

**BIOMECHANICAL VALIDATION OF TRANSFER ASSESSMENT INSTRUMENT
(TAI) IN EVALUATING DIFFERENT INDEPENDENT TRANSFERS IN
WHEELCHAIR USERS**

by

Chung-Ying Tsai

B.S. Physical Therapy, National Yang-Ming University, 2005

M.S. Biomedical Engineering, National Cheng Kung University, 2007

Submitted to the Graduate Faculty of
School of Health and Rehabilitation Science in partial fulfillment
of the requirements for the degree of
Doctor of Philosophy

University of Pittsburgh

2014

UNIVERSITY OF PITTSBURGH
SCHOOL OF HEALTH AND REHABILITATION SCIENCE

This dissertation was presented

by

Chung-Ying Tsai

It was defended on

September 5, 2014

and approved by

Michael L. Boninger, MD, Professor, Department of Physical Medicine and Rehabilitation

Rory A. Cooper, PhD, Distinguished Professor, Department of Rehabilitation Science and

Technology

Jennifer Hastings, PhD, Professor, Department of Physical Therapy, University of Puget

Sound

Laura Rice, PhD, Assistant Professor, Department of Kinesiology and Community Health,

University of Illinois at Urbana-Champaign

Dissertation Advisor: Alicia M. Koontz, PhD, Associate Professor, Department of

Rehabilitation Science and Technology

Copyright © by Chung-Ying Tsai

2014

**BIOMECHANICAL VALIDATION OF TRANSFER ASSESSMENT INSTRUMENT
(TAI) IN EVALUATING DIFFERENT INDEPENDENT TRANSFERS IN
WHEELCHAIR USERS**

Chung-Ying Tsai, PhD

University of Pittsburgh, 2014

Transfers are one of the most essential and physically demanding daily activities for wheelchair users (WUs). The Transfer Assessment Instrument (TAI) is the first tool to standardize the way clinicians evaluate transfer techniques and to help identify specific skills to target during transfer training. The study was to validate the function of the TAI, indicate the effects of transfer skills in performing toilet transfers in two different setups, and evaluate the immediate effects of individualized TAI-based structured transfer training. Up to twenty-six WUs performed transfers to a level-height bench and a toilet with a side and front setup while force plates, load cells, and a motion capture system recorded the biomechanics of their natural transferring skills. Their skills were simultaneously evaluated by two clinicians using the TAI. Logistic and multiple linear regression models were used to determine the relationships between TAI scores and the joint kinetic variables on both arms. Multivariate analysis of variance models were built to test biomechanical differences between using and non-using skill groups during toilet transfers with a side and front setup respectively. Wilcoxon signed-rank test was used to compare the differences of the biomechanical variables between pre and post TAI-based transfer training. The results showed that the completion of TAI skills was associated with lower resultant moments and/or their rates of rise at both shoulders and/or elbows ($p < 0.02$). Some skills increased the moment

magnitude or rate on the leading side ($p<0.03$). Compared to WUs who did not use skills, WUs who scooted forward in their wheelchair and used an appropriate handgrip and head-hip techniques had better shoulder positioning and lower joint forces and moments on both arms in toilet transfers with a side setup ($p<0.04$), and WUs who used close wheelchair positioning had significantly lower trailing arm loading ($p=0.03$) in a front setup. The TAI-based transfer training intervention improved the leading shoulder posture ($p<0.04$) and reduced the joint forces and moments and their rates on both shoulders and trailing elbow and wrist ($p<0.05$). Structured training and the routine practice of TAI skills is recommended to help reduce the risk of developing secondary injuries.

TABLE OF CONTENTS

ACKNOWLEDGEMENTS	XVI
1.0 INTRODUCTION.....	1
1.1 RESEARCH PURPOSE 1: THE KINETIC EFFECTS OF COMPONENT TRANSFER SKILLS IN THE TAI.....	4
1.2 RESEARCH PURPOSE 2: THE EFFECTS OF COMPONENT TRANSFER SKILLS IN TOILET TRANSFERS.....	4
1.3 RESEARCH PURPOSE 3: IMMEDIATE BIOMECHANICAL EFFECTS OF A TRANSFER TRAINING.....	6
2.0 THE RELATIONSHIP BETWEEN INDEPENDENT TRANSFER SKILLS AND UPPER LIMB KINETICS IN WHEELCHAIR USERS	7
2.1 INTRODUCTION	7
2.2 METHODS.....	10
2.2.1 Participants	10
2.2.2 Testing protocol	10
2.2.3 Data analysis	13
2.3 RESULTS	17
2.3.1 Participants	17
2.3.2 TAI variables.....	18

2.3.3	Kinetic variables	19
2.3.4	Correlation test results	21
2.3.5	Logistic regression models for item scores	24
2.3.6	Multiple regression model for part 1 score	28
2.4	DISCUSSION.....	29
2.4.1	Study limitations	34
2.5	CONCLUSION	35
2.6	ACKNOWLEDGEMENTS	36
3.0	THE UPPER LIMB BIOMECHANICAL EFFECTS OF COMPONENT TRANSFER SKILLS IN TWO DIFFERENT SETUPS OF TOILET TRANSFERS IN WHEELCHAIR USERS	37
3.1	INTRODUCTION	37
3.2	METHODS.....	40
3.2.1	Subjects.....	40
3.2.2	Experimental protocol.....	41
3.2.3	Data analysis	44
3.2.4	Statistical analysis.....	47
3.3	RESULTS.....	48
3.3.1	Participants	48
3.3.2	The biomechanical effects of overall transfer skills	49
3.3.3	Deficits in component skills	53
3.3.4	The biomechanical effects of specific component transfer skills for the side setup.....	56

3.3.5	The biomechanical effects of specific component transfer skills for the front setup	63
3.4	DISCUSSION.....	64
3.4.1	Study limitations	73
3.5	CONCLUSION	74
3.6	ACKNOWLEDGEMENTS	75
4.0	THE IMMEDIATE BIOMECHANICAL IMPLICATIONS OF A STRUCTURED COMPONENT SKILLS TRAINING ON INDEPENDENT WHEELCHAIR TRANSFERS	76
4.1	INTRODUCTION	76
4.2	METHODS.....	79
4.2.1	Subjects.....	79
4.2.2	Experimental protocol.....	80
4.2.3	Data analysis	83
4.2.4	Statistical analysis.....	87
4.3	RESULTS	87
4.3.1	Participants	87
4.3.2	TAI scores.....	88
4.3.3	The immediate training effects in biomechanical variables	90
4.4	DISCUSSION.....	98
4.4.1	Study limitations	102
4.5	CONCLUSION	103
4.6	ACKNOWLEDGEMENTS	104

5.0	CONCLUSIONS	105
5.1	STUDY LIMITATIONS	107
5.2	FUTURE WORK.....	108
	APPENDIX A	110
	APPENDIX B	120
	APPENDIX C	127
	APPENDIX D	143
	APPENDIX E	144
	APPENDIX F	145
	APPENDIX G.....	164
	BIBLIOGRAPHY	243

LIST OF TABLES

Table 1. Participants' demographic information	17
Table 2. The items in part 1 of the TAI	18
Table 3. The mean (\pm standard deviation (SD)) of the kinetic variables normalized by body mass (kg).....	20
Table 4. Point-biserial correlation coefficients between TAI items and kinetic variables and Spearman's correlation coefficients between part 1 summary scores and kinetic variables. The table shows the relationships that were significant and had at least medium effect size: $r \geq .3$ or $\leq -.3$	22
Table 5. Logistic regression model results for each TAI item. Odds ratio (Exp(B)) is shown for the predictors that significantly contributed to predicting the TAI item scores. The Nagelkerke R^2 value for each model is reported.	25
Table 6. Multiple linear regression analysis summary for predicting part 1 score.....	28
Table 7. Participants' demographic information	49
Table 8. The values (\pm standard deviation, SD) of maximum kinetic variables and Spearman's correlation coefficients (r) between kinetic variables and P1 summary score in the two setups of toilet transfers. The table shows the significant correlation coefficients.....	50

Table 9. The values (\pm standard deviation, SD) of maximum kinematic variables and Spearman's correlation coefficients (r) between kinematic variables and P1 summary score in the two setups of toilet transfers. The table shows the significant correlation coefficients.	51
Table 10. The items in part 1 of the TAI	53
Table 11. The number of people (% , failure rate) who scored No (0 point) in the selected TAI items respectively and average P1 summary score (\pm SD) in both wheelchair-toilet setups	55
Table 12. The biomechanical effects of item 7 in a wheelchair setup at a side of a toilet	57
Table 13. The biomechanical effects of item 8 in a wheelchair setup at a side of a toilet	58
Table 14. The biomechanical effects of item 9 in a wheelchair setup at a side of a toilet	60
Table 15. The biomechanical effects of item 12 in a wheelchair setup at a side of a toilet	62
Table 16. The biomechanical effects of item 1 skill for the wheelchair setup in front of the toilet	63
Table 17. Participants' demographic information	88
Table 18. The items in part 1 of the TAI and the number of the participants who fail to perform each transfer skill during pre- and post- training testing	89
Table 19. The values (\pm standard deviation, SD) of the kinematic variables and the results of the statistical analysis between pre- and post-training groups.....	91
Table 20. The values (\pm standard deviation, SD) of maximum trailing shoulder kinetic variables and the results of the statistical analysis between pre- and post-training groups	93
Table 21. The values (\pm standard deviation, SD) of maximum trailing elbow kinetic variables and the results of the statistical analysis between pre- and post-training groups	94
Table 22. The values (\pm standard deviation, SD) of maximum trailing wrist kinetic variables and the results of the statistical analysis between pre- and post-training groups	95

Table 23. The values (\pm standard deviation, SD) of maximum leading shoulder kinetic variables and the results of the statistical analysis between pre- and post-training groups	95
Table 24. The values (\pm standard deviation, SD) of maximum leading elbow kinetic variables and the results of the statistical analysis between pre- and post-training groups	97
Table 25. The values (\pm standard deviation, SD) of maximum leading wrist kinetic variables and the results of the statistical analysis between pre- and post-training groups	97
Table 26. Summary of exploratory principle component analysis results for the items in the TAI (N=23).....	113
Table 27. The summary of multiple linear regression analysis for the associations between component scores and kinetic variables.....	115

LIST OF FIGURES

Figure 1. Front (left figure) and top (right figure) views of the transfer station. Abbreviations: WC, wheelchair; FP, force plate.	11
Figure 2. The marker set used in the current study. Abbreviations: FH, forehead; RTMJ, right temporomandibular joint; LTMJ, left temporomandibular joint; STRN, sternum; RAC, right acromioclavicular joint; LAC, left acromioclavicular joint; XYPD, xiphoid; RUA, right upper arm; LUA, left upper arm; RLEP, right lateral epicondyle; LLEP, left lateral epicondyle; RMEP, right medial epicondyle; LMEP, left medial epicondyle; RFA, right forearm; LFA, left forearm; RUS, right ulnar styloid; LUS, left ulnar styloid; RRS, right radial styloid; LRS, left radial styloid; RHC, right hand center; LHC, left hand center; R3MCP, right 3rd metacarpophalangeal joint; L3MCP, left 3rd metacarpophalangeal joint; C7, 7th cervical spinous process; T3, 3rd thoracic spinous process; T8, 8th thoracic spinous process.....	12
Figure 3. Two different wheelchair setups for toilet transfers suggested by Access Board: wheelchair setup at a side of a toilet (A) and in front of a toilet (B) ("Americans with Disabilities Act (ADA) - Accessibility Guidelines for Buildings and Facilities,")	40
Figure 4. The transfer station includes a 10-camera Vicon Nexus motion analysis system (Vicon, Centennial, CO) (A), three force plates under the wheelchair, subjects' feet, and the toilet (Bertec	

Corporation, Columbus, OH) (B), and two load cells (Model MC5 from AMTI, Watertown, MA; Model Omega 160 from ATI, Apex, NC) attached to the two grab bars respectively (C and D). 42

Figure 5. The orientation of the toilet in side (A) and front (B) setups in our transfer station..... 42

Figure 6. The definition of the position angle the study recorded 44

Figure 7. Figure 2: Anatomical (zero) position and shoulder angle orientation relative to trunk coordinate system: A, plane of elevation; B, negative elevation; C, internal rotation (Wu et al., 2005). Abbreviation: GH joint, glenohumeral joint; IJ, incisura jugularis; X_s, Y_s, Z_s, shoulder local coordinate system; X_t, Y_t, Z_t, trunk local coordinate system..... 46

Figure 8. The study setup for level-height transfers (left) and toilet transfers (right). A, simulated wheelchair armrest; B, bench-side grab bar; C, wheelchair force plate; D, bench force plate; E, feet force plate..... 83

Figure 9. Anatomical (zero) position and shoulder angle orientation relative to trunk coordinate system: A, plane of elevation; B, negative elevation; C, internal rotation (Wu et al., 2005). Abbreviation: GH joint, glenohumeral joint; IJ, incisura jugularis; X_s, Y_s, Z_s, shoulder local coordinate system; X_t, Y_t, Z_t, trunk local coordinate system 86

Figure 10. Scree plot between each component and its eigenvalue. The point of inflexion is at the fourth data (component) point. 113

Figure 11. The scatter plot between component 2 scores and average resultant moment on the trailing (right) shoulder 117

Figure 12. The scatter plot between component 2 scores and average resultant moment on the trailing (right) elbow 117

Figure 13. The scatter plot between component 3 scores and average resultant moment on the trailing (right) shoulder 118

Figure 14. The scatter plot between component 2 scores and average resultant moment on the leading (left) wrist..... 119

Figure 15. Dashboard indicator for level-height transfers 123

Figure 16. Dashboard indicator for toilet transfers with a side setup 124

Figure 17. Dashboard indicator for toilet transfers with a front setup..... 125

ACKNOWLEDGEMENTS

Finally, my PhD life is close to the end and I will start another new career in the states. In the 4 years and four months period, I learned a lot and enjoyed a lot. Getting a PhD degree is one of my goals in my life. I can have this kind of achievements, I believe it's not because of my personal endeavor, it's because I have many good advisors and friends helping me.

First, I need to thank my advisor, Dr. Koontz. Without her help, I never can finish my project, my dissertation, have publications, ... , and I even can not come to the states. She is always very nice and patient to listen to me and discuss with me. I know my writing is bad and sometimes I may be a little bit emotional, lazy, and try to avoid troubles. She is always very patient to give me comments, modify my papers, let me understand what she thinks and push me forward. Besides, she is also very supportive and gives me a lot of freedom so I can also pursue what I want to do for my career besides PhD degree. Thank you, Dr. Koontz.

Second, thank all of the shop staffs: Mark, Garrett, Dalton, Josh, Zach, and Ben. The lunch time with them definitely is one of the best parts in my PhD life. It gives me a lot of chances to practicing English, provides me a lot of culture shocks, and also helps me relieve my pressure. They are also very nice and patient to teach me the machining and manufacturing processes which I have zero knowledge about before I join into the big group. Now I can understand what they are discussing and even make my own parts by myself. Without their help,

I also can not finish my project. Without their company, my PhD life would be boring. Thank you all, shop staffs.

I also need to thank all of my committee members, Dr. Boninger, Cooper, Hastings, and Rice. Without their support and suggestion, I can not finish my project smoothly. All of their comments and suggestion make my dissertation more meaningful and comprehensive. I also learn a lot from seeing their attitude about doing research. It's so scientific and conscientious. Thank you.

Thank all of the clinical coordinators, staffs in RST, HERL, and UPMC. Without their help, the whole study can not be preceded.

Thank all of the participants. Without their generosity and contribution, the study can not be done.

Thank all of my friends!!!! I am so lucky that I can have so many friends in Pittsburgh. It's also super cool that I can have friends from different countries. Working and hanging out with the friends from different culture is also a priceless experience for me in my PhD life. Without their company, my life would not be colorful. Without their support, I can not solve all of the difficulties in the states. Thanks, all my wonderful friends.

Last but not least. Thank all of my families' support. My parents always give me a lot of freedom to choose and pursue what I want. Without their support and trust, I may lose myself, be panic, and be hesitated. I am so lucky to have my great younger sister and brother. They are always very sweet to talk to me about the situation in Taiwan and take care of my parents well, so I don't need to worry too much and I can totally focus on my research and career in the states. Although our distance is so far away, the whole families' affection is still strong and close. Thank you, all of my dear families.

1.0 INTRODUCTION

51.2 million people in the U.S. have a physical disability (Steinmetz, 2006), and there were about 265,000 people with spinal cord injuries (SCI) in U.S. in 2010 ("Spinal Cord Injury Facts and Figures at a Glance," 2010). Each year, there are about 12,000 new spinal cord injuries (SCI) many of which will require the use of a wheelchair ("Spinal Cord Injury Facts and Figures at a Glance," 2010). People in this large and expanding population need to use their upper extremities to complete almost all of the activities of daily living (ADLs). The accumulation of high loading on both upper limbs from transfers, weight relief maneuvers, and wheelchair propulsion expose wheelchair users to high risk of overuse injuries, such as rotator cuff tears, elbow pain, and carpal tunnel syndrome (Escobedo, Hunter, Hollister, Patten, & Goldstein, 1997; Koontz, Kankipati, Lin, Cooper, & Boninger, 2011; Sie, Waters, Adkins, & Gellman, 1992).

Wheelchair transfers are one of the most critical predictors for wheelchair users' quality of life and community participation (Mortenson, Miller, Backman, & Oliffe, 2012). Full-time wheelchair users usually perform 14 to 18 wheelchair transfers per day (Finley, McQuade, & Rodgers, 2005). Performing transfers is mandatory and essential for wheelchair users during functional activities, including bathing, hygiene, and driving (Fliess-Douer, Vanlandewijck, & Van Der Woude, 2012). However, studies have indicated that transfers place higher mechanical demand and joint loading on upper extremities than other wheelchair activities, such as wheelchair propulsion and weight-relief lift (Gagnon, Koontz, Mulroy, et al., 2009; Gagnon,

Nadeau, Noreau, Dehail, & Piotte, 2008). During transfers, wheelchair users' hands need to support 60% to 80% of body weight and shoulder pressure increases 3 to 6 times more than resting position (Bayley, Cochran, & Sledge, 1987; Gagnon, Nadeau, Noreau, Dehail, & Gravel, 2008). Also, during transfers the arms are usually in an impingement position which is combined by flexion, abduction and internal rotation (Koontz, Kankipati, et al., 2011). The combination of high loading, high repetition, and awkward joint angles during transfers may be why shoulder pain is most frequently reported during transfers among wheelchair users (Alm, Saraste, & Norrbrink, 2008; Dalyan, Cardenas, & Gerard, 1999).

When daily activities cause pain, wheelchair users may withdraw from community participation, become dependent on others, functionally decline, and have increased medical expenditures (Dalyan et al., 1999; Mortenson et al., 2012; Pentland & Twomey, 1994). Recovery from upper extremity injuries can be difficult because the constant demand of ADLs do not adequately allow a wheelchair user to rest and wait for the injured soft tissue to fully recover. Previous studies have indicated that the medical treatments for shoulder pain has limited benefit in this population (Alm et al., 2008; Curtis et al., 1999; Dalyan et al., 1999). Therefore, prevention may be an important way to keeping wheelchair users' quality of life. Learning to transfer in a way that reduces forces and awkward joint motions is an important strategy for preserving upper limb function (Subbarao, Klopstein, & Turpin, 1995). However, there is no universal standard for wheelchair transfer evaluation and training in clinics. The current standard for evaluating transfer technique is observation by a therapist and a qualitative assessment. Transfer technique evaluations are not scientifically oriented and uniform across rehabilitation facilities (Fliess-Douer et al., 2012; Newton, Kirby, Macphee, Dupuis, & Macleod, 2002).

Results are impacted by the experience of the therapist and their idea of what constitutes a proper transfer, leading to less precise evaluations and a great degree of variability in transfer skills.

Transfer Assessment Instrument (TAI) is the first instrument to evaluate wheelchair users' transfer skills in detail. The TAI was found to be a safe and quick outcome measurement tool that can be easily applied in a clinical setting without extra testing equipment (McClure, Boninger, Ozawa, & Koontz, 2011). The items on the TAI were based on clinical practice guidelines (Boninger, Waters, et al., 2005), current knowledge in the literature (Gagnon, Koontz, Mulroy, et al., 2009), and best clinical practices related to transfers. The TAI contains two parts. Part 1 divides a transfer into 15 component items, which are scored "Yes" (1 point) if the subject performs the specified skill correctly, "No" (0 points) if the subject performs the skill incorrectly, or not applicable "(N/A)" if the item does not apply to the individual (McClure et al., 2011). The 15 items in the part 1 of TAI include three aspects of component transfer skills: transfer preparation, conservation techniques, and the smoothness of transfers (McClure et al., 2011). Part 1 is completed after each transfer. The 12 items in part 2 of the TAI are used to evaluate the consistency of skills and global performance of transfers. They are scored on a Likert Scale ranging from 0 to 4. A '0' means strongly disagree, and '4' means strongly agree. The items in part 2 are completed after all transfers trials have been performed. The TAI has been shown to have an acceptable to high intra- and inter-rater reliability among raters with different clinical backgrounds; good content, face, and construct validity; and no bias for subjects' physical characteristics, such as age and weight (McClure et al., 2011; Tsai, Rice, Hoelmer, Boninger, & Koontz, 2013). However, no study has associated the clinical assessment of transfer skills to biomechanical changes.

1.1 RESEARCH PURPOSE 1: THE KINETIC EFFECTS OF COMPONENT TRANSFER SKILLS IN THE TAI

The purpose of the study described in chapter 2 is to examine the relationship between component transfer skills as measured with the TAI and upper limb joint loading, and to determine if using proper component transfer skills as defined by the TAI results in biomechanical factors that protect the upper limbs for long term use. We hypothesize that better component transfer skills (higher scores on the TAI) will correlate with lower magnitudes and rates of rise of forces and moments at the shoulders, elbows, and wrists. Knowledge of the relationship between TAI skills and joint biomechanics will lead to more effective transfer assessments and help to focus training on skills that protect the upper limbs for long term use.

1.2 RESEARCH PURPOSE 2: THE EFFECTS OF COMPONENT TRANSFER SKILLS IN TOILET TRANSFERS

Studies have shown that different transfer setups, such as high-target, low-target, and far-gap transfers, would influence muscle activations and biomechanics during transfers (Gagnon, Nadeau, Noreau, Dehail, & Gravel, 2008; Wang, Kim, Ford, & Ford, 1994). Toilet transfers present a unique set of challenges for wheelchair users. They often take place in constrained spaces limiting transfer preparation and wheelchair positioning options. The height of the toilet (43.18 to 48.26 cm or 17 to 19") is lower than the average wheelchair and cushion height (55.88 cm or 22" (Toro, Koontz, & Cooper, 2013)) and therefore requires non-level height transfers for most people. There may not be a good position for their hands or optimal use a grab bar which

can provide a mechanical advantage (Toro et al., 2013). All of these factors may make toilet transfers more strenuous.

To our knowledge there is no research addressing wheelchair users' transfer skill deficits and the impact of transfer skills during toilet transfers. The goal of the study described in chapter 3 is to better understand wheelchair users' transfer skill deficits during self-selected transfers to two toilet positions and determine the impact of these transfer skills on upper-limb joint biomechanics during transfers for each toilet position. We compared differences in component transfer skills used and joint biomechanics between two different toilet positions which are Americans with Disabilities Act (ADA) compliant ("Americans with Disabilities Act (ADA) - Accessibility Guidelines for Buildings and Facilities,"): one toilet position required the wheelchair setup to be at the side of the toilet (a narrower angle of approach), and the other toilet position allowed the wheelchair to be set up in front of the toilet (a wider angle of approach). We hypothesize that wheelchair users with overall good component transfer skills (higher TAI part 1 summary score) would have lower force and moment loading on the shoulders, elbows, and wrists on both sides and for both wheelchair-toilet setups. Moreover, we expect to find that the types of component transfer skills (e.g. individual TAI item scores) associated with reduced loading would be the same between the two wheelchair-toilet setups. The results of this study will help to support the need for clinical transfer evaluation and training, and potentially identify the optimal bathroom setup needed for performing biomechanically safe toilet transfers.

1.3 RESEARCH PURPOSE 3: IMMEDIATE BIOMECHANICAL EFFECTS OF A TRANSFER TRAINING

A study indicates that near 50% of wheelchair users do not receive appropriate transfer skill training during rehabilitation in the hospital (Fliess-Douer et al., 2012). Rice et al.'s recent study demonstrated the importance of a structured transfer education program and its long-term training effects for wheelchair users (L. A. Rice et al., 2013). Wheelchair users who received the strict protocol of transfer training in inpatient rehabilitation had higher TAI scores, which mean better transfer quality, compared to the standard care group after one year postdischarge (L. A. Rice et al., 2013). However, no study has investigated whether a structured training program can have good biomechanical effects on wheelchair users' upper limbs. The training program may have the chance to further prevent wheelchair users from acquiring secondary injuries.

The purpose of the study described in chapter 4 is to evaluate the immediate biomechanical effects of TAI-based structured transfer training on wheelchair users' upper limbs. Based on previous studies, we hypothesize that after the training program, wheelchair users will have reduced resultant joint forces and moments on both the leading and trailing arms and less shoulder internal rotation and elevation, and wrist extension angles during transfers compared to before training. Results of this study could help standardize and unify how transfers are being taught in the field and reduce the incidence of upper limb pain and injuries among wheelchair users who perform independent sitting pivot transfers.

2.0 THE RELATIONSHIP BETWEEN INDEPENDENT TRANSFER SKILLS AND UPPER LIMB KINETICS IN WHEELCHAIR USERS

2.1 INTRODUCTION

(This chapter has been published in BioMed Research International, volume 2014, page 12) In 2010 there were about 1.6 million people using wheelchairs for mobility (*2013 Annual Disability Statistics Compendium*, 2013); with that number expanding each year ("Spinal Cord Injury Facts and Figures at a Glance," 2010). Wheelchair users must use their upper extremities for almost all activities of daily living (ADLs) such as getting in and out of bed, transferring to a shower or toilet and transferring in and out of a car.(Fliess-Douer et al., 2012). A full-time wheelchair user will perform on average 14 to 18 transfers per day (Finley et al., 2005). Transfers are a key element of living an active and productive life, and play a vital role in maintaining independence of wheeled mobility device users. If wheelchair users can not transfer freely, their quality of life and community participation will be severely affected (Mortenson et al., 2012).

Transfers are one of the most strenuous wheelchair activities performed (Alm et al., 2008) and nearly half of wheelchair users do not learn how to use proper transfer techniques during rehab (Fliess-Douer et al., 2012). Incorrect transfer skills may predispose wheelchair users to developing upper limb pain and overuse related injuries, such as rotator cuff tears, elbow pain, and carpal tunnel syndrome (Boninger, Waters, et al., 2005; Curtis et al., 1995; Dalyan et

al., 1999; Gellman, Sie, & Waters, 1988; Nichols, Norman, & Ennis, 1979). The onset of pain can lead to social isolation (Mortenson et al., 2012), dependence on others for assistance with ADLs, and increased medical expenditures (Dalyan et al., 1999). Only about half of wheelchair users seek treatment for pain (Alm et al., 2008; Goldstein, Young, & Escobedo, 1997; McCasland, Budiman-Mak, Weaver, Adams, & Miskevics, 2006) and many feel that their symptoms were not improved after treatment (Alm et al., 2008; Goldstein et al., 1997; Subbarao et al., 1995). Therefore, it seems that prevention may be crucial to reducing upper limb pain and overuse injuries. Learning to transfer in a way that reduces forces and awkward joint motions is an important strategy for preserving upper limb function (Subbarao et al., 1995).

During transfers, the shoulders often assume a position of flexion, abduction, and internal rotation (Finley et al., 2005; Gagnon, Nadeau, Noreau, Eng, & Gravel, 2008). This position brings the glenohumeral head in closer alignment to the undersurface of the acromion and has been identified as a critical risk factor for impinging subacromial soft tissue (Yanai, Fuss, & Fukunaga, 2006). Previous studies also indicate that the loading on the upper extremity joints during transfers is greater than any other wheelchair related activity (Gagnon, Nadeau, Noreau, Dehail, & Pottie, 2008). Transfers have been associated with high peak posterior force and shoulder flexion and adductor moments at the shoulders (Gagnon, Koontz, Mulroy, et al., 2009; Gagnon, Nadeau, Noreau, Dehail, & Pottie, 2008; Koontz, Kankipati, et al., 2011). Large posterior forces at the shoulder are thought to contribute to the development of shoulder posterior instability, capsulitis, and tendinitis (Campbell & Koris, 1996). The combination of shoulder posterior and superior forces increases the risk of shoulder impingement syndrome (Finley & Rodgers, 2004). Furthermore, the elbow has been shown to sustain high superior forces during transfers which may cause nerve compression and result in secondary elbow injuries (Koontz,

Kankipati, et al., 2011). Extremes of wrist extension during transfers have also been reported which combined with the weight-bearing loads during transfers may exacerbate wrist injuries such as carpal tunnel syndrome (Keir, Wells, Ranney, & Lavery, 1997; Sie et al., 1992). Using transfer techniques that reduce upper limb joint forces and moments may help prevent injuries (Boninger, Koontz, et al., 2005; Fleisig, Andrews, Dillman, & Escamilla, 1995; Fuchtmeier et al., 2007; Mercer et al., 2006).

The current standard for evaluating transfer technique is observation by the therapist and a qualitative assessment. Transfer technique evaluations are not scientifically oriented and uniform across rehabilitation facilities (Fliess-Douer et al., 2012; Newton et al., 2002). Results are impacted by the experience of the therapist and their idea of what constitutes a proper transfer, leading to less precise evaluations and a great degree of variability in transfer skills. The Transfer Assessment Instrument (TAI) is the first tool to standardize the way clinicians evaluate transfer technique and to help identify specific skills to target during transfer training. The items on the TAI were based on clinical practice guidelines (Boninger, Waters, et al., 2005), current knowledge in the literature (Gagnon, Koontz, Mulroy, et al., 2009), and best clinical practices related to transfers. The TAI has acceptable to high inter- and intra-rater reliability (intraclass correlation coefficient (ICC) values ranging from 0.72 to 0.88) and good face, content, and construct validity (McClure et al., 2011; L. A. Rice et al., 2013; Tsai et al., 2013). However, no study has associated a clinical assessment of transfer skills to biomechanical changes. The purpose of this study is to examine the relationship between transfer skills as measured with the TAI and upper limb joint loading, and to determine if using proper transfer skills as defined by the TAI results in biomechanical factors that protect the upper limbs for long term use. We hypothesize that better transfer skills (higher scores on the TAI) will correlate with lower

magnitudes and rates of rise of forces and moments at the shoulders, elbows, and wrists. Knowledge on the relationship between TAI skills and joint biomechanics will lead to more effective transfer assessments and help to focus training on skills that protect the upper limbs for long term use.

2.2 METHODS

2.2.1 Participants

The study was approved by the Department of Veterans Affairs Institutional Review Board. All testing occurred at the Human Engineering Research Laboratories in Pittsburgh, PA. The subjects participating in the study were required to be over 18 years old and one year post injury or diagnosis, use a wheelchair for the majority of mobility (40 hours/per week), and be unable to stand up without support. Individuals with pressure sores within the past year and history of angina or seizures were excluded.

2.2.2 Testing protocol

After written informed consent was obtained, subjects completed a general demographic questionnaire. Anthropometric measures were collected, such as upper arm length and circumference, to determine the center of mass and moment of inertia for each segment (Hanavan, 1964). Subjects were asked to position themselves next to a bench, which was at a height level to their own wheelchair seats, on a custom-built transfer station (Figure 1) (Koontz,

Lin, Kankipati, Boninger, & Cooper, 2011). The transfer station contains three force plates (Bertec Corporation, Columbus, OH) which were underneath the wheelchair, level bench, and the subject's feet respectively. Two 6-component load cells (Model MC5 from AMTI, Watertown, MA; Model Omega 160 from ATI, Apex, NC) were attached to two steel beams used to simulate an armrest and grab bar (Figure 1). Subjects were asked to naturally position and secure their wheelchairs in the 3×3 square foot (91.44 cm by 91.44 cm) aluminum platform that covered the wheelchair force plate. They were also asked to choose where they wanted to position and secure the bench on the other 3×4 square foot aluminum platform (91.44 cm by 121.92 cm) that covered the bench force plate (Figure 1). The position of the wheelchair grab bar was also adjusted based on the subjects' preference. Reflective markers (Figure 2) were placed on subjects' heads, trunks, and upper extremities to build local coordinate systems (Wu et al., 2005) for each segment. Marker trajectories were collected at 100 Hz using a ten-camera three-dimensional motion capture system (Vicon, Centennial, CO.) Kinetic data from all the force plates and load cells were collected at 1000 Hz.

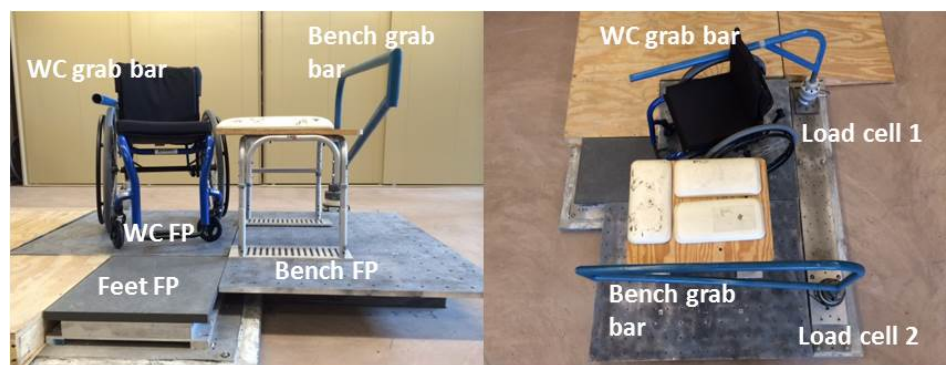


Figure 1. Front (left figure) and top (right figure) views of the transfer station. Abbreviations: WC, wheelchair; FP, force plate.

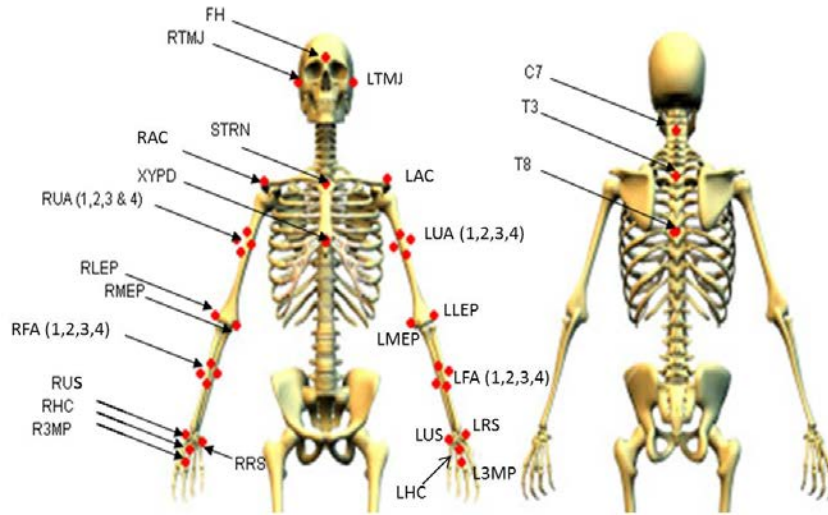


Figure 2. The marker set used in the current study. Abbreviations: FH, forehead; RTMJ, right temporomandibular joint; LTMJ, left temporomandibular joint; STRN, sternum; RAC, right acromioclavicular joint; LAC, left acromioclavicular joint; XYPD, xiphoid; RUA, right upper arm; LUA, left upper arm; RLEP, right lateral epicondyle; LLEP, left lateral epicondyle; RMEP, right medial epicondyle; LMEP, left medial epicondyle; RFA, right forearm; LFA, left forearm; RUS, right ulnar styloid; LUS, left ulnar styloid; RRS, right radial styloid; LRS, left radial styloid; RHC, right hand center; LHC, left hand center; R3MCP, right 3rd metacarpophalangeal joint; L3MCP, left 3rd metacarpophalangeal joint; C7, 7th cervical spinous process; T3, 3rd thoracic spinous process; T8, 8th thoracic spinous process

Subjects were asked to perform up to five trials of level-height bench transfers. In each trial, subjects needed to perform transfers to and from their own wheelchairs in a natural way. Movement from one surface to the other (e.g. wheelchair to bench) was considered as one transfer. They were provided an opportunity to adjust their wheelchair position and familiarize themselves with the setup prior to data collection. Subjects had time to rest in between trials and additional rest was provided as needed. They were asked to use their own approaches to transferring so their transfer movement pattern and techniques would be as natural as possible. Subjects were asked to place their trailing arm (right arm) on the wheelchair grab bar (Figure 1)

when they transferred to the bench on their left side so the reaction forces at the hand could be recorded. On the bench side, subjects were free to place their hand on either the bench or the grab bar. During each trial, up to two study clinicians independently observed and scored each subject's transfer skills using the TAI. All of the participants in the study were evaluated by the same two clinicians. Both were physical therapists who were trained to use the TAI before the study started. The TAI was completed after watching participants perform three to five transfers from the wheelchair to the bench. After independently scoring each subject, the clinicians compared their findings. Any discrepancies in the scoring were discussed and a score reflecting the consensus decision was recorded.

2.2.3 Data analysis

The biomechanical variables were computed using Matlab (Mathworks, Inc., Natick, MA, USA). A zero-lag low-pass 4th order Butterworth filter with cut-off frequency of 7 and 5 Hz was used to filter the kinetic and kinematic data respectively (Koontz, Kankipati, et al., 2011). Only the lift phase of the transfer from the wheelchair to the bench was analyzed in this study. A transfer was determined to begin when a vertical reaction force was detected by the load cell on the wheelchair side grab bar (Figure 1) and ended before a landing spike was detected by the force plate underneath the bench (Kankipati, Koontz, Vega, & Lin, 2011). The end of the lift phase and the beginning of the descent phase is defined by the highest elevated point of the trunk which is indicated by the peak of the C7 and T3 marker trajectories (Kankipati et al., 2011). Hanavan's model was used to calculate center of mass and moment of inertia using the subjects' segment lengths and circumferences (Hanavan, 1964). Three-component forces and moments measured by the load cells and the force plates (Figure 1), the marker data of the trunk and upper

extremities, and the inertial properties of each body segment were inputs into an inverse dynamic model (Cooper, Boninger, Shimada, & Lawrence, 1999). Each segment was assumed as a rigid body and linked together by ball and socket joints. The 3rd metacarpalphalangeal joint was assumed as the point of force application. The output of the inverse dynamic model included upper extremity net joint forces and moments.

The key kinetic variables included average and maximum resultant forces and moments, and maximum rate of rise of resultant force and moment at the shoulders, elbows, and wrists on both sides. Since shoulder pain is more commonly associated with transfers (Dalyan et al., 1999), we analyzed the maximum superior and posterior shoulder forces and extension, abduction, and internal rotation shoulder moments. These variables were selected because they have been linked to shoulder pain, median nerve function, and other upper extremity injuries (Boninger, Koontz, et al., 2005; Finley & Rodgers, 2004; Gagnon, Koontz, Mulroy, et al., 2009; Keeley, Oliver, & Dougherty, 2012; Meislin, Sperling, & Stitik, 2005; Mercer et al., 2006; I. M. Rice, Jayaraman, Hsiao-Wecksler, & Sosnoff, 2013). The resultant force on each joint is indicative of the total joint loading. The maximum rate of rise of resultant force is the peak instantaneous loading rate and impact force on each joint. The resultant moment on each joint represents the rotational demands associated with the muscle forces around the joint and the external forces. The maximum rate of rise of resultant moment indicates the peak rate of moment production on each joint. The superior and posterior shoulder forces were defined as the components of resultant shoulder force acting along the vertical upward and posterior axes of shoulder. Each kinetic variable was normalized by body mass (in kilogram) (Desroches, Gagnon, Nadeau, & Popovic, 2013; Gagnon, Koontz, Mulroy, et al., 2009; Gagnon, Nadeau, Noreau, Dehail, & Pottie, 2008).

Descriptive statistics (means and standard deviations (SD)) were calculated for each variable. Kinetic variables were averaged over a minimum of three and a maximum of five trials.

The TAI contains two parts – parts 1 and 2. Both parts are scored and averaged to produce a third, final score. Only part 1 item scores and part 1 summary scores were used because the part 1 items evaluate whether the individual used specific transfer skills. Part 2 was not analyzed in this study as it encompasses some of the same transfer skills that are measured in Part 1. Part 1 is comprised of 15 items which are scored “Yes” (1 point) when the subject performs the specified skill correctly and “No” (0 points) when the subject performs the skill incorrectly, or not applicable “(N/A)” which means the item does not apply. The part 1 summary score is the summation of each item's score multiplied by 10, and then divided by the number of applicable items, ranging from 0-10 (McClure et al., 2011). TAI items that had a 50% response rate or higher in a N/A category or greater than an 80% response rate in the same non-NA category (e.g. Yes or No) were not considered for further analysis on the individual item scores. Point-biserial correlations were conducted between the remaining items. Among the items that were highly correlated ($r > 0.80$), one was selected for the logistical modeling analysis (see below).

All of the kinetic data and TAI part 1 summary scores (e.g. continuous variables) were examined for normality using the Shapiro-Wilk test. Point-biserial correlation tests between each TAI item score (e.g. dichotomous variable) and the kinetic variables and Spearman's correlation tests between part 1 summary scores and kinetic variables were conducted to identify relationships with at least a medium effect size ($r \geq .30$ or $\leq -.30$ (Cohen, 1992)). In order to verify specific kinetic effects of each transfer skill, logistic regression was used to model the association between individual TAI item scores (dichotomous outcome variable) and kinetic

variables (predictors). Multiple linear regression was used to model the association between the TAI part 1 summary scores (continuous outcome variable) and kinetic variables (predictors). Separate models were created for the left and right sides. For the logistic regression model, histograms and Q-Q plots were used to check the assumption of no outliers. The assumption of multicollinearity for the kinetic variables (predictors) was tested using the variance inflation factors (VIFs) (Myers, 2000). The assumption of linear relationships between continuous predictors and the log of the outcome variable was tested by Box-Cox transformation (Box & Cox, 1964). For the multiple linear regression models, histograms and Q-Q plots were used to check the assumption of no outliers on both predictors and outcome variables. The scatter plot of the standardized residuals against the predicted value was used to test the assumption of linearity. Shapiro-Wilk test was used to check the normality of the error term of the regression model. The assumption of multicollinearity for the predictors was also tested using the VIFs (Myers, 2000). The assumptions of homoscedasticity and independence for multiple linear regression was checked using the Breusch-Pagan test (Breusch & Pagan, 1979) and Durbin-Watson test (Durbin & Watson, 1950) respectively.

Backward elimination was used to determine the subset of predictors (kinetic variables) for each TAI outcome variable. The level of significance was set at $p < 0.05$. All the statistical analyses were performed in SPSS 21 (SPSS Inc., Chicago, IL).

2.3 RESULTS

2.3.1 Participants

Twenty men and three women volunteered to participate in the study. Table 1 shows summary demographic information. Eighteen subjects had a spinal cord injury (SCI); fourteen subjects reported a complete SCI and four subjects an incomplete SCI (three with American Spinal Injury Association (ASIA) Grade B, one with ASIA Grade C). Three subjects had quadriplegia (C4 to C6), nine had high paraplegia (T2 to T7), and six had low paraplegia (T8 to L3) (John, Cherian, & Babu, 2010). The remaining five participants had bilateral tibial and fibular fractures with nerve damage (n=1), double above knee amputation (n=1), muscular dystrophy (n=1), osteogenesis imperfecta (n=1), and myelopathy (n=1).

Table 1. Participants' demographic information

Subjects, n=23	Mean \pm standard deviation (range)
Age (years)	38.30 \pm 11.07 (21 - 55)
Height (meters)	1.67 \pm 0.23 (.99 - 1.85)
Weight (kilograms)	67.14 \pm 19.18 (29.96 - 98.15)
Average duration of using a wheelchair (years)	13.15 \pm 8.13 (1 - 27.25)

2.3.2 TAI variables

Since the TAI part 1 summary scores and final scores were highly correlated ($r=.97$), the TAI part 1 summary scores were used for the multiple regression model. The Part 1 summary scores ranged from 3.08 to 10.00 with an average (\pm SD) of 7.30 (\pm 1.76). Table 2 shows the items in the part 1 of the TAI. Items 1, 2, 6, 7, 9, and 12 met the inclusion criteria for the logistic models (Yes response rate ranges from 39% to 78%, $n=23$). Items 4, 5, 15 were not modeled because of the high number of N/A responses. Items 8, 10, 11, 13, and 14 were not modeled because they had too high of a 'Yes' response rate (e.g. greater than 80% of subjects). Items 3 and 7 scores had the same exact responses for both ($r=1$). Item 7 scores were modeled because it can be applied to both manual and power wheelchair users, whereas item 3 only applies to manual wheelchair users.

Table 2. The items in part 1 of the TAI

Items in part 1 of the TAI
1. *The subject's wheelchair is within 3 inches of the object to which he is transferring on to.
2. *The angle between the subject's wheelchair and the surface to which he is transferring is approximately 20-45 degrees.
3. The subject attempts to position his chair to perform the transfer forward of the rear wheel (i.e., subject does not transfer over the rear wheel).
4. If possible, the subject removes his armrest or attempts to take it out of the way.
5. The subject performs a level or downhill transfer, whenever possible.
6. *The subject places his feet in a stable position (on the floor if possible) before the transfer.

Table 2 (continued)

7. *The subject scoots to the front edge of the wheelchair seat before he transfers (i.e., moves his buttocks to the front 2/3rds of the seat).
8. Hands are in a stable position prior to the start of the transfer.
9. *A handgrip is utilized correctly by the leading arm (when the handgrip is in the individual's base of support).
10. A handgrip is utilized correctly by the trailing arm (when the handgrip is in the individual's base of support).
11. Flight is well controlled.
12. *Head-hip relationship is used.
13. The lead arm is correctly positioned (The arm should not be extremely internally rotated and should be abducted 30-45 deg.)
14. The landing phase of the transfer is smooth and well controlled (i.e., hands are not flying off the support surface and the subject is sitting safely on the target surface.)
15. If an assistant is helping, the assistant supports the subject's arms during the transfer.

Note: *, the items we selected to analyze

2.3.3 Kinetic variables

Means and standard deviations of the selected kinetic variables are shown in Table 3.

Table 3. The mean (\pm standard deviation (SD)) of the kinetic variables normalized by body mass (kg)

Variables	Trailing	Leading	
	(right) side	(left) side	
	Mean (\pm SD)	Mean (\pm SD)	
Shoulder	AveRF (N/Kg)	2.98 (\pm 0.75)	2.52 (\pm 0.54)
	MaxRF (N/Kg)	4.54 (\pm 1.10)	4.24 (\pm 0.97)
	MaxRFRate (N/sec*Kg)	15.95 (\pm 6.09)	13.14 (\pm 5.72)
	AveRM (N*m/Kg)	0.53 (\pm 0.26)	0.60 (\pm 0.17)
	MaxRM (N*m/Kg)	0.87 (\pm 0.38)	1.06 (\pm 0.25)
	MaxRMRate (N*m/sec*Kg)	3.36 (\pm 1.95)	3.96 (\pm 1.38)
	MaxSupF (N/Kg)	1.58 (\pm 0.70)	2.18 (\pm 1.14)
	MaxPosF (N/Kg)	3.22 (\pm 1.17)	3.23 (\pm 0.95)
	MaxIRM (N*m/Kg)	0.10 (\pm 0.11)	0.10 (\pm 0.15)
	MaxAbdM (N*m/Kg)	0.43 (\pm 0.21)	0.42 (\pm 0.26)
	MaxExtenM (N*m/Kg)	0.41 (\pm 0.30)	0.70 (\pm 0.32)
	Elbow	AveRF (N/Kg)	2.76 (\pm 0.71)
MaxRF (N/Kg)		4.35 (\pm 1.07)	4.20 (\pm 1.03)
MaxRFRate (N/sec*Kg)		16.06 (\pm 6.00)	4.66 (\pm 2.91)
AveRM (N*m/Kg)		0.38 (\pm 0.16)	0.21 (\pm 0.10)
MaxRM (N*m/Kg)		0.62 (\pm 0.23)	0.39 (\pm 0.15)
MaxRMRate (N*m/sec*Kg)		2.43 (\pm 1.18)	1.85 (\pm 0.89)

Table 3 (continued)

Wrist	AveRF (N/Kg)	2.69 (± 0.70)	2.34 (± 0.61)
	MaxRF (N/Kg)	4.29 (± 1.05)	4.19 (± 1.06)
	MaxRFRate (N/sec*Kg)	16.21 (± 6.08)	13.17 (± 5.74)
	AveRM (N*m/Kg)	0.22 (± 0.06)	0.15 (± 0.08)
	MaxRM (N*m/Kg)	0.35 (± 0.09)	0.26 (± 0.14)
	MaxRMRate (N*m/sec*Kg)	1.34 (± 0.57)	0.86 (± 0.46)
	<hr/> Abbreviations: Ave, average; Max, maximum; RF, resultant force; RFRate, rate of rise of resultant force; RM, resultant moment; RMRate, rate of rise of resultant moment; SupF, superior force; PosF, posterior force; IRM, internal rotation moment; AbdM, abduction moment; ExtenM, extension moment <hr/>		

2.3.4 Correlation test results

The TAI part 1 summary and item scores were statistically associated and at least moderately correlated ($r \geq .3$ or $\leq -.3$) with one or more of the kinetic variables (Cohen, 1992) (Table 4).

Table 4. Point-biserial correlation coefficients between TAI items and kinetic variables and Spearman's correlation coefficients between part 1 summary scores and kinetic variables. The table shows the relationships that were significant and had at least medium effect size: $r \geq .3$ or $\leq -.3$.

Correlations	Trailing (right) side							Leading (left) side						
	1	2	6	7	9	12	Part1	1	2	6	7	9	12	Part1
Shoulder														
AveRF				-.43*			-.35	-.30	-.31					
MaxRF									-.36					
MaxRFRate			-.31	-.32	-.54*					-.37				
AveRM	.30		-.52 ^{\$}		-.44*								-.34	
MaxRM	.31		-.47*		-.49*									
MaxRMRate	.37		-.51*		-.52*			.37		-.55*		-.39	-.46*	-.39
MaxSupF														
MaxPosF														
MaxIRM			.37						-.56*			.42*		
MaxAbdM						.33			-.32					
MaxExtenM						.31		.35	.30	.43*				.49*
Elbow														

Table 4 (continued)

AveRF	.30									
MaxRF	.31									
MaxRFRate										
AveRM										
MaxRM										
MaxRMRate										
Wrist										
AveRF										
MaxRF										
MaxRFRate										
AveRM										
MaxRM										
MaxRMRate										

*p < 0.05; [§]p < 0.01; Abbreviations: Ave, average; Max, maximum; RF, resultant force; RFRate, rate of rise of resultant force; RM, resultant moment; RMRate, rate of rise of resultant moment; SupF, superior force; PosF, posterior fore; IRM, internal rotation moment; AbdM, abduction moment; ExtenM, extension moment

2.3.5 Logistic regression models for item scores

Lower average resultant shoulder force and higher maximum rate of rise of resultant shoulder moment on the leading (left) side were associated with a ‘Yes’ score on item 1 (Table 5). Subjects with lower maximum internal rotation shoulder moments on the leading (left) side had an increased likelihood of a ‘Yes’ score for item 2. Lower average resultant shoulder moment on the trailing (right) side and lower maximum rate of rise of resultant shoulder moment on the leading (left) side corresponded with a ‘Yes’ score on item 6.

On the trailing (right) side, subjects with lower average resultant moment and maximum rate of rise of resultant moment at the elbow were more likely to have a ‘Yes’ score on item 7. On the leading (left) side, a higher maximum shoulder extension moment was associated with a ‘Yes’ score on item 7 (Table 5).

On the trailing (right) side, a ‘Yes’ score on item 9 corresponded with lower average resultant shoulder moment and lower maximum rate of rise of resultant elbow moment. On the leading (left) side, a ‘Yes’ score on item 9 was associated with lower maximum rate of rise of resultant shoulder moment, higher maximum internal rotation shoulder moment, lower maximum rate of rise of resultant elbow moment, and higher maximum rate of rise of resultant wrist moment (Table 5). Subjects with a lower rate of rise of resultant shoulder moment on the leading (left) side were more likely to score a ‘Yes’ on item 12 (Table 5).

Table 5. Logistic regression model results for each TAI item. Odds ratio (Exp(B)) is shown for the predictors that significantly contributed to predicting the TAI item scores. The Nagelkerke R² value for each model is reported.

Item	Variables	B	χ^2	Sig.	Exp(B)	Model results
Item 1: The subject's wheelchair is within 3 inches of the object to which he is transferring on to.	Leading (left) shoulder AveRF	-2.45	3.55	.06		$\chi^2(2, N=23) = 8.72,$ p = .01, R ² = .42
	Leading (left) shoulder	1.32	3.39	.07		
	MaxRMRate					
Item 2: The angle between the subject's wheelchair and the surface to which he is transferring is approximately 20-45 degrees.	Leading (left) shoulder	-16.53	4.29	.04	.00	$\chi^2(1, N=23) = 9.09,$ p < .01, R ² = .46
	MaxIRM*					
Item 6: The subject places his feet in a stable position (on the floor if possible) before the transfer.	Leading (left) shoulder	-1.34	3.67	.06		$\chi^2(1, N=23) = 7.86,$ p < .01, R ² = .42
	MaxRMRate					
	Trailing (right) shoulder	-5.73	4.19	.04	.00	
AveRM*						
Item 7: The subject scoots to the front edge of the wheelchair seat before he transfers (i.e., moves his buttocks to the	Leading (left) shoulder	3.91	3.54	.06		$\chi^2(1, N=23) = 4.70,$ p = .03, R ² = .27
	MaxExtenM					
	Trailing (right) elbow AveRM	-13.34	2.96	.09		

Table 5 (continued)

front 2/3rds of the seat).	Trailing (right) elbow	-3.70	2.82	.09	$p < .01, R^2 = .69$
	MaxRMRate				
Item 9: A handgrip is utilized correctly by the leading arm (when the handgrip is in the individual's base of support).	Leading (left) shoulder	-1.39	1.62	.20	$\chi^2(4, N=23) = 18.29,$ $p < .01, R^2 = .74$
	MaxRMRate				
	Leading (left) shoulder	22.10	1.85	.17	
	MaxIRM				
	Leading (left) elbow	-4.74	2.21	.14	
	MaxRMRate				
Item 12: Head-hip relationship is used.	Leading (left) wrist	7.51	2.83	.09	$\chi^2(1, N=23) = 5.13,$ $p = .02, R^2 = .27$
	MaxRMRate				
	Trailing (right) shoulder	-9.91	1.43	.23	
	AveRM				
	Trailing (right) elbow	-10.38	4.07	.04	
MaxRMRate*					

Table 5 (continued)

Note: *, the predictor significantly contributed to the regression model. Abbreviations: B, unstandardized regression coefficients; Sig., significance; Exp(B), odds ratio; Ave, average; Max, maximum; RMRate, rate of rise of resultant moment; RF, resultant force; IRM, internal rotation moment; RM, resultant moment; ExtenM, extension moment

2.3.6 Multiple regression model for part 1 score

Lower average resultant trailing (right) elbow moment, lower maximal rate of rise of resultant leading (left) elbow moment and higher maximal leading (left) shoulder extension moment were associated with proper completion of a greater number of transfer skills overall (higher TAI part 1 score) (Table 6).

Table 6. Multiple linear regression analysis summary for predicting part 1 score

Variable	B	SEB	β	sr^2	Sig.	Regression model
Trailing (right) elbow AveRM*	-5.86	2.02	-.53	.29	<.01	F(1,21)=8.40, p<.01, R ² =.29
Leading (left) shoulder MaxExtenM	1.94	.85	.35	.12	.03	F(2,20)=12.54, p<.01, R ² =.56
Leading (left) elbow MaxRMRate*	-1.13	.30	-.57	.31	<.01	

Note: *, the predictor significantly contributed to the regression model. Abbreviations: B,

unstandardized regression coefficients; SEB, standard error of the unstandardized regression coefficients; β , standardized regression coefficients; sr^2 , squared semipartial correlations; Sig., significance; Ave, average; Max, maximum; RM, resultant moment;

ExtenM, extension moment; RMRate, rate of rise of resultant moment

2.4 DISCUSSION

This is the first study to examine the association between proper and improper transfer skills and the resulting forces and moments imparted on the upper limb joints during the transfer process. Specific transfer skills, identified using the TAI, were found to be associated with kinetic variables related to injury risks on the upper extremities (Boninger, Koontz, et al., 2005; Finley & Rodgers, 2004; Gagnon, Koontz, Mulroy, et al., 2009; Keeley et al., 2012; Meislin et al., 2005; Mercer et al., 2006; I. M. Rice et al., 2013). Our study sample included a diverse sample of wheelchair users who had a wide range of transfer skills (e.g. Part 1 summary scores that ranged from 3.08 to 10.00). Despite differences across studies in measurement techniques and subject characteristics, our kinetic variables were in line with those values reported for level transfers in other studies. For example, the studies from Gagnon and Desroches et al. measured upper limb joint forces and moments during transfers among individuals with SCI and indicated that maximum wrist resultant moment ranged from 0.14 Nm/Kg to 0.48 Nm/Kg and shoulder posterior force on both sides were 2.64 N/kg and 3.14 N/kg respectively (Desroches et al., 2013; Gagnon, Nadeau, Noreau, Dehail, & Piote, 2008).

From the regression model results (Table 5 and Table 6), it appears that transfer skills identified by the TAI are closely associated with the magnitude and timing of joint moments. During transfers, the wheelchair user's trunk and his/her arms can be thought as a tripod (Minkel, Hastings, McClure, & Bjerkefors, 2010) which forms a closed kinetic chain (Marciello, Herbison, Cohen, & Schmidt, 1995). The skills used in transfers (e.g. positioning of the wheelchair, using correct handgrips etc.) cause alterations in the moment arms or the distances separating the hands and trunk center of mass and changes in upper limb joint angles (Pynn, Tsai, & Koontz, 2014) that act along with the external forces to produce the resulting moments. Certain transfer skills

helped to reduce the moments imparted on both upper limbs while other skills had the effects of increasing the magnitudes or rates of loading on the leading (left) arm. Proper completion of the skills related to the trailing (right) arm (Part 1 summary score and Items 6, 7 and 9) had the effect of lowering the trailing (right) shoulder and/or elbow peak resultant moment or rate of resultant moment loading. This is significant considering that the trailing arm tends to support a higher percentage of the body weight during sitting-pivot transfers (Forslund, Granstrom, Levi, Westgren, & Hirschfeld, 2007; Gagnon, Nadeau, Noreau, Dehail, & Gravel, 2008).

The six transfer skills as measured by the TAI were modeled because at least 20% of our subject sample scored a “no” for incorrect performance of a particular skill. Four of the six applicable TAI items (transfer skills) dealt with the setup of the wheelchair and body prior to making the transfer. Positioning the wheelchair within 3 inches of the target surface, as measured by item 1, was associated with a reduction in the average resultant shoulder force ($B=-2.45$, $p=.06$) and an increased rate of rise of shoulder resultant moment ($B=1.32$, $p=.07$) (Table 5) on the leading (left) side. The increase in rate of rise may be associated with a shorter time needed to make the transfer when the body is in a position that is closer to the target surface. A proper angle (20 to 45 degrees) between the wheelchair and transfer surface (item 2), was associated with lower peak internal rotation shoulder moment on the leading (left) side ($B=-16.53$, $p=.04$) (Table 5). Angling the wheelchair next to the target as opposed to parallel parking provides a space that can be used to pivot the trunk and lower body over to the target surface. Angling the wheelchair also allows for the user to clear the rear wheel more easily. The pivoting actions of the trunk and lower body and clearing the pathway to the target surface may have helped to reduce the rotational demands on the leading shoulder.

Proper positioning of the feet, (item 6) can provide wheelchair users with greater dynamic postural control during transfers (Gagnon, Koontz, Mulroy, et al., 2009). About 30% of the body weight during sitting pivot transfers is supported by the feet and legs (Gagnon, Nadeau, Noreau, Dehail, & Gravel, 2008). Subjects who scored well on this item had lower resultant moments on the trailing (right) shoulder ($B=-5.73$, $p=.04$) and less maximum rate of rise of resultant moment at the leading (left) shoulder ($B=-1.34$, $p=.06$) (Table 5). “Scooting forward” to the front edge of the wheelchair seat before transfers (item 7) was associated with less trailing (right) elbow moment and its rate of rise ($B=-13.34$ and -3.70 , $p=.09$ and $.09$) (Table 5). Scooting forward brings wheelchair users and their trailing hand positions closer to the target surface which would decrease the lever arm that the applied force is acting through. Our regression model however also indicated that this skill increases leading (left) shoulder extension moment ($B=3.91$, $p=.06$) (Table 5). The increasing shoulder extension moment may have resulted from a shift in loading from the trailing arm to the leading arm. As mentioned, the trailing arm bears more force in a transfer. Getting closer to the surface allows for placing both hands closer to the trunk center of mass which helps to balance the loading more equally across both arms (Kankipati, 2012). For persons who position themselves correctly this will mean seeing less loading on the trailing arm and possibly more loading on the leading arm. In any case higher shoulder extension moment has been shown to increase the risk of pathology, such as ligament edema (Mercer et al., 2006). Close positioning and appropriate angling wheelchair and foot placement may help to mediate the increased shoulder moments experienced on the leading side.

Item 9 evaluates whether wheelchair users use a correct handgrip on the leading arm within their base of support when performing transfers. Clinical practice guidelines encourage

wheelchair users to use handgrips instead of flat hands or fists when performing transfers (Boninger, Waters, et al., 2005). Using flat hands during transfers will cause extreme wrist extension which is one factor identified in the etiology of carpal tunnel syndrome, while a closed-finger fist will result in excessive pressure on the metacarpal joints (Boninger, Waters, et al., 2005; Goodman et al., 2001). The use of handgrips can prevent extreme wrist angles, provide more stability, and help apply forces during transfers (Boninger, Waters, et al., 2005). During transfers, the handgrip choices are limited by the type of transfer surface and the handgrip option available. For the bench transfer evaluated in this study, subjects could either drape their leading fingers over the edge of the bench with the palm resting on the surface, place a flat palm or fist anywhere on top of the bench, or use the adjacent grab bar. If they used a flat palm, closed-finger fist and/or placed their leading hand outside of where the clinicians felt would be their base of support, the subjects were scored a 'no' on this item. Our results from the regression models showed that using a correct leading handgrip (item 9) can lower shoulder resultant moment ($B=-9.91$, $p=.23$) and rate of rise of elbow moment ($B=-10.38$, $p=.04$) on the trailing (right) side and lower the rate of rise of the shoulder and elbow resultant moments on the leading (left) side ($B=-1.39$ and -4.74 , $p=.20$ and $.14$) (Table 5). Because this item combines multiple aspects of handgrips it's difficult to know exactly which attribute (e.g. type of finger grip or hand placement within the base of support) is more responsible for the kinetic outcomes. The rate of rise of the wrist resultant moment increased with better handgrip ($B=7.51$, $p=.09$) which may be associated with the types of handgrips used by the subjects which were not explicitly documented in this study. Future research should be done to investigate the impact that different types of handgrips used in transfers have on the upper limb joint forces and moments.

Wheelchair users who use the head-hips technique appropriately (item 12) experienced lesser rate of rise of moment on the leading (left) shoulder ($B=-.81$, $p=.05$) (Table 5). This technique has been associated with an increase in trunk forward flexion and a shift of the trunk center of mass forward and downward to create a moment which can facilitate lifting the buttocks during the transfer (Allison, Singer, & Marshall, 1996). As with setting up the wheelchair angle appropriately, the increased trunk pivot motions may have helped to reduce the rate of rise of resultant shoulder moment.

Wheelchair users with proper overall transfer skills (higher part 1 summary scores) were more likely to experience lower moments on the trailing (right) elbow ($B=-5.86$, $p<.01$) and lower rate of rise of resultant moment on the leading (left) elbow ($B=-1.13$, $p<.01$) but increased extension shoulder moment on the leading (left) side ($B=1.94$, $p=.03$) (Table 6). Shoulder and elbow movements are related to each other in a close chain activity (Marciello et al., 1995). As observed with the individual TAI items using good skills can shift loading off of one joint onto another or from one arm to the other. Offloading the elbows and loading the shoulders more may make for a more efficient transfer particularly for individuals who lack elbow extension function. Although triceps muscle function can make a transfer easier (assist with lifting the buttocks off the surface) it is not a primary mover in transfers. The primary movers for transfers are the actions of the pectoralis major muscles, serratus anterior and latissimus dorsi muscle groups which are all attached to shoulder (Gagnon, Nadeau, Noreau, Dehail, & Pottie, 2008; Perry, Gronley, Newsam, Reyes, & Mulroy, 1996). The increasing extension shoulder moment may have resulted from the recruitment of the large primary movers, such as the latissimus dorsi and pectoralis major muscles (Gagnon, Koontz, Brindle, Boninger, & Cooper, 2009; Koontz,

Kankipati, et al., 2011) which can drive the movement and shift the body weight during transfers (Gagnon, Nadeau, Desjardins, & Noreau, 2008).

As noted in our regression models (Table 5 and Table 6), some transfer skills as measured by the TAI increased magnitudes and rates of rise of moments. Dashboard indicators were created to summarize and compare the magnitude effects of using certain transfer skills on the biomechanical variables, (please see Appendix B). By properly combining different transfer skills in tandem, the risks associated with secondary injuries can be minimized. For example, wheelchair users should angle their wheelchairs appropriately relative to the target surface (20-45 degrees) to reduce the large internal rotation shoulder moments on the leading side which can occur when using a proper leading handgrip. Using the head-hip technique (item 12 skill), can reduce the increasing rate of rise of leading shoulder moments which was also associated with close wheelchair positioning.

2.4.1 Study limitations

The small sample size may have negatively affected the power of the statistical analyses and response rate for some of the TAI items. For example not all of the items could be modeled because subjects were either too proficient on the item or the item did not apply to their transfer. Also because some of the items analyzed in this study may be related to some extent to each other, the collinearity of items may have an effect on the regression model results. In order to understand the interdependence between items selected in the study and find out the most important components in transfer skills, we performed a secondary analysis – principle component analysis (please see Appendix A). Then we further used regression models to understand the relationship between principle components and kinetic variables (please see

Appendix A). This study only analyzed transfers from a wheelchair to a level-height bench located on the subjects' left side and required them to use the wheelchair side grab bar for positioning of the trailing hand (Figure 1). Subjects were given time to acclimate to the setup prior to testing. Furthermore, a prior study found no differences in muscular demand based on which side (dominant or non-dominant) led the transfer or preferred direction of transfer (Gagnon, Koontz, Brindle, et al., 2009). Wheelchair users have to learn to be flexible with adapting to different setups when they transfer in public places where places to position their hands or the area to position their wheelchairs is limited. Future studies should consider the effects of skills on kinematic variables. Furthermore, the biomechanical effects of transfer training based on TAI principles should be investigated.

2.5 CONCLUSION

The study shows that the transfer skills that can be measured with the TAI are closely associated with the magnitude and timing of joint moments. Certain transfer skills helped to reduce the moments imparted on both upper limbs while other skills had the effects of increasing the magnitudes or rates loading on the leading limb. Different skills have different kinetic effects on the upper extremities (please see summary dashboard indicator in Appendix B). Taking into consideration the kinetic effects from all the transfer skills studied may help to reach better load-relieving effects on the upper extremities during transfers. The study provides insight into the impact that a specific skill can have on upper limb loading patterns. As such the TAI may be useful for measuring the effects of a training intervention on reducing upper limb joint loading.

2.6 ACKNOWLEDGEMENTS

This material is based upon work supported by the Department of Veterans Affairs (B7149I). The contents of this paper do not represent the views of the Department of Veterans Affairs or the United States Government.

3.0 THE UPPER LIMB BIOMECHANICAL EFFECTS OF COMPONENT TRANSFER SKILLS IN TWO DIFFERENT SETUPS OF TOILET TRANSFERS IN WHEELCHAIR USERS

3.1 INTRODUCTION

Wheelchair users depend on their arms to complete most of their daily activities, such as bed and toilet transfers. On average, they need to perform 15 to 20 transfers per day (Finley et al., 2005). Transfers are repetitive and high-loading activities (Gagnon, Nadeau, Noreau, Dehail, & Gravel, 2008; Gagnon, Nadeau, Noreau, Dehail, & Piotte, 2008). Throughout the transfer it is difficult for wheelchair users to avoid awkward arm positions, such as extreme shoulder internal rotation with abduction (Finley et al., 2005; Gagnon et al., 2003). The combination of high repetitions, high loading, and high risk arm positions can cause upper-extremity injuries and pain in this population. Specifically, transfers are one potential cause of rotator cuff injuries, elbow pain, and carpal tunnel syndrome (Boninger, Waters, et al., 2005; Curtis et al., 1995; Dalyan et al., 1999; Gellman et al., 1988; Nichols et al., 1979).

Pain and injury in wheelchair users can affect many aspects of their lives. The onset of upper-extremity pain and injuries may lead to social isolation, dependence, and high medical expenditures (Dalyan et al., 1999; Mortenson et al., 2012). Wheelchair users cannot rest or wait for injuries to fully recover without affecting their abilities to remain independent (Goldstein et

al., 1997). Therefore, injury prevention is very important for this population. Appropriate and correct transfer skills can help reduce the potential of injury during transfers by reducing upper-extremity loading and preventing awkward arm positions (Pynn et al., 2014; C.-Y. Tsai, N. S. Hogaboom, M. L. Boninger, & A. M. Koontz, 2014). However, nearly 50% of wheelchair users do not receive appropriate transfer skill training during rehabilitation in a hospital (Fliess-Douer et al., 2012). Clinicians need a standardized clinical approach for transfer skill evaluation and training that can prevent wheelchair users from secondary injuries.

The Transfer Assessment Instrument (TAI) is a clinical tool for clinicians to evaluate transfer skills. The items listed in the TAI evaluate the performance of different components of a transfer. The tool was developed based on clinical practice guidelines (Boninger, Waters, et al., 2005), current knowledge of the literature (Gagnon, Koontz, Mulroy, et al., 2009), and best clinical practice related to transfers. The TAI evaluation can be finished within 10 minutes and does not require specific testing equipment. The TAI contains two parts. Part 1 divides a transfer into 15 items which represent 15 component transfer skills, such as positioning wheelchair close to the target surface within 3 inches and correctly using handgrip during transfers. Part 2 evaluates the consistency of component skills and global performance of a transfer. The TAI yields high reliability among different raters of different clinical backgrounds and experience. It is unbiased towards subjects' physical characteristics, such as age, weight, and type of disabilities, that may influence transfers (Tsai et al., 2013). TAI also has good face, content, and construct validity (McClure et al., 2011; L. A. Rice et al., 2013). Each TAI item score and summary score are highly correlated with different biomechanical variables that are related to injury mechanisms in the upper extremities (Pynn et al., 2014; C. Y. Tsai, N. S. Hogaboom, M. L.

Boninger, & A. M. Koontz, 2014). Through using the TAI during evaluation, clinicians can objectively identify wheelchair users' transfer skills and quantify the quality of their transfers.

Toilet transfers present a unique set of challenges for wheelchair users. They often take place in small and constrained spaces limiting transfer preparation and wheelchair positioning options. The height of the toilet (43.18 to 48.26 cm or 17 to 19", ADA compliant ("Americans with Disabilities Act (ADA) - Accessibility Guidelines for Buildings and Facilities,") is lower than the average wheelchair and cushion height (55.88 cm or 22" (Toro et al., 2013)) and therefore requires non-level height transfers for most people. There may not be a good position for their hands or optimal use of a grab bar, as the bar may be outside of the wheelchair user's reach or too high to provide a mechanical advantage (Toro et al., 2013). All of these factors may make toilet transfers more strenuous.

To our knowledge there is no research addressing wheelchair users' transfer skill deficits and the impact of transfer skills on the biomechanics of toilet transfers. The goal of this study was to better understand wheelchair users' transfer skill deficits during self-selected transfers to two toilet positions and determine the impact of these transfer skills on upper-limb joint biomechanics during transfers for each toilet position.

The two toilet positions tested in this study were Americans with Disabilities Act (ADA) compliant ("Americans with Disabilities Act (ADA) - Accessibility Guidelines for Buildings and Facilities,") and included: one toilet position that required the wheelchair to be set up at the side of a toilet (a narrower angle of approach), and the other toilet position allowed the wheelchair to be set up in front of a toilet (a wider angle of approach) (Figure 3). We hypothesized that wheelchair users with overall good component transfer skills (higher TAI part 1 summary score) would have lower force and moment loading on the shoulders, elbows, and wrists on both sides

and for both wheelchair-toilet setups. Moreover, we expected to find that the types of component transfer skills (e.g. individual TAI item scores) associated with reduced loading would be the same between the two wheelchair-toilet setups. The results of this study will help to support the need for clinical transfer evaluation and training, and potentially identify the optimal bathroom setup needed for performing biomechanically safe toilet transfers.

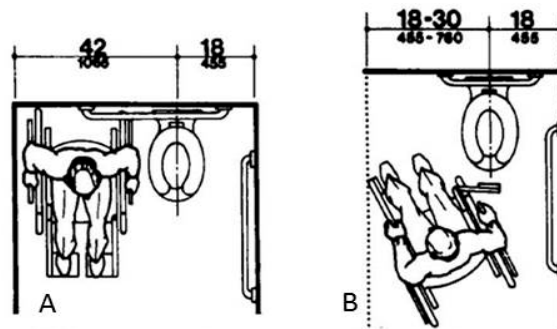


Figure 3. Two different wheelchair setups for toilet transfers suggested by Access Board: wheelchair setup at a side of a toilet (A) and in front of a toilet (B) ("Americans with Disabilities Act (ADA) - Accessibility Guidelines for Buildings and Facilities,")

3.2 METHODS

3.2.1 Subjects

The study was approved by the Department of Veterans Affairs Institutional Review Board. To be included, participants needed to be over the age of 18 years, at least one year post injury or diagnosis, use wheelchairs for the majority of mobility (40 hours/per work), and unable to stand

up without support. Participants with pressure sores, seizures, or angina within one year were excluded. All subjects provided informed consent before completing any study procedures.

3.2.2 Experimental protocol

Subjects first positioned their wheelchairs next to the toilet on the transfer station (Figure 4) (Koontz, Lin, et al., 2011). The station included three force plates (Berotec Corporation, Columbus, OH) located underneath the wheelchair, the toilet, and the subjects' feet, respectively. Two 6-component load cells (Model MC5 from AMTI, Watertown, MA; Model Omega 160 from ATI, Apex, NC) were attached to two steel beams used to simulate a wheelchair armrest and bathroom grab bar. Subjects were asked to naturally position and secure their wheelchairs in the 3*3 square-foot (91.44 cm by 91.44 cm) aluminum platform that covered the wheelchair force plate. They were also asked to choose where they wanted to position and secure the toilet on the other 3*4 square foot aluminum platform (91.44 cm by 121.92 cm) that covered the toilet force plate (Figure 4). The position and height (the height from center of the grab bar to the floor ranges from 24 inch to 28 inch (60.96 cm to 71.12 cm)) of the wheelchair grab bar was also adjusted based on the subjects' preferences. Reflective markers were placed on anatomical landmarks of the subjects' trunk and upper extremities (C.-Y. Tsai et al., 2014; Wu et al., 2005). A ten-camera three-dimensional motion capture system (Vicon, Centennial, CO) was used to collect the marker positions during the transfers. To mimic the side transfer setup of Figure 3, we oriented the toilet facing forward (Figure 5A). For the front setup, the orientation of the toilet was facing toward the wheelchair user (Figure 5B). The grab bar on the toilet side was only available for the side setup due to mounting limitations of the station. The toilet height is 18.5 inches (46.99 cm). The position of the grab bar was 18 inches (45.72 cm) away from the

centerline of the toilet and its height was 33 inches (83.82 cm). Both the toilet and grab bar setups meet ADA regulation ("Access Board, Figure 30b and 30c: Toilet Stalls, Alternate Stalls,").



Figure 4. The transfer station includes a 10-camera Vicon Nexus motion analysis system (Vicon, Centennial, CO) (A), three force plates under the wheelchair, subjects' feet, and the toilet (Bertec Corporation, Columbus, OH) (B), and two load cells (Model MC5 from AMTI, Watertown, MA; Model Omega 160 from ATI, Apex, NC) attached to the two grab bars respectively (C and D).

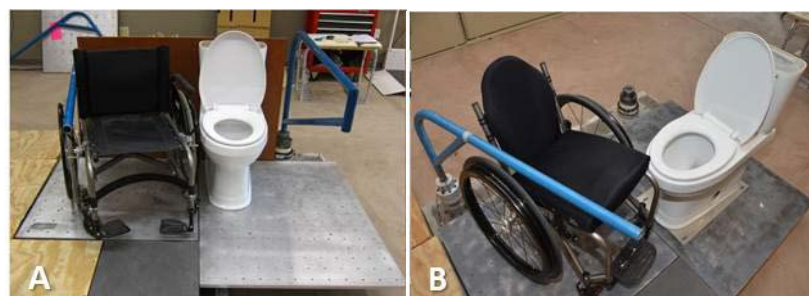


Figure 5. The orientation of the toilet in side (A) and front (B) setups in our transfer station

Subjects were first asked to sit with their arms in an anatomical neutral position to collect a static trial of the marker positions (C.-Y. Tsai et al., 2014). After that, subjects were asked to

perform a minimum of three and a maximum of five trials of toilet transfers in the two wheelchair-toilet setups respectively using their habitual technique – they could position their own wheelchair in any angle and distance they preferred between the wheelchair and toilet. The angle and distance they used were recorded. The angle was defined by the centerline of toilet and wheelchair seat (Figure 6). The recorded distance is the shortest distance between the wheelchair seat and toilet. In each trial, subjects needed to perform transfers from and to their wheelchairs. Transferring from one surface to the other was defined as one transfer. When subjects transferred from their wheelchair to the toilet, they needed to place their trailing (right) hand on the steel beam near the wheelchair (Figure 4C) so forces could be recorded. The order of transfer setup was randomized. Subjects were given at least 10 minutes to rest between the two wheelchair-toilet setups to prevent fatigue. When subjects performed transfers, the same two physical therapists observed and scored their transfer skills using the TAI. Both of the raters were trained to use the TAI before the study started. The TAI was completed after watching subjects perform a minimum of three to a maximum of five transfers from the wheelchair to the toilet in each wheelchair-toilet setup. After independently scoring each subject, the clinicians compared their findings. Any discrepancies in the scoring were discussed and a score reflecting the consensus decision was recorded. Kinetic data from all the force plates and load cells were collected at 1000 Hz for the duration of each transfer, while kinematic data were collected at 100 Hz.

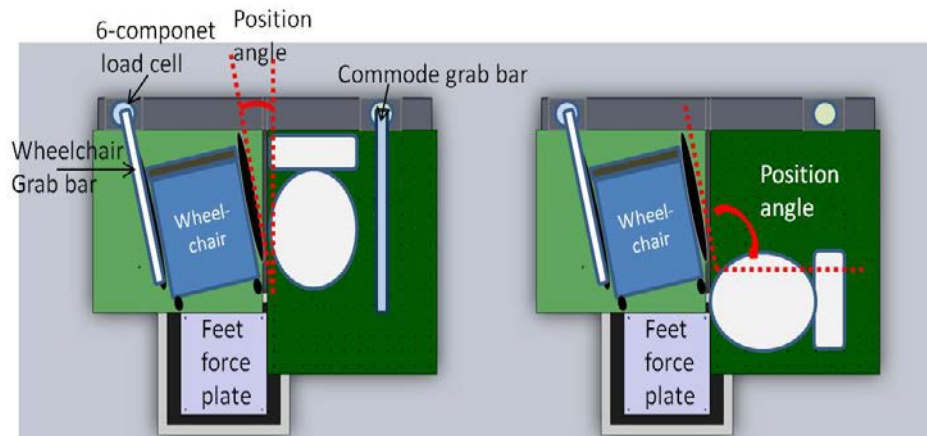


Figure 6. The definition of the position angle the study recorded

3.2.3 Data analysis

Biomechanical variables were computed using Matlab (Mathworks, Inc., Natick, MA, USA). A zero-lag low-pass 4th order Butterworth filter with a cut-off frequency of 7 and 5 Hz was used to filter the kinetic and kinematic data, respectively (Koontz, Kankipati, et al., 2011). A transfer was determined to begin when a vertical reaction force was detected by the load cell on the wheelchair side grab bar (Figure 4C) and ended before a landing spike was detected by the force plate underneath the bench (Kankipati et al., 2011). The end of the lift phase (and beginning of the descent phase) is defined by the highest elevated point of the trunk which is indicated by the peak of the C7 and T3 marker trajectories (Kankipati et al., 2011). Only the lift phase of the transfer from the wheelchair to the toilet was analyzed in the study. The kinematics of transfers was calculated based on the rotation sequences recommended by International Society of Biomechanics (Wu et al., 2005). The Euler angle sequences for shoulder, elbow, and wrist were YXY, ZXY, and ZXY, respectively (Wu et al., 2005). As for trunk, Cardan angle sequence, ZXY (Wu et al., 2005), was used with respect to the trunk coordinate system at initial trunk position.

Hanavan's model was used to calculate centers of mass and moments of inertia using the subjects' segment lengths and circumferences (Hanavan, 1964). The three-component forces and moments measured by the load cells and the force plates (Figure 4), marker data of the trunk and upper extremities, and the inertial properties of each body segment were inputs into an inverse dynamic model (Cooper et al., 1999). Each segment was assumed as a rigid body and linked together by ball and socket joints. The 3rd metacarpalphalangeal joint was assumed as the point of force application. The output of the inverse dynamic model included upper extremity net joint forces and moments.

The key kinetic dependent variables included maximum resultant forces and moments at the shoulders, elbows, and wrists and maximum shoulder posterior force and internal rotation and abduction moments on both sides. The resultant force on each joint is indicative of the total joint loading, while the resultant moment represents rotational demands associated with the muscle and external forces around the joint. Posterior shoulder forces were defined as the components of resultant shoulder force acting along the posterior axis of the shoulder. Each kinetic variable was normalized by body mass (Desroches et al., 2013; Gagnon, Koontz, Mulroy, et al., 2009; Gagnon, Nadeau, Noreau, Dehail, & Piotte, 2008). Several kinematic dependent variables on both sides were analyzed in the present study: maximum shoulder internal rotation, elevation, and plane of elevation angles, minimum shoulder plane of elevation angle (Figure 7), maximum and minimum elbow flexion angles, and maximum wrist extension angle on the both arms. These kinetic and kinematic variables were selected because they have been linked to shoulder pain, such as rotator cuff tears, median nerve function, elbow pain, and other upper extremity injuries (Boninger, Impink, Cooper, & Koontz, 2004; Boninger, Koontz, et al., 2005; Boninger, Waters, et al., 2005; Finley & Rodgers, 2004; Gagnon, Koontz, Mulroy, et al., 2009;

Gagnon, Nadeau, Noreau, Eng, et al., 2008; Keeley et al., 2012; Meislin et al., 2005; Mercer et al., 2006; I. M. Rice et al., 2013). Maximum trunk flexion angle, flexion/extension range of motion (ROM), and right/left side bending ROM were also included to identify the use of head-hips techniques (Allison et al., 1996; Gagnon, Nadeau, Noreau, Eng, et al., 2008). All of the kinetic and kinematic variables were averaged over a minimum of three and a maximum of five trials.

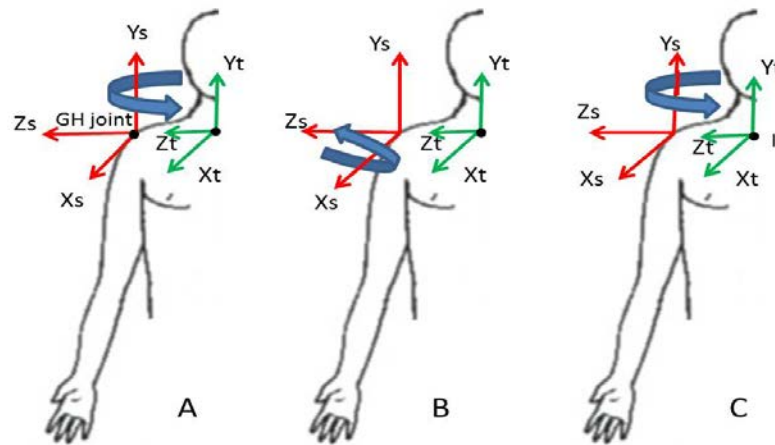


Figure 7. Figure 2: Anatomical (zero) position and shoulder angle orientation relative to trunk coordinate system: A, plane of elevation; B, negative elevation; C, internal rotation (Wu et al., 2005).

Abbreviation: GH joint, glenohumeral joint; IJ, incisura jugularis; Xs, Ys, Zs, shoulder local coordinate system; Xt, Yt, Zt, trunk local coordinate system

The 15 items in part 1 of the TAI are scored “Yes” (1 point) if the subject performs the specified skill correctly, “No” (0 points) if the subject performs the skill incorrectly, or not applicable “(N/A)” if the item does not apply to the individual (McClure et al., 2011). The 15 items in the TAI include three aspects of transfer skills: transfer preparation, conservation techniques, and the smoothness of transfers (McClure et al., 2011). The 12 items in part 2 of the TAI are scored on a Likert Scale ranging from 0 to 4. A ‘0’ means strongly disagree, and ‘4’ means strongly agree. The items in part 2 are completed after all transfers trials have been

performed. This study focused on analyzing the biomechanical effects of preparation and conservation techniques (items on part 1 of the TAI without item 11, 14, and 15) which can be easily learned and adjusted (smoothness of transfers may be influenced by balance control, type of injuries, and muscle strength). Part 2 of the TAI was not analyzed because it encompasses some of the same transfer skills (items) that are measured by the part 1 of the TAI (McClure et al., 2011).

3.2.4 Statistical analysis

The failure rates of individual items in part 1 were calculated by taking the number of subjects who scored a “No” on each item and dividing by the total number of subjects who were applicable for that item. Descriptive statistics (means and standard deviations) were calculated and reported for each biomechanical variable and part 1 summary score. Point-biserial correlations were conducted between TAI part 1 items. Among the items that were highly correlated ($r > 0.80$) with each other in item score, one was selected for further analysis.

All of the kinematic and kinetic variables and part 1 summary scores were examined for normality using the Shapiro-Wilk test. Wilcoxon signed-rank test was used to test the differences of TAI part 1 summary scores between side and front setups. Spearman’s correlation tests (because some variables were non-normally distributed) between part 1 summary scores and kinematic and kinetic variables were conducted to identify the relationships in both toilet transfer setups. Multivariate analysis of variance (MANOVA) models were built to test whether there were biomechanical differences between those who did and did not complete the skill. The independent variable in each model was each Part 1 item score (complete the skill = 1, did not complete the skill = 0). The dependent variables were either the kinematic or kinetic variables.

Five MANOVA models for each item were built in the study: item score with trailing (right) kinetic and kinematic variables respectively, item score with leading (left) kinetic and kinematic variables respectively, and item score with trunk kinematic variables. Following a significant MANOVA, an individual univariate ANOVA for each dependent variable was used. The level of significance was set at 0.05. The effect size (Cohen's *d*) for the magnitude difference in each biomechanical variable between using-skill and non-using-skill group was also calculated. Small effect size in Cohen's *d* is 0.2, medium effect size is 0.5, and large effect size is 0.8 (Cohen, 1992). All the statistical analyses were performed in SPSS (SPSS Inc., Chicago, IL).

3.3 RESULTS

3.3.1 Participants

Twenty-three men and three women volunteered to participate in this study. Table 7 shows summary demographic information. Twenty subjects had a spinal cord injury (SCI); sixteen subjects with SCI reported their injuries as complete and four reported theirs as incomplete (three with American Spinal Injury Association (ASIA) Grade B and one with ASIA Grade C). Three of these subjects had quadriplegia (C4 to C6), nine had high paraplegia (T2 to T7), and eight had low paraplegia (T8 to L3) (John et al., 2010). The remaining six participants without SCI had bilateral tibial and fibular fractures with nerve damage (n=1), double above knee amputation (n=1), muscular dystrophy (n=1), osteogenesis imperfecta (n=1), myelopathy (n=1), and spinal bifida (n=1).

The average height (\pm SD) of our subjects' wheelchair seat plus cushion was 21.53 (\pm 1.05) inches. Five out of twenty-six subjects used the grab bar for the side wheelchair-toilet setup. The rest of the subjects positioned their leading hand on the toilet rim. As for the front wheelchair-toilet setup, all subjects positioned their leading hand on the toilet rim, except one subject positioned the leading hand on the toilet lid during transfers.

Table 7. Participants' demographic information

Subjects, n= 26	Mean \pm standard deviation (range)
Age (years)	37.62 \pm 11.29 (19.00 – 55.00)
Height (meters)	1.66 \pm 0.23 (0.99 (DA) – 2.03)
Weight (kilograms)	67.55 \pm 19.26 (29.96 – 98.15)
Body mass index (kg/m ²)	25.07 \pm 9.51 (15.05 – 65.47 (DA))
Average duration of using a wheelchair (years)	13.47 \pm 8.47 (1.00 – 27.25)
Note: abbreviation: DA, double above knee amputation	

3.3.2 The biomechanical effects of overall transfer skills

The mean and standard deviation (SD) of the selected kinetic and kinematic variables for both the wheelchair-toilet setup are listed in Table 8 and Table 9 respectively. Of note, the maximum shoulder, elbow, and wrist resultant forces on the leading side were larger than the trailing side in both wheelchair-toilet setups.

The Spearman's correlation coefficients between selected kinetic and kinematic variables and part 1 summary score are shown in Table 8 and Table 9. Higher part 1 summary scores

(better transfers) in the side setup were associated with lower maximum resultant forces on the trailing shoulder, elbow, and wrist, lower posterior forces on both shoulders, and lower resultant moment on both elbows and trailing wrist. Better overall transfer skill in the side setup was also associated with higher shoulder plane of elevation angles and lower shoulder elevation angles on the leading side. For the front toilet setup, better transfer skills were related to lower maximum shoulder posterior force and elbow resultant moment on the trailing side and lower shoulder abduction moment on the leading side.

Table 8. The values (\pm standard deviation, SD) of maximum kinetic variables and Spearman's correlation coefficients (r) between kinetic variables and P1 summary score in the two setups of toilet transfers. The table shows the significant correlation coefficients.

		Wheelchair setup at a side of a toilet		Wheelchair setup in front of a toilet	
Maximum kinetic variables (\pm SD)		Value	r with P1	Value	r with P1
	Resultant force (N/Kg)	4.52 \pm 1.06	r = -0.52	4.35 \pm 1.15	
Trailing	Resultant moment (Nm/Kg)	1.01 \pm .29		1.26 \pm 1.86	
(right)	Posterior force (N/Kg)	3.53 \pm .89	r = -0.43	2.82 \pm .97	r = -0.47
shoulder	Internal rotation moment (Nm/Kg)	.01 \pm .08		.06 \pm .13	
	Abduction moment (Nm/Kg)	.32 \pm .26		.38 \pm .22	
Trailing	Resultant force (N/Kg)	4.32 \pm 1.01	r = -0.54	4.12 \pm 1.14	
(right)	Resultant moment (Nm/Kg)	.64 \pm .20	r = -0.68	.56 \pm .22	r = -0.40
elbow					

Table 8 (continued)

Trailing	Resultant force (N/Kg)	4.25±.99	r= -0.54	4.05±1.14	
(right)					
wrist	Resultant moment (Nm/Kg)	.37±.08	r= -0.40	.34±.09	
	Resultant force (N/Kg)	5.05±1.59		4.45±.93	
Leading	Resultant moment (Nm/Kg)	1.39±.78		1.00±.29	
(left)	Posterior force (N/Kg)	3.37±1.34	r= -0.64	3.26±1.06	
shoulder	Internal rotation moment (Nm/Kg)	.16±.73		.03±.16	
	Abduction moment (Nm/Kg)	.40±.18		.37±.18	r= -0.57
Leading	Resultant force (N/Kg)	4.98±1.64		4.43±.98	
(left)					
elbow	Resultant moment (Nm/Kg)	.48±.25	r= -0.67	.41±.29	
Leading	Resultant force (N/Kg)	4.96±1.66		4.43±.99	
(left)					
wrist	Resultant moment (Nm/Kg)	.33±.14		.34±.10	

Table 9. The values (\pm standard deviation, SD) of maximum kinematic variables and Spearman's correlation coefficients (r) between kinematic variables and P1 summary score in the two setups of toilet transfers. The table shows the significant correlation coefficients.

	Wheelchair setup at a side of a toilet	r with P1	Wheelchair setup in front of a toilet	r with P1
Kinematic variables (\pm SD, degree)	Value		Value	

Table 9 (continued)

Trailing (right) shoulder	Maximum internal rotation	61.42±9.34		62.82±7.57
	Maximum elevation	35.78±15.21		43.06±19.39
	Maximum plane of elevation	10.62±13.85		14.09±18.40
	Minimum plane of elevation	-10.72±17.46		-9.94±18.46
Trailing (right) elbow	Minimum flexion	30.08±13.01		41.03±13.88
	Maximum flexion	65.55±18.38		74.85±16.65
Trailing (right) wrist	Maximum extension	59.54±18.21		63.57±17.88
Leading (left) shoulder	Maximum internal rotation	55.31±10.33		61.15±13.31
	Maximum elevation	55.31±19.91	r= -0.46	59.06±17.24
	Maximum plane of elevation	27.94±24.29	r= 0.72	40.24±27.56
	Minimum plane of elevation	-2.28±25.15	r= 0.62	0.99±20.30
Leading (left) elbow	Minimum flexion	17.81±9.77		18.47±11.99
	Maximum flexion	39.32±12.25		43.43±15.53
Leading (left) wrist	Maximum extension	63.44±20.51		71.70±14.58
Trunk	Maximum flexion	23.12±8.76		25.00±11.14
	Flexion/extension ROM	24.26±7.97		25.84±9.58

Table 9 (continued)

Right/Left side bending ROM	19.65±7.12	22.13±6.71
-----------------------------	------------	------------

3.3.3 Deficits in component skills

Table 10 shows all of the items in the part 1 of the TAI. In this study, we analyzed items 1, 2, 6, 7, 8, 9, and 12 in part 1 of the TAI. Items 11, 14, and 15 in part 1 of the TAI were not included in the study because they are used to evaluate the smoothness of a transfer and a dependent transfer. Items 3 and 7 were highly correlated ($r = 1$). Only item 7 was modeled because it can be applied to both manual and power wheelchair users, whereas item 3 only applies to manual wheelchair users. Items 8 and 13 were also highly correlated ($r = 1$). Item 8 was selected because studies have shown that the hand positioning has biomechanical effects on upper extremity loading (Kankipati, 2012; Koontz, Kankipati, et al., 2011). Some subjects' wheelchairs had no armrests or the armrests were fixed so item 4 was not analyzed (more than 40% response rate in "N/A"). Because of the study setup, item 5 and 10 were not applicable items and not analyzed.

Table 10. The items in part 1 of the TAI

Items in part 1 of the TAI

1. * The subject's wheelchair is within 3 inches of the object to which he is transferring on to.
2. * The angle between the subject's wheelchair and the surface to which he is transferring is approximately 20-45 degrees.
3. The subject attempts to position his chair to perform the transfer forward of the rear wheel (i.e., subject does not transfer over the rear wheel).

Table 10 (continued)

4. If possible, the subject removes his armrest or attempts to take it out of the way.
5. The subject performs a level or downhill transfer, whenever possible.
6. * The subject places his feet in a stable position (on the floor if possible) before the transfer.
7. * The subject scoots to the front edge of the wheelchair seat before he transfers (i.e., moves his buttocks to the front 2/3rds of the seat).
8. * Hands are in a stable position prior to the start of the transfer.
9. * A handgrip is utilized correctly by the leading arm (when the handgrip is in the individual's base of support).
10. A handgrip is utilized correctly by the trailing arm (when the handgrip is in the individual's base of support).
11. Flight is well controlled.
12. * Head-hip relationship is used.
13. The lead arm is correctly positioned (The arm should not be extremely internally rotated and should be abducted 30-45 deg.)
14. The landing phase of the transfer is smooth and well controlled (i.e., hands are not flying off the support surface and the subject is sitting safely on the target surface.)
15. If an assistant is helping, the assistant supports the subject's arms during the transfer.

Note: *, the items we selected to analyze.

For the wheelchair setup at the side of the toilet (Figure 5A), the failure rates of all items (component skills) we analyzed ranged from 19 to 69% (Table 11). The average distance and

angle between the wheelchair and toilet our subjects used were 4.52 (± 2.22) inches and 21.52 (± 13.21) degrees.

In the setup where the wheelchair was in front of the toilet (Figure 5B), the failure rates of the items we analyzed ranged from 4 to 60% (Table 11). Item 2 was not applicable (N/A) in the wheelchair setup in front of the toilet because the angle between the wheelchair and toilet in the front setup was always larger than 30 degrees. The average distance and angle between the wheelchair and toilet our subjects used in the front setup were 5.55 (± 3.31) inch and 107.25 (± 8.39) degree.

A 20% or higher failure rate for wheelchair mobility skills has been used to identify skills to emphasize during training (Hosseini, Oyster, Kirby, Harrington, & Boninger, 2012). Comparatively, more than 20% of our subjects failed to complete five component transfer skills in the side setup compared to three skills in the front setup. Items 1, 6, and 12 had more than a 20% failure rate in both toilet setups. Part 1 summary scores were lower for the transfers in the side setup compared to the front setup although the difference was not significant ($p = .11$).

Table 11. The number of people (% failure rate) who scored No (0 point) in the selected TAI items respectively and average P1 summary score (\pm SD) in both wheelchair-toilet setups

TAI items	1	2	6	7	8	9	12	P1 summary
0 point in								
Wheelchair setup at a side of the toilet	18 (69%)	13 (50%)	10 (43%)	5* (19%)	8* (31%)	5* (19%)	15* (58%)	6.99 (± 1.77)

Table 11 (continued)

0 point in								
Wheelchair	14*		8	4	1	1	15	7.83
setup in front	(56%)	N/A	(36%)	(16%)	(4%)	(4%)	(60%)	(±1.25)
of the toilet								

Note: *, the items that resulted in significant differences in the biomechanics between people who did and did not do the skill correctly (see next section); N/A, not applicable

3.3.4 The biomechanical effects of specific component transfer skills for the side setup

Wheelchair users who performed items 7, 8, 9, and 12 skills correctly in toilet transfers with a side setup had significant differences ($p < 0.05$) in kinetic and kinematic variables on their upper arms and trunk compared to people did not perform these skills correctly (Table 12, Table 13, Table 14, and Table 15). When wheelchair users scooted forward to the front edge of the wheelchair seat before performing toilet transfers in the side setup, (item 7 skill), they had a larger maximum plane of elevation (effect size = 1.17) and less shoulder maximum elevation angle (effect size = 1.33) (Table 12) on their leading (left) arm.

Positioning hands in a stable and close position before transfers, TAI item 8 skill, helped wheelchair users to reduce maximum shoulder resultant and internal rotation moments and maximum elbow resultant moment (46%, 112 %, and 53% lower than without using the skill, effect sizes were 1.14, 0.88, and 2.08 respectively), but increased maximum shoulder posterior force and wrist resultant moment in the leading (left) arm (137% and 86% higher than without using the skill, effect sizes were 3.20 and 1.46 respectively) (Table 13). It also helped decrease

trunk side bending ROM and move the leading (left) shoulder plane of elevation closer to the scapular plane, but increased leading (left) wrist extension angle (Table 13).

When wheelchair users used a correct leading handgrip during toilet transfers with a side setup, TAI item 9, they had less maximum shoulder resultant force and posterior force (20% and 28% lower than without using the skill), elbow resultant force and moment (21% and 25% lower than without using the skill), and wrist resultant force (21% lower than without using the skill) on the trailing (right) side, and less maximum shoulder and elbow resultant moment on the leading (left) side (41% and 49% lower than without using the skill) (Table 14). People who used this skill also had less trunk side bending ROM and leading (left) shoulder maximum elevation angle (effect sizes were 1.18 and 1.34). However, when wheelchair users used a proper leading handgrip, they also increased maximum trailing (right) shoulder abduction moment (236% higher than without using the skill but small magnitude), leading (left) shoulder posterior force (124% higher than without using the skill) and internal rotation angle, leading (left) wrist resultant moment (147% higher than without using the skill) and extension angle, and trunk flexion ROM (effect sizes ranged from 1.20 to 2.32) (Table 14).

Using the head-hip relationship technique in toilet transfers with a side setup (item 12) resulted in lower maximum trailing (right) shoulder internal rotation moment (effect size=1.06) (Table 15).

Table 12. The biomechanical effects of item 7 in a wheelchair setup at a side of a toilet

Wheelchair setup at a side of a toilet				
Item	Sig. variables, p value for univariate ANOVA	Use the skill Value ± SD	Not use Value ± SD	MANOVA

Table 12 (continued)

7. The subject scoots to the front edge of the wheelchair seat before he transfers (Failure rate: 19%)	Leading (left) shoulder max. plane of elevation (°), P=.03	32.84±22.84 (Cohen's d=1.17)	7.35±20.61	Sig. group differences in leading (left) kinematic variables, F(7,18)=4.79, P < .01
	Leading (left) shoulder max. elevation angle (°), P=.02	51.11±19.11 (Cohen's d=1.33)	72.93±13.04	

Table 13. The biomechanical effects of item 8 in a wheelchair setup at a side of a toilet

Wheelchair setup at a side of a toilet				
Item	Sig. variables, p value for univariate ANOVA	Use the skill Value ± SD	Not use Value ± SD	MANOVA
8. Hands are in a stable position prior to the start of the transfer. (Failure rate: 31%)	Leading (left) shoulder max. resultant moment (Nm/Kg), P<.01	1.10±.27 (Cohen's d=1.14)	2.04±1.13	Sig. group differences in leading (left) kinetic variables, F(9,16)=13.42
	Leading (left) shoulder max. posterior force (N/Kg), P<.01	4.10±.79 (Cohen's d=3.20)	1.73±.69	

Table 13 (continued)

	Leading (left) shoulder			P < .01
	max. internal rotation	-.08±.09	.67±1.20	
	moment (Nm/Kg), P=.01	(Cohen's d=0.88)		
	Leading (left) elbow			
	max. resultant moment	.36±.10	.77±.26	
	(Nm/Kg), P<.01	(Cohen's d=2.08)		
	Leading (left) wrist max.			
	resultant moment	.39±.09	.21±.15	
	(Nm/Kg), P<.01	(Cohen's d=1.46)		
8. Hands are in a				Sig. group
stable position				differences in
prior to the start	Trunk side bending	17.23±5.61	25.10±7.47	trunk
of the transfer.	ROM (°), P=.01	(Cohen's d=1.19)		kinematic
(Failure rate:				variables,
31%)				F(3,22)=3.46,
				P=.03
8. Hands are in a	Leading (left) shoulder			Sig. group
stable position	max. plane of elevation	37.06±22.54	7.43±13.41	differences in
prior to the start	angle (°), P<.01	(Cohen's d=1.6)		leading (left)
of the transfer.	Leading (left) shoulder			kinematic
(Failure rate:	min. plane of elevation	7.91±22.20	-25.21±13.91	variables,
31%)	angle (°), P<.01	(Cohen's d=1.79)		F(7,18)=8.59,
	Leading (left) wrist max.	70.95±17.36	46.54±17.28	P<.01

Table 13 (continued)

extension angle (°), P<.01	(Cohen's d=1.41)
-------------------------------	------------------

Table 14. The biomechanical effects of item 9 in a wheelchair setup at a side of a toilet

Wheelchair setup at a side of a toilet					
Item	Sig. variables, p value for univariate ANOVA	Use the skill Value ± SD	Not use Value ± SD	MANOVA	
9. A handgrip is utilized correctly by the leading arm (when the handgrip is in the individual's base of support) (Failure rate: 19%)	Trailing (right) shoulder resultant force (N/Kg), P=.04	4.32±1.08 (Cohen's d=1.37)	5.39±.25	Sig. group differences in trailing (right) kinetic variables, F(9,16)=3.80 P=.01	
	Trailing (right) shoulder posterior force (N/Kg), P<.01	3.29±.80 (Cohen's d=1.97)	4.55±.42		
	Trailing (right) shoulder abduction moment (Nm/Kg), P=.04	.37±.26 (Cohen's d=1.20)	.11±.16		
	Trailing (right) elbow resultant force (N/Kg), P=.03	4.11±1.01 (Cohen's d=1.46)	5.18±.23		
	Trailing (right) elbow resultant moment (Nm/Kg), P=.04	.60±.18 (Cohen's d=0.97)	.80±.23		
	Trailing (right) wrist resultant force (N/Kg), P=.03	4.05±1.00 (Cohen's d=1.46)	5.11±.24		
	Leading (left) shoulder	1.22±.61	2.08±1.09		Sig. group

Table 14 (continued)

utilized	resultant moment (Nm/Kg),	(Cohen's d=0.97)		differences in
correctly by the	P=.02			leading (left)
leading arm	Leading (left) shoulder	3.77±1.13		kinetic
(when the	posterior force (N/Kg), P<.01	(Cohen's d=2.26)	1.68±.66	variables,
handgrip is in	Leading (left) elbow resultant	.41±.18		F(9, 16)=5.63
the individual's	moment (Nm/Kg), P<.01	(Cohen's d=1.79)	.81±.26	P<.01
base of support)	Leading (left) wrist resultant	.37±.12		
(Failure rate:	moment (Nm/Kg), P<.01	(Cohen's d=2.32)	.15±.06	
19%)				
<hr/>				
9. A handgrip is				
utilized				Sig. group
correctly by the	Trunk flexion/extension	25.85±7.77		differences in
leading arm	ROM, P=.03	(Cohen's d=1.26)	17.59±5.08	trunk
(when the				kinematic
handgrip is in				variables,
the individual's				F(3, 22)=3.36
base of support)	Trunk side bending ROM (°),	18.19±6.62		P=.04
(Failure rate:	P=.03	(Cohen's d=1.18)	25.80±6.26	
19%)				
<hr/>				
9. A handgrip is	Leading (left) shoulder max.			Sig. group
utilized	internal rotation angle (°),	57.39±10.37		differences in
correctly by the	P=.03	(Cohen's d=1.40)	46.58±3.40	leading (left)

Table 14 (continued)

leading arm				kinematic
(when the	Leading (left) shoulder max.	51.00±18.79		variables,
handgrip is in	elevation angle (°), P=.02	(Cohen's d=1.34)	73.40±14.34	F(7, 18)=3.97
the individual's				P=.01
base of support)				
(Failure rate:	Leading (left) wrist max.	67.95±19.05		
19%)	extension angle (°), P=.02	(Cohen's d=1.33)	44.50±16.07	

Table 15. The biomechanical effects of item 12 in a wheelchair setup at a side of a toilet

Wheelchair setup at a side of a toilet				
Item	Sig. variables, p value for univariate ANOVA	Use the skill Value ± SD	Not use Value ± SD	MANOVA
12. Head-hip relationship is used (Failure rate: 58%)	Trailing (right) shoulder max. internal rotation moment (Nm/Kg), P=.01	-.03±.08 (Cohen's d=1.06)	.05±.07	Sig. group differences in trailing (right) kinetic variables, F(9,16)=3.53 P=.01

3.3.5 The biomechanical effects of specific component transfer skills for the front setup

In toilet transfers with a front setup, only item 1 skill resulted in significant biomechanical differences on the trailing arm. Users who completed Item 1 correctly had significantly lower maximum shoulder, elbow, and wrist resultant forces (22%, 27%, and 23% lower than without using the skill respectively), and lower shoulder posterior force and abduction moment on their trailing (right) arm (28% and 43% lower than without using the skill) compared to people who didn't perform this skill correctly (effect sizes ranged from 0.99 to 1.19) (Table 16).

Table 16. The biomechanical effects of item 1 skill for the wheelchair setup in front of the toilet

Wheelchair setup in front of a toilet				
Item	Sig. variables, p value for univariate ANOVA	Use the skill Value \pm SD	Not use Value \pm SD	MANOVA
1. The subject's wheelchair is within 3 inches of the object to which he is transferring on to (Failure rate: 56%)	Trailing (right) shoulder max. resultant force (N/Kg), p=.02	3.76 \pm 1.16 (Cohen's d=0.99)	4.81 \pm .94	Sig. group differences in trailing (right) kinetic variables, F(9,15)=2.92 p=.03
	Trailing (right) shoulder max. posterior force (N/Kg), p=.02	2.31 \pm .94 (Cohen's d=1.03)	3.21 \pm .81	
	Trailing (right)	.27 \pm .13	.47 \pm .23	

Table 16 (continued)

shoulder max.	(Cohen's d=1.07)	
abduction moment		
(Nm/Kg), p=.02		
<hr/>		
Trailing (right)		
elbow max. resultant	3.34±1.17	4.58±.90
force (N/Kg), p=.02	(Cohen's d=1.19)	
<hr/>		
Trailing (right) wrist		
max. resultant force	3.46±1.17	4.51±.89
(N/Kg), p=0.02	(Cohen's d=1.01)	

3.4 DISCUSSION

This study aimed to describe and relate transfer skills assessed with the TAI to the biomechanics of transferring in two different wheelchair-toilet positions. Consistent with our hypothesis, higher quality transfers skills overall (higher part 1 summary scores) were highly associated with lower force and moment loading on both upper limbs in both toilet transfer setups (Table 8). During toilet transfers with the side wheelchair-toilet setup (Table 9), higher quality transfers were also associated with better leading shoulder positions, such as lesser shoulder elevation and a larger shoulder plane of elevation (Boninger, Waters, et al., 2005; Gagnon, Koontz, Mulroy, et al., 2009; Giphart et al., 2013). Also in the front wheelchair-toilet setup individuals performed better quality transfers and had lower failure rates on items that related to hand placement and handgrip.

TAI scores differed between the different wheelchair-toilet setups (Table 11). The TAI summary score is higher in the front setup (7.83) than the side setup (6.99). The built environment will affect the component transfers skills required to complete a good quality of toilet transfer. When the built environment requires an individual to set up their wheelchairs at the side of a toilet, more than 20% of them were unaware that they needed to: position their wheelchair within three inches (item 1) with 20 to 45 degree angle (item 2) between the wheelchair and transfer target; put feet on the floor (item 6), put their leading hand in a close and stable position (item 8) with correct handgrip (item 9); and use head-hip relationship technique (item 12). In the front toilet setup, wheelchair users didn't notice that they should position their wheelchair within three inches and feet on the floor (item 1 and 6) and use head-hip relationship technique (item 12). We saw a high failure rate of greater than 20% in more than half of the component transfer skills we analyzed (five out of seven in side setup and three out of six in the front setup (Table 11). The side setup in toilet transfers seemed to cause more skill deficits than the front setup. These results indicate that many wheelchair users lack knowledge of proper transfer component skills for toilet transfers.

In addition to toilet height the existence of grab bars in the built environment may have an adverse effect on the upper extremities. These bars, which may be helpful for people who perform stand and pivot transfers may actually be harmful for wheelchair users who perform sitting-pivot transfers. Some of our subjects' (5 out of 26 subjects (19%)) reached out to the grab bar near the toilet in the side setup (Figure 4-D). The position of the grab bar in our setup was in an ADA compliant position (18 inches away from the centerline of the toilet, Figure 4-D and Figure 4-A) ("Americans with Disabilities Act (ADA) - Accessibility Guidelines for Buildings and Facilities,"). Reaching out to the bar caused them to go outside of their base of support and

score a '0' on TAI items 8 and 9. The significant increase found in leading shoulder elevation angle (increase from 50° to 70°, large effect size) and resultant moment (about 70% increase, large effect size) (Table 13Table 14) in this study when people didn't use item 8 and 9 skills in the side setup further indicated the likelihood of adverse effects of the grab bar outside of wheelchair users' base of support. The increased shoulder elevation angle and resultant moment have been identified as important risk factors for shoulder injuries, such as shoulder impingement and rotator cuff tears (Boninger, Waters, et al., 2005; Gagnon, Koontz, Mulroy, et al., 2009). Our subjects didn't know that they should avoid the awkward shoulder position. These results further point to the need for transfer training to educate users on proper hand placement for toilet transfers.

When wheelchair users performed toilet transfers with a side setup, incorrect performance on items 7, 8, 9, and 12 skills caused significant biomechanical effects on the upper limbs and trunk. Scooting to the front edge of the seat before transfers (item 7) moved the plane of shoulder elevation from pure abduction (0 degree of plane of elevation) to the scapular plane (30 to 40 degrees of plane of elevation), while decreasing the elevation angle (Table 12). Shoulder impingement syndrome and rotator cuff injuries have been reported as major injuries for wheelchair users (Escobedo et al., 1997; Finley & Rodgers, 2004). Shoulder abduction and internal rotation angles have been identified as major factors to reducing the subacromial space and causing impingement (Minkel, 2000; Qi, Wakeling, Grange, & Ferguson-Pell, 2013). Smaller excursions of the humeral head are present during full range of motion exercise in scaption (shoulder elevation in scapular plane which is 30 to 40 degrees of plane of elevation (Reinold et al., 2007)) compared to abduction (Giphart et al., 2013); glenohumeral position is also more inferior in this position (Giphart et al., 2013). The approximate 30 degree change in

shoulder plane of elevation accomplished by completing the skill of scooting to the front of the seat may therefore lead to less humeral head movement and shear force in the shoulder joint protecting the shoulder from arthritis (Giphart et al., 2013; Hawkins & Angelo, 1990) and impingement.

Putting hands in a stable and close position before transfers (item 8) affected the leading arm and trunk biomechanics in the side-toilet transfer setup (Table 13). Positioning hands close to the body so there is just enough space for the buttocks to land can shorten shoulder moment arms; ultimately, accomplishment of this skill can reduce the moment loading on the leading side (Table 13) (Minkel et al., 2010). The maximum resultant moments on the leading shoulder and elbow in using the close hand positioning skill during transfers is about half as large as without using the skill (large effect size). The decrease in trunk side bending ROM (Table 13) may help wheelchair users keep their balance and stability during transfers, which is very important in maintaining movement quality and preventing falls (Minkel et al., 2010). The skill also facilitates movement of the shoulder plane of elevation from the coronal plane (around 0 degrees) to the scapular plane (30 degree) (Table 13). The humeral head movement is smaller in the scapular plane (Giphart et al., 2013). The small excursion of humeral head may reduce shoulder shear force and prevent narrowing of subacromial space, which may help prevent shoulder arthritis and impingement (Giphart et al., 2013). The close and stable hand positioning during transfers also produced larger shoulder posterior force, wrist resultant moments, and wrist extension angles (Table 13). These increased biomechanical responses on the leading side may have negative effects and may be related to the use of handgrip.

A correct use of the handgrip by the leading arm during toilet transfers with a side setup (item 9) affected the biomechanics of both arms and movement of the trunk (Table 14). In this

instance, “correct” use means that the fingers are allowed to drape over the edge of the toilet or grasp a grab bar or armrest within wheelchair users’ base of support during transfers. An appropriate handgrip on the leading side reduced the maximum resultant force and/or moment on the leading and trailing shoulders and elbows and the trailing wrist (Table 14). The skill also increased wheelchair users’ trunk flexion/extension ROM, decreased side bending ROM, and decreased leading shoulder elevation angle (Table 14). These findings support the clinical practice guidelines recommendations, which suggest that it is better for wheelchair users to use handgrips during transfers, not flat hands and closed-fists (Boninger, Waters, et al., 2005). The correct handgrip may reduce up to 49% of the shoulder and elbow loading on the both sides (Table 14) by providing more stability for transfers and facilitating the application of hand push/pull force compared to without using a correct handgrip (Boninger, Waters, et al., 2005). The stable handgrip may also provide wheelchair users more freedom to increase trunk flexion/extension movement but decrease side bending. The increased trunk flexion/extension movement when using correct leading handgrip (large effect size, Table 14) found by this study may place the wheelchair user’s center of mass close to the thighs; this would provide more stability and create enough momentum to help lift the buttocks and reduce loading on the upper limbs (Allison et al., 1996; Desroches et al., 2013).

As mentioned, the correct use of a leading handgrip led to mixed biomechanics findings in the side setup. For example, trunk flexion/extension ROM increased while the trunk side bending ROM decreased (Table 14), posterior shoulder force and wrist extension angle and resultant moment on the leading side also increased. These results may be explained in part by the leading hand being placed on the toilet rim which for most of the users in this study was lower than their wheelchair seat height. In transfers the arms and trunk form a closed kinetic

chain (Marciello et al., 1995). The increased trunk flexion combined with lower hand placement may cause the leading shoulder posterior force to increase (Gagnon, Nadeau, Noreau, Dehail, & Pottie, 2008). Positioning the hand close to the trunk and lower than wheelchair seat may also explain the increase in wrist extension angle and wrist moment (Gagnon, Nadeau, Noreau, Eng, & Gravel, 2009). The increased posterior forces, wrist resultant moment and extension angle on the leading side are potentially risk factors for secondary injuries, such as capsulitis, tendinitis, and carpal tunnel syndrome (Campbell & Koris, 1996; Keir et al., 1997; Sie et al., 1992).

Previous studies have shown that the head-hips relationship may help wheelchair users reduce superior shoulder force and recruit larger muscle groups around the shoulder for transfers, and increase shoulder external rotation moment (Finley et al., 2005; Koontz, Kankipati, et al., 2011). This technique is a rotational strategy wherein the center of mass of the trunk is moved forward and downward to create a momentum to lift up buttocks during transfers (Allison et al., 1996). As mentioned, the trunk and arms in transfers form a closed kinetic chain (Marciello et al., 1995). The trunk flexion movement with hands fixed on the transfer target and wheelchair may accompany shoulder external rotation movement. The shoulder external rotation movement may decrease shoulder internal rotation moment during transfers (Table 15). The decreased shoulder internal rotation moment may help to protect wheelchair users from shoulder impingement (Curtis et al., 1995; Escobedo et al., 1997).

The skill of positioning the wheelchair close to the toilet within three inches (item 1) showed significantly lower loading on the trailing (right in the study) side in toilet transfers with a front setup (up to 43% lower loading compared to without using this skill, large effect size, Table 16). These observations were in contrast to the component skills in the side transfer setup. Performing the skill correctly was associated with lower maximum shoulder resultant, posterior

force, and abduction moment, and elbow and wrist resultant forces on the trailing side (Table 16). Close positioning shortens the distance between the wheelchair and the toilet, combined with a lower seat height, may help wheelchair to reach the toilet rim easier. The trailing arm does not need to support the lift as much and control the body across the wheelchair-toilet gap.

We found that shoulder internal rotation moment was significantly decreased after using head-hip relationship skill (item 12) in toilet transfers with a side setup, but the magnitude of the internal rotation moment is about 0.05 N/Kg and the magnitude of moment change was less than 0.1 N*m/Kg between using-skill and non-using-skill groups (Table 15). Whereas all of other biomechanical values seem rather substantive (for example, the reduced magnitude of shoulder resultant force and posterior force on the trailing side were 1.07 and 1.26 N/Kg respectively after using correct handgrip skill, Table 14), and thus are more likely to have beneficial effects on the joints. There is a gap in research that would allow for us to directly link the change of magnitudes we found during transfers when using skills to clinically meaningful outcomes (e.g. how much decreased magnitude in biomechanical variables could reduce injury risk and pain or how much exact joint biomechanical loading would cause injuries). Considering the repetitive nature of transfers low reduced magnitudes may still be detrimental over the long term. Future longitudinal studies that assess the long-term outcomes of following or not following the techniques expressed in TAI could help to elucidate more clearly the impact that 'smaller' but statistically significant differences have on joint health.

The biomechanical effects for transferring to a toilet, which may have a lower seat height than the height of the wheelchair user's seat, may be opposite to those when transferring to a level- and high-target seat. In previous studies investigating level-height transfer biomechanics, wheelchair users have higher maximum hand and joint reaction force on the trailing side than the

leading side (Gagnon, Nadeau, Noreau, Dehail, & Gravel, 2008; C.-Y. Tsai et al., 2014). In a higher height transfer, vertical reaction force on the trailing hand and muscular activity of deltoid and pectoralis major muscles on the trailing side increases, while vertical reaction force on the leading hand slightly decrease (Gagnon, Nadeau, Noreau, Dehail, & Gravel, 2008; Gagnon, Nadeau, et al., 2009). The increased muscular demand on the trailing side in high-target transfers is to support the body weight and push the body to a high surface. However, toilets are usually lower than wheelchair seats so toilet transfers are one kind of low-target surface transfers (Toro et al., 2013). The results in this current study indicate that the leading arm sustained higher force loading than the trailing arm (Table 8). The trailing arm in low-target transfers doesn't need to push as much as in level- and high-surface transfers, but the leading arm may need to provide more effort to support the body weight and stabilize the lowering movement of the trunk compared to level-height transfers. Therefore, low-target transfers won't be easier than level-height transfers (Gagnon, Nadeau, et al., 2009). The results of the study are consistent with the suggestion in Clinical Practice Guideline - wheelchair users should perform level transfers whenever possible (Boninger, Waters, et al., 2005). In effect, transferring to and back from a toilet combines low- and high-target transfers which may increase the loading on both arms. An ADA compliant toilet (current compliant height is 17 to 19 inches) is low for most wheelchair users (who have a seat plus cushion height of about 22 inches (Toro et al., 2013)). Wheelchair users should consider using assistive technology, such as toilet seat riser, to make the toilet seat level in their home and or work environments.

In the toilet transfers with a side setup, four (items 7, 8, 9, and 12) transfer skills measured by the TAI had significant biomechanical effects (all have large effect sizes) in wheelchair users' arms and trunk movement suggesting that the correct use of certain component

skills may be protective when an individual is required to use the side approach. Dashboard indicators were created to summarize and compare the magnitude effects of using certain transfer skills on the biomechanical variables for the two toilet setups (please see Appendix B). Among the transfer skills we measured and analyzed, five skills (items 1, 2, 6, 8, and 12) had more than a 20% failure rate in the side setup. As for the toilet transfer with a front setup, just one transfer skill (item 1) measured by the TAI caused significant biomechanical effects on the wheelchair users' trailing side, and only three skills (item 1, 6, and 12) had more than 20% failure rate. The TAI part 1 summary score in the front setup was also higher than the side setup. These results indicated two issues. First, the grab bar and hand placement options in transfers may largely influence wheelchair users' transfer quality. The grab bar position in the side setup likely predisposed users to choosing a non-ideal hand placement that resulted in harmful biomechanics. Therefore it is important to train wheelchair users how to choose optimal hand placement during toilet transfer in different setups. Second, these findings may imply that a built environment that allows toilet transfers with a front setup may facilitate wheelchair users to perform better quality transfers. They can perform toilet transfers in a more intuitive way and put more attention on positioning their wheelchairs as close to the toilet as possible. The results were inconsistent with our hypothesis that different transfer setups may change the transfer skills needed to improve the quality of transfers. To facilitate wheelchair users to perform safer transfers, transfer skills training and, the design of spaces around a toilet and the grab bar placement in a restroom should be considered together.

3.4.1 Study limitations

The small sample size may have negatively affected the power of the statistical analyses and the response rate for some of the TAI items. Not all of the items could be analyzed to compare the biomechanical differences between using- and non-using skill groups; specifically, subjects were either too proficient on the item (most received a “Yes” response) or the item did not apply to their transfers (“N/A” response). An additional limitation was the transfer station setup. This study only analyzed the transfers from a wheelchair to a toilet located on the subjects’ left side and required the use of the wheelchair side grab bar for positioning of the trailing hand (Figure 2C). To correct for this, subjects were given time to acclimate to the setup prior to testing. Wheelchair users have to learn to be flexible with adapting to different setups when they transfer in public places where places to position their hands or the area to position their wheelchairs are limited. Future studies will investigate where the optimal hand position is and how to determine a good handgrip since hand positioning and handgrip use greatly influence transfer biomechanics. Different environmental settings may influence the use of transfer skills and the effects of skills. We may need to further investigate the effects and needs of transfer skills in different daily setups, such car and bed transfers. We also want to see whether transfer skill training based on TAI principles can help reduce upper extremity loading for different transfer types, such level-height and toilet transfers.

3.5 CONCLUSION

Using the TAI several transfer skill deficits were identified for wheelchair toilet transfers in two different simulated built environments that were also linked to potentially harmful biomechanics. Using good transfer skills has significant effects on reducing the loading on upper limbs in toilet transfers with both the side and front setups. The front wheelchair-toilet setup resulted in lower failed skill rates and the types of failed skills did not affect the biomechanics as much as the types of failed skills that occurred with the side wheelchair-toilet setup. In the front wheelchair-toilet setup, the component skill of close wheelchair positioning is important for lowering transfer loading. When the built environment requires a side wheelchair position, the most protective component skills are: scooting forward movement in the wheelchair seat, utilizing stable and close hand positioning, and utilizing correct handgrip and head-hips relationship technique (see Appendix B, dashboard indicator for a summary of the magnitude effects of using each skill on the biomechanical variables). Because of the intrinsic height difference in toilet transfers and the potentially harmful biomechanical effects concentrating on the leading side alternating the leading side (direction of transfer) should be done if the environment allows.

Clinical transfer training should emphasize different skills based on the toilet space setup and how to choose correct handgrip placement. When wheelchair users try to determine needs for home adaptations for toilet transfers, enabling the ability for front wheelchair positioning and facilitating good handgrip use should be planned. Public restrooms may consider adding space to permit front wheelchair positioning and preventing non-ideal grab bar setup, which may facilitate wheelchair users in performing better quality of transfers.

3.6 ACKNOWLEDGEMENTS

This material is based upon work supported by the Department of Veterans Affairs (B7149I). The contents of this paper do not represent the views of the Department of Veterans Affairs or the United States Government.

4.0 THE IMMEDIATE BIOMECHANICAL IMPLICATIONS OF A STRUCTURED COMPONENT SKILLS TRAINING ON INDEPENDENT WHEELCHAIR TRANSFERS

4.1 INTRODUCTION

Wheelchair transfers are one of the most essential wheelchair activities for wheelchair users (Fliess-Douer et al., 2012). A full time wheelchair user usually needs to perform 15 to 20 transfers each day (Finley et al., 2005). Performing transfers is mandatory for wheelchair users during functional activities, including bathing, hygiene, and driving. Good transfer capability can also increase wheelchair users' community participation and improve their social life (Mortenson et al., 2012). However, transfers are also one of the most strenuous wheelchair activities. The loading on wheelchair users' upper limbs during transfers are higher than other wheelchair activities such as weight relief and wheelchair propulsion (Gagnon, Nadeau, Noreau, Dehail, & Pottie, 2008; Van Drongelen et al., 2005). The high superior and posterior forces at the shoulders, a flexion, abduction, and internal rotation shoulder position, high superior elbow force, and high compression force on an extreme wrist extension angle during transfers have been implicated as risk factors for secondary injuries, such as shoulder impingement, elbow pain, and carpal tunnel syndrome (Boninger, Robertson, Wolff, & Cooper, 1996; Burnham & Steadward, 1994; Campbell & Koris, 1996; Cobb, An, & Cooney, 1995; Curtis et al., 1995; Dalyan et al., 1999; Escobedo et al., 1997; Gagnon, Koontz, Mulroy, et al., 2009; Gagnon,

Nadeau, Noreau, Dehail, & Piotte, 2008; Gellman et al., 1988; Goodman et al., 2001; Keir et al., 1997; Koontz, Kankipati, et al., 2011; Nichols et al., 1979; Pyo et al., 2010; Sie et al., 1992). 65% of individuals with spinal cord injuries (SCIs) are affected by pain when they perform transfers (Dalyan et al., 1999).

Injury prevention is very critical for wheelchair users to maintain quality of life. When daily activities cause pain, wheelchair users may start to withdraw from community participation, become dependent on others, functionally decline, and increase medical expenditures (Dalyan et al., 1999; Mortenson et al., 2012; Pentland & Twomey, 1994). Wheelchair users cannot wait for full recovery from injuries because of the constant demand of the activities of daily living (Pentland & Twomey, 1994).

A good clinical evaluation and training program can be an important first step for injury prevention. The Transfer Assessment Instrument (TAI) is the first clinical tool for clinicians to evaluate wheelchair users' transfer skills in a systematic and quantitative way (McClure et al., 2011). The items in the TAI were developed based on the clinical practice guidelines (Boninger, Waters, et al., 2005), current literature review (Gagnon, Koontz, Mulroy, et al., 2009), and the best clinical practice related to transfers. It only takes about 10 minutes to perform a transfer evaluation with the TAI, and the evaluation needs no extra testing equipment (McClure et al., 2011). The TAI has been proven to have an acceptable to high intra- and inter-rater reliability among raters with different clinical backgrounds; good content, face, and construct validity; and no bias for subjects' physical characteristics, such as age and weight (McClure et al., 2011; C.-Y. Tsai et al., 2014; Tsai et al., 2013). The TAI contains two parts. Part 1 divides a transfer into 15 items which represent 15 component transfer skills, such as positioning wheelchair close to the target surface within 3 inches and correctly using handgrip during transfers. Part 2 evaluate the

consistency of component skills and global performance of a transfer. About 50% of wheelchair users do not receive transfer skills training during their initial hospital stay (Fliess-Douer et al., 2012). Transfer training and evaluation has been largely subjective rather than scientific (Newton et al., 2002). Rice et al.'s recent study demonstrated the importance of a structured transfer education program and its long-term training effects for wheelchair users (L. A. Rice et al., 2013). The wheelchair users who received the strict protocol of transfer training in an inpatient rehabilitation stage had higher TAI scores, which means better transfer quality, compared to the standard care group after one year post discharge (L. A. Rice et al., 2013). However, no study has investigated whether a structured training program results in improved biomechanical effects on wheelchair users' upper limbs.

The component skills in the TAI have been linked with injury-related biomechanical variables (C.-Y. Tsai et al., 2014). Subjects with higher scores on component skills and higher overall summary scores showed reduced peak forces, moments, and impacts on the trailing side (ref chapter 2). However for some skills, leading side moments were higher for persons who performed the skill correctly compared to those who did not (C.-Y. Tsai et al., 2014). Previous studies have shown that the forces on trailing side are higher than leading side for sitting pivot transfers (Gagnon, Nadeau, Noreau, Dehail, & Gravel, 2008; C.-Y. Tsai et al., 2014). Seeing lower loading on the trailing side and higher loading on the leading side may indicate that using the skill helped to balance the loading across both upper extremities. In the prior study comparing taught techniques, it was observed that techniques that decreased trailing side forces and moments caused a shift towards increased forces and moments on the leading side and that keeping the hands close to the body potentially helped to minimize both trailing and leading side forces and moments (Kankipati, Boninger, Gagnon, Cooper, & Koontz, 2014).

The purpose of this study is to evaluate the immediate biomechanical effects of TAI-based structured transfer training on wheelchair users' shoulders, elbows, and wrists. Based on previous studies, we hypothesize that after the training program, wheelchair users will have reduced resultant joint forces and moments on both the leading and trailing arms and less shoulder internal rotation and elevation, and wrist extension angles during transfers compared to before training. Results of this study could help standardize and unify how transfers are being taught in the field and reduce the incidence of upper limb pain and injuries among wheelchair users who perform independent sitting pivot transfers.

4.2 METHODS

4.2.1 Subjects

The study was approved by the Department of Veterans Affairs Institutional Review Board. All of the participants provided informed consent before the test protocol started. The participants in this study needed to use wheelchairs for the majority of mobility (over 40 hours/week), could perform independent transfers without human assistance or using assistive devices, and were at least one year post injuries or diagnosis and over the age of 18 years. Participants who had pressure sores, seizures, and angina in the last year were excluded.

4.2.2 Experimental protocol

The study protocol includes two steps. Step 1 was baseline testing: our research clinicians evaluated and scored participants' transfer quality and collected their joint biomechanical information in their habitual transfers approach. Step 2 was follow-up testing: we recruited participants who performed low-quality transfers in step 1, provided structured transfer training to them, and then re-examined the biomechanics when they performed transfers using the taught techniques.

In step 1 protocol, participants' anthropometric measures were collected first, such as upper arm length and circumference, to determine the center of mass and moment of inertia for each segment (Hanavan, 1964). Subjects were asked to position themselves next to a bench at a height level with their own wheelchair seats and a regular toilet on a custom-built transfer station (Figure 8) (Koontz, Lin, et al., 2011). The transfer station contained three force plates (Bertec Corporation, Columbus, OH) underneath the wheelchair, the level bench (or toilet), and the participant's feet respectively. Two 6-component load cells (Model MC5 from AMTI, Watertown, MA; Model Omega 160 from ATI, Apex, NC) were attached to two steel beams used to simulate an armrest and grab bar (Figure 8A and B). Subjects were asked to naturally position and secure their wheelchairs in the 3x3 square foot (91.44 cm by 91.44 cm) aluminum platform that covered the wheelchair force plate. They were also asked to choose where they wanted to position and secure the bench (or the toilet) on the other 3x4 square foot aluminum platform (91.44 cm by 121.92 cm) that covered the bench force plate (Figure 8). The position of the simulated wheelchair armrest was also adjusted based on the participants' preference. Reflective markers were placed on subjects' heads, trunks, and upper extremities to build local coordinate systems (Wu et al., 2005) for each segment. Marker trajectories were collected at 100

Hz using a ten-camera three-dimensional motion capture system (Vicon, Centennial, CO.). Kinetic data from all the force plates and load cells were collected at 1000 Hz.

Then, participants were asked to perform up to five trials of level-height bench transfers and five trials of toilet transfers. In each trial, participants needed to perform transfers to and from their own wheelchairs in a natural way. Movement from one surface to the other (e.g. wheelchair to bench) was considered as one transfer. Participants were provided an opportunity to adjust their wheelchair position and familiarize themselves with the setup prior to data collection, and had time to rest in between trials. Additional rest was provided as needed. Subjects were asked to place their trailing arm (right arm) on the simulated armrest (Figure 8A) when they transferred to the bench (or toilet) on their left side so the reaction forces at the hand could be recorded. On the leading side (left), participants were free to place their hand on either the bench/toilet or the grab bar. During each trial, two study physical therapists independently observed and scored each participant's component transfer skills using the TAI. All of the participants in the study were evaluated by the same two physical therapists who were trained to use the TAI before the study started. The TAI was completed after watching participants perform three to five transfers from the wheelchair to the bench and to the toilet. After independently scoring each participant, the clinicians compared their findings. Any discrepancies in the scoring were discussed and a score reflecting the consensus decision for level-height bench and toilet transfers, respectively, was recorded.

If the participants' part 1 summary scores were lower than 7.36 in any of the transfers in the step 1 protocol, they were invited back for the step 2 visit within 4 weeks to undergo supervised and individualized training to improve their transfer techniques. The cutoff of the part 1 summary score, 7.36, was determined by the average part 1 summary scores (7.69 and 7.04) in

the previous two studies we conducted for testing TAI's psychometric properties (McClure et al., 2011; Tsai et al., 2013). A total of 81 participants in these two studies were recruited and the TAI was used to evaluate their component transfer skills on a self-selected mat table setup. We assumed that the average score represented the general population's component transfer skills. If our participants' part 1 summary scores were lower than 7.36, they may have poorer than average component transfer skills.

The training protocol in step 2 of the study followed motor learning theories with blocked practice (repeat practice of the same technique) and using knowledge of performance as feedback (McCullagh, Weiss, & Ross, 1989; I. Rice, Gagnon, Gallagher, & Boninger, 2010). In the follow-up visit, the study clinician observed the participants' first transfers using the TAI to affirm the problem(s) to be corrected. Afterwards the participants rested and received a one-on-one training. The clinician discussed advantages and perceived problems in the participants' component transfer skills and demonstrated how to modify them. The training instruction went through the description and demonstration of all the component transfer skills defined by the TAI first and then emphasized the participants' weaknesses based on the TAI evaluation results from the first testing session. Together the participants and clinician discussed new transfer strategies which matched their physical condition and the component transfer skills defined by the TAI. For example, in the training session, subjects and our clinician together adjusted the distance and angle between the wheelchair and transfer surface and found an appropriate handgrip position to determine a good transfer approach which followed the TAI guideline and could be comfortably used by the subject. We may have corrected a participant's wheelchair preparation for transfers (wheelchair approach angle and removing the armrest, item 2 and 4 in part 1 of TAI), lead arm position (item 13 in part 1), or use of a handgrip within the subject's base of support (item 9 in

part 1 of TAI). Then, the subject repeated practicing the new techniques in the same transfer setup (blocked practice) until familiar with them. In the first few practices, verbal feedback on the transfer performance was given immediately, such as scooting forward and using head-hip relationship more, and then was decreased later. The whole training session lasted about 45 minutes.

After the training session, participants followed the same protocol as before (step 1 of the study) in order to immediately retest their biomechanics during level-height bench transfers (5 trials in same visit). The TAI was also completed by one of the same physical therapists as step 1 during the follow-up biomechanical testing.

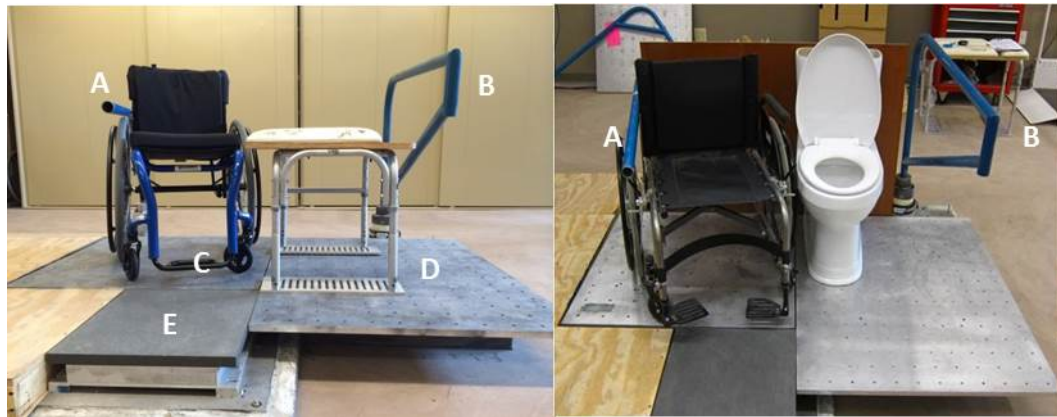


Figure 8. The study setup for level-height transfers (left) and toilet transfers (right). A, simulated wheelchair armrest; B, bench-side grab bar; C, wheelchair force plate; D, bench force plate; E, feet force plate

4.2.3 Data analysis

The biomechanical variables were computed using Matlab (Mathworks, Inc., Natick, MA, USA). A zero-lag low-pass 4th order Butterworth filter with cut-off frequency of 7 and 5 Hz was used to

filter the kinetic and kinematic data respectively (Koontz, Kankipati, et al., 2011). Only the lift phase of the transfer from the wheelchair to the bench was analyzed in this study. A transfer was determined to begin when a vertical reaction force was detected by the load cell on the wheelchair side grab bar (Figure 8) and ended before a landing spike was detected by the force plate underneath the bench (Kankipati et al., 2011). The end of the lift phase and the beginning of the descent phase is defined by the highest elevated point of the trunk which is indicated by the peak of the C7 and T3 marker trajectories (Kankipati et al., 2011). The kinematics of transfers was calculated based on the rotation sequences recommended by International Society of Biomechanics (Wu et al., 2005). Anatomical joint position was the neutral position (zero angle position, Figure 9). The Euler angle sequences for shoulder, elbow, and wrist were YXY, ZXY, and ZXY, respectively (Wu et al., 2005). The joint orientation was described by the coordinate system of distal segment relative to the coordinate system of proximal segment. For example, shoulder joint orientation was described by the upper arm coordinate system relative to the trunk coordinate system. As for the trunk, Cardan angle sequence, ZXY (Wu et al., 2005), was used with respect to the trunk coordinate system at the initial trunk position. Hanavan's model was used to calculate center of mass and moment of inertia using the subjects' segment lengths and circumferences (Hanavan, 1964). Three-component forces and moments measured by the load cells and the force plates (Figure 8), the marker data of the trunk and upper extremities, and the inertial properties of each body segment were inputs into an inverse dynamic model (Cooper et al., 1999). Each segment was assumed as a rigid body and linked together by ball and socket joints. The 3rd metacarpalphalangeal joint was assumed as the point of force application. The output of the inverse dynamic model included upper extremity net joint forces and moments.

Key kinetic variables included maximum resultant forces and moments, and maximum rate of rise of resultant force and moment at the shoulders, elbows, and wrists on both sides. Since shoulder pain is more commonly associated with transfers (Dalyan et al., 1999), the maximum superior and posterior shoulder forces were also analyzed, as well as maximum abduction, extension, and external and internal rotation (ER and IR) shoulder moments, and their rate of rise on both sides. The resultant force on each joint is indicative of the total joint loading. The maximum rate of rise of resultant force is the peak instantaneous loading rate and impact force on each joint. The resultant moment on each joint represents the rotational demands associated with the muscle forces around the joint and the external forces. The maximum rate of rise of resultant moment indicates the peak rate of moment production on each joint. The superior and posterior shoulder forces were defined as the components of resultant shoulder force acting along the vertical upward and posterior axes of shoulder. The shoulder abduction, extension, and ER/IR moments were defined as the components of resultant shoulder moment producing surround the anterior/posterior, medial/lateral, and vertical axes of shoulder respectively. Each kinetic variable was normalized by body mass (in kilogram) (Desroches et al., 2013; Gagnon, Koontz, Mulroy, et al., 2009; Gagnon, Nadeau, Noreau, Dehail, & Piotte, 2008). Several kinematic dependent variables on both sides were analyzed in the present study: maximum shoulder internal rotation, elevation, and plane of elevation angles, minimum shoulder plane of elevation angle (Figure 9), maximum and minimum elbow flexion angles, maximum wrist extension angle, and the range of motion (ROM) of each joint. These kinetic and kinematic variables were selected because they have been linked to shoulder pain, median nerve function, and other upper extremity injuries (Boninger, Koontz, et al., 2005; Finley & Rodgers, 2004; Gagnon, Koontz, Mulroy, et al., 2009; Hurd & Kaufman, 2012; Keeley et al., 2012; Meislin et

al., 2005; Mercer et al., 2006; I. M. Rice et al., 2013). Maximum trunk flexion angle, flexion/extension ROM, and right/left side bending ROM were also included to identify the use of head-hips techniques (Allison et al., 1996; Gagnon, Nadeau, Noreau, Eng, et al., 2008). All of the kinetic and kinematic variables were averaged over a minimum of three and a maximum of five trials.

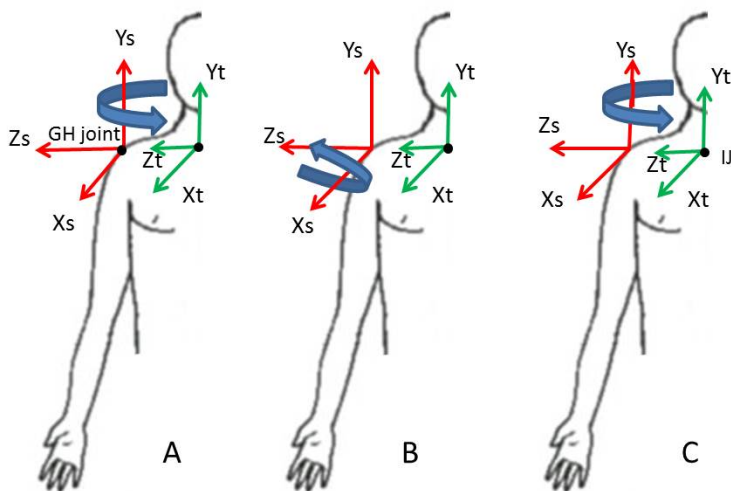


Figure 9. Anatomical (zero) position and shoulder angle orientation relative to trunk coordinate system: A, plane of elevation; B, negative elevation; C, internal rotation (Wu et al., 2005). Abbreviation: GH joint, glenohumeral joint; IJ, incisura jugularis; X_s , Y_s , Z_s , shoulder local coordinate system; X_t , Y_t , Z_t , trunk local coordinate system

The TAI contains three scores. Both part 1 and part 2 are scored and averaged to produce a third score, the final score. All scores range from 0 to 10. Only the part 1 summary score was used to identify component transfer skills because part 1 items evaluate whether the individual used specific component transfer skills (McClure et al., 2011). Part 2 was not analyzed in this study as it encompasses some of the same transfer skills that are measured in Part 1 and its major purpose is to evaluate the consistency of skills. Part 1 items are scored “Yes” (1 point) when the

subject performs the specified component skill correctly, “No” (0 points) when the subject performs the component skill incorrectly, or not applicable “(N/A)” which means the item does not apply. The part 1 summary score is the sum of each item's score multiplied by 10, and then divided by the number of applicable items, ranging from 0-10 (McClure et al., 2011).

4.2.4 Statistical analysis

Descriptive statistics (means and standard deviations (SD)) were calculated and reported for each biomechanical variable. All of the kinetic variables were examined for normality using the Shapiro-Wilk test. Because of the small sample size and non-normally distributed variables, Wilcoxon signed-rank test was used to compare the differences of the selected injury-related biomechanical variables between pre- and post-training. The effect size (Cohen's d) for the magnitude of difference in each biomechanical variable between pre- and post-training groups was also calculated. Based on a previous study, small effect size in Cohen's d is 0.2, medium effect size is 0.5, and large effect size is 0.8 (Cohen, 1992). The level of significance was set at 0.05. All the statistical analyses were performed in SPSS (SPSS Inc., Chicago, IL).

4.3 RESULTS

4.3.1 Participants

Twenty-four people volunteered to participate in the study. Seventeen participants met the criteria for the follow-up testing (part 1 summary score lower than 7.36), but only twelve of them

could come back for the follow-up testing within four weeks after the step 1 testing. One of the twelve participants who finished the two-step protocol had a bilateral above knee amputation. Because his transfer approach was not sitting pivot transfer he was not included in the data analysis in this study.

Table 17 shows summary demographic information for the eleven subjects (8 men and 3 women) who completed the two steps of the study. Ten subjects had a spinal cord injury (SCI); six subjects reported a complete SCI and four subjects an incomplete SCI (three with American Spinal Injury Association (ASIA) Grade B and one with ASIA Grade C). One subjects had quadriplegia (C5 to C6), five had high paraplegia (T2 to T7), and four had low paraplegia (T8 to L1) (John et al., 2010). The remaining one participant had muscular dystrophy.

Table 17. Participants' demographic information

Subjects, n=11	Mean \pm standard deviation (range)
Age (years)	42.18 \pm 10.77 (21 - 55)
Height (meters)	1.70 \pm 0.10 (1.55 - 1.82)
Weight (kilograms)	64.47 \pm 16.84 (39.45 – 95.61)
Average duration of using a wheelchair (years)	16.68 \pm 8.82 (4 – 27.25)

4.3.2 TAI scores

The average of the 11 participants' pre-training part 1 summary score was 6.31 (\pm .98). Table 18 shows our participants' skill deficits in transfers before training. Items 5 and 15 were not applicable in this study setting. Participants performed poorly on almost all of the items. Items

1, 4, 9, 12, and 13 had the most participants who performed poorly. After training, the average of part 1 summary score improved to 9.92 ($\pm .25$). Only one participant did not perform item 12, using head-hip relationship techniques, in transfers after training.

Table 18. The items in part 1 of the TAI and the number of the participants who fail to perform each transfer skill during pre- and post- training testing

Items in part 1 of the TAI	Pre-training, number of subjects fail	Post-training, number of subjects fail
1. The subject's wheelchair is within 3 inches of the object to which he is transferring on to.	8	0
2. The angle between the subject's wheelchair and the surface to which he is transferring is approximately 20-45 degrees.	5	0
3. The subject attempts to position his chair to perform the transfer forward of the rear wheel (i.e., subject does not transfer over the rear wheel).	3	0
4. If possible, the subject removes his armrest or attempts to take it out of the way.	8	0
5. The subject performs a level or downhill transfer, whenever possible.	NA	NA
6. The subject places his feet in a stable position (on the floor if possible) before the transfer.	4	0
7. The subject scoots to the front edge of the wheelchair seat before he transfers (i.e., moves his buttocks to the front 2/3rds of the seat).	3	0
8. Hands are in a stable position prior to the start of the transfer.	6	0
9. A handgrip is utilized correctly by the leading arm (when the handgrip is in the individual's base of support).	8	0
10. A handgrip is utilized correctly by the trailing arm (when the handgrip is in the individual's base of support).	1	0
11. Flight is well controlled.	0	0
12. Head-hip relationship is used.	8	1
13. The lead arm is correctly positioned (The arm should not be extremely internally rotated and should be abducted 30-45 deg.)	8	0
14. The landing phase of the transfer is smooth and well controlled (i.e., hands are not flying off the support surface and the subject is sitting safely on the target surface.)	0	0

Table 18 (continued)

15. If an assistant is helping, the assistant supports the subject's arms during the transfer.	NA	NA
--	----	----

4.3.3 The immediate training effects in biomechanical variables

Table 19 and

Table 20 show our participants' pre- and post- training biomechanical variables and the results of the statistical comparisons (Appendix C shows individual training effects). The structured transfer training had significant biomechanical effects on the trailing (right) shoulder, elbow, and wrist joints and leading (left) shoulder joint.

After the structured training, participants' trailing elbow remained in a more flexed position during transfers and elbow flexion/extension ROM significantly decreased compared to before training ($p < .03$, larger than medium effect size, Table 19). As for the kinetic variables on trailing (right) side, participants' shoulder resultant moment and external rotation moments, rate of rise of shoulder superior/inferior force and adduction/abduction moment (Table 20), and rate of rise of elbow and wrist resultant forces (Table 21 Table 22) significantly decreased after training compared to before training ($p < .05$, up to 49% lower than before training, all of the variables have larger than medium effect size).

As for the kinematics variables on the leading (left) side, participants after training had significantly less shoulder maximum internal rotation and elevation angles and less plane of elevation, elevation, and internal/external rotation ROMs during transfers compared to before training ($p < .04$, at least medium effect size, Table 19). For the kinetic variables, after training participants had lower shoulder resultant and external rotation moments and lower rate of rise of shoulder resultant force, resultant moment, and abduction/adduction and external/internal

rotation moments on the leading side (Table 23) compared to before training ($p < .04$, up to 42% lower than pre-training, at least medium effect size).

Table 19. The values (\pm standard deviation, SD) of the kinematic variables and the results of the statistical analysis between pre- and post-training groups

Kinematic variables (\pm SD, degree)		Pre-training	Post-transfer training	P value
Trailing (right) shoulder	Maximum internal rotation	58.99 \pm 13.75	61.89 \pm 8.08	.42
	Maximum elevation	34.24 \pm 17.37	36.13 \pm 13.27	.93
	Maximum plane of elevation	21.73 \pm 11.44	19.05 \pm 14.55	.48
	Minimum plane of elevation	-13.90 \pm 18.41	-15.53 \pm 11.66	.86
	Plane of elevation ROM	35.51 \pm 18.21	34.15 \pm 10.81	.72
	Elevation ROM	22.82 \pm 9.25	23.34 \pm 8.91	.79
Internal/external rotation ROM		19.38 \pm 6.86	16.25 \pm 6.88	.16
Trailing (right) elbow	Minimum flexion	*38.93 \pm 13.17	*49.98 \pm 20.54 (Cohen's d=0.64)	.03
	Maximum flexion	77.19 \pm 13.19	76.12 \pm 15.85	1.00
	Flexion/extension ROM	*38.25 \pm 14.46	*28.61 \pm 7.38 (Cohen's d=0.84)	<.01
Trailing (right) wrist	Maximum extension	56.98 \pm 15.09	57.34 \pm 13.80	.86
	Flexion/extension ROM	30.47 \pm 15.05	30.29 \pm 12.89	.79
Leading (left)	Maximum internal rotation	*67.11 \pm 11.24	*56.85 \pm 6.71 (Cohen's d=1.11)	.04

Table 19 (continued)

shoulder	Maximum elevation	*58.20±11.09	*48.95±15.64 (Cohen's d=0.68)	.02
	Maximum plane of elevation	46.29±32.96	33.58±14.73	.21
	Minimum plane of elevation	-4.79±26.41	-1.86±12.74	1.00
	Plane of elevation ROM	*51.09±26.94	*34.96±7.97 (Cohen's d=0.81)	.03
	Elevation ROM	*56.11±16.60	*34.37±10.34 (Cohen's d=1.57)	<.01
	Internal/external rotation ROM	*45.58±9.78	*32.56±6.32 (Cohen's d=1.58)	<.01
	Leading (left) elbow	Minimum flexion	25.35±7.91	31.84±14.80
	Maximum flexion	58.20±11.09	60.09±15.56	.93
	Flexion/extension ROM	32.86±12.90	28.61±7.38	.29
Leading (left) wrist	Maximum extension	58.08±26.66	69.84±19.00	.06
	Flexion/extension ROM	45.93±27.63	45.50±25.23	.93
	Maximum flexion	26.38±15.21	32.26±11.75	.29
Trunk	Flexion/extension ROM	31.00±12.05	32.25±11.76	.79
	Right/Left side bending ROM	29.45±6.90	25.69±8.90	.48

*p < 0.05; Abbreviations: ROM, range of motion

Table 20. The values (\pm standard deviation, SD) of maximum trailing shoulder kinetic variables and the results of the statistical analysis between pre- and post-training groups

Joint	Maximum kinetic variables (\pm SD)	Pre-training	Post-transfer training	P value
Trailing (right) shoulder	Resultant force (N/Kg)	4.45 \pm .89	4.59 \pm .54	.66
	Rate of rise of resultant force (N/Kg*s)	15.50 \pm 5.16	13.29 \pm 3.91	.09
	Resultant moment (Nm/Kg)	*.97 \pm .35	*.62 \pm .23 (Cohen's d=1.18)	.04
	Rate of rise of resultant moment (N*m/Kg*s)	3.69 \pm 1.72	2.19 \pm .88	.06
	Superior force (N/Kg)	1.83 \pm .62	1.24 \pm .69	.06
	Posterior force (N/Kg)	3.25 \pm 1.00	3.16 \pm 1.28	.72
	Internal rotation moment (Nm/Kg)	.12 \pm .11	.12 \pm .14	1.00
	External rotation moment (Nm/Kg)	*.59 \pm .33	*.30 \pm .25 (Cohen's d=0.99)	.03
	Abduction moment (Nm/Kg)	.49 \pm .25	.31 \pm .15	.06
	Extension moment (Nm/Kg)	.47 \pm .23	.34 \pm .22	.18
	Rate of rise of anterior/posterior force (N/Kg*s)	7.17 \pm 2.24	7.99 \pm 1.68	.29
	Rate of rise of superior/inferior force	*6.71 \pm 2.43	*4.33 \pm 1.39	0.01

Table 20 (continued)

	(N/Kg*s)		(Cohen's d=1.20)	
			*1.01±.48	
	Rate of rise of adduction/abduction moment (N*m/Kg*s)	*1.60±.74	(Cohen's d=0.95)	.05
	Rate of rise of internal/external rotation moment (N*m/Kg*s)	1.47±.76	1.00±.61	.11
	Rate of rise of flexion/extension moment (N*m/Kg*s)	2.30±.93	1.70±.73	.11

*p < 0.05; Abbreviations: N, Newton; m, meter; kg, kilogram; s, second

Table 21. The values (±standard deviation, SD) of maximum trailing elbow kinetic variables and the results of the statistical analysis between pre- and post-training groups

Joint	Maximum kinetic variables (±SD)	Pre-training	Post-transfer training	P value
	Resultant force (N/Kg)	4.49±.79	4.38±.56	.66
			*13.33±3.92	
Trailing (right) elbow	Rate of rise of resultant force (N/Kg*s)	*15.76±5.23	(Cohen's d=0.53)	.03
	Resultant moment (Nm/Kg)	.68±.23	.65±.24	.33
	Rate of rise of resultant moment (N*m/Kg*s)	2.67±1.26	2.22±.91	.16

*p < 0.05; Abbreviations: N, Newton; m, meter; kg, kilogram; s, second

Table 22. The values (\pm standard deviation, SD) of maximum trailing wrist kinetic variables and the results of the statistical analysis between pre- and post-training groups

Joint	Maximum kinetic variables (\pm SD)	Pre-training	Post-transfer training	P value
Trailing (right) wrist	Resultant force (N/Kg)	4.44 \pm .75	4.32 \pm .57	.53
	Rate of rise of resultant force (N/Kg*s)	*15.78 \pm 5.36	*13.54 \pm 4.22 (Cohen's d=0.46)	.05
	Resultant moment (Nm/Kg)	.35 \pm .07	.34 \pm .07	.59
	Rate of rise of resultant moment (N*m/Kg*s)	1.24 \pm .40	1.07 \pm .33	.09

*p < 0.05; Abbreviations: N, Newton; m, meter; kg, kilogram; s, second

Table 23. The values (\pm standard deviation, SD) of maximum leading shoulder kinetic variables and the results of the statistical analysis between pre- and post-training groups

Joint	Maximum kinetic variables (\pm SD)	Pre-training	Post-transfer training	P value
Leading (left) shoulder	Resultant force (N/Kg)	4.36 \pm .90	4.18 \pm .80	.29
	Rate of rise of resultant force (N/Kg*s)	*12.81 \pm 6.18	*10.35 \pm 3.15 (Cohen's d=0.50)	.04
	Resultant moment (Nm/Kg)	*1.07 \pm .24	*.85 \pm .20	.03

Table 23 (continued)

			(Cohen's d=1.00)	
Rate of rise of resultant moment (N*m/Kg*s)	*3.79±1.54	*2.43±.64	(36% lower, Cohen's d=1.15)	<.01
Superior force (N/Kg)	2.14±.73	2.07±.75		.58
Posterior force (N/Kg)	3.33±.92	3.35±1.27		.67
Internal rotation moment (Nm/Kg)	.05±.08	.08±.17		.48
External rotation moment (Nm/Kg)	*.73±.28	*.56±.16 (23% lower, Cohen's d=0.75)		.05
Abduction moment (Nm/Kg)	.32±.16	.26±.07		.40
Extension moment (Nm/Kg)	.78±.29	.64±.35		.48
Rate of rise of anterior/posterior force (N/Kg*s)	5.32±5.86	3.14±1.74		.16
Rate of rise of superior/inferior force (N/Kg*s)	9.08±3.78	7.26±2.11		.09
Rate of rise of adduction/abduction moment (N*m/Kg*s)	*1.97±1.12	*1.14±.29 (Cohen's d=1.01)		.04
Rate of rise of internal/external	*3.22±1.76	*1.91±.54		.01

Table 23 (continued)

rotation moment (N*m/Kg*s)		(Cohen's d=1.01)	
Rate of rise of flexion/extension moment (N*m/Kg*s)	2.23±1.16	1.63±.66	.21

p < 0.05; Abbreviations: N, Newton; m, meter; kg, kilogram; s, second

Table 24. The values (±standard deviation, SD) of maximum leading elbow kinetic variables and the results of the statistical analysis between pre- and post-training groups

Joint	Maximum kinetic variables (±SD)	Pre-training	Post-transfer training	P value
Leading (left) elbow	Resultant force (N/Kg)	4.31±.96	4.16±.82	.37
	Rate of rise of resultant force (N/Kg*s)	12.81±6.02	10.72±3.40	.08
	Resultant moment (Nm/Kg)	.41±.16	.50±.12	.16
	Rate of rise of resultant moment (N*m/Kg*s)	2.03±1.00	1.99±.97	1.00

p < 0.05; Abbreviations: N, Newton; m, meter; kg, kilogram; s, second

Table 25. The values (±standard deviation, SD) of maximum leading wrist kinetic variables and the results of the statistical analysis between pre- and post-training groups

Joint	Maximum kinetic variables (±SD)	Pre-training	Post-transfer training	P value
Leading	Resultant force (N/Kg)	4.29±.99	4.17±.83	.48

Table 25 (continued)

(left)	Rate of rise of resultant force	12.73±5.96	10.86±3.50	.21
wrist	(N/Kg*s)			
	Resultant moment (Nm/Kg)	.23±.13	.31±.09	.06
	Rate of rise of resultant moment	.72±.33	.88±.26	.21
	(N*m/Kg*s)			

$p < 0.05$; Abbreviations: N, Newton; m, meter; kg, kilogram; s, second

4.4 DISCUSSION

This is the first study investigating the immediate effects of a structured transfer skill training program on wheelchair users' upper limbs from a biomechanical perspective. After the transfer training, our participants' TAI scores notably improved (close to the best score, 10) and their injury-related biomechanical variables also significantly improved (Table 18Table 19Table 20Table 21Table 22Table 23Table 24, andTable 25). Better component transfer skills helped wheelchair users reduce the elbow flexion/extension movement and the moment loading and force impacts on shoulder, elbow, and wrist on the trailing side, as well as reduce the moment loading and force and moment impacts on the leading shoulder. The loading-reducing effects on every upper-limb joint on trailing side, but only on the shoulder on leading side, may be because during transfers wheelchair users' trailing arm supports more body weight than the leading arm (Forslund et al., 2007; Gagnon, Nadeau, Noreau, Dehail, & Gravel, 2008). Therefore, the training effects on the trailing side were more prominent than the leading side.

Within our total of twenty-four participants, seventeen of them (71%) had lower than average TAI scores (7.36). Most of the eleven participants who came back and participated in the

training program were unaware that they needed to: position their wheelchair within three inches (item 1) with 20 to 45 degree angle (item 2) between the wheelchair and transfer target; remove the armrest (item 4), put their leading hand in a close and stable position (item 8) without over shoulder internal rotation and abduction (item 13) and with correct handgrip (item 9); and use head-hip relationship technique (item 12) (Table 18). Some of these transfer skills have been previously shown to be associated with good biomechanical effects. For example, close wheelchair positioning and appropriate angling (item 1 and 2) was linked to lower leading shoulder resultant force and internal rotation moment (C.-Y. Tsai et al., 2014). Using correct and close handgrip (item 9) during transfers was associated with reduced moment impact on the leading shoulder and elbow and resultant moment and moment impact on the trailing shoulder and elbow (C.-Y. Tsai et al., 2014). Using the head-hip relationship (item 12) was linked to a reduced moment impact on leading shoulder (C.-Y. Tsai et al., 2014). Some of these component skills may increase the moment loading on the leading side (Forslund et al., 2007; Gagnon, Nadeau, Noreau, Dehail, & Gravel, 2008). However it's important to note that these associations between biomechanical variables and the TAI were based on self-selected, not trained transfer techniques. Specifically training individuals to strictly follow the TAI led to reducing loading across the trailing arm joints and the leading shoulder joint. Thus, a structured transfer training program is necessary for educating wheelchair users how to transfer in a way that minimizes loading across both shoulders.

The reduction in loading across both shoulders may be explained in part by the changes made during training in the hand placement and shoulder positioning. After the transfer training, our participants had smaller shoulder ROM and less maximum IR and elevation angles on the leading side, as well as lower shoulder resultant moment and rate of rise of superior/inferior

force and abduction/adduction moments on both arms (up to 42% lower than before training, larger than medium effect size), which may protect wheelchair users from shoulder impingement (Boninger, Waters, et al., 2005; Gagnon, Koontz, Mulroy, et al., 2009; Yanai et al., 2006). Wheelchair users' external rotation moments and rate of rise of internal/external rotation moments also significantly decreased (up to 49% lower) on both sides after the training. The decreased external rotation moment and impact may prevent the imbalance between shoulder internal and external rotators which may lead to shoulder instability, impingement, and rotator cuff tears (Burnham, May, Nelson, Steadward, & Reid, 1993; Lee & McMahon, 2002). These results indicate that the structured transfer training program has high potential to helping wheelchair users prevent secondary shoulder injuries.

Our structured transfer training based on the TAI enabled wheelchair users to perform transfers with significantly less elbow ROM and rate of rise of resultant force on the trailing side. The less elbow movement and impact force (15% lower than before training, medium effect) on the elbow may potentially protect them from elbow pain and ulnar mononeuropathy (Boninger et al., 1996; Burnham & Steadward, 1994; Dalyan et al., 1999). This finding was somewhat unexpected as the items in TAI specifically focus on optimizing shoulder and hand positioning. In a transfer which is one kind of closed-chain task, the movement and loading on the shoulder, elbow, and wrist are highly correlated to each other (Marciello et al., 1995). The smaller elbow movement on the trailing side and shoulder ROM on the leading side that resulted from using proper component transfer skills may assist people with poor triceps and shoulder function, such as persons with tetraplegia, to be able to perform high-quality transfers.

During transfers, the maximal extension angle of both wrists is around 84° to 88° (Gagnon, Nadeau, Noreau, Eng, et al., 2008). The extreme wrist extension position during

transfers predisposes wheelchair users to wrist injuries (Keir et al., 1997; Sie et al., 1992). Therefore, the clinical practice guidelines suggest that wheelchair users should use a correct handgrip which means either using a grab-bar within their base of support or draping fingers to grab the edge of the target surface during transfers to prevent extreme wrist angles, provide more stability, and help apply forces during transfers (Boninger, Waters, et al., 2005). The results of the study indicated that the rate of rise of wrist resultant force significantly decreased (14% lower than before training) on the trailing side after training which may decrease the force impact on the wrist joint and median nerve. However, there is a trend of increasing wrist extension angle and resultant moment (35% higher than before training) on the leading side (Table 19 and Table 25). Compared with previous studies, the wrist extension angle on the leading side in this study (average \pm SD is 58.08 ± 26.66) is much smaller, because some of our participants used a closed-finger fist or hyperextension of the metacarpophalangeal (MCP) joint to support body weight during transfers (six out of eleven participants, Appendix D and Appendix E). Although a closed-finger fist and hyperextension MCP joint provides a more neutral wrist position, it will result in excessive pressure on the MCP joints and makes it hard to maintain wrist stability (Boninger, Waters, et al., 2005; Goodman et al., 2001; Minkel et al., 2010). After the structured transfer training, all of our participants changed to using a handgrip during transfers. This resulted in a tradeoff effect related to training the use of a handgrip. The handgrip while increasing the wrist extension angle compared to using a fist and a hyperextended MCP (Appendix D) likely protects the MCP joint from excessive pressure. Although wheelchair users' wrist extension angle increased (average \pm SD is 69.84 ± 19.00) when using a handgrip, the extension angle was still less than the extreme wrist extension angle previously reported in the

literature. These findings point to a need to develop transfer aids and/or assistive technology that help to facilitate a handgrip that minimizes wrist extension angles during transfers.

The study results further support TAI's construct validity. The biomechanics results were consistent with what the TAI was designed to do which is to reduce awkward motions and forces on the upper extremities. This study shows more biomechanical benefits compared to the previous TAI validation study which assessed self-selected transfer techniques (C.-Y. Tsai et al., 2014). Individualized training that encompassed all aspects of TAI, not just specific skill deficits, had the overall effect of lowering the loads on the leading and trailing side. Our structured transfer training program can not only make up the component transfer skills wheelchair users lack, but ensures that all the component skills work together to result in a transfer technique that reduces loading on both upper limbs.

4.4.1 Study limitations

The small sample size may have negatively affected the power of the statistical analyses. The large amount of comparisons between each variable without a correction may inflate the type I error. To support the overall training effect in this study, we added individual's training effects in the Appendix C. The training effects still can be observed in each individual result. There is a gap in research that would allow for us to directly link the change of magnitudes we found after the training program to clinically meaningful outcomes (e.g. how much decreased magnitude in biomechanical variables could reduce injury risk and pain level or how much exact joint biomechanical magnitude would cause injuries). Considering the repetitive nature of transfers low reduced magnitudes may still be detrimental over the long term. This study only analyzed transfers from a wheelchair to a level-height bench located on the subjects' left side and required

them to use the wheelchair side grab bar for positioning of the trailing hand (Figure 8A). Although they needed to use the wheelchair side grab bar, the use of handgrip and arm positioning is still a part of good component transfer skills. Subjects were given enough time to acclimate to the setup and practice the taught transfer skills prior to testing. Wheelchair users must learn to be flexible in adapting to different setups when they transfer in public places where places to position their hands or the area to position their wheelchairs is limited. The TAI rater in the follow-up testing was not blinded and there was no control group to compare the effects of training program. However, the biomechanics after training changed in a way that supported the desired training effects and what the TAI was designed to achieve. Future studies should consider recruiting more participants and investigating the immediate biomechanical effects of the structured transfer training program on different types of transfers, such as high-target and toilet transfers. Future longitudinal studies that assess the long-term outcomes of following or not following the techniques expressed in TAI could help to elucidate more clearly the impact that 'smaller' but statistically significant differences have on joint health.

4.5 CONCLUSION

The results of the study indicate that many wheelchair users lack good component transfer skills. Our structured transfer training program based on the TAI principle has good immediate biomechanical effects on wheelchair users' upper limbs. When wheelchair users transfer after training, they have significantly smaller trailing elbow and leading shoulder ROM, trailing and leading shoulder moment loading and impacts, and trailing elbow and wrist force impacts compared to pre-training. A structured transfer training program may have the potential to keep

wheelchair users from developing secondary injuries and may need to be further emphasized in in-patient hospital stays or outpatient clinics.

4.6 ACKNOWLEDGEMENTS

This material is based upon work supported by the Department of Veterans Affairs (B7149I). The contents of this paper do not represent the views of the Department of Veterans Affairs or the United States Government.

5.0 CONCLUSIONS

Through the results of three chapters in the study, we can understand that transfer skills, setups, and training program are very important for wheelchair users in performing a safe and efficient transfer. The combination of good transfer skills, appropriate transfer setups, and structured transfer training program may have great potential to protecting wheelchair users' upper limbs for long term use.

The component transfer skills that can be measured with the TAI are closely associated with the magnitude and impact of joint moments. Certain component transfer skills helped to reduce the moments imparted on both upper limbs while other skills had the effects of increasing the magnitudes or rates loading on the leading limb. Different component skills have different kinetic effects on the upper extremities. Good transfer skills not only reduce the loading on both of upper limbs, but also balance the force and moment between the two limbs. Taking into consideration the kinetic effects from all the component transfer skills studied may help to reach better load-relieving effects on the upper extremities during transfers. For example, wheelchair users should angle their wheelchairs appropriately relative to the target surface (20-45 degrees) to reduce the large internal rotation shoulder moments on the leading side which can occur when using a proper leading handgrip.

Using the TAI several transfer skill deficits were identified for wheelchair toilet transfers in two different simulated built environments that were also linked to potentially harmful

biomechanics. The front wheelchair-toilet setup resulted in lower failed skill rates and the types of failed skills did not affect the biomechanics as much as the types of failed skills that occurred with the side wheelchair-toilet setup. In the front wheelchair-toilet setup, the component skill of close wheelchair positioning is important for lowering transfer loading. When the built environment requires a side wheelchair position, the most protective component skills are: scooting forward movement, utilizing stable and close hand positioning, and utilizing correct handgrip and head-hips relationship technique. Because of the intrinsic height difference in toilet transfers alternating the leading side (direction of transfer) should be done if the environment allows. Clinical transfer training should emphasize different skills based on the toilet space setup and how to choose correct handgrip placement. When wheelchair users try to determine needs for home adaptations for toilet transfers, enabling the ability for front wheelchair positioning and facilitating good handgrip use should be planned. Public restrooms may consider adding space to permit front wheelchair positioning and preventing non-ideal grab bar setup, which may facilitate wheelchair users in performing better quality of transfers.

The structured transfer training program based on the TAI principle has good immediate biomechanical effects on wheelchair users' upper limbs. When wheelchair users transfer after training, they have significantly smaller trailing elbow and leading shoulder ROM, trailing and leading shoulder moment loading and impacts, and trailing elbow and wrist force impacts compared to pre-training. A structured transfer training program may have the potential to keep wheelchair users from developing secondary injuries and may need to be further emphasized in in-patient hospital stays or outpatient clinics.

5.1 STUDY LIMITATIONS

The small sample size may have negatively affected the power of the statistical analyses and response rate for some of the TAI items. For example not all of the items could be modeled and analyzed to compare the biomechanical differences between using- and non-using skill groups because subjects were either too proficient on the item (most received a “Yes” response) or the item did not apply to their transfer (“N/A” response).

The large amount of comparisons between each variable without a correction may inflate the type I error. To support the overall training effect in this study, we added individual’s training effects in the Appendix C. The training effects still can be observed in each individual result.

This study only analyzed transfers from a wheelchair to a level-height bench or a toilet located on the subjects’ left side and required them to use the wheelchair side grab bar for positioning of the trailing hand (Figure 8A). Although they needed to use the wheelchair side grab bar, the use of handgrip and arm positioning is still a part of good component transfer skills. Subjects were given time to acclimate to the setup prior to testing. Wheelchair users have to learn to be flexible with adapting to different setups when they transfer in public places where places to position their hands or the area to position their wheelchairs is limited.

The TAI rater in the follow-up testing was not blinded, and there was no control group to comparing the effects of training program. However, the biomechanics after training changed in a way that supported the desired training effects and what the TAI was designed to achieve.

5.2 FUTURE WORK

Future studies should collect and analyze subjective feedback from the subject on the learned techniques and perceived exertion to understand how subjects felt about using the new techniques. It's possible that while the biomechanics showed 'improvement' after training the subjects may have felt it was more difficult or awkward to apply the techniques in practice. Other physical attributes such as pain levels and the amount of trunk control, strength, and flexibility may also influence a person's ability to execute the techniques promoted in the TAI. A transfer training program may need to consider a holistic approach (e.g. balance, strength, and range of motion exercises) to enabling the desired movement strategies. We also need studies to better understand disparities in transfer techniques that may be associated with gender, age, pain, balance, muscle strength, physical flexibility, and transfer experiences. Future ultrasound imaging studies and musculoskeletal modeling of the upper extremities would help to elucidate the impact of techniques on soft tissue and loading through individual muscle tendons and ligaments within the joints. These results can provide a deeper understanding of the potential impact of using proper transfer skills on reducing injury risk.

From these study results, we also realized the importance of a good handgrip which greatly influences transfer biomechanics. How to determine an optimal handgrip placement and developing some assistive technology which can facilitate wheelchair users using good handgrip during transfers are also critical topics for helping wheelchair users perform efficient and safe transfers.

Creating a population-based database of wheelchair user's transfer deficits using the TAI evaluation could be helpful for education and training purposes. Plans are underway to develop a TAI assessment and training mobile app that would enable for such a reference database to be

created. As differences were found among the different types of transfers examined in this dissertation, future studies may need to investigate the immediate biomechanical effects of a structured transfer training program on other types of transfers, such as high-target and car transfers. Further, long term effects of the transfer training program are important and critical for clinical application. The long term effects of the transfer training program also need to be researched. .

Wide-spread dissemination and use of the TAI and training program is the other important area of future work. Development of the TAI evaluation mobile app, and a virtual transfer coaching system that can interact with the patient and provide feedback on technique, and publishing and presenting TAI related research at international conferences are all good approaches to spreading the application of the TAI.

APPENDIX A

PRINCIPLE COMPONENT ANALYSIS AND MULTIPLE LINEAR REGRESSION ANALYSIS OF TAI ITEM SCORES

Purpose: A secondary analysis was conducted to 1) examine and explore the interdependence among the part 1 items of the TAI and 2) model the relationship between the component factors resulting from a principle component analysis (PCA) of the TAI items and the same upper limb kinetic variables studied in Chapter 2. By performing this secondary analysis we aimed to identify clearer elements (e.g. PCA components) of transfer skill that reduce the upper limb loading during transfers.

Methods: The data for this secondary analysis comes from the 23 subjects who participated in the Chapter 2 study. They performed level-height transfers (up to 5 trials of transfers from their wheelchair to bench) while two study clinicians evaluated their transfer skills using the TAI (please refer to 2.2.1 and 2.2.2). A principal component analysis (PCA) was conducted on the 6 items in the TAI we selected in chapter 2 with orthogonal rotation (varimax) using SPSS 21 (SPSS Inc., Chicago, IL). These items were selected because they didn't have high correlation with other items in the TAI and high response rates (>80%) in one of the categories of Yes or No (please refer to 2.2.3). The Kaiser-Meyer-Olkin (KMO) measure was

used to verify the sampling adequacy for the analysis ('between 0.5 to 0.7 is mediocre; between 0.7 and 0.8 is good; between 0.8 and 0.9 is great; above 0.9 is superb' according to Kaiser, 1974 (H. Kaiser, 1974)). Eigenvalues for each component in the data were computed. Multiple linear regression was used to model the association between the component scores and kinetic variables. Separate models were created for the left and right sides. The assumption of multicollinearity for the kinetic variables (predictors) was tested using the variance inflation factors (VIFs). The results of the VIFs and backward elimination were used to determine the subset of predictors (kinetic variables) for each component score model (please refer to 2.2.3).

Results: The result of KMO measure is 0.55 (mediocre). Two components had eigenvalues larger than 1 (Kaiser's criterion (H. F. Kaiser, 1960)). The scree plot (Figure 10) was slightly ambiguous but showed the point of inflection that occurred at the fourth data point (component) and justified retaining three components. These components combined explained 76.49% of the variance. Table 26 shows the component loadings after rotation. Each component is made up by the variables with higher than 0.72 factor loading (Stevens (2002) suggested that for a sample size of 50 a loading of 0.722 can be considered significant)(Stevens, 2002). Component 1 included item 2 (appropriate wheelchair angling) and 12 (using head-hip relationship) which are reflective of using a "rotational strategy". Component 2 included item 9 (using correct leading handgrip) and 7 (scotting forward to the front edge of wheelchair) and represent a "close hand positioning technique". Component 3 included item 1 (close wheelchair positioning) and 6 (positioning the feet on the stable surface) which represent "transfer preparation technique".

Table 27 shows the results of multiple linear regression analysis. Wheelchair users who applied a close hand positioning technique (component 2) during transfers had lower average

resultant moments on the trailing shoulder and elbow and lower maximum rate of rise of resultant moment on both elbows, but higher average resultant moment at the leading wrist. Lower average resultant moment on the trailing shoulder and lower maximum rate of rise of resultant moment on the leading shoulder were highly associated with using an appropriate transfer preparation technique (component 3). Using a rotational strategy (component 1) during transfers was not significantly associated with the upper limb joint kinetics.

Wheelchair users with higher component 2 scores had average resultant moments on the trailing shoulder that were about 40% less than users with lower component 2 scores (component 2 scores increased from 0 to 1.65, and the trailing shoulder resultant moment decreased from 0.63 N*m/Kg to 0.39 N*m/Kg, Figure 11), and average resultant moment on the trailing elbow that was about 50% less than users with lower scores (scores increased from 0 to 1.65, and moments decreased from 0.54 N*m/Kg to 0.28 N*m/Kg, Figure 12). Using proper component 3 techniques reduced about 40% of the trailing shoulder resultant moment during transfers (scores increased from -0.93 to 0.68, and resultant moments decreased from 0.72 N*m/Kg to 0.47 N*m/Kg, Figure 13). Considering both the 40% to 50% decrease in the shoulder and elbow resultant moment and high frequency of daily transfer activities, using proper component 2 and 3 skills, such as using a correct handgrip, scooting forward movement, close positioning, and stable feet position, may greatly alleviate the cumulative loading on wheelchair users' shoulders and elbows. However, using component 2 skills increased the leading wrist resultant moment by 65% (component 2 scores increased from 0 to 1.65, and wrist resultant moments increased from 0.13 N*m/Kg to 0.21 N*m/Kg, Figure 14).

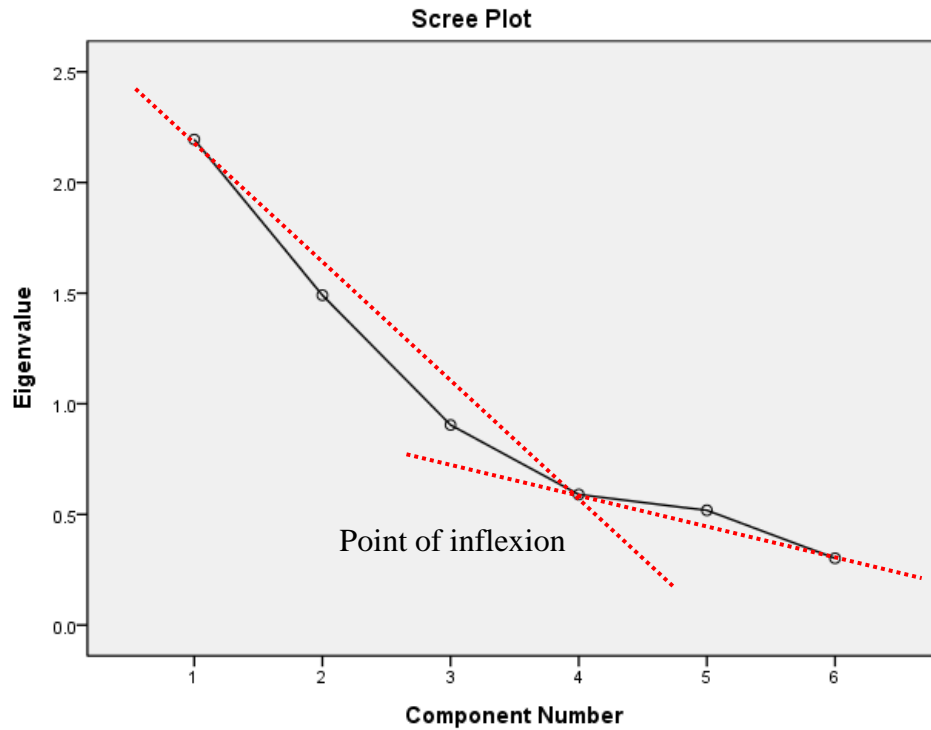


Figure 10. Scree plot between each component and its eigenvalue. The point of inflexion is at the fourth data (component) point.

Table 26. Summary of exploratory principle component analysis results for the items in the TAI (N=23)

Rotated factor loadings			
Item	Rotational strategy	Close hand positioning	Transfer preparation
2. The angle between the subject's wheelchair and the surface to which he	0.89*	-0.27	<0.1

Table 18 (continued)

is transferring is			
approximately 20-			
45 degrees.			
12. Head-hip	0.79*	0.31	0.14
relationship is used.			
9. A handgrip is			
utilized correctly by			
the leading arm			
(when the handgrip	<0.10	0.86*	0.12
is in the			
individual's base of			
support).			
7. The subject			
scoots to the front			
edge of the			
wheelchair seat			
before he transfers	0.13	0.80*	0.14
(i.e., moves his			
buttocks to the			
front 2/3rds of the			
seat).			
1. The subject's	0.42	<0.10	-0.93*
wheelchair is			

Table 18 (continued)

within 3 inches of

the object to which

he is transferring

on to.

6. The subject

places his feet in a

stable position (on

<0.10

0.22

0.68*

the floor if possible)

before the transfer.

Eigenvalues

1.62

1.59

1.38

% of variance

27.00

26.57

22.93

Note: *, factor loadings are larger than 0.72 (Stevens, 2002)

Table 27. The summary of multiple linear regression analysis for the associations between component scores and kinetic variables

Components	Variables	B	SEB	β	sr^2	Sig.	Model results
Component 1: Rotational strategy (item 2 and 12)	Right wrist	-1.86	2.39	-0.17	0.03	0.45	F(1,21)=0.61,
	Ave_RM						P=0.45, R ² =0.03
Component 2: Close hand	Left shoulder	0.74	0.44	0.34	0.16	0.12	F(1,21)=2.79,
	Max_ExtM						P=0.11, R ² =0.12
Component 2: Close hand	Right shoulder	-0.90	0.32	-0.35	0.12	0.01	F(3,19)=16.09,
	Ave_RM*						P<0.01,

Table 19 (continued)

positioning (item 9 and 7)	Right elbow	-1.16	0.64	-0.28	0.05	0.08	$R^2 = 0.72$
	Ave_RM						
	Right elbow	-0.82	0.23	-0.55	0.20	<0.01	
	Max_RateRiseRM*						
	Left elbow	-0.32	0.13	-0.43	0.18	0.02	F(3,19)=4.69,
	Max_RateRiseRM*						P=0.01,
	Left wrist	4.09	1.44	0.49	0.24	0.01	$R^2 = 0.41$
	Ave_RM*						
							F(1, 21)=4.99,
Component	Right shoulder	-1.11	0.50	-0.44	0.19	0.04	P=0.04,
3: Transfer	Ave_RM*						$R^2 = 0.19$
preparation							F(1, 21)=8.77,
(item 1 and 6)	Left shoulder	-0.26	0.09	-0.54	0.29	<0.01	P<0.01,
	Max_RateRiseRM*						$R^2 = 0.30$

Note: *, the predictor significantly contributed to the regression model. Abbreviations: B, unstandardized regression coefficients; SEB, standard error of the unstandardized regression coefficients; β , standardized regression coefficients; sr^2 , squared semipartial correlations; Sig., significance; Ave, average; Max, maximum; RM, resultant moment; ExtM, extension moment; RateRiseRM, rate of rise of resultant moment

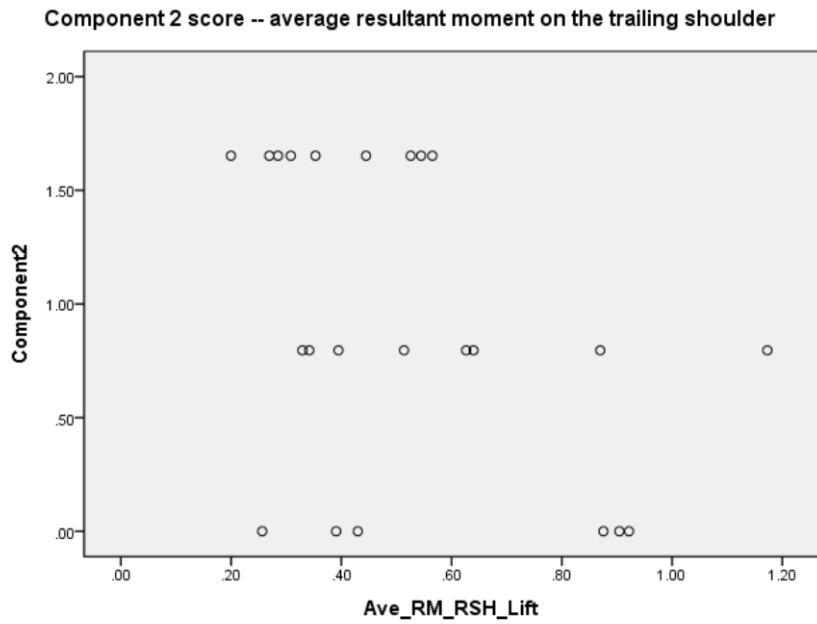


Figure 11. The scatter plot between component 2 scores and average resultant moment on the trailing (right) shoulder

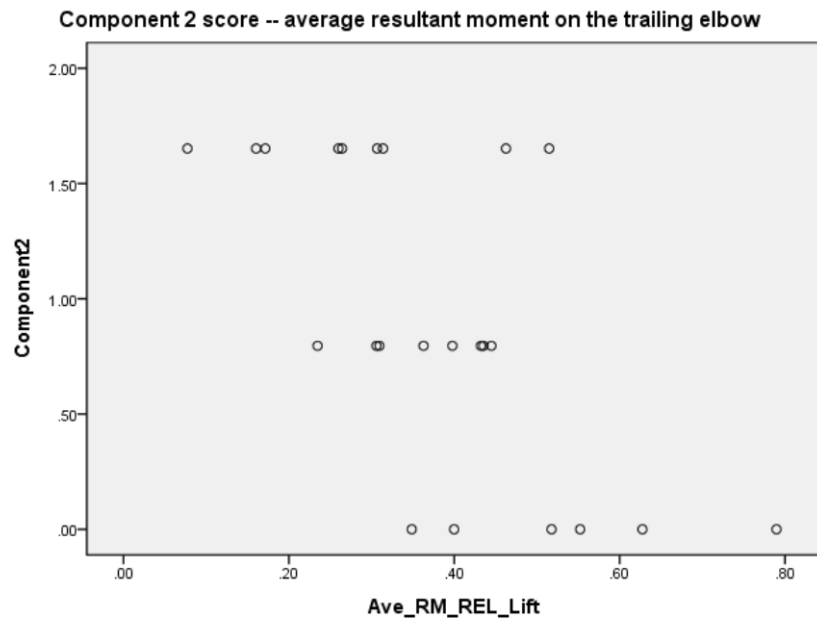


Figure 12. The scatter plot between component 2 scores and average resultant moment on the trailing (right) elbow

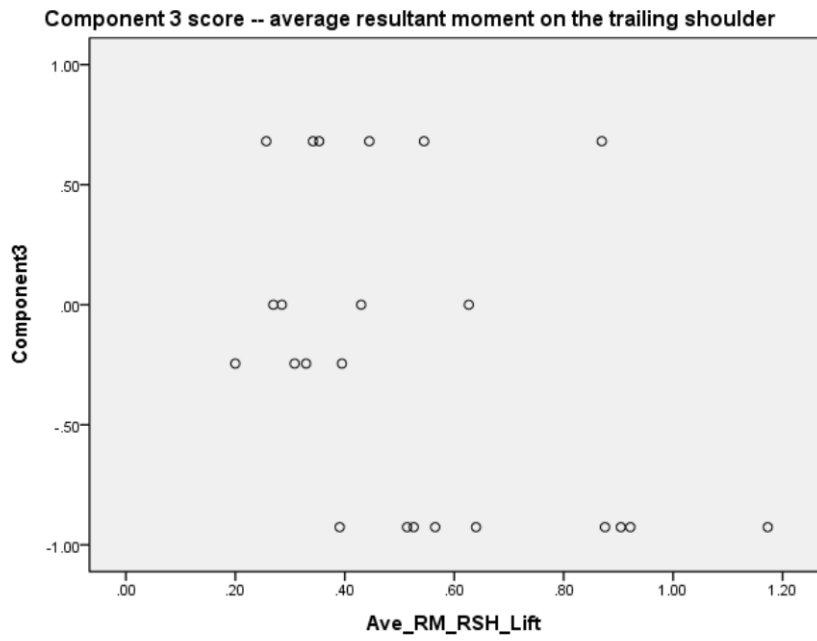


Figure 13. The scatter plot between component 3 scores and average resultant moment on the trailing (right) shoulder

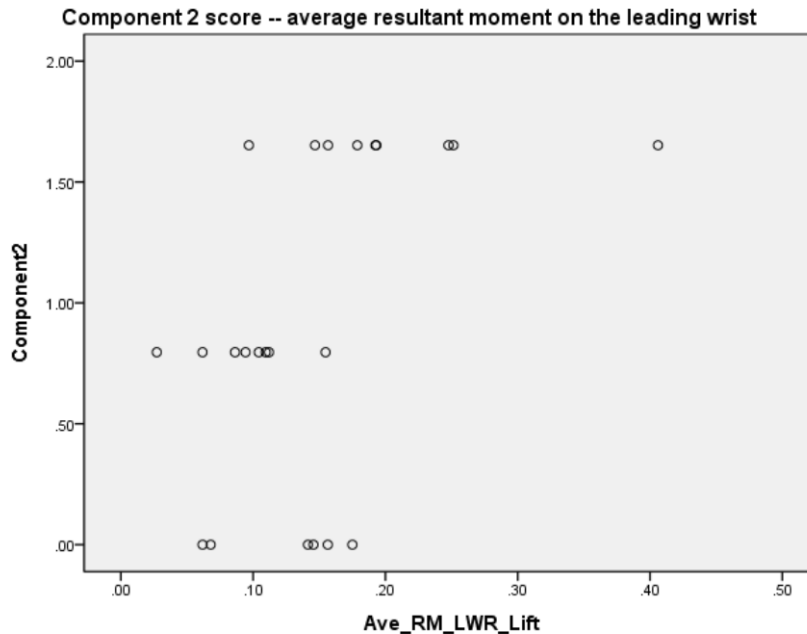


Figure 14. The scatter plot between component 2 scores and average resultant moment on the leading (left) wrist

Discussion: These results suggest that clinicians should emphasize the component 2 and 3 skills during training- close hand positioning and appropriate transfer preparation, such as using a correct handgrip, scooting forward to the front edge of the wheelchair seat, close wheelchair positioning, and putting feet on the ground, to help wheelchair users perform better quality of transfers. Because close hand positioning resulted in increased wrist moments, future research should focus on how to reduce the wrist loading during transfers, such as investigating the ideal position (angle and distance) for handgrip or developing assistive devices for facilitating optimal handgrip during transfers.

APPENDIX B

DASHBOARD INDICATORS TO SUMMARIZE THE BIOMECHANICAL EFFECTS OF COMPONENT TRANSFER SKILLS FOR DIFFERENT TRANSFERS

Purpose: Dashboard indicators were developed to summarize the biomechanical effects of selected component transfer skills for the level-height transfers, and toilet transfers with a side setup and front setup. The dashboard approach provides a simple menu that shows the magnitude impact of the selected transfer component skills on upper limb biomechanics.

Methods: Three categories were created: reduces loading (green), neutral (yellow), increases loading (red). The effect of each skill in reducing loading, or causing a neutral or increased loading effect was based on statistically significant variables in our regression models ((please refer to 2.3.3, 2.3.5, 3.3.2, 3.3.4, and 3.3.5), effect sizes and a clinical relevance criteria. Effect sizes (Cohen's d) were calculated for the kinematic and kinetic variables between using-skill and non-using-skill groups. The magnitude of the joint kinetic variables of at least 0.33 N/Kg or 0.33 N*m/Kg was set as a threshold for determining clinical relevance. This threshold equates to about 22 N (or 5 pounds) of net loading on the joints (e.g. joint kinetic variables were normalized to body mass ($0.33 \text{ N/Kg} \times \text{average body weight, } 67.55 \text{ Kg} = 22.29 \text{ N}$, please refer to 2.3.1, 2.2.3, 3.3.1, and 3.2.3)). This threshold was based on a cadaver study that showed that 22

N tension on the long head of biceps tendon had a significant effect of shifting the glenohumeral (GH) joint center and altering GH rotational ranges of motion and translations (Youm, ElAttrache, Tibone, McGarry, & Lee, 2009). Although establishing a threshold on results of a cadaver study, and on a single tendon in the shoulder has obvious limitations (e.g. no active muscle movers and stabilizers) we could find no studies from the literature that directly linked the amount and extensiveness of mechanical loading to the development of cumulative types of shoulder injuries in live subjects.

“Reduces loading” (green) was assigned to skills that had statistical significance and larger than medium effect sizes for reducing upper limb loading which was at least 0.33 N/Kg or 0.33 N*m/Kg in magnitude or facilitating better joint positioning, such as moving the shoulder plane of elevation to the scapular plane, compared to without using the skill (note that small effect size for Cohen’s d is 0.2, medium effect size is 0.5, and large effect size is 0.8 (Cohen, 1992)).

“Increases loading” (red) was assigned to skills that had statistical significance and larger than medium effect sizes for increasing upper limb loading which was at least 0.33 N/Kg or 0.33 N*m/Kg in magnitude or resulting in a more awkward joint position, such as greater wrist extension angles.

“Neutral” (yellow) was assigned to skills that had significant biomechanical effects and at least a medium effect size, but had mixed biomechanical outcomes (e.g. some biomechanical variables increased and some decreased).

Results: For the level transfers, 15 biomechanical variables (predictors) were included in the 6 regression models (6 item score models) with statistical significance (please refer to 2.3.5 and 2.3.6). The effect sizes for the magnitude of differences in these 15 biomechanical variables

between using- and non-using-skill group ranged from 0.56 (medium effect) to 1.65 (very large effect). Besides maximum internal rotation shoulder moment on the trailing and leading sides, all of the other variables were larger than 0.33 N/Kg or 0.33 N*m/Kg in magnitude.

For the toilet transfers with a side setup, 4 MANOVA models for 4 items had statistical significance between using- and non-using-skill groups and included 27 biomechanical variables (please refer to 3.3.4). The effect sizes for the differences of these 27 biomechanical variables between using- and non-using-skill groups ranged from 0.88 (large effect) to 3.2 (very large effect). Besides maximum internal rotation shoulder moment on the trailing and leading sides, all of the other variables were larger than 0.33 N/Kg or 0.33 N*m/Kg in magnitude.

As for toilet transfers with a front setup, one MANOVA model had statistical significance between the using- and non-using-skill groups and included 5 biomechanical variables (please refer to 3.3.5). The effect sizes for the differences in the 5 biomechanical variables between using- and non-using-skill groups ranged from 0.99 to 1.19 (large effects). All of the variables were larger than 0.33 N/Kg or 0.33 N*m/Kg in magnitude. Figures 15 to 17 show the dashboard indicators for level-height transfers, toilet transfers with a side setup, and toilet transfers with a front setup respectively.

	Reduce loading		Neutral	Increase loading		
<u>Level-height transfer</u> Item	Leading shoulder	Leading elbow	Leading wrist	Trailing shoulder	Trailing elbow	Trailing wrist
Item 1: Position within 3 inches of the object to which he is transferring on to.	1. Resultant force ↓ 2. Rate of rise of resultant moment ↑					
Item 2: The angle between the wheelchair and the surface is about 20-45 degrees.						
Item 6: Places feet in a stable position (on the floor if possible) before the transfer.	Rate of rise of resultant moment ↓			Ave. resultant moment ↓		
Item 7: Scoots to the front edge of the wheelchair seat before he transfers	Extension moment ↑				1. Ave. resultant moment ↓ 2. Rate of rise of resultant moment ↓	
Item 9: A correct handgrip is utilized by the leading arm	1. Rate of rise of resultant moment ↓	Rate of rise of resultant moment ↓	Rate of rise of resultant moment ↑	Ave. resultant moment ↓	Rate of rise of resultant moment ↓	
Item 12: Head-hip relationship is used.	Rate of rise of resultant moment ↓					

Figure 15. Dashboard indicator for level-height transfers

	Reduce loading		Neutral		Increase loading	
<i>Toilet transfer, side setup</i>	Leading shoulder	Leading elbow	Leading wrist	Trailing shoulder	Trailing elbow	Trailing wrist
Item 1: Position within 3 inches of the object to which he is transferring on to.						
Item 2: The angle between the wheelchair and the surface is about 20-45 degrees.						
Item 6: Places feet in a stable position (on the floor if possible) before the transfer.						
Item 7: Scoots to the front edge of the wheelchair seat before he transfers	1.Scapular plane movement 2. Elevation angle ↓					
Item 8: Hands are in a stable position	1. Resultant moment ↓ 2. Posterior force ↑ 3. Move on scapular plane	Resultant moment ↓	1.Resultant moment ↑ 2.Extension angle ↑			
Item 9: A correct handgrip is utilized by the leading arm	1. Resultant moment ↓ 2. Posterior force ↑ 3. Elevation angle ↓ 4. Internal rotation angle ↑	Resultant moment ↓	1.Resultant moment ↑ 2.Extension angle ↑	1. Resultant force ↓ 2. Posterior force ↓ 3. Abduction moment ↑	1. Resultant force ↓ 2. Resultant moment ↓	Resultant force ↓
Item 12: Head-hip relationship is used.						

Figure 16. Dashboard indicator for toilet transfers with a side setup

	Reduce loading		Neutral	Increase loading		
<i>Toilet transfer, front setup</i> Item	Leading shoulder	Leading elbow	Leading wrist	Trailing shoulder	Trailing elbow	Trailing wrist
Item 1: Position within 3 inches of the object to which he is transferring on to.				1. Resultant force ↓ 2. Posterior force ↓ 3. Abduction moment ↓	Resultant force ↓	Resultant force ↓
Item 2: The angle between the wheelchair and the surface is about 20-45 degrees.						
Item 6: Places feet in a stable position (on the floor if possible) before the transfer.						
Item 7: Scoots to the front edge of the wheelchair seat before he transfers						
Item 8: Hands are in a stable position						
Item 9: A correct handgrip is utilized by the leading arm						
Item 12: Head-hip relationship is used.						

Figure 17. Dashboard indicator for toilet transfers with a front setup

Discussion: These dashboard indicators provide good summary information for the effects of transfer skills. Different component skills have different biomechanical effects with both statistical and clinical significance. The effects of skills are also different in different types of transfers. Generally, by using the combination of different component transfer skills wheelchair users can reduce shoulder and elbow loading on both sides during transfers. However, the use and position of handgrip (item 8 and 9) may highly relate to increased wrist resultant moment and extension angles which are two risk factors for carpal tunnel syndrome. Therefore, identifying transfer techniques or environmental adaptations (e.g. grab bars or handles) that can reduce wrist loading and extension angles during transfers while keeping the elbow and shoulder loads at a minimum is important future work.

APPENDIX C

INDIVIDUAL'S TRAINING EFFECTS

S1 training effects

Age: 34

Type of disability: complete SCI, T8-9

Body mass: 57.16 Kg

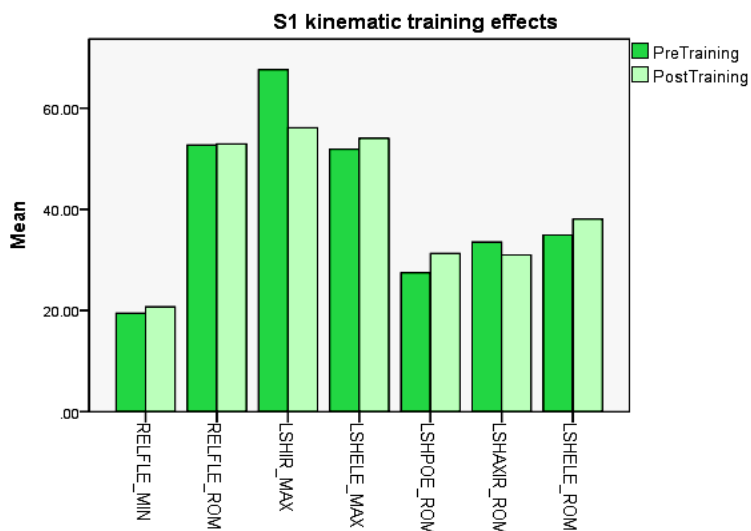
Height: 179.07 cm

Lowest TAI P1 score: 5.83;

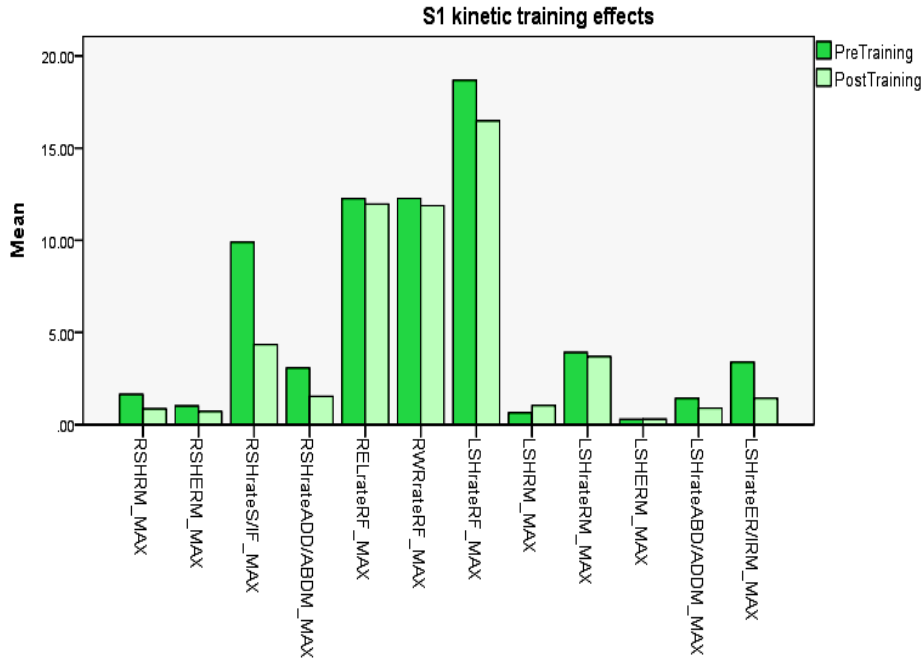
Correction: item 3 (does not transfer over the rear wheel), 6

(places his feet in a stable position), 7 (scoots to the front edge), 9 (correct leading handgrip), and

12 (head-hip relationship)



Abbreviations: REL, right elbow; FLE, flexion, MIN, minimum; ROM, range of motion; LSH, left shoulder; IR, internal rotation; MAX, maximum; ELE, elevation; POE, plane of elevation; AXIR, axial rotation



Abbreviations: RSH, right shoulder; RM, resultant moment; MAX, maximum; ERM, external rotation moment; rate S/IF, rate of rise of superior/inferior force; rateADD/ABDM, rate of rise of adduction/abduction moment; REL, right elbow; rateRF, rate of rise of resultant force; RWR, right wrist; LSH, left shoulder; RM, resultant moment; rateRM, rate of rise of resultant moment; ERM, external rotation moment; rateER/IRM, rate of rise of external/internal rotation moment

S2 training effects

S2 Age: 50

Type of disability: incomplete SCI (ASIA: C), T2

Body mass: 86.94 Kg

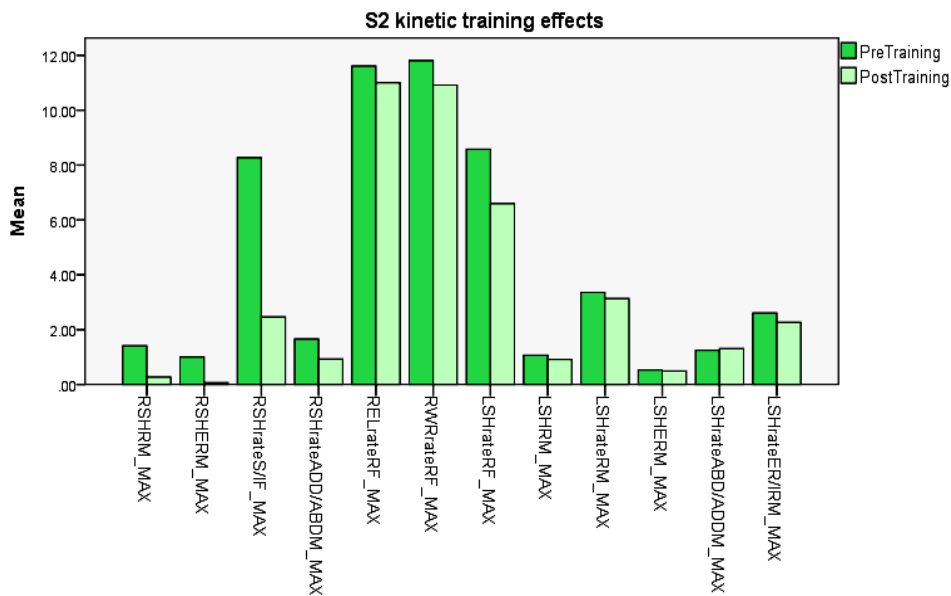
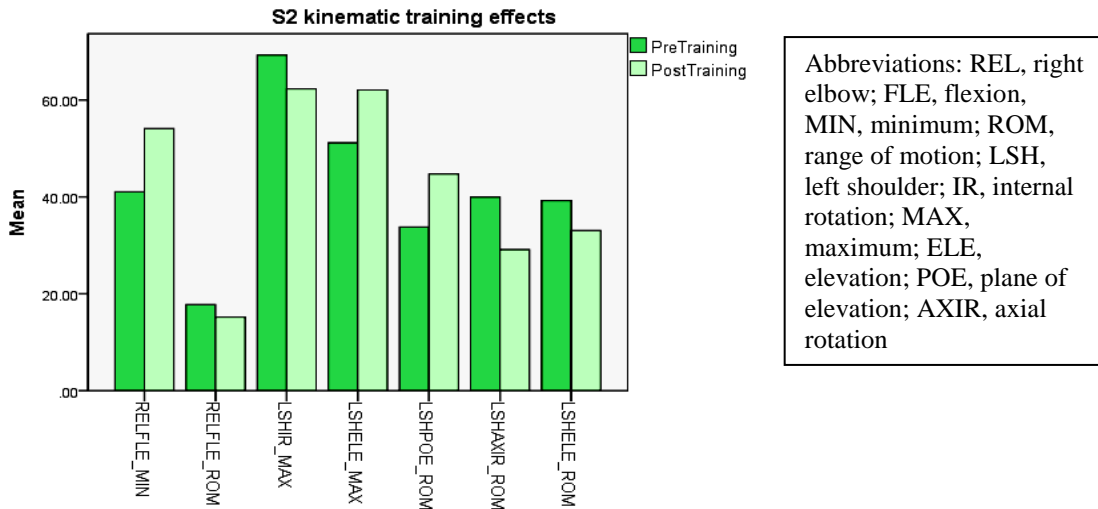
Height: 157.48 cm

Lowest TAI P1 score: 5.83;

TAI corrections: item 1 (wheelchair within 3 inches of the

object), 3 (does not transfer over the rear wheel), 7 (scoots to the front edge), 8 (Hands are in a stable position), 9 (correct leading handgrip), 12 (head-hip relationship), 13 (arms not in

extremely internally rotated & should be abducted 30-45 deg)



Abbreviations: RSH, right shoulder; RM, resultant moment; MAX, maximum; ERM, external rotation moment; rate S/IF, rate of rise of superior/inferior force; rateADD/ABDM, rate of rise of adduction/abduction moment; REL, right elbow; rateRF, rate of rise of resultant force; RWR, right wrist; LSH, left shoulder; RM, resultant moment; rateRM, rate of rise of resultant moment; ERM, external rotation moment; rateER/IRM, rate of rise of external/internal rotation moment

S3 training effects

S3 Age: 39

Type of disability: incomplete SCI (ASIA: B), T12

Body mass: 70.60 Kg

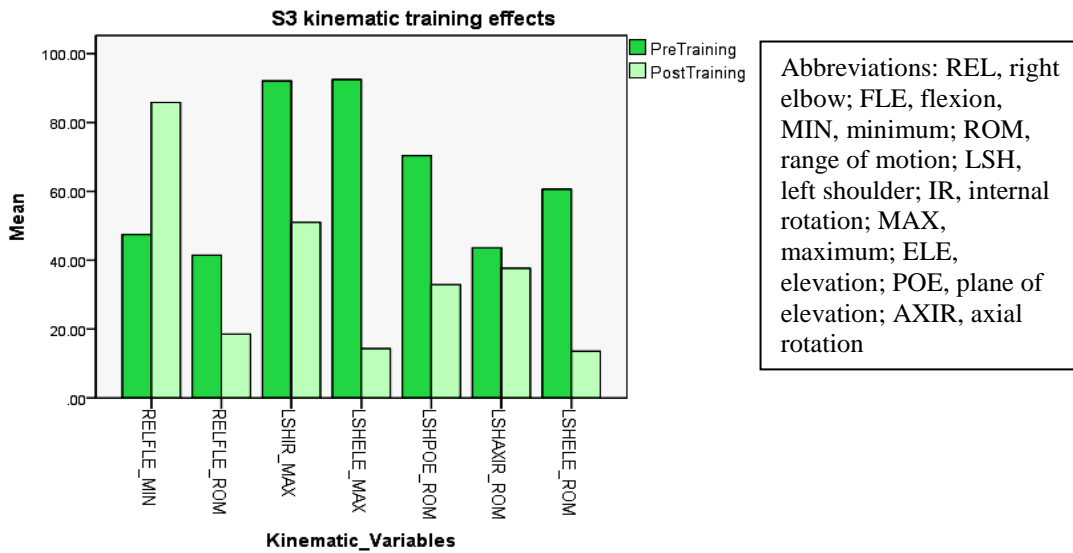
Height: 167.64 cm

Lowest TAI P1 score: 6.92;

TAI corrections: item 1 (wheelchair within 3 inches of the

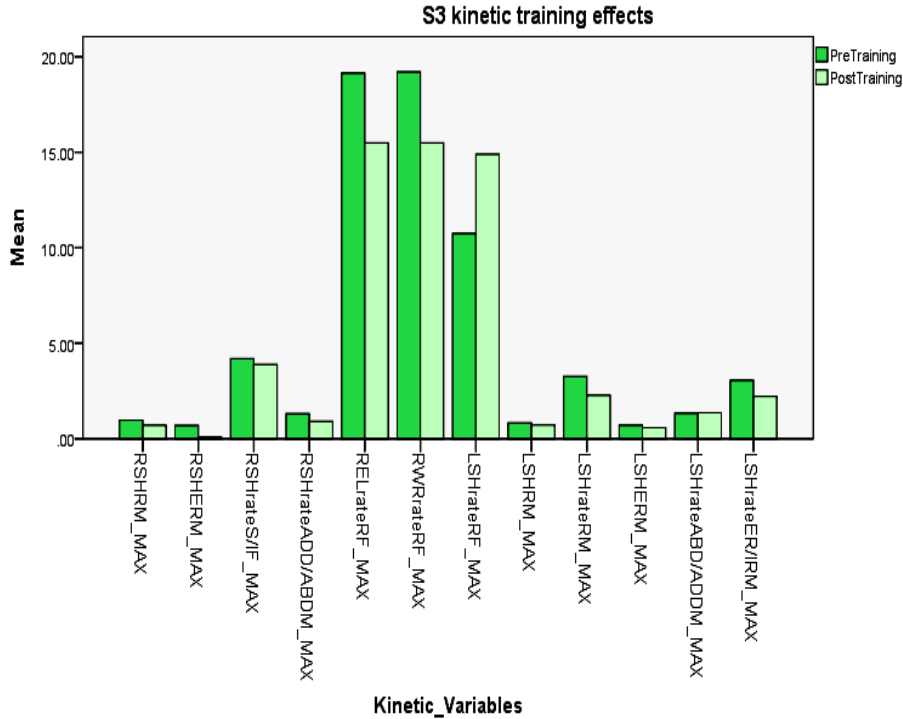
object), 2 (the angle between wheelchair and the surface is 20-45 degrees), 4 (removes the

armrest), 6 (places his feet in a stable position), 9 (correct leading handgrip)



Age: 39; Type of disability: incomplete SCI (ASIA: B), T12; Body mass: 70.60 Kg; Height: 167.64 cm

TAI deficits: item 1, 2, 4, 6, 9, 10



Abbreviations: RSH, right shoulder; RM, resultant moment; MAX, maximum; ERM, external rotation moment; rate S/IF, rate of rise of superior/inferior force; rateADD/ABDM, rate of rise of adduction/abduction moment; REL, right elbow; rateRF, rate of rise of resultant force; RWR, right wrist; LSH, left shoulder; RM, resultant moment; rateRM, rate of rise of resultant moment; ERM, external rotation moment; rateER/IRM, rate of rise of external/internal rotation moment

S4 training effects

S4 Age: 33

Type of disability: complete SCI, T6-7

Body mass: 55.93 Kg

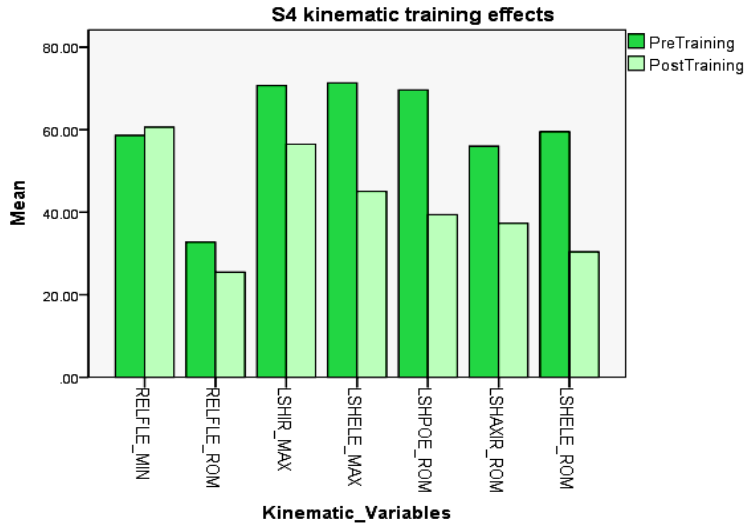
Height: 162.56 cm

Lowest TAI P1 score: 6.92;

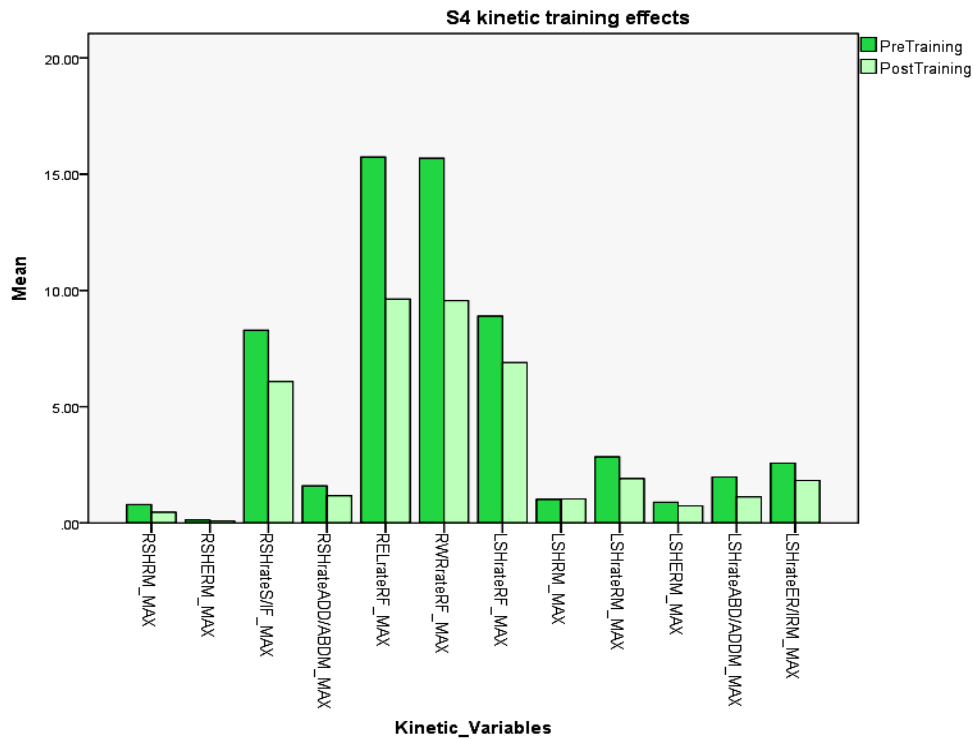
TAI corrections: item 1 (wheelchair within 3 inches of the

object), 4 (removes the armrest), 9 (correct leading handgrip), 12 (head-hip relationship), 13

(arms not in extremely internally rotated & should be abducted 30-45 deg)



Abbreviations: REL, right elbow; FLE, flexion, MIN, minimum; ROM, range of motion; LSH, left shoulder; IR, internal rotation; MAX, maximum; ELE, elevation; POE, plane of elevation; AXIR, axial rotation



Abbreviations: RSH, right shoulder; RM, resultant moment; MAX, maximum; ERM, external rotation moment; rate S/IF, rate of rise of superior/inferior force; rateADD/ABDM, rate of rise of adduction/abduction moment; REL, right elbow; rateRF, rate of rise of resultant force; RWR, right wrist; LSH, left shoulder; RM, resultant moment; rateRM, rate of rise of resultant moment; ERM, external rotation moment; rateER/IRM, rate of rise of external/internal rotation moment

S5 training effects

S5 Age: 33

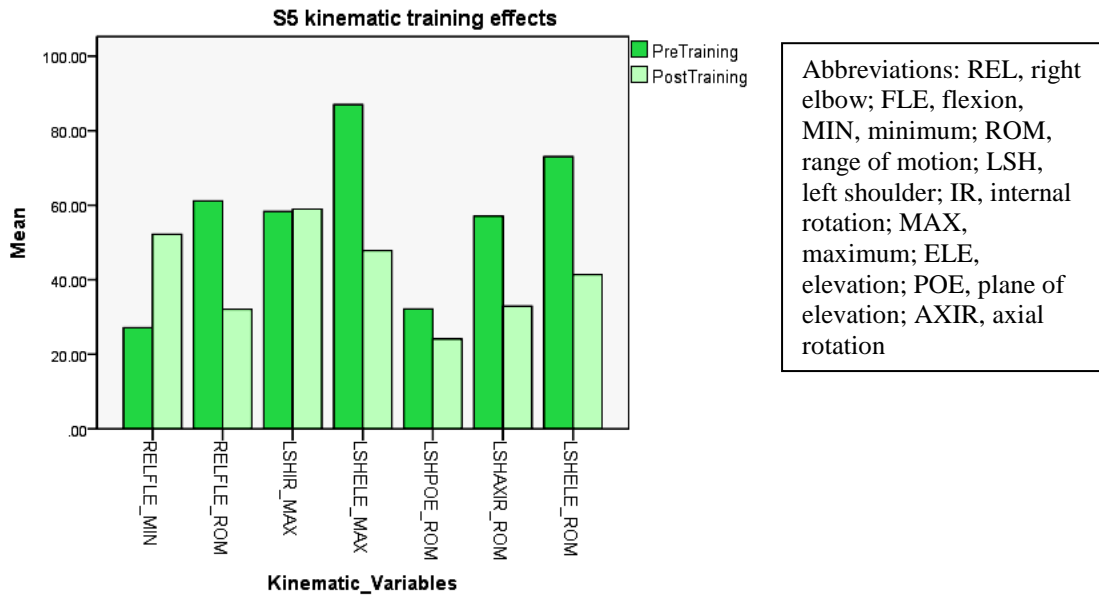
Type of disability: incomplete SCI (ASIA: B), T5

Body mass: 95.61 Kg

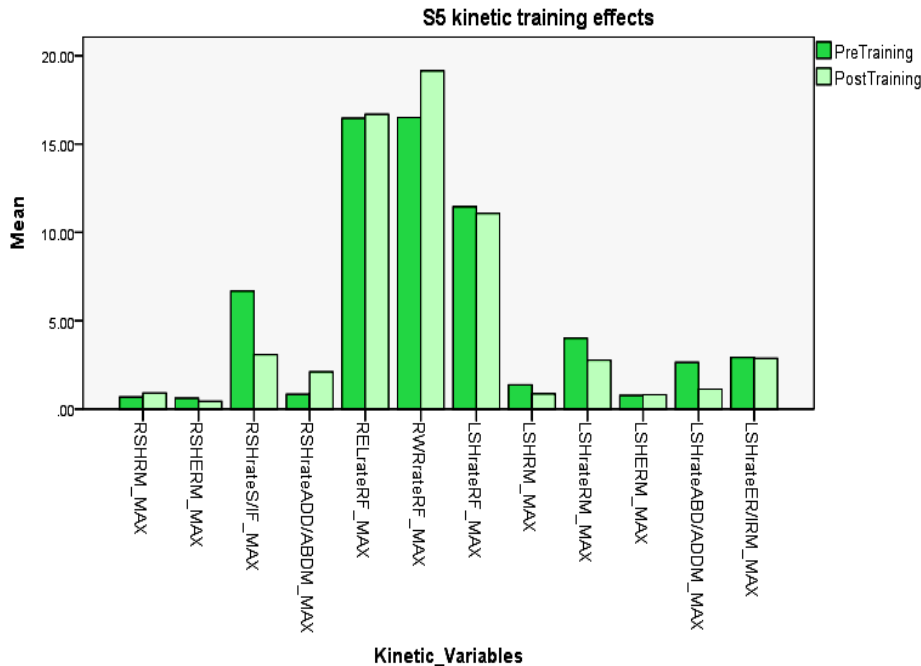
Height: 182.25 cm

Lowest TAI P1 score: 6.54;

TAI corrections: item 1 (wheelchair within 3 inches of the object), 4 (removes the armrest), 9 (correct leading handgrip), 12 (head-hip relationship), 13 (arms not in extremely internally rotated & should be abducted 30-45 deg)



Age: 33; Type of disability: incomplete SCI (ASIA: B), T5; Body mass: 95.61 Kg; Height: 182.25 cm



Abbreviations: RSH, right shoulder; RM, resultant moment; MAX, maximum; ERM, external rotation moment; rate S/IF, rate of rise of superior/inferior force; rateADD/ABDM, rate of rise of adduction/abduction moment; REL, right elbow; rateRF, rate of rise of resultant force; RWR, right wrist; LSH, left shoulder; RM, resultant moment; rateRM, rate of rise of resultant moment; ERM, external rotation moment; rateER/IRM, rate of rise of external/internal rotation moment

S6 training effects

S6 Age: 55

Type of disability: complete SCI, T4-5

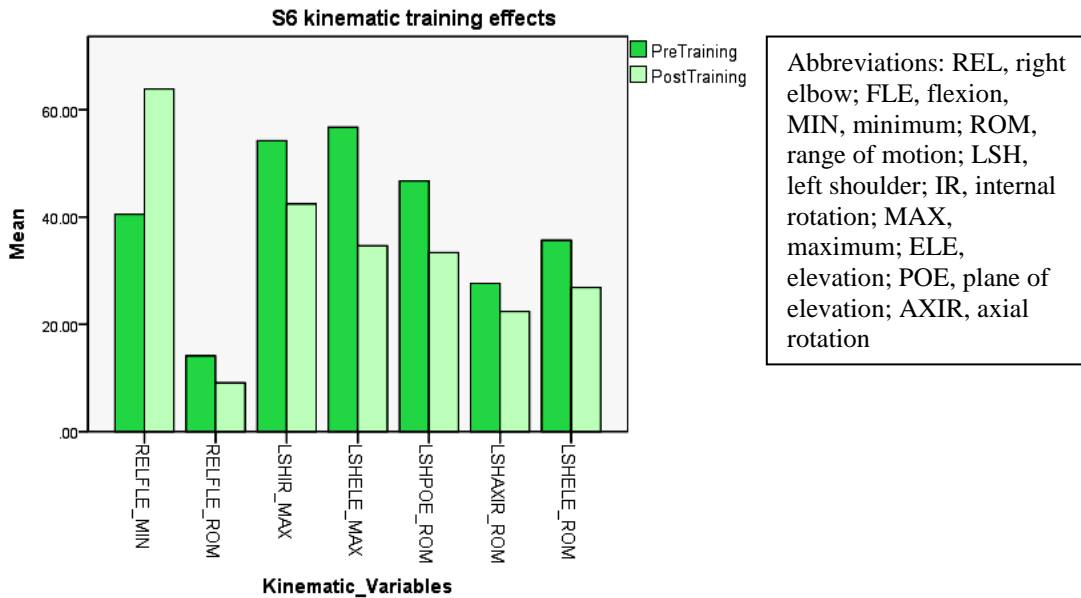
Body mass: 44.95 Kg

Height: 154.94 cm

Lowest TAI P1 score: 6.54;

TAI corrections: item 1 (wheelchair within 3 inches of the

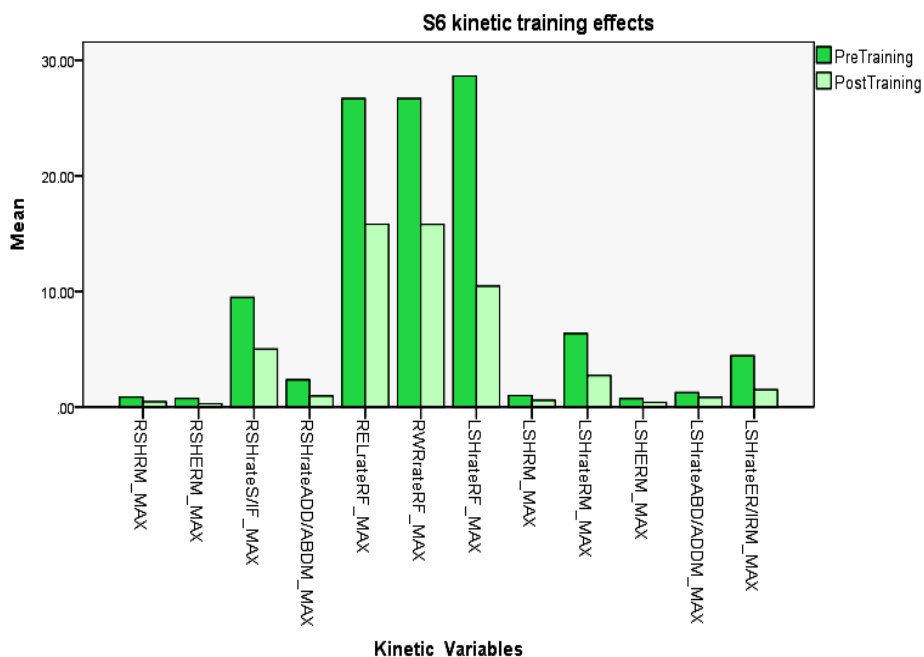
object), 4 (removes the armrest), 6 (places his feet in a stable position), 9 (correct leading handgrip), 12 (head-hip relationship)



Abbreviations: REL, right elbow; FLE, flexion, MIN, minimum; ROM, range of motion; LSH, left shoulder; IR, internal rotation; MAX, maximum; ELE, elevation; POE, plane of elevation; AXIR, axial rotation

Age: 55; Type of disability: complete SCI, T4-5; Body mass: 44.95 Kg; Height: 154.94

TAI deficits: item 1, 4, 6, 9, 10, 12



Abbreviations: RSH, right shoulder; RM, resultant moment; MAX, maximum; ERM, external rotation moment; rate S/IF, rate of rise of superior/inferior force; rateADD/ABDM, rate of rise of adduction/abduction moment; REL, right elbow; rateRF, rate of rise of resultant force; RWR, right wrist; LSH, left shoulder; RM, resultant moment; rateRM, rate of rise of resultant moment; ERM, external rotation moment; rateER/IRM, rate of rise of external/internal rotation moment

S7 training effects

S7 Age: 51

Type of disability: complete SCI, T4-5

Body mass: 59.02 Kg

Height: 172.72 cm

Lowest TAI P1 score: 3.85;

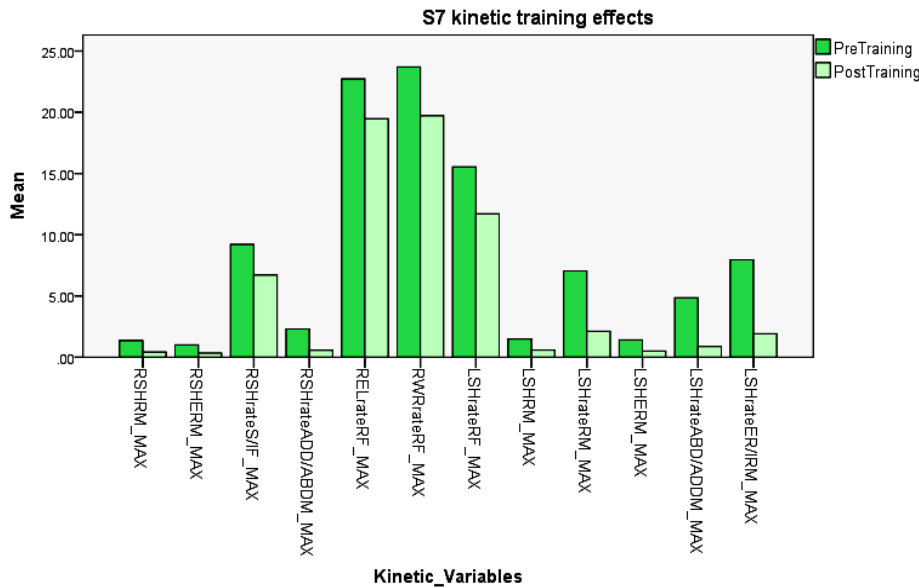
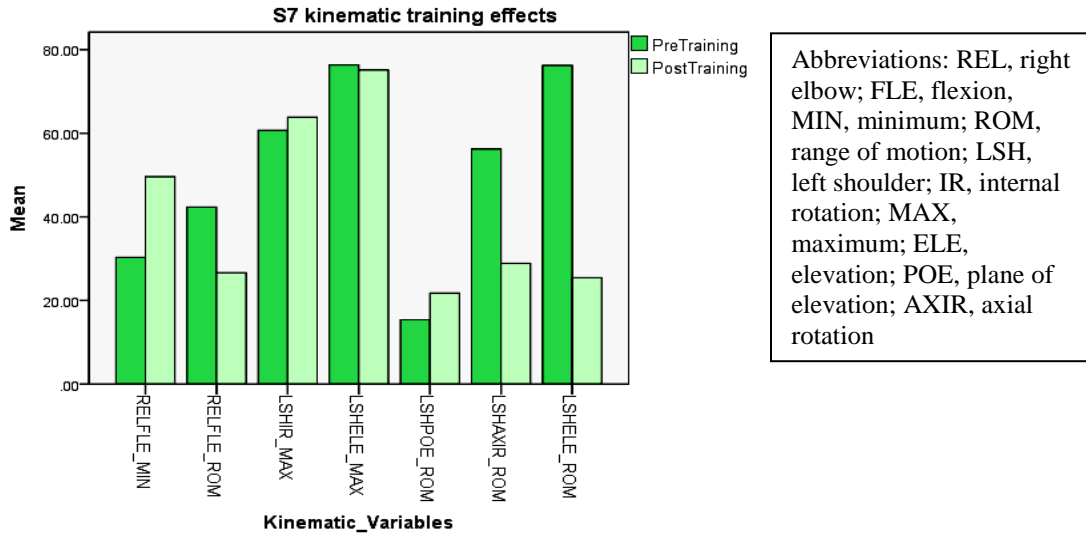
TAI corrections: item 1 (wheelchair within 3 inches of the

object), 2 (the angle between wheelchair and the surface is 20-45 degrees), 3 (does not transfer

over the rear wheel), 4 (removes the armrest), 6 (places his feet in a stable position), 7 (scoots to

the front edge), 8 (Hands are in a stable position), 9 (correct leading handgrip), 12 (head-hip

relationship), 13 (arms not in extremely internally rotated & should be abducted 30-45 deg)



Abbreviations: RSH, right shoulder; RM, resultant moment; MAX, maximum; ERM, external rotation moment; rate S/IF, rate of rise of superior/inferior force; rateADD/ABDM, rate of rise of adduction/abduction moment; REL, right elbow; rateRF, rate of rise of resultant force; RWR, right wrist; LSH, left shoulder; RM, resultant moment; rateRM, rate of rise of resultant moment; ERM, external rotation moment; rateER/IRM, rate of rise of external/internal rotation moment

S8 training effects

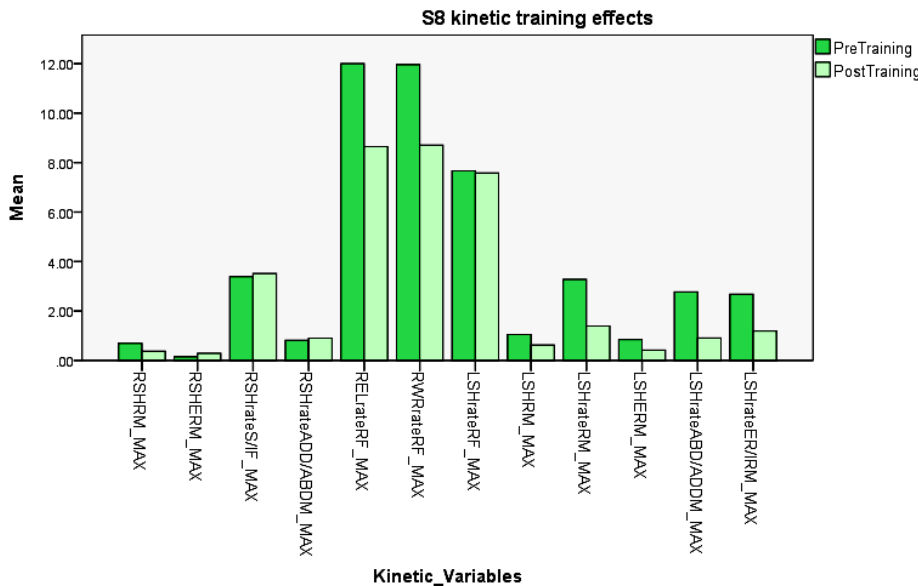
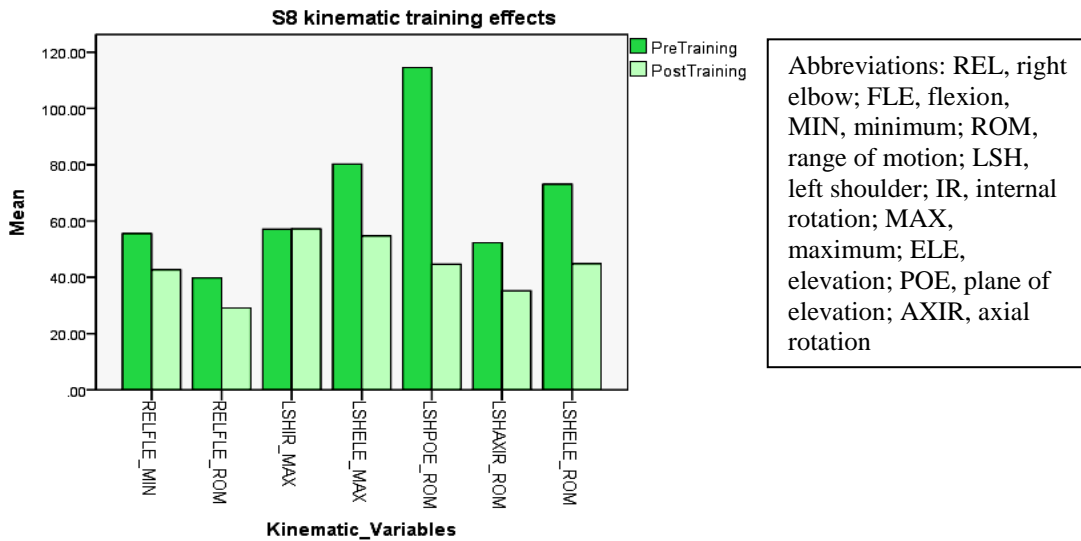
S8 Age: 21

Type of disability: complete SCI, T9-12

Body mass: 63.15 Kg

Height: 180.34 cm

Lowest TAI P1 score: 5.77; TAI corrections: item 1 (wheelchair within 3 inches of the object), 2 (the angle between wheelchair and the surface is 20-45 degrees), 3 (does not transfer over the rear wheel), 4 (removes the armrest), 6 (places his feet in a stable position), 7 (scoots to the front edge), 8 (Hands are in a stable position), 9 (correct leading handgrip), 12 (head-hip relationship), 13 (arms not in extremely internally rotated & should be abducted 30-45 deg)



Abbreviations: RSH, right shoulder; RM, resultant moment; MAX, maximum; ERM, external rotation moment; rate S/IF, rate of rise of superior/inferior force; rateADD/ABDM, rate of rise of adduction/abduction moment; REL, right elbow; rateRF, rate of rise of resultant force; RWR,

right wrist; LSH, left shoulder; RM, resultant moment; rateRM, rate of rise of resultant moment; ERM, external rotation moment; rateER/IRM, rate of rise of external/internal rotation moment

S9 training effects

S9 Age: 50

Type of disability: muscular dystrophy

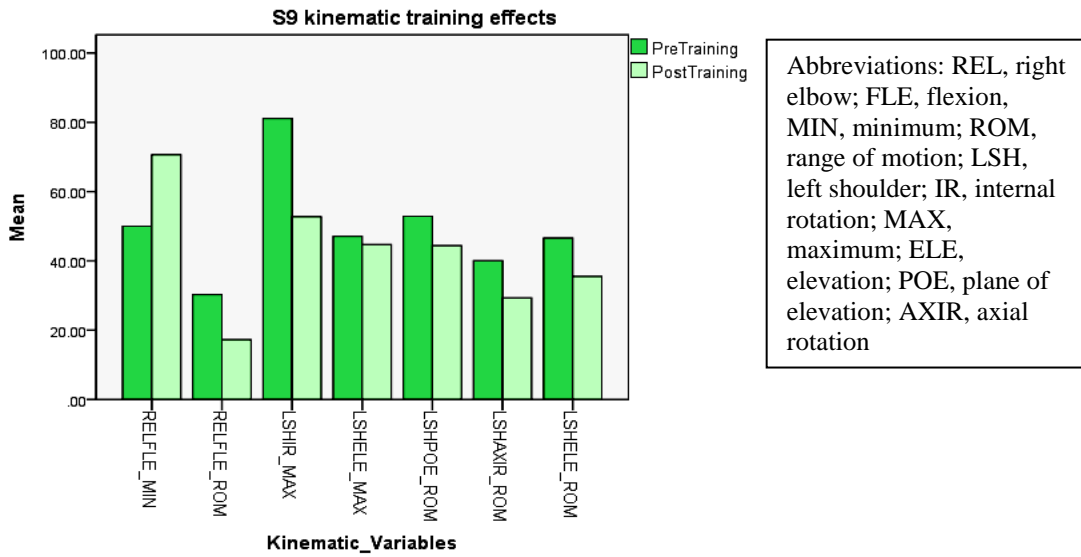
Body mass: 39.45 Kg

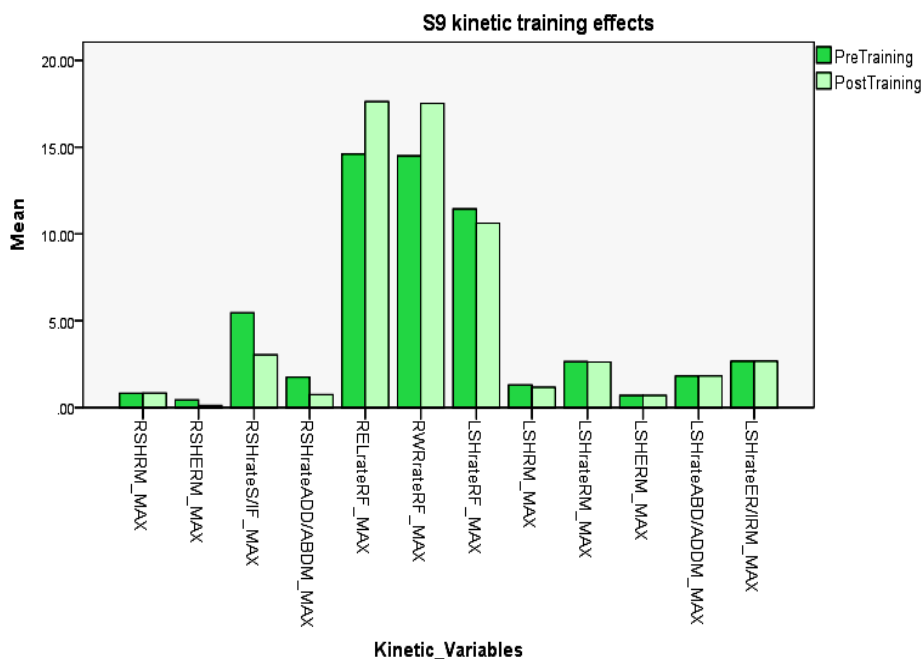
Height: 161.93 cm

Lowest TAI P1 score: 7.31;

TAI corrections: item 1 (wheelchair within 3 inches of the

object), 2 (the angle between wheelchair and the surface is 20-45 degrees), 4 (removes the armrest), 13 (arms not in extremely internally rotated & should be abducted 30-45 deg)





Abbreviations: RSH, right shoulder; RM, resultant moment; MAX, maximum; ERM, external rotation moment; rate S/IF, rate of rise of superior/inferior force; rateADD/ABDM, rate of rise of adduction/abduction moment; REL, right elbow; rateRF, rate of rise of resultant force; RWR, right wrist; LSH, left shoulder; RM, resultant moment; rateRM, rate of rise of resultant moment; ERM, external rotation moment; rateER/IRM, rate of rise of external/internal rotation moment

S10 training effects

S10 Age: 51

Type of disability: incomplete SCI (ASIA: B), C5-6

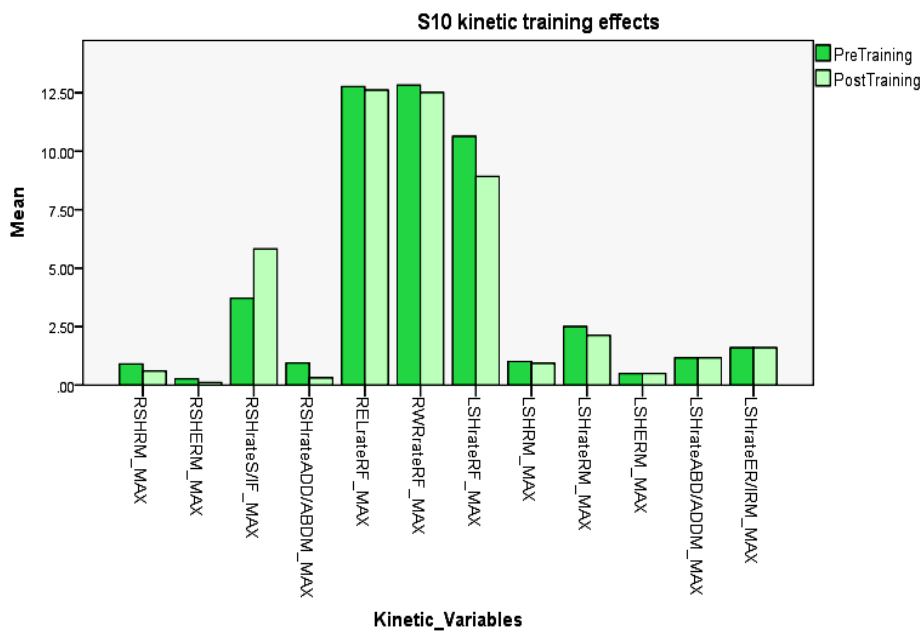
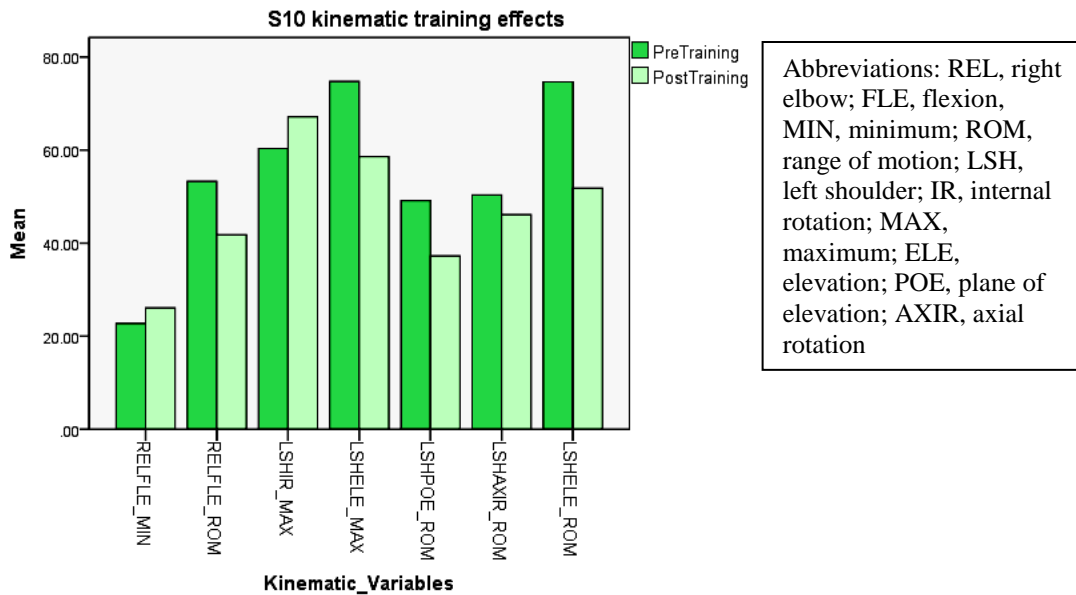
Body mass: 60.11 Kg

Height: 179.07 cm

Lowest TAI P1 score: 6.67;

TAI corrections: item 1 (wheelchair within 3 inches of the

object), 8 (Hands are in a stable position), 9 (correct leading handgrip), 12 (head-hip relationship), 13 (arms not in extremely internally rotated & should be abducted 30-45 deg)



Abbreviations: RSH, right shoulder; RM, resultant moment; MAX, maximum; ERM, external rotation moment; rate S/IF, rate of rise of superior/inferior force; rateADD/ABDM, rate of rise of adduction/abduction moment; REL, right elbow; rateRF, rate of rise of resultant force; RWR, right wrist; LSH, left shoulder; RM, resultant moment; rateRM, rate of rise of resultant moment; ERM, external rotation moment; rateER/IRM, rate of rise of external/internal rotation moment

S11 training effects

S11 Age: 47

Type of disability: complete SCI, T12-L1

Body mass: 76.27 Kg

Height: 175.26 cm

Lowest TAI P1 score: 5.77;

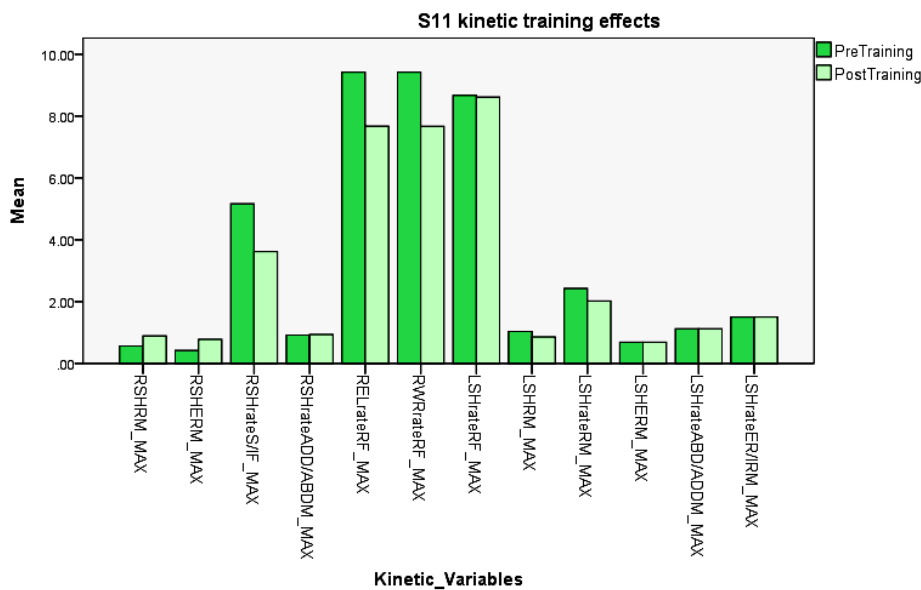
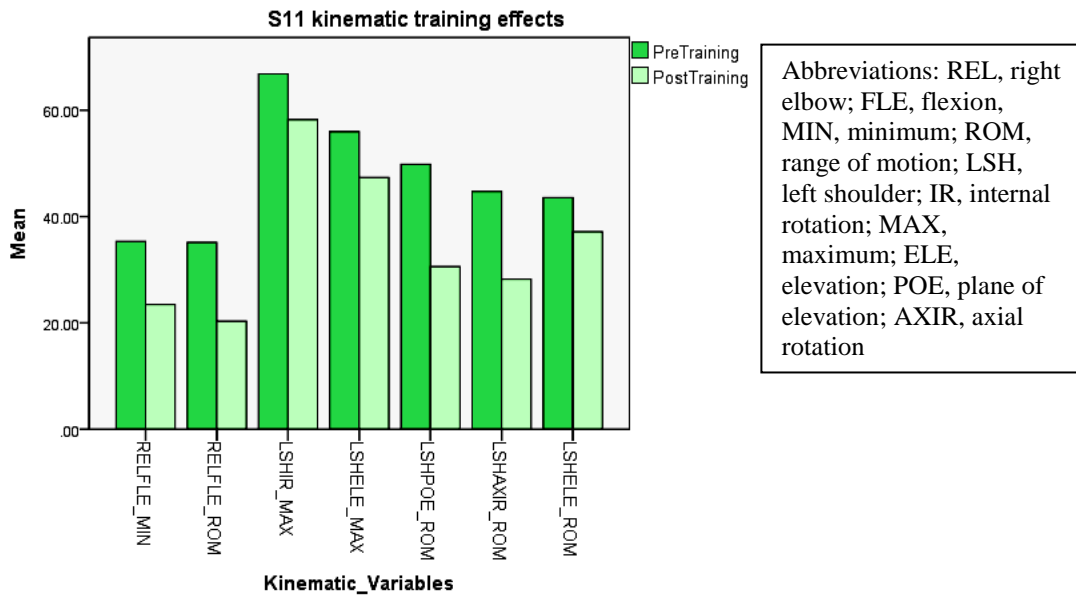
TAI corrections: item 2 (the angle between wheelchair and

the surface is 20-45 degrees), 3 (does not transfer over the rear wheel), 4 (removes the armrest),

6 (places his feet in a stable position), 8 (Hands are in a stable position), 9 (correct leading

handgrip), 12 (head-hip relationship), 13 (arms not in extremely internally rotated & should be

abducted 30-45 deg)



Abbreviations: RSH, right shoulder; RM, resultant moment; MAX, maximum; ERM, external rotation moment; rate S/IF, rate of rise of superior/inferior force; rateADD/ABDM, rate of rise of adduction/abduction moment; REL, right elbow; rateRF, rate of rise of resultant force; RWR, right wrist; LSH, left shoulder; RM, resultant moment; rateRM, rate of rise of resultant moment; ERM, external rotation moment; rateER/IRM, rate of rise of external/internal rotation moment

APPENDIX D

HANDGRIP EFFECTS ON MAXIMUM WRIST EXTENSION ANGLE DURING TRANSFERS

The effects of handgrip correction on maximum wrist extension angle

Pre-training leading wrist maximum extension angle	Pre-training leading wrist maximum extension angle	TAI correction
102.11°	96.7°	Flat hand to close handgrip
23.28°	61.98°	Fist to close handgrip
40.03°	47.09°	Hyperextension MCP to close handgrip
65.67°	61.6°	Flat hand to close handgrip
42.08°	56.5°	Hyperextension MCP to close handgrip
28.12°	71.64°	Hyperextension MCP to close handgrip
41.9°	57.92°	Far target handgrip to close handgrip
67.9°	84.93°	Hyperextension MCP to close handgrip
90.22°	105.85°	Close handgrip to close handgrip
88.79°	50.39°	Flat hand to close handgrip
48.77°	73.61°	Hyperextension MCP to close handgrip

APPENDIX E

HANDGRIP EFFECTS ON MAXIMUM WRIST RESULTANT MOMENT DURING TRANSFERS

The effects of handgrip correction on maximum wrist resultant moment

Pre-training leading wrist maximum resultant moment (N*m/Kg)	Pre-training leading wrist maximum resultant moment (N*m/Kg)	TAI correction
0.34	0.28	Flat hand to close handgrip
0.05	0.14	Fist to close handgrip
0.19	0.27	Hyperextension MCP to close handgrip
0.18	0.26	Flat hand to close handgrip
0.12	0.35	Hyperextension MCP to close handgrip
0.13	0.29	Hyperextension MCP to close handgrip
0.1	0.36	Far target handgrip to close handgrip
0.27	0.35	Hyperextension MCP to close handgrip
0.38	0.35	Close handgrip to close handgrip
0.44	0.25	Flat hand to close handgrip
0.34	0.49	Hyperextension MCP to close handgrip

APPENDIX F

MATLAB CODE: KINEMATICS

```
clc
clear all
close all

% Kinematics for both upper extremities during wheelchair transfer
% filter the raw data first
% decide one transfer cycle
% Calculate rotation matrix of joint (based on natural posture) *
% Chung-Ying Tsai, 11/13/2012

allfile_m = importdata('TPIIFR17_LB01.csv', ',', 11); %(filename,saperate,kinematic data from
line 11+1)
allfile_f = importdata('TPIIFR17_LB01.csv', ',', 11821); %(filename,saperate,kinetic data from
line 13735+1)
load anat_posL.txt; % Reference Vector for LEL $ LEM in L.C.S
load anat_posR.txt; % Reference Vector for REL $ REM in L.C.S
load anat_posT.txt; % Reference Vector for STRN $ XYPD in L.C.S
load anat_Leg.txt; % Anatomic rotation matrix for left UE(natureal posture)
load anat_Reg.txt; % Anatomic rotation matrix for right UE(natureal posture)
fg=[0 0 -9.807]; % gravity in G.L.S

% filter for kinetic data, Load cell:44 45 46 Force, 47 48 49 moment
Fs2=1000; %Sampling Rate Frequency [Hz]
Fc2=7; %Cutoff Frequency for kinetic data[Hz]
w2=2*(Fc2/Fs2); %cutoff/corner frequency in radians
[b2,a2]=butter(4,w2,'low');
f_kinetic=filtfilt(b2,a2,allfile_f.data); %filtfilt=zerolag(zerophase)
ds_kinetic=downsample(f_kinetic,10);
```

```

% filter for kinematic data
Fs3=100; % Sampling Rate Frequency [Hz]
Fc3=5; % Cutoff Frequency for kinematic data[Hz]
w3=2*(Fc3/Fs3); % cutoff/corner frequency in radians
[b3,a3]=butter(4,w3,'low');
all_data=filtfilt(b3,a3,allfile_m.data(:,,:)); %filtfilt=zerolag(zerophase)
% all_data=allfile_m.data(:,,:);
% Cut one transfer cycle
LC_FZ=ds_kinetic(:,46);
BN_FZ=ds_kinetic(:,10);
figure (1);
plot(LC_FZ,'b');
hold;
plot(BN_FZ,'r');
title('WC to BN: Select start from Load Cell(blue), and end from bench(red)')
% xlabel('Frame','fontsize', 16)
% ylabel('Force (N)','fontsize', 16)
[t1_x,t1_y] = ginput(2);
t1_x=round(t1_x); % frame number for one transfer cycle
k_start=t1_x(1);
k_end=t1_x(2);
close figure 1

save cycframe.dat t1_x -ascii;

TOP=all_data(k_start:k_end,2:4); % with LoadCell makers and no bench markers:start from 50
% include LoadCell makers and benchmarkers:start from 59
RTMJ=all_data(k_start:k_end,5:7);
LTMJ=all_data(k_start:k_end,8:10);
RAC=all_data(k_start:k_end,11:13);
RUA1=all_data(k_start:k_end,14:16);
RUA2=all_data(k_start:k_end,17:19);
RUA3=all_data(k_start:k_end,20:22);
RUA4=all_data(k_start:k_end,23:25);
RLE=all_data(k_start:k_end,26:28);
% RME=all_data(k_start:k_end,29:31);
RFA1=all_data(k_start:k_end,29:31);
RFA2=all_data(k_start:k_end,32:34);
RFA3=all_data(k_start:k_end,35:37);
RFA4=all_data(k_start:k_end,38:40);
RUS=all_data(k_start:k_end,41:43);
RRS=all_data(k_start:k_end,44:46);
RCH=all_data(k_start:k_end,47:49);
R3MCP=all_data(k_start:k_end,50:52);
LAC=all_data(k_start:k_end,53:55);
LUA1=all_data(k_start:k_end,56:58);

```

```

LUA2=all_data(k_start:k_end,59:61);
LUA3=all_data(k_start:k_end,62:64);
LUA4=all_data(k_start:k_end,65:67);
LLE=all_data(k_start:k_end,68:70);
% LME=all_data(k_start:k_end,74:76);
LFA1=all_data(k_start:k_end,71:73);
LFA2=all_data(k_start:k_end,74:76);
LFA3=all_data(k_start:k_end,77:79);
LFA4=all_data(k_start:k_end,80:82);
LUS=all_data(k_start:k_end,83:85);
LRS=all_data(k_start:k_end,86:88);
LCH=all_data(k_start:k_end,89:91);
L3MCP=all_data(k_start:k_end,92:94);
C7=all_data(k_start:k_end,95:97);
T3=all_data(k_start:k_end,98:100);
T8=all_data(k_start:k_end,101:103);
XYPD=all_data(k_start:k_end,104:106);
STRN=all_data(k_start:k_end,107:109);

% Calculate local coordinate position for REM and REL (elbow markers)%
% and shoulder joint center %
% create upper arm triad c.s
n=length(TOP(:,1));
for i=1:n
%   X_RUA=norm1((RUA2(i,:)-RUA4(i,:)));
%   Y_RUA=norm1(cross(RUA1(i,:)-0.5*(RUA2(i,:)+RUA4(i,:)),X_RUA));
%   Z_RUA=norm1(cross(X_RUA,Y_RUA));
%   CS_RUA=[X_RUA' Y_RUA' Z_RUA'];
%
%   % The position data for REM, REL & RSH in G.C.S
%
%   X_LUA=norm1((LUA2(i,:)-LUA4(i,:)));
%   Y_LUA=norm1(cross(LUA1(i,:)-0.5*(LUA2(i,:)+LUA4(i,:)),X_LUA));
%   Z_LUA=norm1(cross(X_LUA,Y_LUA));
%   CS_LUA=[X_LUA' Y_LUA' Z_LUA'];

X_RFA=norm1((RFA2(i,:)-RFA4(i,:)));
Y_RFA=norm1(cross(RFA1(i,:)-0.5*(RFA2(i,:)+RFA4(i,:)),X_RFA));
Z_RFA=norm1(cross(X_RFA,Y_RFA));
CS_RFA=[X_RFA' Y_RFA' Z_RFA'];

% The position data for RUS, RRS, REM, and RLM in G.C.S
%   GRUS(i,:)=(CS_RFA*anat_posR(3,:)+(0.5*(RFA2(i,:)+RFA4(i,:))))';
%   GRRS(i,:)=(CS_RFA*anat_posR(4,:)+(0.5*(RFA2(i,:)+RFA4(i,:))))';
%   GRME(i,:)=(CS_RFA*anat_posR(1,:)+(0.5*(RFA2(i,:)+RFA4(i,:))))';
%   GRLE(i,:)=(CS_RFA*anat_posR(2,:)+(0.5*(RFA2(i,:)+RFA4(i,:))))';

```

```

X_LFA=norm1((LFA2(i,:)-LFA4(i,:)));
Y_LFA=norm1(cross(LFA1(i,:)-0.5*(LFA2(i,:)+LFA4(i,:)),X_LFA));
Z_LFA=norm1(cross(X_LFA,Y_LFA));
CS_LFA=[X_LFA' Y_LFA' Z_LFA'];

% The position data for RUS, RRS, REM, and RLM in G.C.S
% GLUS(i,:)=(CS_LFA*anat_posL(3,:)+(0.5*(LFA2(i,:)+LFA4(i,:))))';
% GLRS(i,:)=(CS_LFA*anat_posL(4,:)+(0.5*(LFA2(i,:)+LFA4(i,:))))';
GLME(i,:)=(CS_LFA*anat_posL(1,:)+(0.5*(LFA2(i,:)+LFA4(i,:))))';
% GLLE(i,:)=(CS_LFA*anat_posL(2,:)+(0.5*(LFA2(i,:)+LFA4(i,:))))';

Y_TRN=norm1(T3(i,:)-T8(i,:));
Z_TRN=norm1(cross(C7(i,:)-T8(i,:),Y_TRN));
X_TRN=norm1(cross(Y_TRN,Z_TRN));
CS_TRN=[X_TRN' Y_TRN' Z_TRN'];

% The position data for STRN and XYPD in G.C.S.
GSTRN(i,:)=(CS_TRN*anat_posT(1,:)+(T8(i,:)))';
GXYPD(i,:)=(CS_TRN*anat_posT(2,:)+(T8(i,:)))';
end

% M=[TOP RTMJ LTMJ RAC RUA1 RUA2 RUA3 RUA4 GRLE GRME RFA1 RFA2 RFA3
RFA4 GRUS GRRS...
% RCH R3MCP LAC LUA1 LUA2 LUA3 LUA4 GLLE GLME LFA1 LFA2 LFA3 LFA4
GLUS GLRS LCH...
% L3MCP C7 T3 T8 GXYPD GSTRN];

M=[TOP RTMJ LTMJ RAC RUA1 RUA2 RUA3 RUA4 RLE GRME RFA1 RFA2 RFA3
RFA4 RUS RRS...
RCH R3MCP LAC LUA1 LUA2 LUA3 LUA4 LLE GLME LFA1 LFA2 LFA3 LFA4 LUS
LRS LCH...
L3MCP C7 T3 T8 GXYPD GSTRN];

save marker_tot.dat M -ascii;

for j=1:n
% Trunk: x:forward (ad/ab), y:upward (LRotation/RRotation), z:toward right (Flex/Ext)
Y_TRUNK=norm1(0.5*(GSTRN(j,:)+C7(j,:))-0.5*(GXYPD(j,:)+T8(j,:)));
Z_TRUNK=norm1(cross(GXYPD(j,:)-T8(j,:), Y_TRUNK));
X_TRUNK=norm1(cross(Y_TRUNK,Z_TRUNK));
CS_TRUNK=[X_TRUNK' Y_TRUNK' Z_TRUNK']; % Trunk Coordinate System %

LOLAC(j,:)=(CS_TRUNK'*LAC(j,:))';
LOLAC_z=-LOLAC(j,3);

```

```

LOLAC(j,3)=LOLAC_z;
GMLAC(j,:)=(CS_TRUNK*LOLAC(j,:))';

LOGLLE(j,:)=(CS_TRUNK*LLE(j,:))';
LOGLLE_z=-LOGLLE(j,3);
LOGLLE(j,3)=LOGLLE_z;
GMGLLE(j,:)=(CS_TRUNK*LOGLLE(j,:))';

LOGLME(j,:)=(CS_TRUNK*GLME(j,:))';
LOGLME_z=-LOGLME(j,3);
LOGLME(j,3)=LOGLME_z;
GMGLME(j,:)=(CS_TRUNK*LOGLME(j,:))';

LOGLUS(j,:)=(CS_TRUNK*LUS(j,:))';
LOGLUS_z=-LOGLUS(j,3);
LOGLUS(j,3)=LOGLUS_z;
GMGLUS(j,:)=(CS_TRUNK*LOGLUS(j,:))';

LOGLRS(j,:)=(CS_TRUNK*LRS(j,:))';
LOGLRS_z=-LOGLRS(j,3);
LOGLRS(j,3)=LOGLRS_z;
GMGLRS(j,:)=(CS_TRUNK*LOGLRS(j,:))';

LOLCH(j,:)=(CS_TRUNK*LCH(j,:))';
LOLCH_z=-LOLCH(j,3);
LOLCH(j,3)=LOLCH_z;
GMLCH(j,:)=(CS_TRUNK*LOLCH(j,:))';

LOL3MCP(j,:)=(CS_TRUNK*L3MCP(j,:))';
LOL3MCP_z=-LOL3MCP(j,3);
LOL3MCP(j,3)=LOL3MCP_z;
GML3MCP(j,:)=(CS_TRUNK*LOL3MCP(j,:))';

% R_Upperarm:
% x:forward (ad/ab), y:upward (IRotation/ERotation), z:toward right(Flex/Ext)
Y_RHUMERUS=norm1(RAC(j,:)-0.5*(RLE(j,:)+GRME(j,:)));
X_RHUMERUS=norm1(cross(RLE(j,:)-RAC(j,:),GRME(j,:)-RAC(j,:)));
Z_RHUMERUS=norm1(cross(X_RHUMERUS,Y_RHUMERUS));
CS_RHUMERUS=[X_RHUMERUS' Y_RHUMERUS' Z_RHUMERUS']; % Humerus
Coordinate System %

% R_forearm:
% x:forward (val/var), y:upward (pronatino/supination), z:toward right(Flex/Ext)
Y_RFOREARM=norm1(0.5*(RLE(j,:)+GRME(j,:))-RUS(j,:));
X_RFOREARM=norm1(cross((RRS(j,:)-0.5*(RLE(j,:)+GRME(j,:))),(RUS(j,:)-
0.5*(RLE(j,:)+GRME(j,:))));

```

```

Z_RFOREARM=norm1(cross(X_RFOREARM,Y_RFOREARM));
CS_RFOREARM=[X_RFOREARM' Y_RFOREARM' Z_RFOREARM']; % Forearm
Coordinate System %

% R_hand:
% x:forward (U_Devi/R_Devi), y:upward (pronatino/supination), z:toward right(Flex/Ext)
Y_RHAND=norm1(0.5*(RUS(j,:)+RRS(j,:))-R3MCP(j,:));
X_RHAND=norm1(cross(Y_RHAND,RRS(j,:)-RUS(j,:)));
Z_RHAND=norm1(cross(X_RHAND,Y_RHAND));
CS_RHAND=[X_RHAND' Y_RHAND' Z_RHAND']; % R_HAND Coordinate System %

% L_Upperarm:
% x:forward (ad/ab), y:upward (IRotation/ERotation), z:toward right(Flex/Ext)
Y_LHUMERUS=norm1(GMLAC(j,:)-0.5*(GMGLLE(j,:)+GMGLME(j,:)));
X_LHUMERUS=norm1(cross(GMGLLE(j,:)-GMLAC(j,:),GMGLME(j,:)-GMLAC(j,:)));
Z_LHUMERUS=norm1(cross(X_LHUMERUS,Y_LHUMERUS));
CS_LHUMERUS=[X_LHUMERUS' Y_LHUMERUS' Z_LHUMERUS']; % Humerus
Coordinate System %

% L_forearm:
% x:forward (val/var), y:upward (pronatino/supination), z:toward right(Flex/Ext)
Y_LFOREARM=norm1(0.5*(GMGLLE(j,:)+GMGLME(j,:))-GMGLUS(j,:));
X_LFOREARM=norm1(cross((GMGLRS(j,:)-
0.5*(GMGLLE(j,:)+GMGLME(j,:))),(GMGLUS(j,:)-0.5*(GMGLLE(j,:)+GMGLME(j,:)))));
Z_LFOREARM=norm1(cross(X_LFOREARM,Y_LFOREARM));
CS_LFOREARM=[X_LFOREARM' Y_LFOREARM' Z_LFOREARM']; % Forearm
Coordinate System %

% L_hand:
% x:forward (U_Devi/R_Devi), y:upward (pronatino/supination), z:toward right(Flex/Ext)
Y_LHAND=norm1(0.5*(GMGLUS(j,:)+GMGLRS(j,:))-GML3MCP(j,:));
X_LHAND=norm1(cross(Y_LHAND,GMGLRS(j,:)-GMGLUS(j,:)));
Z_LHAND=norm1(cross(X_LHAND,Y_LHAND));
CS_LHAND=[X_LHAND' Y_LHAND' Z_LHAND']; % L_HAND Coordinate System %

% Rotation matrix of the segments %
R(j*3-2:j*3,:)= [CS_TRUNK CS_RHUMERUS CS_RFOREARM CS_RHAND
CS_LHUMERUS CS_LFOREARM CS_LHAND];

% Calaulate rotation matrix of Joints %
RrRGH(j*3-2:j*3,:)=CS_TRUNK'*CS_RHUMERUS; % shoulder
RrREL(j*3-2:j*3,:)=CS_RHUMERUS'*CS_RFOREARM; % elbow
RrRWT(j*3-2:j*3,:)=CS_RFOREARM'*CS_RHAND; % wrist

RrLGH(j*3-2:j*3,:)=CS_TRUNK'*CS_LHUMERUS; % shoulder
RrLEL(j*3-2:j*3,:)=CS_LHUMERUS'*CS_LFOREARM; % elbow

```

```

RrLWT(j*3-2:j*3,:)=CS_LFOREARM'*CS_LHAND; % wrist

RrTrunk(j*3-2:j*3,:)=R(1:3,1:3)*R(j*3-2:j*3,1:3);

% Calculate euler angle
RGHA=180/pi*euler2(RrRGH(j*3-2:j*3,:),[2 1 2], 'float'); %plane of elevation, IR/ER,
down/elevation
    if RGHA(1,3)>0
        RGHA(1,3)=-RGHA(1,3);
    end
RELA=180/pi*euler2(RrREL(j*3-2:j*3,:),[3 1 2], 'float'); %flexion/extension, varus/valgus,
pronation/supination
RWRA=180/pi*euler2(RrRWT(j*3-2:j*3,:),[3 1 2], 'float'); %flexion/extension, ulnar/radial
deviation, pronation/supination
%   RGHA(1,1)=180/pi*atan(RrRGH(3*j-2,2)/RrRGH(3*j,2));
%   RGHA(1,2)=180/pi*acos(RrRGH(3*j-1,2));
%   RGHA(1,3)=-180/pi*atan2(RrRGH(3*j-1,1),RrRGH(3*j-1,3));

LGHA=180/pi*euler2(RrLGH(j*3-2:j*3,:),[2 1 2], 'float');
if LGHA(1,3)>0
    LGHA(1,3)=-LGHA(1,3);
end
LELA=180/pi*euler2(RrLEL(j*3-2:j*3,:),[3 1 2], 'float');
LWRA=180/pi*euler2(RrLWT(j*3-2:j*3,:),[3 1 2], 'float');
%   LGHA(1,1)=180/pi*atan(RrLGH(3*j-2,2)/RrLGH(3*j,2));
%   LGHA(1,2)=180/pi*acos(RrLGH(3*j-1,2));
%   LGHA(1,3)=-180/pi*atan2(RrLGH(3*j-1,1),RrLGH(3*j-1,3));

TrunkA=180/pi*euler2(RrTrunk(j*3-2:j*3,:),[3 1 2], 'float'); % extension/flexion, R-
sidebending/L, L-axialR/R

REU(j,:)=j RGHA RELA RWRA TrunkA];
LEU(j,:)=j LGHA LELA LWRA];

% Calculate position data for segmental COG%
% Based on Biomechanics and Motor Control of Human Movement/David A.
% Winter, p.98

RELC(j,:)=0.5*(GRME(j,:)+RLE(j,:)); % elbow center
RSHC(j,:)=RAC(j,:); % shoulder center
RUAcog(j,:)=RELC(j,:)+.564*(RSHC(j,:)-RELC(j,:)); % COG of upper arm
RWRC(j,:)=0.5*(RRS(j,:)+RUS(j,:)); % wrist center
RFacog(j,:)=RWRC(j,:)+.570*(RELC(j,:)-RWRC(j,:)); % COG of forearm
RHcog(j,:)=RWRC(j,:)+0.506*(RWRC(j,:)-R3MCP(j,:)); % Cog of hand
RHcont(j,:)=R3MCP(j,:); % contact point of hand

```

```

LELC(j,:)=0.5*(GLME(j,:)+LLE(j,:));      % elbow center
LSHC(j,:)=LAC(j,:);                      % shoulder center
LUAcog(j,:)=LELC(j,:)+.564*(LSHC(j,:)-LELC(j,:)); % COG of upper arm
LWRC(j,:)=0.5*(LRS(j,:)+LUS(j,:));      % wrist center
LFAcog(j,:)=LWRC(j,:)+.570*(LELC(j,:)-LWRC(j,:)); % COG of forearm
LHcog(j,:)=LWRC(j,:)+0.506*(LWRC(j,:)-L3MCP(j,:)); % Cog of hand
LHcont(j,:)=L3MCP(j,:);                 % contact point of hand

```

```

% Calculate segmental proximal and distal moment arm in L.C.S %

```

```

Rlppu=inv(CS_RHUMERUS)*(RSHC(j,:)-RUAcog(j,:));
Rldpu=inv(CS_RHUMERUS)*(RELC(j,:)-RUAcog(j,:));
Rlppf=inv(CS_RFOREARM)*(RELC(j,:)-RFAcog(j,:));
Rldpf=inv(CS_RFOREARM)*(RWRC(j,:)-RFAcog(j,:));
Rlpph=inv(CS_RHAND)*(RWRC(j,:)-RHcog(j,:));
Rldph=inv(CS_RHAND)*(RHcont(j,:)-RHcog(j,:));

```

```

Llppu=inv(CS_LHUMERUS)*(LSHC(j,:)-LUAcog(j,:));
Lldpu=inv(CS_LHUMERUS)*(LELC(j,:)-LUAcog(j,:));
Llppf=inv(CS_LFOREARM)*(LELC(j,:)-LFAcog(j,:));
Lldpf=inv(CS_LFOREARM)*(LWRC(j,:)-LFAcog(j,:));
Llpph=inv(CS_LHAND)*(LWRC(j,:)-LHcog(j,:));
Lldph=inv(CS_LHAND)*(LHcont(j,:)-LHcog(j,:));

```

```

Rsegcog(j,:)= [j RUAcog(j,:) RFAcog(j,:) RHcog(j,:)];
Rsegarm(j,:)= [Rlppu' Rldpu' Rlppf' Rldpf' Rlpph' Rldph'];
Rjcent(j,:)= [i RSHC(j,:) RELC(j,:) RWRC(j,:) RHcont(j,:)];

```

```

Lsegcog(j,:)= [j LUAcog(j,:) LFAcog(j,:) LHcog(j,:)];
Lsegarm(j,:)= [Llppu' Lldpu' Llppf' Lldpf' Llpph' Lldph'];
Ljcent(j,:)= [i LSHC(j,:) LELC(j,:) LWRC(j,:) LHcont(j,:)];

```

```

% calculate the euler parameter for each segment

```

```

ptTR(j,:)= [i param(CS_TRUNK)];
ptRHU(j,:)= [i param(CS_RHUMERUS)];
ptRFA(j,:)= [i param(CS_RFOREARM)];
ptRH(j,:)= [i param(CS_RHAND)];
ptLHU(j,:)= [i param(CS_LHUMERUS)];
ptLFA(j,:)= [i param(CS_LFOREARM)];
ptLH(j,:)= [i param(CS_LHAND)];

```

```

end

```

```

% Trunk linear movement, forward/backward (X), transverse (Y), height (Z)
Trunk_FBROM=max(GSTRN(:,1))-min(GSTRN(:,1));

```

```

Trunk_TRROM=max(GSTRN(:,2))-min(GSTRN(:,2));
Trunk_HTROM=max(GSTRN(:,3))-min(GSTRN(:,3));
Trunk_LROM=[Trunk_FBRROM Trunk_TRROM Trunk_HTROM];

%%%%%%%%%%
%% Export rotation matrix data to files %

RJRM=[RrRGH RrREL RrRWT RrTrunk];
save Rjointmat.dat RJRM -ascii; % Joint angle matrix

LJRM=[RrLGH RrLEL RrLWT];
save Ljointmat.dat LJRM -ascii; % Joint angle matrix

save lcsmat.dat R -ascii; % segmental orientation

%% euler angle
save ReuangLB01.dat REU -ascii;
save LeuangLB01.dat LEU -ascii;
save TrunkLROMLB01.dat Trunk_LROM -ascii; %Trunk linear movement, forward/backward
(X), transverse (Y), height (Z)

save Rcog.dat Rsegcog -ascii; % COG
save Lcog.dat Lsegcog -ascii; % COG
save Rlcsarm.dat Rsegarm -ascii; % moment arm in L.C.C
save Llcsarm.dat Lsegarm -ascii; % moment arm in L.C.C
save Rjcenter.dat Rjcent -ascii; % Joint center
save Ljcenter.dat Ljcent -ascii; % Joint center

save paraTR.dat ptTR -ascii; % euler parameter of trunk
save paraRHU.dat ptRHU -ascii; % euler parameter of upperarm
save paraRFA.dat ptRFA -ascii; % forearm
save paraRH.dat ptRH -ascii; % hand
save paraLHU.dat ptLHU -ascii; % euler parameter of upperarm
save paraLFA.dat ptLFA -ascii; % forearm
save paraLH.dat ptLH -ascii; % hand

%%%%%%%%%%
figure(1)
plot(REU(:,1),REU(:,2),'-ro',REU(:,1),REU(:,3),'-b',REU(:,1),REU(:,4));
title('Right/Trailing arm-shoulder');
legend('plane of elevation(0:abd, 90:flex)', 'axial rotation:IR/ER', 'elevation (negative)');

figure(2)
plot(REU(:,1),REU(:,5),'-ro',REU(:,1),REU(:,6),'-b',REU(:,1),REU(:,7));

```



```

ReuangCM=filtfilt(b2,a2,ReuangLB01); %filtfilt=zerolag(zerophase)

RUE=ReuangCM;
LUE=LeuangCM;

%%%%% determine the descent phase %%%%%%%%%%%
load marker_tot.dat;
C7 = marker_tot(:,100:102);
T3 = marker_tot(:,103:105);
figure;
plot(C7(:,3),'blue')
hold all
plot(T3(:,3),'red')
title('Select the first dip and fast dropping point from red (T3)or blue line (C7)')
[t1_x,t1_y] = ginput(2);
t1_x=round(t1_x);
end_lift=t1_x(2);
prelift_descent=t1_x;
save start_descent_prelift.txt prelift_descent -ascii;
%%%%%%%%%%
%%%%%%%%%%
% load starting_descent.dat;
% end_lift=starting_descent;

R_SHO=RUE(:,2:4);
R_EL=RUE(:,5:7);
R_WR=RUE(:,8:10);
L_SHO=LUE(:,2:4);
L_EL=LUE(:,5:7);
L_WR=LUE(:,8:10);
Trunk=RUE(:,11:13);

%%%%%%%%% peak angle on right shoudler in a whole transfer process
[RSH_POE_MAX, RSHPOE_MAXI]=max(R_SHO(:,1)); % shoulder flexion plane
[RSH_POE_MIN, RSHPOE_MINI]=min(R_SHO(:,1)); % shoulder extension plane
RSH_POE_ROM=RSH_POE_MAX-RSH_POE_MIN;
[RSH_AXIR_MAX, RSHAXIR_MAXI]=max(R_SHO(:,2)); % shoulder IR
[RSH_AXIR_MIN, RSHAXIR_MINI]=min(R_SHO(:,2)); % shoulder ER
RSH_AXIR_ROM=RSH_AXIR_MAX-RSH_AXIR_MIN;
[RSH_ELE_MAX, RSHELE_MAXI]=max(R_SHO(:,3)); % shoulder move down
[RSH_ELE_MIN, RSHELE_MINI]=min(R_SHO(:,3)); % shoulder elevation
RSH_ELE_ROM=RSH_ELE_MAX-RSH_ELE_MIN;

%%%%%%%%% peak angle on right shoulder in the lift phase of a transfer process
[RSH_POE_MAX_LF, RSHPOE_MAXI_LF]=max(R_SHO(1:end_lift,1)); % shoulder
flexion plane

```

```

[RSH_POE_MIN_LF, RSHPOE_MINI_LF]=min(R_SHO(1:end_lift,1)); % shoulder
extension plane
RSHPOE_MAXphase_LF=RSHPOE_MAXI_LF/end_lift;
RSHPOE_MINphase_LF=RSHPOE_MINI_LF/end_lift;
RSH_POE_ROM_LF=RSH_POE_MAX_LF-RSH_POE_MIN_LF;
[RSH_AXIR_MAX_LF, RSHAXIR_MAXI_LF]=max(R_SHO(1:end_lift,2)); %
shoulder IR
[RSH_AXIR_MIN_LF, RSHAXIR_MINI_LF]=min(R_SHO(1:end_lift,2)); % shoulder
ER
RSHAXIR_MAXphase_LF=RSHAXIR_MAXI_LF/end_lift;
RSHAXIR_MINphase_LF=RSHAXIR_MINI_LF/end_lift;
RSH_AXIR_ROM_LF=RSH_AXIR_MAX_LF-RSH_AXIR_MIN_LF;
[RSH_ELE_MAX_LF, RSHELE_MAXI_LF]=max(R_SHO(1:end_lift,3)); % shoulder
move down
[RSH_ELE_MIN_LF, RSHELE_MINI_LF]=min(R_SHO(1:end_lift,3)); % shoulder
elevation
RSHELE_MAXphase_LF=RSHELE_MAXI_LF/end_lift;
RSHELE_MINphase_LF=RSHELE_MINI_LF/end_lift;
RSH_ELE_ROM_LF=RSH_ELE_MAX_LF-RSH_ELE_MIN_LF;

%%%%%% peak angle on right elbow in a whole transfer process
[REL_FLE_MAX, RELFLE_MAXI]=max(R_EL(:,1)); % elbow flexion
[REL_FLE_MIN, RELFLE_MINI]=min(R_EL(:,1)); % elbow extension
REL_FLE_ROM=REL_FLE_MAX-REL_FLE_MIN;
[REL_VAR_MAX, RELVAR_MAXI]=max(R_EL(:,2)); % elbow varus
[REL_VAR_MIN, RELVAR_MINI]=min(R_EL(:,2)); % elbow varus/valgus
REL_VAR_ROM=REL_VAR_MAX-REL_VAR_MIN;
[REL_PRO_MAX, RELPRO_MAXI]=max(R_EL(:,3)); % elbow pronation
[REL_PRO_MIN, RELPRO_MINI]=min(R_EL(:,3)); % elbow pronation/supination
REL_PRO_ROM=REL_PRO_MAX-REL_PRO_MIN;

%%%%%% peak angle on right elbow in the lift phase of a transfer process
[REL_FLE_MAX_LF, RELFLE_MAXI_LF]=max(R_EL(1:end_lift,1)); % elbow
flexion
[REL_FLE_MIN_LF, RELFLE_MINI_LF]=min(R_EL(1:end_lift,1)); % elbow
extension
RELFLE_MAXphase_LF=RELFLE_MAXI_LF/end_lift;
RELFLE_MINphase_LF=RELFLE_MINI_LF/end_lift;
REL_FLE_ROM_LF=REL_FLE_MAX_LF-REL_FLE_MIN_LF;
[REL_VAR_MAX_LF, RELVAR_MAXI_LF]=max(R_EL(1:end_lift,2)); % elbow
varus
[REL_VAR_MIN_LF, RELVAR_MINI_LF]=min(R_EL(1:end_lift,2)); % elbow
varus/valgus
RELVAR_MAXphase_LF=RELVAR_MAXI_LF/end_lift;
RELVAR_MINphase_LF=RELVAR_MINI_LF/end_lift;
REL_VAR_ROM_LF=REL_VAR_MAX_LF-REL_VAR_MIN_LF;

```

```

[REL_PRO_MAX_LF, RELPRO_MAXI_LF]=max(R_EL(1:end_lift,3)); % elbow
pronation
[REL_PRO_MIN_LF, RELPRO_MINI_LF]=min(R_EL(1:end_lift,3)); % elbow
pronation/supination
RELPRO_MAXphase_LF=RELPRO_MAXI_LF/end_lift;
RELPRO_MINphase_LF=RELPRO_MINI_LF/end_lift;
REL_PRO_ROM_LF=REL_PRO_MAX_LF-REL_PRO_MIN_LF;

%%%%%% peak angle on right wrist in a whole transfer proces
[RWR_FLE_MAX, RWRFLE_MAXI]=max(R_WR(:,1)); % wrist flexion
[RWR_FLE_MIN, RWRFLE_MINI]=min(R_WR(:,1)); % wrist extension
RWR_FLE_ROM=RWR_FLE_MAX-RWR_FLE_MIN;
[RWR_ULD_MAX, RWRULD_MAXI]=max(R_WR(:,2)); % wrist ulnar deviation
[RWR_ULD_MIN, RWRULD_MINI]=min(R_WR(:,2)); % wrist extension
RWR_ULD_ROM=RWR_ULD_MAX-RWR_ULD_MIN;
[RWR_PRO_MAX, RWRPRO_MAXI]=max(R_WR(:,3)); % wrist pronation
[RWR_PRO_MIN, RWRPRO_MINI]=min(R_WR(:,3)); % wrist pronation/supination
RWR_PRO_ROM=RWR_PRO_MAX-RWR_PRO_MIN;

%%%%%% peak angle on right wrist in the lift phase of a transfer process
flexion
[RWR_FLE_MAX_LF, RWRFLE_MAXI_LF]=max(R_WR(1:end_lift,1)); % wrist
extension
[RWR_FLE_MIN_LF, RWRFLE_MINI_LF]=min(R_WR(1:end_lift,1)); % wrist
extension
RWRFLE_MAXphase_LF=RWRFLE_MAXI_LF/end_lift;
RWRFLE_MINphase_LF=RWRFLE_MINI_LF/end_lift;
RWR_FLE_ROM_LF=RWR_FLE_MAX_LF-RWR_FLE_MIN_LF;
[RWR_ULD_MAX_LF, RWRULD_MAXI_LF]=max(R_WR(1:end_lift,2)); % wrist
ulnar deviation
[RWR_ULD_MIN_LF, RWRULD_MINI_LF]=min(R_WR(1:end_lift,2)); % wrist
extension
RWRULD_MAXphase_LF=RWRULD_MAXI_LF/end_lift;
RWRULD_MINphase_LF=RWRULD_MINI_LF/end_lift;
RWR_ULD_ROM_LF=RWR_ULD_MAX_LF-RWR_ULD_MIN_LF;
[RWR_PRO_MAX_LF, RWRPRO_MAXI_LF]=max(R_WR(1:end_lift,3)); % wrist
pronation
[RWR_PRO_MIN_LF, RWRPRO_MINI_LF]=min(R_WR(1:end_lift,3)); % wrist
pronation/supination
RWRPRO_MAXphase_LF=RWRPRO_MAXI_LF/end_lift;
RWRPRO_MINphase_LF=RWRPRO_MINI_LF/end_lift;
RWR_PRO_ROM_LF=RWR_PRO_MAX_LF-RWR_PRO_MIN_LF;

% [TR_FLE_MAX, TRFLE_MAXI]=max(Trunk(:,1));
% [TR_FLE_MIN, TRFLE_MINI]=min(Trunk(:,1));
% TR_FLE_ROM=TR_FLE_MAX-TR_FLE_MIN;
% [TR_SB_MAX, TRSB_MAXI]=max(Trunk(:,2));

```

```

% [TR_SB_MIN, TRSB_MINI]=min(Trunk(:,2));
% TR_SB_ROM=TR_SB_MAX-TR_SB_MIN;
% [TR_AR_MAX, TRAR_MAXI]=max(Trunk(:,3));
% [TR_AR_MIN, TRAR_MINI]=min(Trunk(:,3));
% TR_AR_ROM=TR_AR_MAX-TR_AR_MIN;

%LEFT SIDE
%%%%%%%% peak angle on left shoulder in a whole transfer process
[LSH_POE_MAX, LSHPOE_MAXI]=max(L_SHO(:,1)); % shoulder flexion plane
[LSH_POE_MIN, LSHPOE_MINI]=min(L_SHO(:,1)); % shoulder extension plane
LSH_POE_ROM=LSH_POE_MAX-LSH_POE_MIN;
[LSH_AXIR_MAX, LSHAXIR_MAXI]=max(L_SHO(:,2)); % shoulder IR
[LSH_AXIR_MIN, LSHAXIR_MINI]=min(L_SHO(:,2)); % shoulder ER
LSH_AXIR_ROM=LSH_AXIR_MAX-LSH_AXIR_MIN;
[LSH_ELE_MAX, LSHELE_MAXI]=max(L_SHO(:,3)); % shoulder move down
[LSH_ELE_MIN, LSHELE_MINI]=min(L_SHO(:,3)); % shoulder elevation
LSH_ELE_ROM=LSH_ELE_MAX-LSH_ELE_MIN;

%%%%%%%% peak angle on left shoulder in the lift phase of a transfer process
flexion plane
[LSH_POE_MAX_LF, LSHPOE_MAXI_LF]=max(L_SHO(1:end_lift,1)); % shoulder
extension plane
[LSH_POE_MIN_LF, LSHPOE_MINI_LF]=min(L_SHO(1:end_lift,1)); % shoulder
LSHPOE_MAXphase_LF=LSHPOE_MAXI_LF/end_lift;
LSHPOE_MINphase_LF=LSHPOE_MINI_LF/end_lift;
LSH_POE_ROM_LF=LSH_POE_MAX_LF-LSH_POE_MIN_LF;
shoulder IR
[LSH_AXIR_MAX_LF, LSHAXIR_MAXI_LF]=max(L_SHO(1:end_lift,2)); %
ER
[LSH_AXIR_MIN_LF, LSHAXIR_MINI_LF]=min(L_SHO(1:end_lift,2)); %
LSHAXIR_MAXphase_LF=LSHAXIR_MAXI_LF/end_lift;
LSHAXIR_MINphase_LF=LSHAXIR_MINI_LF/end_lift;
LSH_AXIR_ROM_LF=LSH_AXIR_MAX_LF-LSH_AXIR_MIN_LF;
move down
[LSH_ELE_MAX_LF, LSHELE_MAXI_LF]=max(L_SHO(1:end_lift,3)); % shoulder
elevation
[LSH_ELE_MIN_LF, LSHELE_MINI_LF]=min(L_SHO(1:end_lift,3)); % shoulder
LSHELE_MAXphase_LF=LSHELE_MAXI_LF/end_lift;
LSHELE_MINphase_LF=LSHELE_MINI_LF/end_lift;
LSH_ELE_ROM_LF=LSH_ELE_MAX_LF-LSH_ELE_MIN_LF;

%%%%%%%% peak angle on left elbow in a whole transfer process
[LEL_FLE_MAX, LELFLE_MAXI]=max(L_EL(:,1)); % elbow flexion
[LEL_FLE_MIN, LELFLE_MINI]=min(L_EL(:,1)); % elbow extension
LEL_FLE_ROM=LEL_FLE_MAX-LEL_FLE_MIN;
[LEL_VAR_MAX, LELVAR_MAXI]=max(L_EL(:,2)); % elbow varus

```

```

[LEL_VAR_MIN, LELVAR_MINI]=min(L_EL(:,2)); % elbow varus/valgus
LEL_VAR_ROM=LEL_VAR_MAX-LEL_VAR_MIN;
[LEL_PRO_MAX, LELPRO_MAXI]=max(L_EL(:,3)); % elbow pronation
[LEL_PRO_MIN, LELPRO_MINI]=min(L_EL(:,3)); % elbow pronation/supination
LEL_PRO_ROM=LEL_PRO_MAX-LEL_PRO_MIN;

%%%%% peak angle on left elbow in the lift phase of a transfer process
[LEL_FLE_MAX_LF, LELFLE_MAXI_LF]=max(L_EL(1:end_lift,1)); % elbow flexion
[LEL_FLE_MIN_LF, LELFLE_MINI_LF]=min(L_EL(1:end_lift,1)); % elbow
extension
LELFLE_MAXphase_LF=LELFLE_MAXI_LF/end_lift;
LELFLE_MINphase_LF=LELFLE_MINI_LF/end_lift;
LEL_FLE_ROM_LF=LEL_FLE_MAX_LF-LEL_FLE_MIN_LF;
[LEL_VAR_MAX_LF, LELVAR_MAXI_LF]=max(L_EL(1:end_lift,2)); % elbow varus
[LEL_VAR_MIN_LF, LELVAR_MINI_LF]=min(L_EL(1:end_lift,2)); % elbow
varus/valgus
LELVAR_MAXphase_LF=LELVAR_MAXI_LF/end_lift;
LELVAR_MINphase_LF=LELVAR_MINI_LF/end_lift;
LEL_VAR_ROM_LF=LEL_VAR_MAX_LF-LEL_VAR_MIN_LF;
[LEL_PRO_MAX_LF, LELPRO_MAXI_LF]=max(L_EL(1:end_lift,3)); % elbow
pronation
[LEL_PRO_MIN_LF, LELPRO_MINI_LF]=min(L_EL(1:end_lift,3)); % elbow
pronation/supination
LELPRO_MAXphase_LF=LELPRO_MAXI_LF/end_lift;
LELPRO_MINphase_LF=LELPRO_MINI_LF/end_lift;
LEL_PRO_ROM_LF=LEL_PRO_MAX_LF-LEL_PRO_MIN_LF;

%%%%% peak angle on left wrist in a whole transfer process
[LWR_FLE_MAX, LWRFLE_MAXI]=max(L_WR(:,1)); % wrist flexion
[LWR_FLE_MIN, LWRFLE_MINI]=min(L_WR(:,1)); % wrist extension
LWR_FLE_ROM=LWR_FLE_MAX-LWR_FLE_MIN;
[LWR_ULD_MAX, LWRULD_MAXI]=max(L_WR(:,2)); % wrist ulnar deviation
[LWR_ULD_MIN, LWRULD_MINI]=min(L_WR(:,2)); % wrist extension
LWR_ULD_ROM=LWR_ULD_MAX-LWR_ULD_MIN;
[LWR_PRO_MAX, LWRPRO_MAXI]=max(L_WR(:,3)); % wrist pronation
[LWR_PRO_MIN, LWRPRO_MINI]=min(L_WR(:,3)); % wrist pronation/supination
LWR_PRO_ROM=LWR_PRO_MAX-LWR_PRO_MIN;

%%%%% peak angle on left wrist in the lift phase of a transfer process
[LWR_FLE_MAX_LF, LWRFLE_MAXI_LF]=max(L_WR(1:end_lift,1)); % wrist
flexion
[LWR_FLE_MIN_LF, LWRFLE_MINI_LF]=min(L_WR(1:end_lift,1)); % wrist
extension
LWRFLE_MAXphase_LF=LWRFLE_MAXI_LF/end_lift;
LWRFLE_MINphase_LF=LWRFLE_MINI_LF/end_lift;
LWR_FLE_ROM_LF=LWR_FLE_MAX_LF-LWR_FLE_MIN_LF;

```

```

[LWR_ULD_MAX_LF, LWRULD_MAXI_LF]=max(L_WR(1:end_lift,2)); % wrist
ulnar deviation
[LWR_ULD_MIN_LF, LWRULD_MINI_LF]=min(L_WR(1:end_lift,2)); % wrist
extension
LWRULD_MAXphase_LF=LWRULD_MAXI_LF/end_lift;
LWRULD_MINphase_LF=LWRULD_MINI_LF/end_lift;
LWR_ULD_ROM_LF=LWR_ULD_MAX_LF-LWR_ULD_MIN_LF;
[LWR_PRO_MAX_LF, LWRPRO_MAXI_LF]=max(L_WR(1:end_lift,3)); % wrist
pronation
[LWR_PRO_MIN_LF, LWRPRO_MINI_LF]=min(L_WR(1:end_lift,3)); % wrist
pronation/supination
LWRPRO_MAXphase_LF=LWRPRO_MAXI_LF/end_lift;
LWRPRO_MINphase_LF=LWRPRO_MINI_LF/end_lift;
LWR_PRO_ROM_LF=LWR_PRO_MAX_LF-LWR_PRO_MIN_LF;

%%%%%% peak angle on TRUNK in a whole transfer process
[TR_FLE_MAX, TRFLE_MAXI]=max(Trunk(:,1)); % Trunk extension
[TR_FLE_MIN, TRFLE_MINI]=min(Trunk(:,1)); % Trunk flexion
TR_FLE_ROM=TR_FLE_MAX-TR_FLE_MIN;
[TR_SideB_MAX, TRSideB_MAXI]=max(Trunk(:,2)); % trunk right side bending
[TR_SideB_MIN, TRSideB_MINI]=min(Trunk(:,2)); % trunk left side bending
TR_SideB_ROM=TR_SideB_MAX-TR_SideB_MIN;
[TR_AxialR_MAX, TRAxialR_MAXI]=max(Trunk(:,3)); % trunk left axial rotation
[TR_AxialR_MIN, TRAxialR_MINI]=min(Trunk(:,3)); % trunk right axial rotation
TR_AxialR_ROM=TR_AxialR_MAX-TR_AxialR_MIN;

%%%%%% peak angle on TRUNK in the lift phase of a transfer process
[TR_FLE_MAX_LF, TRFLE_MAXI_LF]=max(Trunk(1:end_lift,1)); % Trunk extension
[TR_FLE_MIN_LF, TRFLE_MINI_LF]=min(Trunk(1:end_lift,1)); % Trunk flexion
TRFLE_MAXphase_LF=TRFLE_MAXI_LF/end_lift;
TRFLE_MINphase_LF=TRFLE_MINI_LF/end_lift;
TR_FLE_ROM_LF=abs(TR_FLE_MAX_LF-TR_FLE_MIN_LF);
[TR_SideB_MAX_LF, TRSideB_MAXI_LF]=max(Trunk(1:end_lift,2)); % trunk right
side bending
[TR_SideB_MIN_LF, TRSideB_MINI_LF]=min(Trunk(1:end_lift,2)); % trunk left side
bending
TRSideB_MAXphase_LF=TRSideB_MAXI_LF/end_lift;
TRSideB_MINphase_LF=TRSideB_MINI_LF/end_lift;
TR_SideB_ROM_LF=abs(TR_SideB_MAX_LF-TR_SideB_MIN_LF);
[TR_AxialR_MAX_LF, TRAxialR_MAXI_LF]=max(Trunk(1:end_lift,3)); % trunk left
axial rotation
[TR_AxialR_MIN_LF, TRAxialR_MINI_LF]=min(Trunk(1:end_lift,3)); % trunk right
axial rotation
TRAxialR_MAXphase_LF=TRAxialR_MAXI_LF/end_lift;
TRAxialR_MINphase_LF=TRAxialR_MINI_LF/end_lift;
TR_AxialR_ROM_LF=abs(TR_AxialR_MAX_LF-TR_AxialR_MIN_LF);

```

```

% Peak value =[index
%         value]
RSH_PEAK=[RSHPOE_MAXI RSHPOE_MINI RSHAXIR_MAXI RSHAXIR_MINI
RSHELE_MAXI RSHELE_MINI;...
RSH_POE_MAX RSH_POE_MIN RSH_AXIR_MAX RSH_AXIR_MIN
RSH_ELE_MAX RSH_ELE_MIN];
REL_PEAK=[REL_FLE_MAXI REL_FLE_MINI RELVAR_MAXI RELVAR_MINI
RELPRO_MAXI RELPRO_MINI;...
REL_FLE_MAX REL_FLE_MIN REL_VAR_MAX REL_VAR_MIN
REL_PRO_MAX REL_PRO_MIN];
RWR_PEAK=[RWR_FLE_MAXI RWR_FLE_MINI RWRULD_MAXI RWRULD_MINI
RWRPRO_MAXI RWRPRO_MINI;...
RWR_FLE_MAX RWR_FLE_MIN RWR_ULD_MAX RWR_ULD_MIN
RWR_PRO_MAX RWR_PRO_MIN];
TR_PEAK=[TR_FLE_MAXI TR_FLE_MINI TR_SideB_MAXI TR_SideB_MINI
TR_AxialR_MAXI TR_AxialR_MINI;...
TR_FLE_MAX TR_FLE_MIN TR_SideB_MAX TR_SideB_MIN TR_AxialR_MAX
TR_AxialR_MIN];

RSH_PEAK_LF=[RSHPOE_MAXI_LF RSHPOE_MINI_LF RSHAXIR_MAXI_LF
RSHAXIR_MINI_LF RSHELE_MAXI_LF RSHELE_MINI_LF;...
RSHPOE_MAXphase_LF RSHPOE_MINphase_LF RSHAXIR_MAXphase_LF
RSHAXIR_MINphase_LF RSHELE_MAXphase_LF RSHELE_MINphase_LF;...
RSH_POE_MAX_LF RSH_POE_MIN_LF RSH_AXIR_MAX_LF
RSH_AXIR_MIN_LF RSH_ELE_MAX_LF RSH_ELE_MIN_LF];
REL_PEAK_LF=[REL_FLE_MAXI_LF REL_FLE_MINI_LF RELVAR_MAXI_LF
RELVAR_MINI_LF RELPRO_MAXI_LF RELPRO_MINI_LF;...
REL_FLE_MAXphase_LF REL_FLE_MINphase_LF RELVAR_MAXphase_LF
RELVAR_MINphase_LF RELPRO_MAXphase_LF RELPRO_MINphase_LF;...
REL_FLE_MAX_LF REL_FLE_MIN_LF REL_VAR_MAX_LF
REL_VAR_MIN_LF REL_PRO_MAX_LF REL_PRO_MIN_LF];
RWR_PEAK_LF=[RWR_FLE_MAXI_LF RWR_FLE_MINI_LF RWRULD_MAXI_LF
RWRULD_MINI_LF RWRPRO_MAXI_LF RWRPRO_MINI_LF;...
RWR_FLE_MAXphase_LF RWR_FLE_MINphase_LF RWRULD_MAXphase_LF
RWRULD_MINphase_LF RWRPRO_MAXphase_LF RWRPRO_MINphase_LF;...
RWR_FLE_MAX_LF RWR_FLE_MIN_LF RWR_ULD_MAX_LF
RWR_ULD_MIN_LF RWR_PRO_MAX_LF RWR_PRO_MIN_LF];
TR_PEAK_LF=[TR_FLE_MAXI_LF TR_FLE_MINI_LF TR_SideB_MAXI_LF
TR_SideB_MINI_LF TR_AxialR_MAXI_LF TR_AxialR_MINI_LF;...
TR_FLE_MAXphase_LF TR_FLE_MINphase_LF TR_SideB_MAXphase_LF
TR_SideB_MINphase_LF TR_AxialR_MAXphase_LF TR_AxialR_MINphase_LF;...
TR_FLE_MAX_LF TR_FLE_MIN_LF TR_SideB_MAX_LF TR_SideB_MIN_LF
TR_AxialR_MAX_LF TR_AxialR_MIN_LF];

```

```

LSH_PEAK=[LSHPOE_MAXI LSHPOE_MINI LSHAXIR_MAXI LSHAXIR_MINI
LSHELE_MAXI LSHELE_MINI;...
LSH_POE_MAX LSH_POE_MIN LSH_AXIR_MAX LSH_AXIR_MIN
LSH_ELE_MAX LSH_ELE_MIN];
LEL_PEAK=[LELFLE_MAXI LELFLE_MINI LELVAR_MAXI LELVAR_MINI
LELPRO_MAXI LELPRO_MINI;...
LEL_FLE_MAX LEL_FLE_MIN LEL_VAR_MAX LEL_VAR_MIN
LEL_PRO_MAX LEL_PRO_MIN];
LWR_PEAK=[LWRFLE_MAXI LWRFLE_MINI LWRULD_MAXI LWRULD_MINI
LWRPRO_MAXI LWRPRO_MINI;...
LWR_FLE_MAX LWR_FLE_MIN LWR_ULD_MAX LWR_ULD_MIN
LWR_PRO_MAX LWR_PRO_MIN];

LSH_PEAK_LF=[LSHPOE_MAXI_LF LSHPOE_MINI_LF LSHAXIR_MAXI_LF
LSHAXIR_MINI_LF LSHELE_MAXI_LF LSHELE_MINI_LF;...
LSHPOE_MAXphase_LF LSHPOE_MINphase_LF LSHAXIR_MAXphase_LF
LSHAXIR_MINphase_LF LSHELE_MAXphase_LF LSHELE_MINphase_LF;...
LSH_POE_MAX_LF LSH_POE_MIN_LF LSH_AXIR_MAX_LF
LSH_AXIR_MIN_LF LSH_ELE_MAX_LF LSH_ELE_MIN_LF];
LEL_PEAK_LF=[LELFLE_MAXI_LF LELFLE_MINI_LF LELVAR_MAXI_LF
LELVAR_MINI_LF LELPRO_MAXI_LF LELPRO_MINI_LF;...
LELFLE_MAXphase_LF LELFLE_MINphase_LF LELVAR_MAXphase_LF
LELVAR_MINphase_LF LELPRO_MAXphase_LF LELPRO_MINphase_LF;...
LEL_FLE_MAX_LF LEL_FLE_MIN_LF LEL_VAR_MAX_LF
LEL_VAR_MIN_LF LEL_PRO_MAX_LF LEL_PRO_MIN_LF];
LWR_PEAK_LF=[LWRFLE_MAXI_LF LWRFLE_MINI_LF LWRULD_MAXI_LF
LWRULD_MINI_LF LWRPRO_MAXI_LF LWRPRO_MINI_LF;...
LWRFLE_MAXphase_LF LWRFLE_MINphase_LF LWRULD_MAXphase_LF
LWRULD_MINphase_LF LWRPRO_MAXphase_LF LWRPRO_MINphase_LF;...
LWR_FLE_MAX_LF LWR_FLE_MIN_LF LWR_ULD_MAX_LF
LWR_ULD_MIN_LF LWR_PRO_MAX_LF LWR_PRO_MIN_LF];

% ROM=[Shoulder_elevationPlane Shoulder_IR/ER Shoulder_down/elevation]
% Elbow_flexion/extension Elbow_var/valgus Elbow_pronation/supination]
% Wrist_flexion/extension Wrist_ulnar/radialdeviation Wrist_pronation/supination]
RUE_ROM=[RSH_POE_ROM RSH_AXIR_ROM RSH_ELE_ROM; REL_FLE_ROM
REL_VAR_ROM REL_PRO_ROM;...
RWR_FLE_ROM RWR_ULD_ROM RWR_PRO_ROM; TR_FLE_ROM
TR_SideB_ROM TR_AxialR_ROM];
LUE_ROM=[LSH_POE_ROM LSH_AXIR_ROM LSH_ELE_ROM; LEL_FLE_ROM
LEL_VAR_ROM LEL_PRO_ROM;...
LWR_FLE_ROM LWR_ULD_ROM LWR_PRO_ROM];
% Trunk_ROM=[TR_FLE_ROM TR_SB_ROM TR_AR_ROM];

RUE_ROM_LF=[RSH_POE_ROM_LF RSH_AXIR_ROM_LF RSH_ELE_ROM_LF;
REL_FLE_ROM_LF REL_VAR_ROM_LF REL_PRO_ROM_LF;...

```

```
RWR_FLE_ROM_LF RWR_ULD_ROM_LF RWR_PRO_ROM_LF;  
TR_FLE_ROM_LF TR_SideB_ROM_LF TR_AxialR_ROM_LF];  
LUE_ROM_LF=[LSH_POE_ROM_LF LSH_AXIR_ROM_LF LSH_ELE_ROM_LF;  
LEL_FLE_ROM_LF LEL_VAR_ROM_LF LEL_PRO_ROM_LF];...  
LWR_FLE_ROM_LF LWR_ULD_ROM_LF LWR_PRO_ROM_LF];  
% Trunk_ROM=[TR_FLE_ROM TR_SB_ROM TR_AR_ROM];
```

```
save RSHpeak.txt RSH_PEAK -ascii;  
save RELpeak.txt REL_PEAK -ascii;  
save RWRpeak.txt RWR_PEAK -ascii;  
save LSHpeak.txt LSH_PEAK -ascii;  
save LELpeak.txt LEL_PEAK -ascii;  
save LWRpeak.txt LWR_PEAK -ascii;  
save Trunkpeak.txt TR_PEAK -ascii;  
save RightROM.txt RUE_ROM -ascii;  
save LeftROM.txt LUE_ROM -ascii;
```

```
save RSHpeak_lift.txt RSH_PEAK_LF -ascii;  
save RELpeak_lift.txt REL_PEAK_LF -ascii;  
save RWRpeak_lift.txt RWR_PEAK_LF -ascii;  
save LSHpeak_lift.txt LSH_PEAK_LF -ascii;  
save LELpeak_lift.txt LEL_PEAK_LF -ascii;  
save LWRpeak_lift.txt LWR_PEAK_LF -ascii;  
save Trunkpeak_lift.txt TR_PEAK_LF -ascii  
save RightROM_lift.txt RUE_ROM_LF -ascii;  
save LeftROM_lift.txt LUE_ROM_LF -ascii;
```



```

swfa=0.5*(0.04*weightlbs-0.5); %segment weight of forearm in lbs (Hanavan)
swha=0.5*(0.01*weightlbs-0.7); %segment weight of hand in lbs (Hanavan)
handdens=1.16/.001; %hand density in kg/m^3 from Winter
fadens=1.13/.001; %forearm in kg/m^3 density
uadens=1.07/.001; %upper arm in kg/m^3 densit

allfile_m = importdata('TPIIFR17_LB01.csv', ',', 11); %(filename,saperate,kinematic data
from line 11+1), get the kinematic data
allfile_f = importdata('TPIIFR17_LB01.csv', ',', 11821); %(filename,saperate,kinetic data
from line 13735+1), get the kinetic data
load base_BNFP.dat; % run Baseline_f.m first
load base_WCLC.dat;
load LeuangLB01.dat;
load ReuangLB01.dat;
Leuang=LeuangLB01;
Reuang=ReuangLB01;

fg=[0 0 -9.807]; % gravity in G.L.S
% filter for kinetic data, Load cell:44 45 46 Force, 47 48 49 moment
Fs2=1000; %Sampling Rate Frequency [Hz]
Fc2=7; %Cutoff Frequency for kinetic data[Hz]
w2=2*(Fc2/Fs2); %cutoff/corner frequency in radians
[b2,a2]=butter(4,w2,'low');
f_kinetic=filtfilt(b2,a2,allfile_f.data); %filtfilt=zerolag(zerophase)
ds_kinetic=downsample(f_kinetic,10);

% find the transfer cycle
load marker_tot.dat;
% marker_tot=[TOP RTMJ LTMJ RAC RUA1 RUA2 RUA3 RUA4 GRLE GRME
RFA1 RFA2 RFA3 RFA4 GRUS GRRS...
% RCH R3MCP LAC LUA1 LUA2 LUA3 LUA4 GLLE GLME LFA1 LFA2 LFA3
LFA4 GLUS GLRS LCH...
% L3MCP C7 T3 T8 GXYPD GSTRN];
% (previous) kin = [C7_global T3_global T8_global RSHO_global RMEP_global
RLEP_global RRS_global RUT_global R3MP_global,.....
% LSHO_global LMEP_global LLEP_global LRS_global LUT_global L3MP_global];
Fs1=100; %Sampling Rate Frequency [Hz]
Fc1=5; %Cutoff Frequency for kinematic data[Hz]
w1=2*(Fc1/Fs1); %cutoff/corner frequency in radians
[b1,a1]=butter(4,w1,'low');
f_marker_tot=filtfilt(b1,a1,marker_tot); %filtfilt=zerolag(zerophase)

kin=f_marker_tot;
[r,c]=size(kin);
n=length(kin(:,1));

```

```

% [R_st,C_st]=find(floor(allfile_m.data(:,2)*10000)==floor(kin(1,1)*10000)); %start
frame
% [R_end,C_end]=find(floor(allfile_m.data(:,2)*10000)==floor(kin(n,1)*10000)); %end
frame
% frame_index=[R_st R_end];
% save frame.txt frame_index -ascii;
load cycframe.dat;
R_st=cycframe(1);
R_end=cycframe(2);

% filename = ['AnalyzedKinematicData_TX', '46', 'V','A', 'L','1'];
% load (filename);
% filename_f = ['AnalyzedKineticData_TX', '46', 'V','A', 'L','1'];
% load (filename_f);

%%%%%%%% Right (trailing) hand reaction force %%%%%%%%%%%%%%
LC_fm=ds_kinetic(R_st:R_end, 44:49);
LC_FX=LC_fm(:,1)-base_WCLC(1,1); % deduct the baseline value
LC_FY=LC_fm(:,2)-base_WCLC(1,2);
LC_FZ=LC_fm(:,3)-base_WCLC(1,3); %Right hand vertical force
LC_MX=LC_fm(:,4)-base_WCLC(1,4);
LC_MY=LC_fm(:,5)-base_WCLC(1,5);
LC_MZ=LC_fm(:,6)-base_WCLC(1,6);
% LC_FX=LC_fm(:,1); % deduct the baseline value
% LC_FY=LC_fm(:,2);
% LC_FZ=LC_fm(:,3); %Right hand vertical force
% LC_MX=LC_fm(:,4);
% LC_MY=LC_fm(:,5);
% LC_MZ=LC_fm(:,6);
LC_fm(:,1)=LC_FX; LC_fm(:,2)=LC_FY; LC_fm(:,3)=LC_FZ; LC_fm(:,4)=LC_MX;
LC_fm(:,5)=LC_MY; LC_fm(:,6)=LC_MZ;
LC_force = LC_fm(:,1:3);
LC_force2 = LC_force;
figure (1); plot (LC_fm(:,1:3)); title('Right hand reaction force');
save WCLC_FM.txt LC_fm -ascii;

%%%%%%%% Bench force plate %%%%%%%%%%%%%%
BN_fm=ds_kinetic(R_st:R_end, 8:13);
BN_FX=BN_fm(:,1)-base_BNFP(1,1); % deduct the baseline value
BN_FY=BN_fm(:,2)-base_BNFP(1,2);
BN_FZ=BN_fm(:,3)-base_BNFP(1,3);
BN_MX=BN_fm(:,4)-base_BNFP(1,4);
BN_MY=BN_fm(:,5)-base_BNFP(1,5);
BN_MZ=BN_fm(:,6)-base_BNFP(1,6);
BN_fm(:,1)=BN_FX; BN_fm(:,2)=BN_FY; BN_fm(:,3)=BN_FZ; BN_fm(:,4)=BN_MX;
BN_fm(:,5)=BN_MY; BN_fm(:,6)=BN_MZ;

```



```

Lwristcen=0.5*(Lradsty+Lulnsty); %wrist center
Llmepe=kin(:,73:75); %Left medial epicondyle
Llatep=kin(:,70:72); %lateral epicondyle
Lacro=kin(:,55:57); %acromion

%upper arm
Ruapr=Raxilc/(2*pi); %upper arm proximal radius (shoulder)
Ruadr=Relbc/(2*pi); %upper arm distal radius (elbow)
Ruavol=(pi*Rualen/3*(Ruapr^2+Ruapr*Ruadr+Ruadr^2)); %segment volume in
m^3 (modeled as elliptical cylinder (Hanavan))
Ruamass=uadens*Ruavol; %upper arm mass in kg (density in kg/m^3)
Ruamu=Ruadr/Ruapr; %radius ratio constant "mu" defined by Hanavan
Ruasigma=1+Ruamu+Ruamu^2; %constant "sigma" defined by Hanavan
RuaAA=(9/(20*pi))*((1+Ruamu+Ruamu^2+Ruamu^3+Ruamu^4)/(Ruasigma^2));
%constant AA defined by Hanavan

RuaBB=(3/80)*((1+4*Ruamu+10*Ruamu^2+4*Ruamu^3+Ruamu^4)/(Ruasigma^2));
%constant BB defined by Hanavan

%check to make sure y is longitudinal and x,z are perpendicular to
%longitudinal
RuaIxx=Ruamass*((RuaAA*(Ruamass/(uadens*Rualen)))+RuaBB*(Rualen^2));
%moment of inertia perpendicular to longitudinal axis(kg*m^2)
RuaIzz=RuaIxx; %moment of inertia perpendicular to longitudinal axis(kg*m^2)
RuaIyy=(3/10)*Ruamass*((Ruapr^5-Ruadr^5)/(Ruapr^3-Ruadr^3));%moment of
inertia about the longitudinal axis of the upper arm (kg*m^2)
RuaIxy=0;
RuaIxz=0;
RuaIyz=0;
RuaI=[RuaIxx RuaIxy RuaIxz; RuaIxy RuaIyy RuaIyz; RuaIxz RuaIyz RuaIzz];
%matrix of upper arm mass moments of inertia

Ruacmratio=((Ruapr^2+2*Ruapr*Ruadr+3*Ruadr^2)/(4*(Ruapr^2+Ruapr*Ruadr+Ruadr^2));
%upper arm center of mass ratio (center of mass/length)with respect to proximal end (Hanavan)
Ruacm=Ruacmratio*(Rlatep-Racro)+Racro; %3-D coordinates of upper arm center
of mass

%forearm
Rfapr=Relbc/(2*pi); %forearm proximal radius (elbow)
Rfadr=Rwrc/(2*pi); %forearm distal radius (wrist)
Rfavol=(pi*Rfalen/3*(Rfapr^2+Rfapr*Rfadr+Rfadr^2)); %segment volume in m^3
(modeled as elliptical cylinder (Hanavan))
Rfamass=fadens*Rfavol; %forearm mass in kg (density in kg/m^3)
Rfamu=Ruadr/Ruapr; %radius ratio constant "mu" defined by Hanavan
Rfasigma=1+Ruamu+Ruamu^2; %constant "sigma" defined by Hanavan

```

```

    RfaAA=(9/(20*pi))*((1+Rfamuu+Rfamuu^2+Rfamuu^3+Rfamuu^4)/(Rfasigma^2));
%constant AA defined by Hanavan
    RfaBB=(3/80)*((1+4*Rfamuu+10*Rfamuu^2+4*Rfamuu^3+Rfamuu^4)/(Rfasigma^2));
%constant BB defined by Hanavan
    RfaIyy=Rfamass*((RfaAA*(Rfamass/(fadens*Rfalen)))+RfaBB*(Rfalen^2));
%moment of inertia perpendicular to longitudinal axis(kg*m^2)
    RfaIzz=RfaIyy; %moment of inertia perpendicular to longitudinal axis(kg*m^2)
    RfaIxx=(3/10)*Rfamass*((Rfapr^5-Rfadr^5)/(Rfapr^3-Rfadr^3));%moment of
inertia about the longitudinal axis of the forearm (kg*m^2)
    RfaIxy=0;
    RfaIxz=0;
    RfaIyz=0;
    RfaI=[RfaIxx RfaIxy RfaIxz; RfaIxy RfaIyy RfaIyz; RfaIxz RfaIyz RfaIzz];
%matrix of forearm mass moments of inertia

Rfacmratio=((Rfapr^2+2*Rfapr*Rfadr+3*Rfadr^2))/(4*(Rfapr^2+Rfapr*Rfadr+Rfadr^2));
%upper arm center of mass ratio (center of mass/length) with respect to proximal end (Hanavan)
    Rfacm=Rfacmratio*(Rwristcen-Rlatep)+Rlatep; %3-D coordinates of forearm
center of mass

    %hand
    Rhandrad=Rfistc/(2*pi); %hand radius
    Rhandvol=(4/3)*pi*Rhandrad^3; %hand volume in m^3
    Rhandmass=handdens*Rhandvol; %hand mass in kg
    RhandIany=(2/5)*Rhandmass*Rhandrad^2; %hand mass moment of inertia about
any axis (kg*m^2)
    RhandI=[RhandIany 0 0; 0 RhandIany 0; 0 0 RhandIany];
    Rhandcmratio=0.5; %center of mass ratio for the hand (sphere) (Hanavan)
    Rhandcm=Rhandcmratio*(Rthirdmp-Rwristcen)+Rwristcen; %3-D coordinates of
hand center of mass

    %Save all segment masses into a matrix
    %1x3 matrix
    Rmassall=[Rhandmass Rfamass Ruamass];

    %Save all center of mass locations in a matrix
    %kinrows(1200)x9 matrix
    Rcmall=[Rhandcm Rfacm Ruacm];

    %upper arm
    Luapr=Laxilc/(2*pi); %upper arm proximal radius (shoulder)
    Luadr=Lelbc/(2*pi); %upper arm distal radius (elbow)
    Luavol=(pi*Lualen/3*(Luapr^2+Luapr*Luadr+Luadr^2)); %segment volume in
m^3 (modeled as elliptical cylinder (Hanavan))
    Luamass=uadens*Luavol; %upper arm mass in kg (density in kg/m^3)
    Luamu=Luadr/Luapr; %radius ratio constant "mu" defined by Hanavan

```

```

    Luasigma=1+Luamu+Luamu^2; %constant "sigma" defined by Hanavan
    LuaAA=(9/(20*pi))*((1+Luamu+Luamu^2+Luamu^3+Luamu^4)/(Luasigma^2));
%constant AA defined by Hanavan

LuaBB=(3/80)*((1+4*Luamu+10*Luamu^2+4*Luamu^3+Luamu^4)/(Luasigma^2)); %constant
BB defined by Hanavan

    %check to make sure y is longitudinal and x,z are perpendicular to
    %longitudinal
    LuaIxx=Luamass*((LuaAA*(Luamass/(uadens*Lualen)))+LuaBB*(Lualen^2));
%moment of inertia perpendicular to longitudinal axis(kg*m^2)
    LuaIzz=LuaIxx; %moment of inertia perpendicular to longitudinal axis(kg*m^2)
    LuaIyy=(3/10)*Luamass*((Luapr^5-Luadr^5)/(Luapr^3-Luadr^3));%moment of
inertia about the longitudinal axis of the upper arm (kg*m^2)
    LuaIxy=0;
    LuaIxz=0;
    LuaIyz=0;
    LuaI=[LuaIxx LuaIxy LuaIxz; LuaIxy LuaIyy LuaIyz; LuaIxz LuaIyz LuaIzz];
%matrix of upper arm mass moments of inertia

Luacmratio=((Luapr^2+2*Luapr*Luadr+3*Luadr^2))/(4*(Luapr^2+Luapr*Luadr+Luadr^2));
%upper arm center of mass ratio (center of mass/length)with respect to proximal end (Hanavan)
    Luacm=Luacmratio*(Llatep-Lacro)+Lacro; %3-D coordinates of upper arm center
of mass

    %forearm
    Lfapr=Lelbc/(2*pi); %forearm proximal radius (elbow)
    Lfadr=Lwrc/(2*pi); %forearm distal radius (wrist)
    Lfavol=(pi*Lfalen/3*(Lfapr^2+Lfapr*Lfadr+Lfadr^2)); %segment volume in m^3
(modeled as elliptical cylinder (Hanavan))
    Lfamass=fadens*Lfavol; %forearm mass in kg (density in kg/m^3)
    Lfamu=Luadr/Luapr; %radius ratio constant "mu" defined by Hanavan
    Lfasigma=1+Luamu+Luamu^2; %constant "sigma" defined by Hanavan
    LfaAA=(9/(20*pi))*((1+Lfamu+Lfamu^2+Lfamu^3+Lfamu^4)/(Lfasigma^2));
%constant AA defined by Hanavan
    LfaBB=(3/80)*((1+4*Lfamu+10*Lfamu^2+4*Lfamu^3+Lfamu^4)/(Lfasigma^2));
%constant BB defined by Hanavan
    LfaIyy=Lfamass*((LfaAA*(Lfamass/(fadens*Lfalen)))+LfaBB*(Lfalen^2));
%moment of inertia perpendicular to longitudinal axis(kg*m^2)
    LfaIzz=LfaIyy; %moment of inertia perpendicular to longitudinal axis(kg*m^2)
    LfaIxx=(3/10)*Lfamass*((Lfapr^5-Lfadr^5)/(Lfapr^3-Lfadr^3));%moment of
inertia about the longitudinal axis of the forearm (kg*m^2)
    LfaIxy=0;
    LfaIxz=0;
    LfaIyz=0;

```

```
LfaI=[LfaIxx LfaIxy LfaIxz; LfaIxy LfaIyy LfaIyz; LfaIxz LfaIyz LfaIzz]; %matrix
of forearm mass moments of inertia
```

```
Lfacmratio=((Lfapr^2+2*Lfapr*Lfadr+3*Lfadr^2))/(4*(Lfapr^2+Lfapr*Lfadr+Lfadr^2));
% upper arm center of mass ratio (center of mass/length) with respect to proximal end (Hanavan)
Lfacm=Lfacmratio*(Lwristcen-Llatep)+Llatep; %3-D coordinates of forearm center
of mass
```

```
%hand
Lhandrad=Lfistc/(2*pi); %hand radius
Lhandvol=(4/3)*pi*Lhandrad^3; %hand volume in m^3
Lhandmass=handdens*Lhandvol; %hand mass in kg
LhandIany=(2/5)*Lhandmass*Lhandrad^2; %hand mass moment of inertia about
any axis (kg*m^2)
```

```
LhandI=[LhandIany 0 0; 0 LhandIany 0; 0 0 LhandIany];
Lhandcmratio=0.5; %center of mass ratio for the hand (sphere) (Hanavan)
Lhandcm=Lhandcmratio*(Lthirdmp-Lwristcen)+Lwristcen; %3-D coordinates of
hand center of mass
```

```
%Save all segment masses into a matrix
% 1x3 matrix
Lmassall=[Lhandmass Lfamass Luamass];
```

```
%Save all center of mass locations in a matrix
%kinrows(1200)x9 matrix
Lcmall=[Lhandcm Lfacm Luacm];
```

```
%-----Calculate absolute limb angular positions-----
-----%
```

```
% Upper Arm
Rupperarmvector=Rlatep-Racro; % vector along the long axis of the upper arm
Ruazyangle=atan2(Rupperarmvector(:,2),Rupperarmvector(:,3)); %absolute upper
arm angle in ZY plane
Ruaxzangle=atan2(Rupperarmvector(:,3),Rupperarmvector(:,1)); %absolute upper
arm angle in XZ plane
Ruaxyangle=atan2(Rupperarmvector(:,2),Rupperarmvector(:,1)); %absolute upper
arm angle in XY plane
```

```
%Forearm
Rforearmvector=Rwristcen-Rlatep; % vector along the long axis of the forearm
Rfazyangle=atan2(Rforearmvector(:,2),Rforearmvector(:,3)); %absolute forearm
angle in ZY plane
Rfaxzangle=atan2(Rforearmvector(:,3),Rforearmvector(:,1)); %absolute forearm
angle in XZ plane
Rfaxyangle=atan2(Rforearmvector(:,2),Rforearmvector(:,1)); %absolute forearm
angle in XY plane
```

```

%Hand
Rhandvector=Rthirdmp-Rwristcen; % vector along the long axis of the hand
Rhandzyangle=atan2(Rhandvector(:,2),Rhandvector(:,3)); %absolute hand angle in
ZY plane
Rhandxzangle=atan2(Rhandvector(:,3),Rhandvector(:,1)); %absolute hand angle in
XZ plane
Rhandxyangle=atan2(Rhandvector(:,2),Rhandvector(:,1)); %absolute hand angle in
XY plane

%L Upper Arm
Lupperarmvector=Llatep-Lacro; % vector along the long axis of the upper arm
Luazyangle=atan2(Lupperarmvector(:,2),Lupperarmvector(:,3)); %absolute upper
arm angle in ZY plane
Luaxzangle=atan2(Lupperarmvector(:,3),Lupperarmvector(:,1)); %absolute upper
arm angle in XZ plane
Luaxyangle=atan2(Lupperarmvector(:,2),Lupperarmvector(:,1)); %absolute upper
arm angle in XY plane

%L Forearm
Lforearmvector=Lwristcen-Llatep; % vector along the long axis of the forearm
Lfazyangle=atan2(Lforearmvector(:,2),Lforearmvector(:,3)); %absolute forearm
angle in ZY plane
Lfaxzangle=atan2(Lforearmvector(:,3),Lforearmvector(:,1)); %absolute forearm
angle in XZ plane
Lfaxyangle=atan2(Lforearmvector(:,2),Lforearmvector(:,1)); %absolute forearm
angle in XY plane

%L Hand
Lhandvector=Lthirdmp-Lwristcen; % vector along the long axis of the hand
Lhandzyangle=atan2(Lhandvector(:,2),Lhandvector(:,3)); %absolute hand angle in
ZY plane
Lhandxzangle=atan2(Lhandvector(:,3),Lhandvector(:,1)); %absolute hand angle in
XZ plane
Lhandxyangle=atan2(Lhandvector(:,2),Lhandvector(:,1)); %absolute hand angle in
XY plane

%-----Calculate angular velocities and accelerations-----
-----%
% Velcities and accelerations calculated according to 3 point centered different
method (Winter)

%store absolute angles in a single matrix
%kinrows(1200)x9 matrix
Rangles=[Ruazyangle Ruaxzangle Ruaxyangle Rfazyangle Rfaxzangle Rfaxyangle
Rhandzyangle Rhandxzangle Rhandxyangle];

```

```

    Langles=[Luazyangle Luaxzangle Luaxyangle Lfazyangle Lfaxzangle Lfaxyangle
    Lhandzyangle Lhandxzangle Lhandxyangle];

```

```

%    check to make sure all angles are in proper quadrant
for row=1:kinrows
    for col=1:9
        if Rangles(row,col) <= -pi
            Rangles(row,col)=(Rangles(row,col)+2*pi);
        elseif Rangles(row,col) > pi
            Rangles(row,col)=(Rangles(row,col)-2*pi);
        end
    end
end

for row2=1:kinrows
    for col2=1:9
        if Langles(row2,col2) <= -pi
            Langles(row2,col2)=(Langles(row2,col2)+2*pi);
        elseif Langles(row2,col2) > pi
            Langles(row2,col2)=(Langles(row2,col2)-2*pi);
        end
    end
end

%calculate velocities
for count1=2:(kinrows-1)
    Rvelocities(count1,1:9)=(Rangles(count1+1,:)-Rangles(count1-1,:))/(2*dt);
    count1=count1+1;
end
%correct # of rows
Rvelocities(1,1:9)=Rvelocities(2,1:9);
Rvelocities(kinrows,1:9)=Rvelocities((kinrows-1),1:9);

for count2=2:(kinrows-1)
    Lvelocities(count2,1:9)=(Langles(count2+1,:)-Langles(count2-1,:))/(2*dt);
    count2=count2+1;
end
%correct # of rows
Lvelocities(1,1:9)=Lvelocities(2,1:9);
Lvelocities(kinrows,1:9)=Lvelocities((kinrows-1),1:9);

%calculate accelerations
for index1=2:(kinrows-2)
    Raccelerations(index1,1:9)=(Rvelocities(index1+1,:)-Rvelocities(index1-
1,))/(2*dt);
    index1=index1+1;

```

```

end
%correct # of rows
Raccelerations(1,1:9)= Raccelerations(2,1:9);
Raccelerations((kinrows-1),1:9)= Raccelerations((kinrows-2),1:9);
Raccelerations(kinrows,1:9)= Raccelerations((kinrows-2),1:9);

for index2=2:(kinrows-2)
    Laccelerations(index2,1:9)=(Lvelocities(index2+1,:)-Lvelocities(index2-
1,:))/(2*dt);
    index2=index2+1;
end
%correct # of rows
Laccelerations(1,1:9)= Laccelerations(2,1:9);
Laccelerations((kinrows-1),1:9)= Laccelerations((kinrows-2),1:9);
Laccelerations(kinrows,1:9)= Laccelerations((kinrows-2),1:9);

%%% solve the gimbal lock problem %%%
for row=1:kinrows;
    for col=1:9;
        if Rvelocities(row,col)< -5; % detect gimble lock position
            Rvelocities(row,col)=0;
        elseif Rvelocities (row,col)> 5; % the cut-off is decided by the range of velocity
of every joint in each subject
            Rvelocities(row,col)=0;
        end
    end
end
[rowV, colV]=find(Rvelocities==0);
Rvelocities(rowV(:,colV(:)))=NaN;

Rvelocities1=spline(1:length(Rvelocities),Rvelocities(:,colV(1)),1:length(Rvelocities));
%spline(old x, old y, new x)
Rvelocities(:,colV(1))=Rvelocities1(:,:); %smooth the first set of gimbal lock data
Rvelocities2=zeros(9,length(Rvelocities));
for q1=2:length(colV);
    if colV(q1,1)~=colV((q1-1),1);

Rvelocities2(colV(q1,:))=spline(1:length(Rvelocities),Rvelocities(:,colV(q1)),1:length(Rvelociti
es)); %spline(old x, old y, new x)
    Rvelocities(:,colV(q1))=Rvelocities2(colV(q1,:)); % smooth other sets of gimbla
lock data
    end
end

for row2=1:kinrows;
    for col2=1:9;

```

```

        if Lvelocities(row2,col2)< -5; % detect gimble lock position
            Lvelocities(row2,col2)=0;
        elseif Lvelocities(row2,col2)> 5; % the cut-off is decided by the range of
velocity of every joint in each subject
            Lvelocities(row2,col2)=0;
        end
    end
end
[rowV2, colV2]=find(Lvelocities==0);
Lvelocities(rowV2(:,colV2(:))=NaN;

Lvelocities1=spline(1:length(Lvelocities),Lvelocities(:,colV2(1)),1:length(Lvelocities));
% spline(old x, old y, new x)
Lvelocities(:,colV2(1))=Lvelocities1(:,:); %smooth the first set of gimbal lock data
Lvelocities2=zeros(9,length(Lvelocities));
for q=2:length(colV2);
    if colV2(q,1)~=colV2((q-1),1);

Lvelocities2(colV2(q,:)=spline(1:length(Lvelocities),Lvelocities(:,colV2(q)),1:length(Lvelocitie
s)); % spline(old x, old y, new x)
    Lvelocities(:,colV2(q))=Lvelocities2(colV2(q,:)); % smooth other sets of gimbla
lock data
    end
end

for row=1:kinrows;
    for col=1:9;
        if Raccelerations(row,col)< -50; % the cut-off is decided by the range of
acceleration of every joint in each subject
            Raccelerations(row,col)=0;
        elseif Raccelerations(row,col)> 50;
            Raccelerations(row,col)=0;
        end
    end
end
[rowA, colA]=find(Raccelerations==0);
Raccelerations(rowA(:,colA(:))=NaN;

Raccelerations1=spline(1:length(Raccelerations),Raccelerations(:,colA(1)),1:length(Racceleratio
ns)); % spline(old x, old y, new x)
Raccelerations(:,colA(1))=Raccelerations1(:,:); %smooth the first set of gimbal lock
data
Raccelerations2=zeros(9,length(Raccelerations));
for q3=2:length(colA);
    if colA(q3,1)~=colA((q3-1),1);

```

```

Raccelerations2(colA(q3,:)=spline(1:length(Raccelerations),Raccelerations(:,colA(q3)),1:length
(Raccelerations)); %spline(old x, old y, new x)
    Raccelerations(:,colA(q3))=Raccelerations2(colA(q3,:)); % smooth other sets of
gimbla lock data
    end
end

for row=1:kinrows;
    for col=1:9;
        if Laccelerations(row,col)< -50; % the cut-off is decided by the range of
acceleration of every joint in each subject
            Laccelerations(row,col)=0;
        elseif Laccelerations(row,col)> 50;
            Laccelerations(row,col)=0;
        end
    end
end
[ rowA2, colA2]=find(Laccelerations==0);
Laccelerations(rowA2(:,),colA2(:,))=NaN;

Laccelerations1=spline(1:length(Laccelerations),Laccelerations(:,colA2(1)),1:length(Laccelerati
ons)); %spline(old x, old y, new x)
Laccelerations(:,colA2(1))=Laccelerations1(:,:); %smooth the first set of gimbal
lock data
Laccelerations2=zeros(9,length(Laccelerations));
for q4=2:length(colA2);
    if colA2(q4,1)~=colA2((q4-1),1);

Laccelerations2(colA2(q4,:)=spline(1:length(Laccelerations),Laccelerations(:,colA2(q4)),1:leng
th(Laccelerations)); %spline(old x, old y, new x)
    Laccelerations(:,colA2(q4))=Laccelerations2(colA2(q4,:)); % smooth other sets
of gimbla lock data
    end
end

%-----Calculate linear velocities and accelerations-----
%-----%
% Velcities and accelerations calculated according to 3 point centered different
method (Winter)

%Calculate linear velocities and accelerations for center of mass of each segment

%linear velocities of center of mass
for count2=2:(kinrows-1)
    Rcmvel(count2,1:9)=(Rcmall(count2+1,:)-Rcmall(count2-1,:))/(2*dt);

```

```

        count2=count2+1;
    end
    %correct # of rows
    Rcmvel(1,1:9)=Rcmvel(2,1:9);
    Rcmvel(kinrows,1:9)=Rcmvel((kinrows-1),1:9);

    %linear accelerations of center of mass;
    for index2=2:(kinrows-2)
        Rcmaccel(index2,1:9)=(Rcmvel(index2+1,:)-Rcmvel(index2-1,:))/(2*dt);
        index2=index2+1;
    end
    %correct # of rows
    Rcmaccel(1,1:9)=Rcmaccel(2,1:9);
    Rcmaccel((kinrows-1),1:9)=Rcmaccel((kinrows-2),1:9);
    Rcmaccel(kinrows,1:9)=Rcmaccel((kinrows-2),1:9);

    for count3=2:(kinrows-1)
        Lcmvel(count3,1:9)=(Lcmvel(count3+1,:)-Lcmvel(count3-1,:))/(2*dt);
        count3=count3+1;
    end
    %correct # of rows
    Lcmvel(1,1:9)=Lcmvel(2,1:9);
    Lcmvel(kinrows,1:9)=Lcmvel((kinrows-1),1:9);

    %linear accelerations of center of mass;
    for index3=2:(kinrows-2)
        Lcmaccel(index3,1:9)=(Lcmvel(index3+1,:)-Lcmvel(index3-1,:))/(2*dt);
        index3=index3+1;
    end
    %correct # of rows
    Lcmaccel(1,1:9)=Lcmaccel(2,1:9);
    Lcmaccel((kinrows-1),1:9)=Lcmaccel((kinrows-2),1:9);
    Lcmaccel(kinrows,1:9)=Lcmaccel((kinrows-2),1:9);

    %-----Calculate Net Joint Reaction Forces and Moments-----
    -----%
    %Reference is Cooper et al. Glenohumeral Joint Kinematics and Kinetics.....Am J
    Phys Med Rehab 1999.
    %All variable names in reference to Cooper et al.

    %Define blank arrays to be filled (defined) later
    %Hand matrices
    PHI_rD_Rhand=zeros(6,1,kinrows); %kinrows=#data points in kinematic file
    M_Rhand=zeros(6,1,kinrows);
    Mg_Rhand=zeros(6,1,kinrows);
    omega_Rhand=zeros(6,6,kinrows);

```

```

T_Rhand=zeros(3,3,kinrows);
Ip_Rhand=zeros(3,3,kinrows);
I_Rhand=zeros(6,6,kinrows);
w_Rhand=zeros(6,1,kinrows);
omegaIw_Rhand=zeros(6,1,kinrows);
a_Rhand=zeros(6,1,kinrows);
Ia_Rhand=zeros(6,1,kinrows);
rP_Rhand=zeros(6,1,kinrows);

```

```

%Forearm matrices

```

```

PHI_rD_Rfa=zeros(6,1,kinrows); %kinrows=#data points in kinematic file
M_Rfa=zeros(6,1,kinrows);
Mg_Rfa=zeros(6,1,kinrows);
omega_Rfa=zeros(6,6,kinrows);
T_Rfa=zeros(3,3,kinrows);
Ip_Rfa=zeros(3,3,kinrows);
I_Rfa=zeros(6,6,kinrows);
w_Rfa=zeros(6,1,kinrows);
omegaIw_Rfa=zeros(6,1,kinrows);
a_Rfa=zeros(6,1,kinrows);
Ia_Rfa=zeros(6,1,kinrows);
rP_Rfa=zeros(6,1,kinrows);

```

```

%Upper arm matrices

```

```

PHI_rD_Rua=zeros(6,1,kinrows); %kinrows=#data points in kinematic file
M_Rua=zeros(6,1,kinrows);
Mg_Rua=zeros(6,1,kinrows);
omega_Rua=zeros(6,6,kinrows);
T_Rua=zeros(3,3,kinrows);
Ip_Rua=zeros(3,3,kinrows);
I_Rua=zeros(6,6,kinrows);
w_Rua=zeros(6,1,kinrows);
omegaIw_Rua=zeros(6,1,kinrows);
a_Rua=zeros(6,1,kinrows);
Ia_Rua=zeros(6,1,kinrows);
rP_Rua=zeros(6,1,kinrows);

```

%Phi Matrix (distances between proximal and distal landmarks with -1 on diagonals) EQN. 20

```

PHI_Rhand=zeros(6,6,kinrows);
PHI_Rfa=zeros(6,6,kinrows);
PHI_Rua=zeros(6,6,kinrows);
for i=1:6
    PHI_Rhand(i,i,1:kinrows)=-1; %put -1 along diagonal
    PHI_Rfa(i,i,1:kinrows)=-1; %put -1 along diagonal
    PHI_Rua(i,i,1:kinrows)=-1; %put -1 along diagonal

```

end

```
%%%%%%%%%%%%%% Left arm %%%%%%%%%%%%%%%  
% Hand matrices  
PHI_rD_Lhand=zeros(6,1,kinrows); %kinrows=#data points in kinematic file  
M_Lhand=zeros(6,1,kinrows);  
Mg_Lhand=zeros(6,1,kinrows);  
omega_Lhand=zeros(6,6,kinrows);  
T_Lhand=zeros(3,3,kinrows);  
Ip_Lhand=zeros(3,3,kinrows);  
I_Lhand=zeros(6,6,kinrows);  
w_Lhand=zeros(6,1,kinrows);  
omegaIw_Lhand=zeros(6,1,kinrows);  
a_Lhand=zeros(6,1,kinrows);  
Ia_Lhand=zeros(6,1,kinrows);  
rP_Lhand=zeros(6,1,kinrows);  
  
% Forearm matrices  
PHI_rD_Lfa=zeros(6,1,kinrows); %kinrows=#data points in kinematic file  
M_Lfa=zeros(6,1,kinrows);  
Mg_Lfa=zeros(6,1,kinrows);  
omega_Lfa=zeros(6,6,kinrows);  
T_Lfa=zeros(3,3,kinrows);  
Ip_Lfa=zeros(3,3,kinrows);  
I_Lfa=zeros(6,6,kinrows);  
w_Lfa=zeros(6,1,kinrows);  
omegaIw_Lfa=zeros(6,1,kinrows);  
a_Lfa=zeros(6,1,kinrows);  
Ia_Lfa=zeros(6,1,kinrows);  
rP_Lfa=zeros(6,1,kinrows);  
  
% Upper arm matrices  
PHI_rD_Lua=zeros(6,1,kinrows); %kinrows=#data points in kinematic file  
M_Lua=zeros(6,1,kinrows);  
Mg_Lua=zeros(6,1,kinrows);  
omega_Lua=zeros(6,6,kinrows);  
T_Lua=zeros(3,3,kinrows);  
Ip_Lua=zeros(3,3,kinrows);  
I_Lua=zeros(6,6,kinrows);  
w_Lua=zeros(6,1,kinrows);  
omegaIw_Lua=zeros(6,1,kinrows);  
a_Lua=zeros(6,1,kinrows);  
Ia_Lua=zeros(6,1,kinrows);  
rP_Lua=zeros(6,1,kinrows);
```

```

%Phi Matrix (distances between proximal and distal landmarks with -1 on
diagonals) EQN. 20
PHI_Lhand=zeros(6,6,kinrows);
PHI_Lfa=zeros(6,6,kinrows);
PHI_Lua=zeros(6,6,kinrows);
for i=1:6
    PHI_Lhand(i,i,1:kinrows)=-1; %put -1 along diagonal
    PHI_Lfa(i,i,1:kinrows)=-1; %put -1 along diagonal
    PHI_Lua(i,i,1:kinrows)=-1; %put -1 along diagonal
end

%%%%%%%%%%%%% Combine force data
%%%%%%%%%%%%%
%Hand segment
rD_Rhand=zeros(kinrows,6);
rD_Lhand=zeros(kinrows,6);
%Assume hand has a point contact with the pushrim at the third mp
%Therefore SW forces are input to the third mp, but there is no moment arm
between the pushrim and the thirdmp, so the input moments are zero
for t=1:kinrows
    %if step(t,1) > 0, % will only input SW forces when hand is on the rim,
determined by step function
    rD_Rhand(t,1:3)=-(LC_force(t,1:3)); %reaction forces at hand are the negative of
the forces applied to the pushrim
    %    plot(forces(:,2))
    %end %
end
%    figure
%    plot(rD_hand(:,2))
rD_Rhand=rD_Rhand';

for t=1:kinrows
    %if step(t,1) > 0, % will only input SW forces when hand is on the rim,
determined by step function
    rD_Lhand(t,1:3)=-(bench_force(t,1:3)); %reaction forces at hand are the negative
of the forces applied to the pushrim
    %    plot(forces(:,2))
    %end %
end
%    figure
%    plot(rD_hand(:,2))
rD_Lhand=rD_Lhand';

for t=1:kinrows
    %fill in Phi_hand matrix with distances between third mp and wrist center
%Signs in PHI matrix are different from Cooper et al. because his

```

```

    %paper assumes distances rather than directional vectors
    PHI_Rhand(4,2,t)=-((Rthirdmp(t,3)-Rwristcen(t,3))); %negative of vector from
prox to dist. in z direction EQN.20 (-Zdp)
    PHI_Rhand(5,1,t)=(Rthirdmp(t,3)-Rwristcen(t,3)); % vector from prox to dist. in z
direction EQN.20 (Zdp)
    PHI_Rhand(4,3,t)=-((Rthirdmp(t,2)-Rwristcen(t,2))); %negative of vector from
prox to dist. in y direction EQN.20 (-Ydp)
    PHI_Rhand(6,1,t)=(Rthirdmp(t,2)-Rwristcen(t,2)); % vector from prox to dist. in
y direction EQN.20 (Ydp)
    PHI_Rhand(6,2,t)=-((Rthirdmp(t,1)-Rwristcen(t,1))); %negative of vector from
prox to dist. in x direction EQN.20 (-Xdp)
    PHI_Rhand(5,3,t)=(Rthirdmp(t,1)-Rwristcen(t,1)); % vector from prox to dist. in x
direction EQN.20 (Xdp)

```

```

    PHI_Lhand(4,2,t)=-((Lthirdmp(t,3)-Lwristcen(t,3))); %negative of vector from
prox to dist. in z direction EQN.20 (-Zdp)
    PHI_Lhand(5,1,t)=(Lthirdmp(t,3)-Lwristcen(t,3)); % vector from prox to dist. in z
direction EQN.20 (Zdp)
    PHI_Lhand(4,3,t)=-((Lthirdmp(t,2)-Lwristcen(t,2))); %negative of vector from
prox to dist. in y direction EQN.20 (-Ydp)
    PHI_Lhand(6,1,t)=(Lthirdmp(t,2)-Lwristcen(t,2)); % vector from prox to dist. in
y direction EQN.20 (Ydp)
    PHI_Lhand(6,2,t)=-((Lthirdmp(t,1)-Lwristcen(t,1))); %negative of vector from
prox to dist. in x direction EQN.20 (-Xdp)
    PHI_Lhand(5,3,t)=(Lthirdmp(t,1)-Lwristcen(t,1)); % vector from prox to dist. in x
direction EQN.20 (Xdp)

```

%EQN. 21 PHI matrix times the reaction forces and moments at the distal end of the segment

```

PHI_rD_Rhand(:, :, t)=PHI_Rhand(:, :, t)*rD_Rhand(1:6,t);
PHI_rD_Lhand(:, :, t)=PHI_Lhand(:, :, t)*rD_Lhand(1:6,t);

```

```

%EQN. 20 Define M matrix for hand (mass and moment arm vector)
M_Rhand(2,1,t)=Rhandmass;
M_Rhand(4,1,t)=Rhandmass*-1*(Rhandcm(t,3)-Rwristcen(t,3));%hand mass
times distance in z direction b/w wrist center and hand center of mass
%negative corrects for direction of moment
M_Rhand(6,1,t)=Rhandmass*(Rhandcm(t,1)-Rwristcen(t,1));%hand mass times
distance in x direction b/w wrist center and hand center of mass

```

```

%EQN. 20 Define M matrix for hand (mass and moment arm vector)
M_Lhand(2,1,t)=Lhandmass;
M_Lhand(4,1,t)=Lhandmass*-1*(Lhandcm(t,3)-Lwristcen(t,3));%hand mass
times distance in z direction b/w wrist center and hand center of mass
%negative corrects for direction of moment

```

M_Lhand(6,1,t)=Lhandmass*(Lhandcm(t,1)-Lwristcen(t,1));%hand mass times distance in x direction b/w wrist center and hand center of mass

%EQN. 21 Calculate M*g matrix

Mg_Rhand(:,1,t)=M_Rhand(:,1,t)*g; %M matrix times gravity

Mg_Lhand(:,1,t)=M_Lhand(:,1,t)*g; %M matrix times gravity

%EQN. 20 Calculate Capital Omega matrix

omega_Rhand(4,5,t)=-(Rvelocities(t,9)); %negative angular velocity @ z axis

omega_Rhand(5,4,t)=(Rvelocities(t,9)); %angular velocity @ z axis

omega_Rhand(4,6,t)=(Rvelocities(t,8)); %angular velocity @ y axis

omega_Rhand(6,4,t)=-(Rvelocities(t,8)); %negative angular velocity @ y axis

omega_Rhand(5,6,t)=-(Rvelocities(t,7)); %negative angular velocity @ x axis

omega_Rhand(6,5,t)=(Rvelocities(t,7)); %angular velocity @ x axis

omega_Lhand(4,5,t)=-(Lvelocities(t,9)); %negative angular velocity @ z axis

omega_Lhand(5,4,t)=(Lvelocities(t,9)); %angular velocity @ z axis

omega_Lhand(4,6,t)=(Lvelocities(t,8)); %angular velocity @ y axis

omega_Lhand(6,4,t)=-(Lvelocities(t,8)); %negative angular velocity @ y axis

omega_Lhand(5,6,t)=-(Lvelocities(t,7)); %negative angular velocity @ x axis

omega_Lhand(6,5,t)=(Lvelocities(t,7)); %angular velocity @ x axis

%EQN.18 Set up transformation matrix to convert inertias about

%segment axes to inertias about global x,y,z axes

%angles(7)=psi_hand; angles(8)=theta_hand; angles(9)=phi_hand

T_Rhand(1,1,t)=cos(Rangles(t,9))*cos(Rangles(t,8));

T_Rhand(1,2,t)=sin(Rangles(t,9))*cos(Rangles(t,8));

T_Rhand(1,3,t)=-sin(Rangles(t,8)); %

Why negative %

T_Rhand(2,1,t)=-

sin(Rangles(t,9))*cos(Rangles(t,7))+cos(Rangles(t,9))*sin(Rangles(t,8))*sin(Rangles(t,7));

T_Rhand(2,2,t)=cos(Rangles(t,9))*cos(Rangles(t,7))+sin(Rangles(t,9))*sin(Rangles(t,8))*sin(Rangles(t,7));

T_Rhand(2,3,t)=cos(Rangles(t,8))*sin(Rangles(t,7));

T_Rhand(3,1,t)=sin(Rangles(t,9))*sin(Rangles(t,7))+cos(Rangles(t,9))*sin(Rangles(t,8))*cos(Rangles(t,7));

T_Rhand(3,2,t)=-

cos(Rangles(t,9))*sin(Rangles(t,7))+cos(Rangles(t,7))*sin(Rangles(t,8))*cos(Rangles(t,7));

T_Rhand(3,3,t)=cos(Rangles(t,8))*cos(Rangles(t,7));

T_Lhand(1,1,t)=cos(Langles(t,9))*cos(Langles(t,8));

T_Lhand(1,2,t)=sin(Langles(t,9))*cos(Langles(t,8));

T_Lhand(1,3,t)=-sin(Langles(t,8));

```

T_Lhand(2,1,t)=-
sin(Langles(t,9))*cos(Langles(t,7))+cos(Langles(t,9))*sin(Langles(t,8))*sin(Langles(t,7));

T_Lhand(2,2,t)=cos(Langles(t,9))*cos(Langles(t,7))+sin(Langles(t,9))*sin(Langles(t,8))*sin(Lan
gles(t,7));
T_Lhand(2,3,t)=cos(Langles(t,8))*sin(Langles(t,7));

T_Lhand(3,1,t)=sin(Langles(t,9))*sin(Langles(t,7))+cos(Langles(t,9))*sin(Langles(t,8))*cos(Lan
gles(t,7));
T_Lhand(3,2,t)=-
cos(Langles(t,9))*sin(Langles(t,7))+cos(Langles(t,7))*sin(Langles(t,8))*cos(Langles(t,7));
T_Lhand(3,3,t)=cos(Langles(t,8))*cos(Langles(t,7));

%EQN.18 Calculate inertias about global x,y,z
Ip_Rhand(:, :, t)=T_Rhand(:, :, t)*RhandI*T_Rhand(:, :, t);
Ip_Lhand(:, :, t)=T_Lhand(:, :, t)*RhandI*T_Lhand(:, :, t);

%All inertia characteristics of the hand (angular velocity and
%acceleration) will not be included in the calculated because they
%have a very small contribution and are susceptible to noise

%EQN. 20 Set up angular velocity vector(lowercase omega-- will call "w")
%w_hand(:, :, t)=[0;0;0;velocities(t,7);velocities(t,8);velocities(t,9)];

%EQN. 21 Calculate product of angular velocity matrices (omega*I*w)
%omegaIw_hand(:, :, t)=omega_hand(:, :, t)*I_hand(:, :, t)*w_hand(:, :, t);

%EQN. 20 Define acceleration vector(linear [of center of mass] and angular
accelerations)

%a_hand(:, :, t)=[cmaccel(t,1);cmaccel(t,2);cmaccel(t,3);accelerations(t,7);accelerations(t,8);accel
erations(t,9)];

%EQN. 21 Calculate matrix that combines inertial properties and linear
accelerations
%Ia_hand(:, :, t)=I_hand(:, :, t)*a_hand(:, :, t);

%EQN. 21 Calculate reaction force at wrist center in global coordinate system
rP_Rhand(:, :, t)=PHI_rD_Rhand(:, :, t)+Mg_Rhand(:, :, t);
rP_Lhand(:, :, t)=PHI_rD_Lhand(:, :, t)+Mg_Lhand(:, :, t);
% plot3(rP_hand(1:3,1,t)) %checking the forces

fxr_hand(t,1)= rD_Rhand(1,t);
fyr_hand(t,1)= rD_Rhand(2,t);
fzr_hand(t,1)= rD_Rhand(3,t);

```

```

fxr_Lhand(t,1)= rD_Lhand(1,t);
fyr_Lhand(t,1)= rD_Lhand(2,t);
fzr_Lhand(t,1)= rD_Lhand(3,t);

resultant_force_R3mp(t,1)=sqrt(rD_Rhand(1,t)^2+rD_Rhand(2,t)^2+rD_Rhand(3,t)^2);

resultant_force_L3mp(t,1)=sqrt(rD_Lhand(1,t)^2+rD_Lhand(2,t)^2+rD_Lhand(3,t)^2);
end

%Forearm segment
rD_Rfa=-rP_Rhand; %reaction forces at hand are the negative of the forces applied
to the wrist (negative applied in PHI matrix below)
rD_Lfa=-rP_Lhand;

for t=1:kinrows
    %fill in Phi_fa matrix with distances between wrist center and lateral epicondyle
    %Signs in PHI matrix are different from Cooper et al. because his
    %paper assumes distances rather than directional vectors
    PHI_Rfa(4,2,t)=-(Rwristcen(t,3)-Rlatep(t,3)); %negative of vector from prox to
dist. in z direction EQN.20 (-Zdp)
    PHI_Rfa(5,1,t)=(Rwristcen(t,3)-Rlatep(t,3)); %vector from prox to dist. in z
direction EQN.20 (Zdp)
    PHI_Rfa(4,3,t)=-((Rwristcen(t,2)-Rlatep(t,2))); %negative of vector from prox to
dist. in y direction EQN.20 (-Ydp)
    PHI_Rfa(6,1,t)=((Rwristcen(t,2)-Rlatep(t,2))); %vector from prox to dist. in y
direction EQN.20 (Ydp)
    PHI_Rfa(6,2,t)=-(Rwristcen(t,1)-Rlatep(t,1)); %negative of vector from prox to
dist. in x direction EQN.20 (-Xdp)
    PHI_Rfa(5,3,t)=(Rwristcen(t,1)-Rlatep(t,1)); %vector from prox to dist. in x
direction EQN.20 (Xdp)

    PHI_Lfa(4,2,t)=-(Lwristcen(t,3)-Llatep(t,3)); %negative of vector from prox to
dist. in z direction EQN.20 (-Zdp)
    PHI_Lfa(5,1,t)=(Lwristcen(t,3)-Llatep(t,3)); %vector from prox to dist. in z
direction EQN.20 (Zdp)
    PHI_Lfa(4,3,t)=-((Lwristcen(t,2)-Llatep(t,2))); %negative of vector from prox to
dist. in y direction EQN.20 (-Ydp)
    PHI_Lfa(6,1,t)=((Lwristcen(t,2)-Llatep(t,2))); %vector from prox to dist. in y
direction EQN.20 (Ydp)
    PHI_Lfa(6,2,t)=-(Lwristcen(t,1)-Llatep(t,1)); %negative of vector from prox to
dist. in x direction EQN.20 (-Xdp)
    PHI_Lfa(5,3,t)=(Lwristcen(t,1)-Llatep(t,1)); %vector from prox to dist. in x
direction EQN.20 (Xdp)

```

the segment %EQN. 21 PHI matrix times the reaction forces and moments at the distal end of

```
PHI_rD_Rfa(:, :, t) = PHI_Rfa(:, :, t) * rD_Rfa(1:6, t);  
PHI_rD_Lfa(:, :, t) = PHI_Lfa(:, :, t) * rD_Lfa(1:6, t);
```

```
%EQN. 20 Define M matrix for forearm (mass and moment arm vector)  
M_Rfa(2, 1, t) = Rfamass;  
M_Rfa(4, 1, t) = Rfamass * -1 * (Rfacm(t, 3) - Rlatep(t, 3)); % forearm mass times  
distance in z direction b/w latep and forearm center of mass  
% negative corrects for direction of moment  
M_Rfa(6, 1, t) = Rfamass * (Rfacm(t, 1) - Rlatep(t, 1)); % forearm mass times distance in  
x direction b/w latep and forearm center of mass
```

```
%EQN. 20 Define M matrix for forearm (mass and moment arm vector)  
M_Lfa(2, 1, t) = Lfamass;  
M_Lfa(4, 1, t) = Lfamass * -1 * (Lfacm(t, 3) - Llatep(t, 3)); % forearm mass times  
distance in z direction b/w latep and forearm center of mass  
% negative corrects for direction of moment  
M_Lfa(6, 1, t) = Lfamass * (Lfacm(t, 1) - Llatep(t, 1)); % forearm mass times distance in  
x direction b/w latep and forearm center of mass
```

```
%EQN. 21 Calculate M*g matrix  
Mg_Rfa(:, 1, t) = M_Rfa(:, 1, t) * g; % M matrix times gravity  
Mg_Lfa(:, 1, t) = M_Lfa(:, 1, t) * g; % M matrix times gravity
```

```
%EQN. 20 Calculate Capital Omega matrix  
omega_Rfa(4, 5, t) = -(Rvelocities(t, 6)); % negative angular velocity @ z axis  
omega_Rfa(5, 4, t) = (Rvelocities(t, 6)); % angular velocity @ z axis  
omega_Rfa(4, 6, t) = (Rvelocities(t, 5)); % angular velocity @ y axis  
omega_Rfa(6, 4, t) = -(Rvelocities(t, 5)); % negative angular velocity @ y axis  
omega_Rfa(5, 6, t) = -(Rvelocities(t, 4)); % negative angular velocity @ x axis  
omega_Rfa(6, 5, t) = (Rvelocities(t, 4)); % angular velocity @ x axis
```

```
%EQN. 20 Calculate Capital Omega matrix  
omega_Lfa(4, 5, t) = -(Lvelocities(t, 6)); % negative angular velocity @ z axis  
omega_Lfa(5, 4, t) = (Lvelocities(t, 6)); % angular velocity @ z axis  
omega_Lfa(4, 6, t) = (Lvelocities(t, 5)); % angular velocity @ y axis  
omega_Lfa(6, 4, t) = -(Lvelocities(t, 5)); % negative angular velocity @ y axis  
omega_Lfa(5, 6, t) = -(Lvelocities(t, 4)); % negative angular velocity @ x axis  
omega_Lfa(6, 5, t) = (Lvelocities(t, 4)); % angular velocity @ x axis
```

```
%EQN.18 Set up transformation matrix to convert inertias about  
% segment axes to inertias about global x,y,z axes  
% angles(4)=psi_fa; angles(5)=theta_fa; angles(6)=phi_fa  
T_Rfa(1, 1, t) = cos(Rangles(t, 6)) * cos(Rangles(t, 5));  
T_Rfa(1, 2, t) = sin(Rangles(t, 6)) * cos(Rangles(t, 5));
```

```

T_Rfa(1,3,t)=-sin(Rangles(t,5));
T_Rfa(2,1,t)=-
sin(Rangles(t,6))*cos(Rangles(t,4))+cos(Rangles(t,6))*sin(Rangles(t,5))*sin(Rangles(t,4));

T_Rfa(2,2,t)=cos(Rangles(t,6))*cos(Rangles(t,4))+sin(Rangles(t,6))*sin(Rangles(t,5))*sin(Rangles(t,4));
T_Rfa(2,3,t)=cos(Rangles(t,5))*sin(Rangles(t,4));

T_Rfa(3,1,t)=sin(Rangles(t,6))*sin(Rangles(t,4))+cos(Rangles(t,6))*sin(Rangles(t,5))*cos(Rangles(t,4));
T_Rfa(3,2,t)=-
cos(Rangles(t,6))*sin(Rangles(t,4))+cos(Rangles(t,4))*sin(Rangles(t,5))*cos(Rangles(t,4));
T_Rfa(3,3,t)=cos(Rangles(t,5))*cos(Rangles(t,4));

%EQN.18 Set up transformation matrix to convert inertias about
%segment axes to inertias about global x,y,z axes
%angles(4)=psi_fa; angles(5)=theta_fa; angles(6)=phi_fa
T_Lfa(1,1,t)=cos(Langles(t,6))*cos(Langles(t,5));
T_Lfa(1,2,t)=sin(Langles(t,6))*cos(Langles(t,5));
T_Lfa(1,3,t)=-sin(Langles(t,5));
T_Lfa(2,1,t)=-
sin(Langles(t,6))*cos(Langles(t,4))+cos(Langles(t,6))*sin(Langles(t,5))*sin(Langles(t,4));

T_Lfa(2,2,t)=cos(Langles(t,6))*cos(Langles(t,4))+sin(Langles(t,6))*sin(Langles(t,5))*sin(Langles(t,4));
T_Lfa(2,3,t)=cos(Langles(t,5))*sin(Langles(t,4));

T_Lfa(3,1,t)=sin(Langles(t,6))*sin(Langles(t,4))+cos(Langles(t,6))*sin(Langles(t,5))*cos(Langles(t,4));
T_Lfa(3,2,t)=-
cos(Langles(t,6))*sin(Langles(t,4))+cos(Langles(t,4))*sin(Langles(t,5))*cos(Langles(t,4));
T_Lfa(3,3,t)=cos(Langles(t,5))*cos(Langles(t,4));

%EQN.18 Calculate inertias about global x,y,z
Ip_Rfa(:, :, t)=T_Rfa(:, :, t)*RfaI*T_Rfa(:, :, t)';
Ip_Lfa(:, :, t)=T_Lfa(:, :, t)*LfaI*T_Lfa(:, :, t)';

%EQN.20 Set up I matrix that contains mass and inertia information
I_Rfa(1,1,t)=Rfamass;
I_Rfa(2,2,t)=Rfamass;
I_Rfa(3,3,t)=Rfamass;
I_Rfa(4:6,4:6,t)=Ip_Rfa(:, :, t);

I_Lfa(1,1,t)=Lfamass;
I_Lfa(2,2,t)=Lfamass;
I_Lfa(3,3,t)=Lfamass;

```

```

I_Lfa(4:6,4:6,t)=Ip_Lfa(:, :, t);

%EQN. 20 Set up angular velocity vector(lowercase omega-- will call "w")
w_Rfa(:, :, t)=[0;0;0;Rvelocities(t,4);Rvelocities(t,5);Rvelocities(t,6)];
w_Lfa(:, :, t)=[0;0;0;Lvelocities(t,4);Lvelocities(t,5);Lvelocities(t,6)];

%EQN. 21 Calculate product of angular velocity matrices (omega*I*w)
omegaIw_Rfa(:, :, t)=omega_Rfa(:, :, t)*I_Rfa(:, :, t)*w_Rfa(:, :, t);
omegaIw_Lfa(:, :, t)=omega_Lfa(:, :, t)*I_Lfa(:, :, t)*w_Lfa(:, :, t);

%EQN. 20 Define acceleration vector(linear [of center of mass] and angular
accelerations)

%a_fa(:, :, t)=[cmaccel(t,4);cmaccel(t,5);cmaccel(t,6);accelerations(t,4);accelerations(t,5);accelerations(t,6)];
a_Rfa(:, :, t)=[Rcmaccel(t,4);Rcmaccel(t,5);Rcmaccel(t,6);0;0;Raccelerations(t,6)];
a_Lfa(:, :, t)=[Lcmaccel(t,4);Lcmaccel(t,5);Lcmaccel(t,6);0;0;Laccelerations(t,6)];
%xz and yz plane angular accelerations ignored because they are
%prone to quadrant changes when the arm is vertical. contributions
%are negligible in these two planes

%EQN. 21 Calculate matrix that combines inertial properties and linear
accelerations
Ia_Rfa(:, :, t)=I_Rfa(:, :, t)*a_Rfa(:, :, t);
Ia_Lfa(:, :, t)=I_Lfa(:, :, t)*a_Lfa(:, :, t);

%EQN. 21 Calculate reaction force at elbow center in global coordinate system
rP_Rfa(:, :, t)=PHI_rD_Rfa(:, :, t)-Ia_Rfa(:, :, t)-omegaIw_Rfa(:, :, t)+Mg_Rfa(:, :, t);
rP_Lfa(:, :, t)=PHI_rD_Lfa(:, :, t)-Ia_Lfa(:, :, t)-omegaIw_Lfa(:, :, t)+Mg_Lfa(:, :, t);

%      plot3(rP_fa(1:3,1,t)) %checking the forces
end

% Upper arm segment
rD_Rua=-rP_Rfa; %reaction forces at shoulder are the negative of the forces applied
to the elbow (negative applied in PHI matrix below)
rD_Lua=-rP_Lfa;

for t=1:kinrows
    %fill in Phi_ua matrix with distances between lateral epicondyle and acromion
    %Signs in PHI matrix are different from Cooper et al. because his
    %paper assumes distances rather than directional vectors
    PHI_Rua(4,2,t)=(Rlatep(t,3)-Racro(t,3)); %negative of vector from prox to dist.
in z direction EQN.20 (-Zdp)
    PHI_Rua(5,1,t)=(Rlatep(t,3)-Racro(t,3)); %vector from prox to dist. in z direction
EQN.20 (Zdp)

```

```

        PHI_Rua(4,3,t)=-((Rlatep(t,2)-Racro(t,2))); %negative of vector from prox to dist.
in y direction EQN.20 (-Ydp)
        PHI_Rua(6,1,t)=((Rlatep(t,2)-Racro(t,2))); %vector from prox to dist. in y
direction EQN.20 (Ydp)
        PHI_Rua(6,2,t)=-((Rlatep(t,1)-Racro(t,1))); %negative of vector from prox to dist.
in x direction EQN.20 (-Xdp)
        PHI_Rua(5,3,t)=((Rlatep(t,1)-Racro(t,1))); %vector from prox to dist. in x direction
EQN.20 (Xdp)

        PHI_Lua(4,2,t)=-((Llatep(t,3)-Lacro(t,3))); %negative of vector from prox to dist.
in z direction EQN.20 (-Zdp)
        PHI_Lua(5,1,t)=((Llatep(t,3)-Lacro(t,3))); %vector from prox to dist. in z direction
EQN.20 (Zdp)
        PHI_Lua(4,3,t)=-((Llatep(t,2)-Lacro(t,2))); %negative of vector from prox to dist.
in y direction EQN.20 (-Ydp)
        PHI_Lua(6,1,t)=((Llatep(t,2)-Lacro(t,2))); %vector from prox to dist. in y
direction EQN.20 (Ydp)
        PHI_Lua(6,2,t)=-((Llatep(t,1)-Lacro(t,1))); %negative of vector from prox to dist.
in x direction EQN.20 (-Xdp)
        PHI_Lua(5,3,t)=((Llatep(t,1)-Lacro(t,1))); %vector from prox to dist. in x direction
EQN.20 (Xdp)

%EQN. 21 PHI matrix times the reaction forces and moments at the distal end of
the segment
PHI_rD_Rua(:, :, t)=PHI_Rua(:, :, t)*rD_Rua(1:6,t);
PHI_rD_Lua(:, :, t)=PHI_Lua(:, :, t)*rD_Lua(1:6,t);

%EQN. 20 Define M matrix for upperarm (mass and moment arm vector)
M_Rua(2,1,t)=Ruamass;
M_Rua(4,1,t)=Ruamass*(1-Ruacmratio)*PHI_Rua(4,2,t);
M_Rua(6,1,t)=Ruamass*(1-Ruacmratio)*PHI_Rua(6,2,t);

M_Lua(2,1,t)=Luamass;
M_Lua(4,1,t)=Luamass*(1-Luacmratio)*PHI_Lua(4,2,t);
M_Lua(6,1,t)=Luamass*(1-Luacmratio)*PHI_Lua(6,2,t);

M_Rua(2,1,t)=Ruamass;
M_Rua(4,1,t)=Ruamass*-1*(Ruacm(t,3)-Racro(t,3));%upperarm mass times
distance in z direction b/w acromion and upperarm center of mass
%negative corrects for direction of moment
M_Rua(6,1,t)=Ruamass*(Ruacm(t,1)-Racro(t,1));%upperarm mass times distance
in x direction b/w acromion and upperarm center of mass

M_Lua(2,1,t)=Luamass;
M_Lua(4,1,t)=Luamass*-1*(Luacm(t,3)-Lacro(t,3));%upperarm mass times
distance in z direction b/w acromion and upperarm center of mass

```

```

%negative corrects for direction of moment
M_Lua(6,1,t)=Luamass*(Luacm(t,1)-Lacro(t,1));%upperarm mass times distance
in x direction b/w acromion and upperarm center of mass

```

```

%EQN. 21 Calculate M*g matrix
Mg_Rua(:,1,t)=M_Rua(:,1,t)*g; %M matrix times gravity
Mg_Lua(:,1,t)=M_Lua(:,1,t)*g; %M matrix times gravity

```

```

%EQN. 20 Calculate Capital Omega matrix
omega_Rua(4,5,t)=-(Rvelocities(t,3)); %negative angular velocity @ z axis
omega_Rua(5,4,t)=(Rvelocities(t,3)); %angular velocity @ z axis
omega_Rua(4,6,t)=(Rvelocities(t,2)); %angular velocity @ y axis
omega_Rua(6,4,t)=-(Rvelocities(t,2)); %negative angular velocity @ y axis
omega_Rua(5,6,t)=-(Rvelocities(t,1)); %negative angular velocity @ x axis
omega_Rua(6,5,t)=(Rvelocities(t,1)); %angular velocity @ x axis

```

```

omega_Lua(4,5,t)=-(Lvelocities(t,3)); %negative angular velocity @ z axis
omega_Lua(5,4,t)=(Lvelocities(t,3)); %angular velocity @ z axis
omega_Lua(4,6,t)=(Lvelocities(t,2)); %angular velocity @ y axis
omega_Lua(6,4,t)=-(Lvelocities(t,2)); %negative angular velocity @ y axis
omega_Lua(5,6,t)=-(Lvelocities(t,1)); %negative angular velocity @ x axis
omega_Lua(6,5,t)=(Lvelocities(t,1)); %angular velocity @ x axis

```

```

%EQN.18 Set up transformation matrix to convert inertias about
%segment axes to inertias about global x,y,z axes
%angles(1)=psi_ua; angles(2)=theta_ua; angles(3)=phi_ua
T_Rua(1,1,t)=cos(Rangles(t,3))*cos(Rangles(t,2));
T_Rua(1,2,t)=sin(Rangles(t,3))*cos(Rangles(t,2));
T_Rua(1,3,t)=-sin(Rangles(t,2));
T_Rua(2,1,t)=-
sin(Rangles(t,3))*cos(Rangles(t,1))+cos(Rangles(t,3))*sin(Rangles(t,2))*sin(Rangles(t,1));

T_Rua(2,2,t)=cos(Rangles(t,3))*cos(Rangles(t,1))+sin(Rangles(t,3))*sin(Rangles(t,2))*sin(Rang
les(t,1));
T_Rua(2,3,t)=cos(Rangles(t,2))*sin(Rangles(t,1));

T_Rua(3,1,t)=sin(Rangles(t,3))*sin(Rangles(t,1))+cos(Rangles(t,3))*sin(Rangles(t,2))*cos(Rang
les(t,1));
T_Rua(3,2,t)=-
cos(Rangles(t,3))*sin(Rangles(t,1))+cos(Rangles(t,1))*sin(Rangles(t,1))*cos(Rangles(t,1));
T_Rua(3,3,t)=cos(Rangles(t,2))*cos(Rangles(t,1));

T_Lua(1,1,t)=cos(Langles(t,3))*cos(Langles(t,2));
T_Lua(1,2,t)=sin(Langles(t,3))*cos(Langles(t,2));
T_Lua(1,3,t)=-sin(Langles(t,2));

```

```

T_Lua(2,1,t)=-
sin(Langles(t,3))*cos(Langles(t,1))+cos(Langles(t,3))*sin(Langles(t,2))*sin(Langles(t,1));

T_Lua(2,2,t)=cos(Langles(t,3))*cos(Langles(t,1))+sin(Langles(t,3))*sin(Langles(t,2))*sin(Langles(t,1));
T_Lua(2,3,t)=cos(Langles(t,2))*sin(Langles(t,1));

T_Lua(3,1,t)=sin(Langles(t,3))*sin(Langles(t,1))+cos(Langles(t,3))*sin(Langles(t,2))*cos(Langles(t,1));
T_Lua(3,2,t)=-
cos(Langles(t,3))*sin(Langles(t,1))+cos(Langles(t,1))*sin(Langles(t,1))*cos(Langles(t,1));
T_Lua(3,3,t)=cos(Langles(t,2))*cos(Langles(t,1));

%EQN.18 Calculate inertias about global x,y,z
Ip_Rua(:, :, t)=T_Rua(:, :, t)*Rual*T_Rua(:, :, t)';
Ip_Lua(:, :, t)=T_Lua(:, :, t)*LuaI*T_Lua(:, :, t)';

%EQN.20 Set up I matrix that contains mass and inertia information
I_Rua(1,1,t)=Ruamass;
I_Rua(2,2,t)=Ruamass;
I_Rua(3,3,t)=Ruamass;
I_Rua(4:6,4:6,t)=Ip_Rua(:, :, t);

I_Lua(1,1,t)=Luamass;
I_Lua(2,2,t)=Luamass;
I_Lua(3,3,t)=Luamass;
I_Lua(4:6,4:6,t)=Ip_Lua(:, :, t);

%EQN. 20 Set up angular velocity vector(lowercase omega-- will call "w")
w_Rua(:, :, t)=[0;0;0;Rvelocities(t,1);Rvelocities(t,2);Rvelocities(t,3)];
w_Lua(:, :, t)=[0;0;0;Lvelocities(t,1);Lvelocities(t,2);Lvelocities(t,3)];

%EQN. 21 Calculate product of angular velocity matrices (omega*I*w)
omegaIw_Rua(:, :, t)=omega_Rua(:, :, t)*I_Rua(:, :, t)*w_Rua(:, :, t);
omegaIw_Lua(:, :, t)=omega_Lua(:, :, t)*I_Lua(:, :, t)*w_Lua(:, :, t);

%EQN. 20 Define acceleration vector(linear [of center of mass] and angular
accelerations)

%a_ua(:, :, t)=[cmaccel(t,7);cmaccel(t,8);cmaccel(t,9);accelerations(t,1);accelerations(t,2);accelerations(t,3)];
a_Rua(:, :, t)=[Rcmaccel(t,7);Rcmaccel(t,8);Rcmaccel(t,9);0;0;Raccelerations(t,3)];
a_Lua(:, :, t)=[Lcmaccel(t,7);Lcmaccel(t,8);Lcmaccel(t,9);0;0;Laccelerations(t,3)];
%xz and yz plane angular accelerations ignored because they are
%prone to quadrant changes when the arm is vertical. contributions
%are negligible in these two planes

```

```

%EQN. 21 Calculate matrix that combines inertial properties and linear
accelerations
Ia_Rua(:,:,t)=I_Rua(:,:,t)*a_Rua(:,:,t);
Ia_Lua(:,:,t)=I_Lua(:,:,t)*a_Lua(:,:,t);

%EQN. 21 Calculate reaction force at shoulder center in global coordinate system
rP_Rua(:,:,t)=PHI_rD_Rua(:,:,t)-Ia_Rua(:,:,t)-omegaIw_Rua(:,:,t)+Mg_Rua(:,:,t);
rP_Lua(:,:,t)=PHI_rD_Lua(:,:,t)-Ia_Lua(:,:,t)-omegaIw_Lua(:,:,t)+Mg_Lua(:,:,t);

%      plot3(rP_ua(1:3,1,t)) %checking the forces

% previously use for checking results
% left in for future troubleshooting
%      if n==1
%          fxr_shoulder(1,t)=-rP_ua(1,1,t);
%          fyr_shoulder(1,t)=-rP_ua(2,1,t);
%          fzr_shoulder(1,t)=-rP_ua(3,1,t);
%          mxr_shoulder(1,t)=-rP_ua(4,1,t);
%          myr_shoulder(1,t)=-rP_ua(5,1,t);
%          m zr_shoulder(1,t)=-rP_ua(6,1,t);
%
resultant_force_shoulder(1,t)=sqrt(rP_ua(1,1,t)^2+rP_ua(2,1,t)^2+rP_ua(3,1,t)^2);
%
resultant_moment_shoulder(1,t)=sqrt(rP_ua(4,1,t)^2+rP_ua(5,1,t)^2+rP_ua(6,1,t)^2);
%      else
%          fxl_shoulder(1,t)=-rP_ua(1,1,t);
%          fyl_shoulder(1,t)=-rP_ua(2,1,t);
%          fzl_shoulder(1,t)=-rP_ua(3,1,t);
%          mxl_shoulder(1,t)=-rP_ua(4,1,t);
%          myl_shoulder(1,t)=-rP_ua(5,1,t);
%          mzl_shoulder(1,t)=-rP_ua(6,1,t);
%      end
%
%      %static check of shoulder Fy forces
%      check_sho_fy(t,1)=-
forces(t,2)+massall(1,1)*9.8+massall(1,2)*9.8+massall(1,3)*9.8;

%----- Calculate Local Coordinate Systems for Segments-----
%
%-----Hand local coordinate system-----%

%temporary k axis of hand (use to calculate i)
%Local x (i): point forward; Local y (j): point upward; Local
%z (k): point to the right

```

```

%if n==1 %vector points to right for both sides in standard anatomical position
v1_Rhand(t,1:3)=Rradsty(t,1:3)-Rulnsty(t,1:3); %vector 1, not normalized
k_Rhand_temp(t,1:3)= v1_Rhand(t,1:3)/norm(v1_Rhand(t,1:3)); %normalized
vector 1 (temporary k vector)
% else %vector points to right for both sides in standard anatomical position
% v1_hand(t,1:3)=ulnsty(t,1:3)-radsty(t,1:3); %vector 1, not normalized
% k_hand_temp(t,1:3)= v1_hand(t,1:3)/norm(v1_hand(t,1:3)); %normalized
vector 1 (temporary k vector)
% end
v1_Lhand(t,1:3)=Lulnsty(t,1:3)-Lradsty(t,1:3); % vector 1, not normalized
k_Lhand_temp(t,1:3)= v1_Lhand(t,1:3)/norm(v1_Lhand(t,1:3)); %normalized
vector 1 (temporary k vector)

%j axis of the hand
v2_Rhand(t,1:3)=Rwristcen(t,1:3)-Rthirdmp(t,1:3); %vector 2, not normalized
j_Rhand(t,1:3)= v2_Rhand(t,1:3)/norm(v2_Rhand(t,1:3)); %normalized vector 2
(j vector)

v2_Lhand(t,1:3)=Lwristcen(t,1:3)-Lthirdmp(t,1:3); %vector 2, not normalized
j_Lhand(t,1:3)= v2_Lhand(t,1:3)/norm(v2_Lhand(t,1:3)); %normalized vector 2 (j
vector)

%i axis of the hand
v3_Rhand(t,1:3)=cross(j_Rhand(t,1:3),k_Rhand_temp(t,1:3));%vector 3, not
normalized
i_Rhand(t,1:3)=v3_Rhand(t,1:3)/norm(v3_Rhand(t,1:3)); %normalized vector 2
(k vector)

v3_Lhand(t,1:3)=cross(j_Lhand(t,1:3),k_Lhand_temp(t,1:3));%vector 3, not
normalized
i_Lhand(t,1:3)=v3_Lhand(t,1:3)/norm(v3_Lhand(t,1:3)); %normalized vector 2 (k
vector)

%k axis of the hand
v4_Rhand(t,1:3)=cross(i_Rhand(t,1:3),j_Rhand(t,1:3));%vector 4, not normalized
k_Rhand(t,1:3)=v4_Rhand(t,1:3)/norm(v4_Rhand(t,1:3)); %normalized vector 2
(i vector)

v4_Lhand(t,1:3)=cross(i_Lhand(t,1:3),j_Lhand(t,1:3));%vector 4, not normalized
k_Lhand(t,1:3)=v4_Lhand(t,1:3)/norm(v4_Lhand(t,1:3)); %normalized vector 2 (i
vector)

%rotation matrix for hand
rot_Rhand(1,1:3,t)=i_Rhand(t,1:3); %first row is i unit vector
rot_Rhand(2,1:3,t)=j_Rhand(t,1:3); %second row is j unit vector
rot_Rhand(3,1:3,t)=k_Rhand(t,1:3); %third row is k unit vector

```

```

rot_Lhand(1,1:3,t)=i_Lhand(t,1:3); %first row is i unit vector
rot_Lhand(2,1:3,t)=j_Lhand(t,1:3); %second row is j unit vector
rot_Lhand(3,1:3,t)=k_Lhand(t,1:3); %third row is k unit vector

%-----Forearm local coordinate system-----%

%temporary k axis of forearm (use to calculate i)
% if n==1 %vector points to right for both sides in standard anatomical position
v1_Rfa(t,1:3)=Rradsty(t,1:3)-Rulnsty(t,1:3); %vector 1, not normalized
k_Rfa_temp(t,1:3)= v1_Rfa(t,1:3)/norm(v1_Rfa(t,1:3)); %normalized vector 1
(temporary k vector)
% else %vector points to right for both sides in standard anatomical position
% v1_fa(t,1:3)=ulnsty(t,1:3)-radsty(t,1:3); %vector 1, not normalized
% k_fa_temp(t,1:3)= v1_fa(t,1:3)/norm(v1_fa(t,1:3)); %normalized vector 1
(temporary k vector)
% end
v1_Lfa(t,1:3)=Lulnsty(t,1:3)-Lradsty(t,1:3); %vector 1, not normalized
k_Lfa_temp(t,1:3)= v1_Lfa(t,1:3)/norm(v1_Lfa(t,1:3)); %normalized vector 1
(temporary k vector)

%j axis of the forearm
v2_Rfa(t,1:3)=Rlatep(t,1:3)-Rulnsty(t,1:3); %vector 2, not normalized
j_Rfa(t,1:3)= v2_Rfa(t,1:3)/norm(v2_Rfa(t,1:3)); %normalized vector 2 (j vector)

v2_Lfa(t,1:3)=Llatep(t,1:3)-Lulnsty(t,1:3); %vector 2, not normalized
j_Lfa(t,1:3)= v2_Lfa(t,1:3)/norm(v2_Lfa(t,1:3)); %normalized vector 2 (j vector)

%i axis of the forearm
v3_Rfa(t,1:3)=cross(j_Rfa(t,1:3),k_Rfa_temp(t,1:3));%vector 3, not normalized
i_Rfa(t,1:3)=v3_Rfa(t,1:3)/norm(v3_Rfa(t,1:3)); %normalized vector 2 (i vector)

v3_Lfa(t,1:3)=cross(j_Lfa(t,1:3),k_Lfa_temp(t,1:3));%vector 3, not normalized
i_Lfa(t,1:3)=v3_Lfa(t,1:3)/norm(v3_Lfa(t,1:3)); %normalized vector 2 (i vector)

%k axis of the forearm
v4_Rfa(t,1:3)=cross(i_Rfa(t,1:3),j_Rfa(t,1:3));%vector 4, not normalized
k_Rfa(t,1:3)=v4_Rfa(t,1:3)/norm(v4_Rfa(t,1:3)); %normalized vector 2 (k vector)

v4_Lfa(t,1:3)=cross(i_Lfa(t,1:3),j_Lfa(t,1:3));%vector 4, not normalized
k_Lfa(t,1:3)=v4_Lfa(t,1:3)/norm(v4_Lfa(t,1:3)); %normalized vector 2 (k vector)

%rotation matrix for forearm
rot_Rfa(1,1:3,t)=i_Rfa(t,1:3); %first row is i unit vector
rot_Rfa(2,1:3,t)=j_Rfa(t,1:3); %second row is j unit vector
rot_Rfa(3,1:3,t)=k_Rfa(t,1:3); %third row is k unit vector

```

```

rot_Lfa(1,1:3,t)=i_Lfa(t,1:3); %first row is i unit vector
rot_Lfa(2,1:3,t)=j_Lfa(t,1:3); %second row is j unit vector
rot_Lfa(3,1:3,t)=k_Lfa(t,1:3); %third row is k unit vector
%-----Humerus local coordinate system-----%
%Reference is Cooper et al. Glenohumeral Joint Kinematics and Kinetics.....Am J
Phys Med Rehab 1999.
%EQN. 1-2,5

%temporary i axis of upper arm (use to calculate k)
v1_Rua(t,1:3)=Rulnsty(t,1:3)-Rlatep(t,1:3); %vector 1, not normalized
i_Rua_temp(t,1:3)= v1_Rua(t,1:3)/norm(v1_Rua(t,1:3)); %normalized vector 1
(temporary i vector)

v1_Lua(t,1:3)=Lulnsty(t,1:3)-Llatep(t,1:3); %vector 1, not normalized
i_Lua_temp(t,1:3)= v1_Lua(t,1:3)/norm(v1_Lua(t,1:3)); %normalized vector 1
(temporary i vector)

%j axis of the upper arm (called j_s in cooper's paper)
v2_Rua(t,1:3)=Racro(t,1:3)-Rlatep(t,1:3); %vector 2, not normalized
j_Rua(t,1:3)= v2_Rua(t,1:3)/norm(v2_Rua(t,1:3)); %normalized vector 2 (j
vector)

v2_Lua(t,1:3)=Lacro(t,1:3)-Llatep(t,1:3); %vector 2, not normalized
j_Lua(t,1:3)= v2_Lua(t,1:3)/norm(v2_Lua(t,1:3)); %normalized vector 2 (j
vector)

%k axis of the upper arm (called k_s in cooper's paper)
v3_Rua(t,1:3)=cross(i_Rua_temp(t,1:3),j_Rua(t,1:3));%vector 3, not normalized
k_Rua(t,1:3)=v3_Rua(t,1:3)/norm(v3_Rua(t,1:3)); %normalized vector 2 (k
vector)

v3_Lua(t,1:3)=cross(i_Lua_temp(t,1:3),j_Lua(t,1:3));%vector 3, not normalized
k_Lua(t,1:3)=v3_Lua(t,1:3)/norm(v3_Lua(t,1:3)); %normalized vector 2 (k
vector)

%i axis of the upper arm (called i_s in cooper's paper)
v4_Rua(t,1:3)=cross(j_Rua(t,1:3),k_Rua(t,1:3));%vector 4, not normalized
i_Rua(t,1:3)=v4_Rua(t,1:3)/norm(v4_Rua(t,1:3)); %normalized vector 2 (i vector)

v4_Lua(t,1:3)=cross(j_Lua(t,1:3),k_Lua(t,1:3));%vector 4, not normalized
i_Lua(t,1:3)=v4_Lua(t,1:3)/norm(v4_Lua(t,1:3)); %normalized vector 2 (i vector)

%rotation matrix for upper arm
rot_Rua(1,1:3,t)=i_Rua(t,1:3); %first row is i unit vector
rot_Rua(2,1:3,t)=j_Rua(t,1:3); %second row is j unit vector

```

```

rot_Rua(3,1:3,t)=k_Rua(t,1:3); %third row is k unit vector

rot_Lua(1,1:3,t)=i_Lua(t,1:3); %first row is i unit vector
rot_Lua(2,1:3,t)=j_Lua(t,1:3); %second row is j unit vector
rot_Lua(3,1:3,t)=k_Lua(t,1:3); %third row is k unit vector
%-----Trunk local coordinate system-----%
%Cooper used a triad on the chest to create coordinate system
%I updated the coordinate system to follow the same convention, but
%avoided using the chest triad

%      shocen(t,1)=(kin(t,14)+kin(t,41))/2;
%      shocen(t,2)=(kin(t,15)+kin(t,42))/2;
%      shocen(t,3)=(kin(t,16)+kin(t,43))/2;

j_Gtrnn(t,1:3)=t3(t,1:3)-t8(t,1:3); % vector j, not normalized
j_tr(t,1:3)= j_Gtrnn(t,1:3)/norm(j_Gtrnn(t,1:3)); %normalized j vector

%intermediate axis of the trunk points anteriorly
i_Gtrint(t,1:3)=kin(t,109:111)-kin(t,106:108);

%k axis of trunk (points to the right in setpo)
k_Gtrnn(t,1:3)=cross(i_Gtrint(t,1:3),j_tr(t,1:3)); %vector k, not normalized
k_tr(t,1:3)= k_Gtrnn(t,1:3)/norm(k_Gtrnn(t,1:3));

%i axis of the trunk
i_Gtrnn(t,1:3)=cross(j_tr(t,1:3),k_tr(t,1:3));
i_tr(t,1:3)=i_Gtrnn(t,1:3)/norm(i_Gtrnn(t,1:3)); %normalized i vector

%rotation matrix for trunk
rot_tr(1,1:3,t)=i_tr(t,1:3); %first row is i unit vector
rot_tr(2,1:3,t)=j_tr(t,1:3); %second row is j unit vector
rot_tr(3,1:3,t)=k_tr(t,1:3); %third row is k unit vector

%      figure
%      plot(rot_tr(1))
%      hold on
%      plot(rot_tr(2),'r')
%      hold on
%      plot(rot_tr(3),'g')

%-----Calculate reaction forces/moments in anatomical coordinate systems----
-----%
right
% Local x (i): point forward; Local y (j): point upward; Local z (k): point to the
%forces at the wrist

```

```

forces      f_Rwrist(1:3,1,t)=rot_Rfa(:,:,t)*-rP_Rhand(1:3,1,t); %local forces=T*global
forces      f_Lwrist(1:3,1,t)=rot_Lfa(:,:,t)*-rP_Lhand(1:3,1,t); %local forces=T*global

%moments at the wrist
moments     m_Rwrist(1:3,1,t)=rot_Rfa(:,:,t)*-rP_Rhand(4:6,1,t); %local moments=T*global
moments     m_Lwrist(1:3,1,t)=rot_Lfa(:,:,t)*-rP_Lhand(4:6,1,t); %local moments=T*global

%reformat variables for plotting
%           if n==1
%           fm_Rwrist(t,1)=f_Rwrist(1,1,t);
%           fm_Rwrist(t,2)=f_Rwrist(2,1,t);
%           fm_Rwrist(t,3)=f_Rwrist(3,1,t);
%           fm_Rwrist(t,4)=m_Rwrist(1,1,t);
%           fm_Rwrist(t,5)=m_Rwrist(2,1,t);
%           fm_Rwrist(t,6)=m_Rwrist(3,1,t);

%           rf_Rwrist(t,1)=sqrt(fm_Rwrist(t,1)^2+ fm_Rwrist(t,2)^2 + fm_Rwrist(t,3)^2);
%           rm_Rwrist(t,1)=sqrt(fm_Rwrist(t,4)^2+ fm_Rwrist(t,5)^2 + fm_Rwrist(t,6)^2);

%           fm_Lwrist(t,1)=f_Lwrist(1,1,t);
%           fm_Lwrist(t,2)=f_Lwrist(2,1,t);
%           fm_Lwrist(t,3)=f_Lwrist(3,1,t);
%           fm_Lwrist(t,4)=m_Lwrist(1,1,t);
%           fm_Lwrist(t,5)=m_Lwrist(2,1,t);
%           fm_Lwrist(t,6)=m_Lwrist(3,1,t);

%           rf_Lwrist(t,1)=sqrt(fm_Lwrist(t,1)^2+ fm_Lwrist(t,2)^2 + fm_Lwrist(t,3)^2);
%           rm_Lwrist(t,1)=sqrt(fm_Lwrist(t,4)^2+ fm_Lwrist(t,5)^2 + fm_Lwrist(t,6)^2);

%forces at the elbow
f_Relbow(1:3,1,t)=rot_Rua(:,:,t)*-rP_Rfa(1:3,1,t); %local forces=T*global forces
f_Lelbow(1:3,1,t)=rot_Lua(:,:,t)*-rP_Lfa(1:3,1,t); %local forces=T*global forces

%moments at the wrist
moments     m_Relbow(1:3,1,t)=rot_Rua(:,:,t)*-rP_Rfa(4:6,1,t); %local moments=T*global
moments     m_Lelbow(1:3,1,t)=rot_Lua(:,:,t)*-rP_Lfa(4:6,1,t); %local moments=T*global

%reformat variables for plotting
%           if n==1
%           fm_Relbow(t,1)=f_Relbow(1,1,t);

```

```

fm_Relbow(t,2)=f_Relbow(2,1,t);
fm_Relbow(t,3)=f_Relbow(3,1,t);
fm_Relbow(t,4)=m_Relbow(1,1,t);
fm_Relbow(t,5)=m_Relbow(2,1,t);
fm_Relbow(t,6)=m_Relbow(3,1,t);
rf_Relbow(t,1)=sqrt(fm_Relbow(t,1)^2+ fm_Relbow(t,2)^2 +
fm_Relbow(t,3)^2);
rm_Relbow(t,1)=sqrt(fm_Relbow(t,4)^2+ fm_Relbow(t,5)^2 +
fm_Relbow(t,6)^2);

fm_Lelbow(t,1)=f_Lelbow(1,1,t);
fm_Lelbow(t,2)=f_Lelbow(2,1,t);
fm_Lelbow(t,3)=f_Lelbow(3,1,t);
fm_Lelbow(t,4)=m_Lelbow(1,1,t);
fm_Lelbow(t,5)=m_Lelbow(2,1,t);
fm_Lelbow(t,6)=m_Lelbow(3,1,t);
rf_Lelbow(t,1)=sqrt(fm_Lelbow(t,1)^2+ fm_Lelbow(t,2)^2 +
fm_Lelbow(t,3)^2);
rm_Lelbow(t,1)=sqrt(fm_Lelbow(t,4)^2+ fm_Lelbow(t,5)^2 +
fm_Lelbow(t,6)^2);

%forces at the shoulder
%EQN. 27 from Cooper et al.
f_Rshoulder(1:3,1,t)=rot_tr(:, :,t)*-rP_Rua(1:3,1,t); %local forces=T*global forces
f_Lshoulder(1:3,1,t)=rot_tr(:, :,t)*-rP_Lua(1:3,1,t); %local forces=T*global forces

%moments at the shoulder
%EQN. 28 from Cooper et al.
m_Rshoulder(1:3,1,t)=rot_tr(:, :,t)*-rP_Rua(4:6,1,t); %local moments=T*global
moments
m_Lshoulder(1:3,1,t)=rot_tr(:, :,t)*-rP_Lua(4:6,1,t); %local moments=T*global
moments

%reformat variables for plotting
% if n==1
fm_Rsho(t,1)=f_Rshoulder(1,1,t);
fm_Rsho(t,2)=f_Rshoulder(2,1,t);
fm_Rsho(t,3)=f_Rshoulder(3,1,t);
fm_Rsho(t,4)=m_Rshoulder(1,1,t);
fm_Rsho(t,5)=m_Rshoulder(2,1,t);
fm_Rsho(t,6)=m_Rshoulder(3,1,t);
rf_Rsho(t,1)=sqrt(fm_Rsho(t,1)^2+ fm_Rsho(t,2)^2 + fm_Rsho(t,3)^2);
rm_Rsho(t,1)=sqrt(fm_Rsho(t,4)^2+ fm_Rsho(t,5)^2 + fm_Rsho(t,6)^2);

```

```

fm_Lsho(t,1)=f_Lshoulder(1,1,t);
fm_Lsho(t,2)=f_Lshoulder(2,1,t);
fm_Lsho(t,3)=f_Lshoulder(3,1,t);
fm_Lsho(t,4)=m_Lshoulder(1,1,t);
fm_Lsho(t,5)=m_Lshoulder(2,1,t);
fm_Lsho(t,6)=m_Lshoulder(3,1,t);
rf_Lsho(t,1)=sqrt(fm_Lsho(t,1)^2+ fm_Lsho(t,2)^2 + fm_Lsho(t,3)^2);
rm_Lsho(t,1)=sqrt(fm_Lsho(t,4)^2+ fm_Lsho(t,5)^2 + fm_Lsho(t,6)^2);

```

end

```

save localFM_Rwrist.txt fm_Rwrist -ascii;
save resultantF_Rwrist.txt rf_Rwrist -ascii;
save resultantM_Rwrist.txt rm_Rwrist -ascii;
save localFM_Lwrist.txt fm_Lwrist -ascii;
save resultantF_Lwrist.txt rf_Lwrist -ascii;
save resultantM_Lwrist.txt rm_Lwrist -ascii;
save localFM_Relbow.txt fm_Relbow -ascii;
save resultantF_Relbow.txt rf_Relbow -ascii;
save resultantM_Relbow.txt rm_Relbow -ascii;
save localFM_Lelbow.txt fm_Lelbow -ascii;
save resultantF_Lelbow.txt rf_Lelbow -ascii;
save resultantM_Lelbow.txt rm_Lelbow -ascii;
save localFM_Rshoulder.txt fm_Rsho -ascii;
save resultantF_Rshoulder.txt rf_Rsho -ascii;
save resultantM_Rshoulder.txt rm_Rsho -ascii;
save localFM_Lshoulder.txt fm_Lsho -ascii;
save resultantF_Lshoulder.txt rf_Lsho -ascii;
save resultantM_Lshoulder.txt rm_Lsho -ascii;

```

figure (3);

```

subplot(3,1,1);plot(fm_Rwrist(:,2));title('Right wrist superior force (+)');
subplot(3,1,2);plot (fm_Rwrist(:,6),'r');title('Right wrist flex(+)/exten moment');
subplot(3,1,3);plot (Reuang(:,8),'g');title('Right wrist flex(+)/exten angle');

```

figure (4);

```

subplot(3,1,1);plot (fm_Lwrist(:,2));title('Left wrist superior force (+)');
subplot(3,1,2);plot (fm_Lwrist(:,6),'r');title('Left wrist flex(+)/exten moment');
subplot(3,1,3);plot (Leuang(:,8),'g');title('Left wrist flex(+)/exten angle');

```

figure (5);

```

subplot(3,1,1);plot (fm_Relbow(:,2));title('Right elbow superior force (+)');
subplot(3,1,2);plot (fm_Relbow(:,6),'r');title('Right elbow flex(+)/exten moment');
subplot(3,1,3);plot (Reuang(:,5),'g');title('Right elbow flex(+)/exten angle');

```

figure (6);

```

subplot(3,1,1);plot (fm_Lelbow(:,2));title('Left elbow superior force (+)');
subplot(3,1,2);plot (fm_Lelbow(:,6),'r');title('Left elbow flex(+)/exten moment');
subplot(3,1,3);plot (Leuang(:,5),'g');title('Left elbow flex(+)/exten angle');

```

```

figure (7);
subplot(3,1,1);plot (fm_Rsho(:,2));title('Right shoulder superior force (+)');
subplot(3,1,2);plot (fm_Rsho(:,4),'r');title('Right shoulder add(+)/abd moment');
subplot(3,1,3);plot (Reuang(:,3),'g');title('Right shoulder IR angle (+)');
figure (8);
subplot(3,1,1);plot (fm_Lsho(:,2));title('Left shoulder superior force (+)');
subplot(3,1,2);plot (fm_Lsho(:,4),'r');title('Left shoulder abd(+)/add moment');
subplot(3,1,3);plot (Leuang(:,3),'g');title('Left shoulder IR angle (+)');

%%%%%%%%%%%%%%%%%%%%%%%%%%%%%%%%%%%%%%%%%%%%%%%%%%%%%%%%%%%%%%%%%%%%%%%%
%%%%%%%%%%%%%%%%%%%%%%%%%%%%%%%%%%%%%%%%%%%%%%%%%%%%%%%%%%%%%%%%%%%%%%%%
%%%%%%%%%%%%%%%%%%%%%%%%%%%%%%%%%%%%%%%%%%%%%%%%%%%%%%%%%%%%%%%%%%%%%%%% Calculate the variables
%%%%%%%%%%%%%%%%%%%%%%%%%%%%%%%%%%%%%%%%%%%%%%%%%%%%%%%%%%%%%%%%%%%%%%%%
clc
clear all

%%%%%%%%% hand reation force %%%%%%%%%
load BNFP_FM.txt
load WCLC_FM.txt

BN_FM=BNFP_FM(:,:);
LC_FM=WCLC_FM(:,:);

BN_FX=BN_FM(:,1);
BN_FY=BN_FM(:,2);
BN_FZ=BN_FM(:,3);
BN_MX=BN_FM(:,4);
BN_MY=BN_FM(:,5);
BN_MZ=BN_FM(:,6);
LHand_resultantF=sqrt((BN_FX.^2+BN_FY.^2+BN_FZ.^2)); %Left hand resultant
force
LHand_HorizontalF=sqrt((BN_FX.^2+BN_FY.^2)); %Left hand horizontal force

LC_FX=LC_FM(:,1);
LC_FY=LC_FM(:,2);
LC_FZ=LC_FM(:,3);
LC_MX=LC_FM(:,4);
LC_MY=LC_FM(:,5);
LC_MZ=LC_FM(:,6);
RHand_resultantF=sqrt((LC_FX.^2+LC_FY.^2+LC_FZ.^2)); %Right hand resultant
force
RHand_HorizontalF=sqrt((LC_FX.^2+LC_FY.^2)); %Right hand horizontal force

% load start_descent.txt
load start_descent_prelift.txt
start_descent=start_descent_prelift(2);

```

```

lift_phase=start_descent/length(BNFP_FM)*100;

%%%%%% Right (trailing) hand reaction force in the whole transfer %%%%%%%%%%%
ave_LCFZ=mean(abs(LC_FZ));
ave_RHandRF=mean(abs(RHand_resultantF));
ave_RHandHF=mean(abs(RHand_HorizontalF));

max_LCFZ=max(abs(LC_FZ));
max_RHandRF=max(abs(RHand_resultantF));
max_RHandHF=max(abs(RHand_HorizontalF));
ave_max_trailingF=[ave_LCFZ ave_RHandHF ave_RHandRF; max_LCFZ
max_RHandHF max_RHandRF];
save ave_max_trailingF.txt ave_max_trailingF -ascii;

%%%%%% Right (trailing) hand reaction force in lift phase %%%%%%%%%%%
[peak_trailingVF_lift, trailing_VFIdx_lift]=max(LC_FZ(1:start_descent,:));
[peak_trailingHF_lift,
trailing_HFIdx_lift]=max(RHand_HorizontalF(1:start_descent,:));
[peak_trailingRF_lift, trailing_RFIdx_lift]=max(RHand_resultantF(1:start_descent,:));
trailing_VFIdx_liftPhase=trailing_VFIdx_lift/start_descent;
trailing_HFIdx_liftPhase=trailing_HFIdx_lift/start_descent;
trailing_RFIdx_liftPhase=trailing_RFIdx_lift/start_descent;
ave_LCFZ_lift=mean(abs(LC_FZ(1:start_descent,:)));
ave_RHandRF_lift=mean(abs(RHand_resultantF(1:start_descent,:)));
ave_RHandHF_lift=mean(abs(RHand_HorizontalF(1:start_descent,:)));
peak_trailingF_lift=[trailing_VFIdx_liftPhase trailing_HFIdx_liftPhase
trailing_RFIdx_liftPhase; peak_trailingVF_lift peak_trailingHF_lift peak_trailingRF_lift ...
; ave_LCFZ_lift ave_RHandHF_lift ave_RHandRF_lift];
save max_trailingF_lift.txt peak_trailingF_lift -ascii;

%%%%%% Left (leading) hand reaction force in lift phase
%%%%%%%%%%
[peak_leadingVF_lift, leading_VFIdx_lift]=max(BN_FZ(1:start_descent,:));
[peak_leadingHF_lift,
leading_HFIdx_lift]=max(LHand_HorizontalF(1:start_descent,:));
[peak_leadingRF_lift, leading_RFIdx_lift]=max(LHand_resultantF(1:start_descent,:));
leading_VFIdx_liftPhase=leading_VFIdx_lift/start_descent;
leading_HFIdx_liftPhase=leading_HFIdx_lift/start_descent;
leading_RFIdx_liftPhase=leading_RFIdx_lift/start_descent;
ave_BNFZ_lift=mean(BN_FZ(1:start_descent,:));
ave_LHandHF_lift=mean(abs(LHand_HorizontalF(1:start_descent,:)));
ave_LHandRF_lift=mean(abs(LHand_resultantF(1:start_descent,:)));
peak_leadingF_lift=[leading_VFIdx_liftPhase leading_HFIdx_liftPhase
leading_RFIdx_liftPhase; peak_leadingVF_lift peak_leadingHF_lift peak_leadingRF_lift ...
;ave_BNFZ_lift ave_LHandHF_lift ave_LHandRF_lift];

```

save max_leadingF_lift.txt peak_leadingF_lift -ascii; %peak vertical force, peak horizontal force, and peak resultant force

```
%%%%%%%% Landing force %%%%%%%%%%%%%%
[peak_landingVF, peak_landingVFI]=max(BN_FZ(:,1));
landingHF=LHand_HorizontalF(peak_landingVFI,1);
landingRF=LHand_resultantF(peak_landingVFI,1);
landingF=[peak_landingVF landingHF landingRF lift_phase];
save max_landingF.txt landingF -ascii;
```

```
%%%%%%%% joint reaction force and joint moment %%%%%%%%%
%%%%%%%% resultant force and force rate in LIFT phase %%%%%%%%%
load resultantF_Rshoulder.txt
load resultantF_Lshoulder.txt
load resultantF_Relbow.txt
load resultantF_Lelbow.txt
load resultantF_Rwrist.txt
load resultantF_Lwrist.txt
```

```
[peak_RF_RSH, peak_RF_RSHIndex]=max(resultantF_Rshoulder(1:start_descent,:));
[peak_RF_LSH, peak_RF_LSHIndex]=max(resultantF_Lshoulder(1:start_descent,:));
[peak_RF_REL, peak_RF_RELIndex]=max(resultantF_Relbow(1:start_descent,:));
[peak_RF_LEL, peak_RF_LELIndex]=max(resultantF_Lelbow(1:start_descent,:));
[peak_RF_RWR, peak_RF_RWRIndex]=max(resultantF_Rwrist(1:start_descent,:));
[peak_RF_LWR, peak_RF_LWRIndex]=max(resultantF_Lwrist(1:start_descent,:));
peak_RF_RSHIndex_LiftPhase=peak_RF_RSHIndex/start_descent;
peak_RF_LSHIndex_LiftPhase=peak_RF_LSHIndex/start_descent;
peak_RF_RELIndex_LiftPhase=peak_RF_RELIndex/start_descent;
peak_RF_LELIndex_LiftPhase=peak_RF_LELIndex/start_descent;
peak_RF_RWRIndex_LiftPhase=peak_RF_RWRIndex/start_descent;
peak_RF_LWRIndex_LiftPhase=peak_RF_LWRIndex/start_descent;
```

```
ave_RF_RSH=mean(resultantF_Rshoulder(1:start_descent,:));
ave_RF_LSH=mean(resultantF_Lshoulder(1:start_descent,:));
ave_RF_REL=mean(resultantF_Relbow(1:start_descent,:));
ave_RF_LEL=mean(resultantF_Lelbow(1:start_descent,:));
ave_RF_RWR=mean(resultantF_Rwrist(1:start_descent,:));
ave_RF_LWR=mean(resultantF_Lwrist(1:start_descent,:));
```

```
[min_RF_RSH, min_RF_RSHIndex]=min(resultantF_Rshoulder(1:start_descent,:));
[min_RF_LSH, min_RF_LSHIndex]=min(resultantF_Lshoulder(1:start_descent,:));
[min_RF_REL, min_RF_RELIndex]=min(resultantF_Relbow(1:start_descent,:));
[min_RF_LEL, min_RF_LELIndex]=min(resultantF_Lelbow(1:start_descent,:));
[min_RF_RWR, min_RF_RWRIndex]=min(resultantF_Rwrist(1:start_descent,:));
[min_RF_LWR, min_RF_LWRIndex]=min(resultantF_Lwrist(1:start_descent,:));
min_RF_RSHIndex_LiftPhase=min_RF_RSHIndex/start_descent;
```

```

min_RF_LSHIndex_LiftPhase=min_RF_LSHIndex/start_descent;
min_RF_RELIndex_LiftPhase=min_RF_RELIndex/start_descent;
min_RF_LELIndex_LiftPhase=min_RF_LELIndex/start_descent;
min_RF_RWRIndex_LiftPhase=min_RF_RWRIndex/start_descent;
min_RF_LWRIndex_LiftPhase=min_RF_LWRIndex/start_descent;

R_peakJRF_lift=[ave_RF_RSH ave_RF_REL ave_RF_RWR; peak_RF_RSH
peak_RF_REL peak_RF_RWR; peak_RF_RSHIndex_LiftPhase peak_RF_RELIndex_LiftPhase
peak_RF_RWRIndex_LiftPhase];
L_peakJRF_lift=[ave_RF_LSH ave_RF_LEL ave_RF_LWR; peak_RF_LSH
peak_RF_LEL peak_RF_LWR; peak_RF_LSHIndex_LiftPhase peak_RF_LELIndex_LiftPhase
peak_RF_LWRIndex_LiftPhase];
save Right_JointResultantF.txt R_peakJRF_lift -ascii;
save Left_JointResultantF.txt L_peakJRF_lift -ascii;

Ave_RFRate_RSH=(peak_RF_RSH-min_RF_RSH)*100/(peak_RF_RSHIndex-
min_RF_RSHIndex); % force rate of loading (Newton/second)
Sim_RFRate_RSH=diff(resultantF_Rshoulder(1:start_descent,:)).*100; % simultaneous
force rate of loading (Newton/second)
[Max_Sim_RFRate_RSH, Max_Sim_RFRate_RSHIndex]=max(Sim_RFRate_RSH(:,,:));
% maximal simultaneous force rate of loading
Max_Sim_RFRate_RSHPhase=Max_Sim_RFRate_RSHIndex/(start_descent-1);

Ave_RFRate_LSH=(peak_RF_LSH-min_RF_LSH)*100/(peak_RF_LSHIndex-
min_RF_LSHIndex); % force rate of loading (Newton/second)
Sim_RFRate_LSH=diff(resultantF_Lshoulder(1:start_descent,:)).*100; % simultaneous
force rate of loading (Newton/second)
[Max_Sim_RFRate_LSH, Max_Sim_RFRate_LSHIndex]=max(Sim_RFRate_LSH(:,,:));
% maximal simultaneous force rate of loading
Max_Sim_RFRate_LSHPhase=Max_Sim_RFRate_LSHIndex/(start_descent-1);

Ave_RFRate_REL=(peak_RF_REL-min_RF_REL)*100/(peak_RF_RELIndex-
min_RF_RELIndex); % force rate of loading (Newton/second)
Sim_RFRate_REL=diff(resultantF_Relbow(1:start_descent,:)).*100; % simultaneous
force rate of loading (Newton/second)
[Max_Sim_RFRate_REL, Max_Sim_RFRate_RELIndex]=max(Sim_RFRate_REL(:,,:));
% maximal simultaneous force rate of loading
Max_Sim_RFRate_RELPhase=Max_Sim_RFRate_RELIndex/(start_descent-1);

Ave_RFRate_LEL=(peak_RF_LEL-min_RF_LEL)*100/(peak_RF_LELIndex-
min_RF_LELIndex); % force rate of loading (Newton/second)
Sim_RFRate_LEL=diff(resultantF_Lelbow(1:start_descent,:)).*100; % simultaneous
force rate of loading (Newton/second)
[Max_Sim_RFRate_LEL, Max_Sim_RFRate_LELIndex]=max(Sim_RFRate_LEL(:,,:));
% maximal simultaneous force rate of loading
Max_Sim_RFRate_LELPhase=Max_Sim_RFRate_LELIndex/(start_descent-1);

```

```

    Ave_RFRate_RWR=(peak_RF_RWR-min_RF_RWR)*100/(peak_RF_RWRIndex-
min_RF_RWRIndex); % force rate of loading (Newton/second)
    Sim_RFRate_RWR=diff(resultantF_Rwrist(1:start_descent,:)).*100; % simultaneous
force rate of loading (Newton/second)
    [Max_Sim_RFRate_RWR,
Max_Sim_RFRate_RWRIndex]=max(Sim_RFRate_RWR(:,:)); % maximal simultaneous force
rate of loading
    Max_Sim_RFRate_RWRPhase=Max_Sim_RFRate_RWRIndex/(start_descent-1);

    Ave_RFRate_LWR=(peak_RF_LWR-min_RF_LWR)*100/(peak_RF_LWRIndex-
min_RF_LWRIndex); % force rate of loading (Newton/second)
    Sim_RFRate_LWR=diff(resultantF_Lwrist(1:start_descent,:)).*100; % simultaneous
force rate of loading (Newton/second)
    [Max_Sim_RFRate_LWR,
Max_Sim_RFRate_LWRIndex]=max(Sim_RFRate_LWR(:,:)); % maximal simultaneous force
rate of loading
    Max_Sim_RFRate_LWRPhase=Max_Sim_RFRate_LWRIndex/(start_descent-1);

    R_ResultantFR=[Ave_RFRate_RSH Max_Sim_RFRate_RSH
Max_Sim_RFRate_RSHPhase; Ave_RFRate_REL Max_Sim_RFRate_REL
Max_Sim_RFRate_RELPhase;...
    Ave_RFRate_RWR Max_Sim_RFRate_RWR Max_Sim_RFRate_RWRPhase];
    L_ResultantFR=[Ave_RFRate_LSH Max_Sim_RFRate_LSH
Max_Sim_RFRate_LSHPhase; Ave_RFRate_LEL Max_Sim_RFRate_LEL
Max_Sim_RFRate_LELPhase;...
    Ave_RFRate_LWR Max_Sim_RFRate_LWR Max_Sim_RFRate_LWRPhase];
    save Right_ResultantFRate.txt R_ResultantFR -ascii;
    save Left_ResultantFRate.txt L_ResultantFR -ascii;

    %%%% resultant moment and moment rate in LIFT phase %%%%
    load resultantM_Rshoulder.txt
    load resultantM_Lshoulder.txt
    load resultantM_Relbow.txt
    load resultantM_Lelbow.txt
    load resultantM_Rwrist.txt
    load resultantM_Lwrist.txt

    [peak_RM_RSH, peak_RM_RSHIndex]=max(resultantM_Rshoulder(1:start_descent,:));
    [peak_RM_LSH, peak_RM_LSHIndex]=max(resultantM_Lshoulder(1:start_descent,:));
    [peak_RM_REL, peak_RM_RELIndex]=max(resultantM_Relbow(1:start_descent,:));
    [peak_RM_LEL, peak_RM_LELIndex]=max(resultantM_Lelbow(1:start_descent,:));
    [peak_RM_RWR, peak_RM_RWRIndex]=max(resultantM_Rwrist(1:start_descent,:));
    [peak_RM_LWR, peak_RM_LWRIndex]=max(resultantM_Lwrist(1:start_descent,:));
    peak_RM_RSHIndex_LiftPhase=peak_RM_RSHIndex/start_descent;
    peak_RM_LSHIndex_LiftPhase=peak_RM_LSHIndex/start_descent;

```

```

peak_RM_RELIndex_LiftPhase=peak_RM_RELIndex/start_descent;
peak_RM_LELIndex_LiftPhase=peak_RM_LELIndex/start_descent;
peak_RM_RWRIndex_LiftPhase=peak_RM_RWRIndex/start_descent;
peak_RM_LWRIndex_LiftPhase=peak_RM_LWRIndex/start_descent;

```

```

ave_RM_RSH=mean(resultantM_Rshoulder(1:start_descent,:));
ave_RM_LSH=mean(resultantM_Lshoulder(1:start_descent,:));
ave_RM_REL=mean(resultantM_Relbow(1:start_descent,:));
ave_RM_LEL=mean(resultantM_Lelbow(1:start_descent,:));
ave_RM_RWR=mean(resultantM_Rwrist(1:start_descent,:));
ave_RM_LWR=mean(resultantM_Lwrist(1:start_descent,:));

```

```

[min_RM_RSH, min_RM_RSHIndex]=min(resultantM_Rshoulder(1:start_descent,:));
[min_RM_LSH, min_RM_LSHIndex]=min(resultantM_Lshoulder(1:start_descent,:));
[min_RM_REL, min_RM_RELIndex]=min(resultantM_Relbow(1:start_descent,:));
[min_RM_LEL, min_RM_LELIndex]=min(resultantM_Lelbow(1:start_descent,:));
[min_RM_RWR, min_RM_RWRIndex]=min(resultantM_Rwrist(1:start_descent,:));
[min_RM_LWR, min_RM_LWRIndex]=min(resultantM_Lwrist(1:start_descent,:));
min_RM_RSHIndex_LiftPhase=min_RM_RSHIndex/start_descent;
min_RM_LSHIndex_LiftPhase=min_RM_LSHIndex/start_descent;
min_RM_RELIndex_LiftPhase=min_RM_RELIndex/start_descent;
min_RM_LELIndex_LiftPhase=min_RM_LELIndex/start_descent;
min_RM_RWRIndex_LiftPhase=min_RM_RWRIndex/start_descent;
min_RM_LWRIndex_LiftPhase=min_RM_LWRIndex/start_descent;

```

```

R_peakJRM_lift=[ave_RM_RSH ave_RM_REL ave_RM_RWR; peak_RM_RSH
peak_RM_REL peak_RM_RWR; peak_RM_RSHIndex_LiftPhase
peak_RM_RELIndex_LiftPhase peak_RM_RWRIndex_LiftPhase];

```

```

L_peakJRM_lift=[ave_RM_LSH ave_RM_LEL ave_RM_LWR; peak_RM_LSH
peak_RM_LEL peak_RM_LWR; peak_RM_LSHIndex_LiftPhase
peak_RM_LELIndex_LiftPhase peak_RM_LWRIndex_LiftPhase];
save Right_JointResultantM.txt R_peakJRM_lift -ascii;
save Left_JointResultantM.txt L_peakJRM_lift -ascii;

```

```

Ave_RMRate_RSH=(peak_RM_RSH-min_RM_RSH)*100/(peak_RM_RSHIndex-
min_RM_RSHIndex); % force rate of loading (Newton/second)

```

```

Sim_RMRate_RSH=diff(resultantM_Rshoulder(1:start_descent,:)).*100; % simultaneous
force rate of loading (Newton/second)

```

```

[Max_Sim_RMRate_RSH,
Max_Sim_RMRate_RSHIndex]=max(Sim_RMRate_RSH(:,:)); % maximal simultaneous force
rate of loading

```

```

Max_Sim_RMRate_RSHPhase=Max_Sim_RMRate_RSHIndex/(start_descent-1);

```

```

Ave_RMRate_LSH=(peak_RM_LSH-min_RM_LSH)*100/(peak_RM_LSHIndex-
min_RM_LSHIndex); % force rate of loading (Newton/second)

```

```

    Sim_RMRate_LSH=diff(resultantM_Lshoulder(1:start_descent,:)).*100; % simultaneous
force rate of loading (Newton/second)
    [Max_Sim_RMRate_LSH,
Max_Sim_RMRate_LSHIndex]=max(Sim_RMRate_LSH(:,:)); % maximal simultaneous force
rate of loading
    Max_Sim_RMRate_LSHPhase=Max_Sim_RMRate_LSHIndex/(start_descent-1);

    Ave_RMRate_REL=(peak_RM_REL-min_RM_REL)*100/(peak_RM_RELIndex-
min_RM_RELIndex); % force rate of loading (Newton/second)
    Sim_RMRate_REL=diff(resultantM_Relbow(1:start_descent,:)).*100; % simultaneous
force rate of loading (Newton/second)
    [Max_Sim_RMRate_REL,
Max_Sim_RMRate_RELIndex]=max(Sim_RMRate_REL(:,:)); % maximal simultaneous force
rate of loading
    Max_Sim_RMRate_RELPhase=Max_Sim_RMRate_RELIndex/(start_descent-1);

    Ave_RMRate_LEL=(peak_RM_LEL-min_RM_LEL)*100/(peak_RM_LELIndex-
min_RM_LELIndex); % force rate of loading (Newton/second)
    Sim_RMRate_LEL=diff(resultantM_Lelbow(1:start_descent,:)).*100; % simultaneous
force rate of loading (Newton/second)
    [Max_Sim_RMRate_LEL,
Max_Sim_RMRate_LELIndex]=max(Sim_RMRate_LEL(:,:)); % maximal simultaneous force
rate of loading
    Max_Sim_RMRate_LELPhase=Max_Sim_RMRate_LELIndex/(start_descent-1);

    Ave_RMRate_RWR=(peak_RM_RWR-min_RM_RWR)*100/(peak_RM_RWRIndex-
min_RM_RWRIndex); % force rate of loading (Newton/second)
    Sim_RMRate_RWR=diff(resultantM_Rwrist(1:start_descent,:)).*100; % simultaneous
force rate of loading (Newton/second)
    [Max_Sim_RMRate_RWR,
Max_Sim_RMRate_RWRIndex]=max(Sim_RMRate_RWR(:,:)); % maximal simultaneous force
rate of loading
    Max_Sim_RMRate_RWRPhase=Max_Sim_RMRate_RWRIndex/(start_descent-1);

    Ave_RMRate_LWR=(peak_RM_LWR-min_RM_LWR)*100/(peak_RM_LWRIndex-
min_RM_LWRIndex); % force rate of loading (Newton/second)
    Sim_RMRate_LWR=diff(resultantM_Lwrist(1:start_descent,:)).*100; % simultaneous
force rate of loading (Newton/second)
    [Max_Sim_RMRate_LWR,
Max_Sim_RMRate_LWRIndex]=max(Sim_RMRate_LWR(:,:)); % maximal simultaneous force
rate of loading
    Max_Sim_RMRate_LWRPhase=Max_Sim_RMRate_LWRIndex/(start_descent-1);

    R_ResultantMR=[Ave_RMRate_RSH Max_Sim_RMRate_RSH
Max_Sim_RMRate_RSHPhase; Ave_RMRate_REL Max_Sim_RMRate_REL
Max_Sim_RMRate_RELPhase;...

```

```

    Ave_RMRate_RWR Max_Sim_RMRate_RWR Max_Sim_RMRate_RWRPhase];
    L_ResultantMR=[Ave_RMRate_LSH Max_Sim_RMRate_LSH
Max_Sim_RMRate_LSHPhase; Ave_RMRate_LEL Max_Sim_RMRate_LEL
Max_Sim_RMRate_LELPhase;...

```

```

    Ave_RMRate_LWR Max_Sim_RMRate_LWR Max_Sim_RMRate_LWRPhase];
    save Right_ResultantMRate.txt R_ResultantMR -ascii;
    save Left_ResultantMRate.txt L_ResultantMR -ascii;

```

```

%% component forces in LIFT phase % % % %

```

```

load localFM_Rshoulder.txt
load localFM_Lshoulder.txt
load localFM_Relbow.txt
load localFM_Lelbow.txt
load localFM_Rwrist.txt
load localFM_Lwrist.txt

```

```

%% Right shoulder component force

```

```

[peak_FX_RSH, peak_FX_RSHIndex]=max(localFM_Rshoulder(1:start_descent,1));
peak_FX_RSHphase=peak_FX_RSHIndex/start_descent;
[peak_FY_RSH, peak_FY_RSHIndex]=max(localFM_Rshoulder(1:start_descent,2));
peak_FY_RSHphase=peak_FY_RSHIndex/start_descent;
[peak_FZ_RSH, peak_FZ_RSHIndex]=max(localFM_Rshoulder(1:start_descent,3));
peak_FZ_RSHphase=peak_FZ_RSHIndex/start_descent;
[peak_MX_RSH, peak_MX_RSHIndex]=max(localFM_Rshoulder(1:start_descent,4));
peak_MX_RSHphase=peak_MX_RSHIndex/start_descent;
[peak_MY_RSH, peak_MY_RSHIndex]=max(localFM_Rshoulder(1:start_descent,5));
peak_MY_RSHphase=peak_MY_RSHIndex/start_descent;
[peak_MZ_RSH, peak_MZ_RSHIndex]=max(localFM_Rshoulder(1:start_descent,6));
peak_MZ_RSHphase=peak_MZ_RSHIndex/start_descent;

```

```

[min_FX_RSH, min_FX_RSHIndex]=min(localFM_Rshoulder(1:start_descent,1));
min_FX_RSHphase=min_FX_RSHIndex/start_descent;
[min_FY_RSH, min_FY_RSHIndex]=min(localFM_Rshoulder(1:start_descent,2));
min_FY_RSHphase=min_FY_RSHIndex/start_descent;
[min_FZ_RSH, min_FZ_RSHIndex]=min(localFM_Rshoulder(1:start_descent,3));
min_FZ_RSHphase=min_FZ_RSHIndex/start_descent;
[min_MX_RSH, min_MX_RSHIndex]=min(localFM_Rshoulder(1:start_descent,4));
min_MX_RSHphase=min_MX_RSHIndex/start_descent;
[min_MY_RSH, min_MY_RSHIndex]=min(localFM_Rshoulder(1:start_descent,5));
min_MY_RSHphase=min_MY_RSHIndex/start_descent;
[min_MZ_RSH, min_MZ_RSHIndex]=min(localFM_Rshoulder(1:start_descent,6));
min_MZ_RSHphase=min_MZ_RSHIndex/start_descent;

```

```

RSH_peakJComFM_lift=[peak_FX_RSH peak_FY_RSH peak_FZ_RSH
peak_MX_RSH peak_MY_RSH peak_MZ_RSH;...

```

```

    peak_FX_RSHphase peak_FY_RSHphase peak_FZ_RSHphase peak_MX_RSHphase
peak_MY_RSHphase peak_MZ_RSHphase];
    RSH_minJComFM_lift=[min_FX_RSH min_FY_RSH min_FZ_RSH min_MX_RSH
min_MY_RSH min_MZ_RSH;...
    min_FX_RSHphase min_FY_RSHphase min_FZ_RSHphase min_MX_RSHphase
min_MY_RSHphase min_MZ_RSHphase];
    save RSH_MaxJointComFM_Lift.txt RSH_peakJComFM_lift -ascii;
    save RSH_MinJointComFM_Lift.txt RSH_minJComFM_lift -ascii;

    %%%%%%%%% Right Shoulder component force rate
    Sim_FXRate_RSH=diff(localFM_Rshoulder(1:start_descent,1)).*100; % simultaneous
force rate of loading (Newton/second)
    [Max_Sim_FXRate_RSH, Max_Sim_FXRate_RSHIndex]=max(Sim_FXRate_RSH(:,,:));
% maximal simultaneous force rate of loading
    Max_Sim_FXRate_RSHPhase=Max_Sim_FXRate_RSHIndex/(start_descent-1); %
%phase at the max. simultaneous force rate

    Sim_FYRate_RSH=diff(localFM_Rshoulder(1:start_descent,2)).*100; % simultaneous
force rate of loading (Newton/second)
    [Max_Sim_FYRate_RSH, Max_Sim_FYRate_RSHIndex]=max(Sim_FYRate_RSH(:,,:));
% maximal simultaneous force rate of loading
    Max_Sim_FYRate_RSHPhase=Max_Sim_FYRate_RSHIndex/(start_descent-1); %
%phase at the max. simultaneous force rate

    Sim_FZRate_RSH=diff(localFM_Rshoulder(1:start_descent,3)).*100; % simultaneous
force rate of loading (Newton/second)
    [Max_Sim_FZRate_RSH, Max_Sim_FZRate_RSHIndex]=max(Sim_FZRate_RSH(:,,:));
% maximal simultaneous force rate of loading
    Max_Sim_FZRate_RSHPhase=Max_Sim_FZRate_RSHIndex/(start_descent-1); %
%phase at the max. simultaneous force rate

    Sim_MXRate_RSH=diff(localFM_Rshoulder(1:start_descent,4)).*100; % simultaneous
force rate of loading (Newton/second)
    [Max_Sim_MXRate_RSH,
Max_Sim_MXRate_RSHIndex]=max(Sim_MXRate_RSH(:,,:)); % maximal simultaneous force
rate of loading
    Max_Sim_MXRate_RSHPhase=Max_Sim_MXRate_RSHIndex/(start_descent-1); %
%phase at the max. simultaneous force rate

    Sim_MYRate_RSH=diff(localFM_Rshoulder(1:start_descent,5)).*100; % simultaneous
force rate of loading (Newton/second)
    [Max_Sim_MYRate_RSH,
Max_Sim_MYRate_RSHIndex]=max(Sim_MYRate_RSH(:,,:)); % maximal simultaneous force
rate of loading
    Max_Sim_MYRate_RSHPhase=Max_Sim_MYRate_RSHIndex/(start_descent-1); %
%phase at the max. simultaneous force rate

```

```

    Sim_MZRate_RSH=diff(localFM_Rshoulder(1:start_descent,6)).*100; % simultaneous
force rate of loading (Newton/second)
    [Max_Sim_MZRate_RSH,
Max_Sim_MZRate_RSHIndex]=max(Sim_MZRate_RSH(:,:)); % maximal simultaneous force
rate of loading
    Max_Sim_MZRate_RSHPhase=Max_Sim_MZRate_RSHIndex/(start_descent-1); %
%phase at the max. simultaneous force rate

```

```

    RSH_JComFMrate_lift=[Max_Sim_FXRate_RSH Max_Sim_FXRate_RSHPhase
Max_Sim_FYRate_RSH Max_Sim_FYRate_RSHPhase Max_Sim_FZRate_RSH
Max_Sim_FZRate_RSHPhase;...
    Max_Sim_MXRate_RSH Max_Sim_MXRate_RSHPhase Max_Sim_MYRate_RSH
Max_Sim_MYRate_RSHPhase Max_Sim_MZRate_RSH Max_Sim_MZRate_RSHPhase];
    save RSH_JointComFMrate_Lift.txt RSH_JComFMrate_lift -ascii;

```

```

%%% % Left shoulder component force
[peak_FX_LSH, peak_FX_LSHIndex]=max(localFM_Lshoulder(1:start_descent,1));
peak_FX_LSHphase=peak_FX_LSHIndex/start_descent;
[peak_FY_LSH, peak_FY_LSHIndex]=max(localFM_Lshoulder(1:start_descent,2));
peak_FY_LSHphase=peak_FY_LSHIndex/start_descent;
[peak_FZ_LSH, peak_FZ_LSHIndex]=max(localFM_Lshoulder(1:start_descent,3));
peak_FZ_LSHphase=peak_FZ_LSHIndex/start_descent;
[peak_MX_LSH, peak_MX_LSHIndex]=max(localFM_Lshoulder(1:start_descent,4));
peak_MX_LSHphase=peak_MX_LSHIndex/start_descent;
[peak_MY_LSH, peak_MY_LSHIndex]=max(localFM_Lshoulder(1:start_descent,5));
peak_MY_LSHphase=peak_MY_LSHIndex/start_descent;
[peak_MZ_LSH, peak_MZ_LSHIndex]=max(localFM_Lshoulder(1:start_descent,6));
peak_MZ_LSHphase=peak_MZ_LSHIndex/start_descent;

```

```

[min_FX_LSH, min_FX_LSHIndex]=min(localFM_Lshoulder(1:start_descent,1));
min_FX_LSHphase=min_FX_LSHIndex/start_descent;
[min_FY_LSH, min_FY_LSHIndex]=min(localFM_Lshoulder(1:start_descent,2));
min_FY_LSHphase=min_FY_LSHIndex/start_descent;
[min_FZ_LSH, min_FZ_LSHIndex]=min(localFM_Lshoulder(1:start_descent,3));
min_FZ_LSHphase=min_FZ_LSHIndex/start_descent;
[min_MX_LSH, min_MX_LSHIndex]=min(localFM_Lshoulder(1:start_descent,4));
min_MX_LSHphase=min_MX_LSHIndex/start_descent;
[min_MY_LSH, min_MY_LSHIndex]=min(localFM_Lshoulder(1:start_descent,5));
min_MY_LSHphase=min_MY_LSHIndex/start_descent;
[min_MZ_LSH, min_MZ_LSHIndex]=min(localFM_Lshoulder(1:start_descent,6));
min_MZ_LSHphase=min_MZ_LSHIndex/start_descent;

```

```

    LSH_peakJComFM_lift=[peak_FX_LSH peak_FY_LSH peak_FZ_LSH peak_MX_LSH
peak_MY_LSH peak_MZ_LSH;...

```

```

    peak_FX_LSHphase peak_FY_LSHphase peak_FZ_LSHphase peak_MX_LSHphase
    peak_MY_LSHphase peak_MZ_LSHphase];
    LSH_minJComFM_lift=[min_FX_LSH min_FY_LSH min_FZ_LSH min_MX_LSH
    min_MY_LSH min_MZ_LSH;...
    min_FX_LSHphase min_FY_LSHphase min_FZ_LSHphase min_MX_LSHphase
    min_MY_LSHphase min_MZ_LSHphase];
    save LSH_MaxJointComFM_Lift.txt LSH_peakJComFM_lift -ascii;
    save LSH_MinJointComFM_Lift.txt LSH_minJComFM_lift -ascii;

    %%%%%%%%% Left Shoulder component force rate
    Sim_FXRate_LSH=diff(localFM_Lshoulder(1:start_descent,1)).*100; % simultaneous
    force rate of loading (Newton/second)
    [Max_Sim_FXRate_LSH, Max_Sim_FXRate_LSHIndex]=max(Sim_FXRate_LSH(:,:));
    % maximal simultaneous force rate of loading
    Max_Sim_FXRate_LSHPhase=Max_Sim_FXRate_LSHIndex/(start_descent-1); %
    %phase at the max. simultaneous force rate

    Sim_FYRate_LSH=diff(localFM_Lshoulder(1:start_descent,2)).*100; % simultaneous
    force rate of loading (Newton/second)
    [Max_Sim_FYRate_LSH, Max_Sim_FYRate_LSHIndex]=max(Sim_FYRate_LSH(:,:));
    % maximal simultaneous force rate of loading
    Max_Sim_FYRate_LSHPhase=Max_Sim_FYRate_LSHIndex/(start_descent-1); %
    %phase at the max. simultaneous force rate

    Sim_FZRate_LSH=diff(localFM_Lshoulder(1:start_descent,3)).*100; % simultaneous
    force rate of loading (Newton/second)
    [Max_Sim_FZRate_LSH, Max_Sim_FZRate_LSHIndex]=max(Sim_FZRate_LSH(:,:));
    % maximal simultaneous force rate of loading
    Max_Sim_FZRate_LSHPhase=Max_Sim_FZRate_LSHIndex/(start_descent-1); %
    %phase at the max. simultaneous force rate

    Sim_MXRate_LSH=diff(localFM_Lshoulder(1:start_descent,4)).*100; % simultaneous
    force rate of loading (Newton/second)
    [Max_Sim_MXRate_LSH,
    Max_Sim_MXRate_LSHIndex]=max(Sim_MXRate_LSH(:,:)); % maximal simultaneous force
    rate of loading
    Max_Sim_MXRate_LSHPhase=Max_Sim_MXRate_LSHIndex/(start_descent-1); %
    %phase at the max. simultaneous force rate

    Sim_MYRate_LSH=diff(localFM_Lshoulder(1:start_descent,5)).*100; % simultaneous
    force rate of loading (Newton/second)
    [Max_Sim_MYRate_LSH,
    Max_Sim_MYRate_LSHIndex]=max(Sim_MYRate_LSH(:,:)); % maximal simultaneous force
    rate of loading
    Max_Sim_MYRate_LSHPhase=Max_Sim_MYRate_LSHIndex/(start_descent-1); %
    %phase at the max. simultaneous force rate

```

```

    Sim_MZRate_LSH=diff(localFM_Lshoulder(1:start_descent,6)).*100; % simultaneous
force rate of loading (Newton/second)
    [Max_Sim_MZRate_LSH,
Max_Sim_MZRate_LSHIndex]=max(Sim_MZRate_LSH(:,:)); % maximal simultaneous force
rate of loading
    Max_Sim_MZRate_LSHPhase=Max_Sim_MZRate_LSHIndex/(start_descent-1); %
%phase at the max. simultaneous force rate

```

```

    LSH_JComFMrate_lift=[Max_Sim_FXRate_LSH Max_Sim_FXRate_LSHPhase
Max_Sim_FYRate_LSH Max_Sim_FYRate_LSHPhase Max_Sim_FZRate_LSH
Max_Sim_FZRate_LSHPhase;...
    Max_Sim_MXRate_LSH Max_Sim_MXRate_LSHPhase Max_Sim_MYRate_LSH
Max_Sim_MYRate_LSHPhase Max_Sim_MZRate_LSH Max_Sim_MZRate_LSHPhase];
    save LSH_JointComFMrate_Lift.txt LSH_JComFMrate_lift -ascii;

```

```

%% %% Right elbow component force
[peak_FX_REL, peak_FX_RELIndex]=max(localFM_Relbow(1:start_descent,1));
peak_FX_RELphase=peak_FX_RELIndex/start_descent;
[peak_FY_REL, peak_FY_RELIndex]=max(localFM_Relbow(1:start_descent,2));
peak_FY_RELphase=peak_FY_RELIndex/start_descent;
[peak_FZ_REL, peak_FZ_RELIndex]=max(localFM_Relbow(1:start_descent,3));
peak_FZ_RELphase=peak_FZ_RELIndex/start_descent;
[peak_MX_REL, peak_MX_RELIndex]=max(localFM_Relbow(1:start_descent,4));
peak_MX_RELphase=peak_MX_RELIndex/start_descent;
[peak_MY_REL, peak_MY_RELIndex]=max(localFM_Relbow(1:start_descent,5));
peak_MY_RELphase=peak_MY_RELIndex/start_descent;
[peak_MZ_REL, peak_MZ_RELIndex]=max(localFM_Relbow(1:start_descent,6));
peak_MZ_RELphase=peak_MZ_RELIndex/start_descent;

```

```

[min_FX_REL, min_FX_RELIndex]=min(localFM_Relbow(1:start_descent,1));
min_FX_RELphase=min_FX_RELIndex/start_descent;
[min_FY_REL, min_FY_RELIndex]=min(localFM_Relbow(1:start_descent,2));
min_FY_RELphase=min_FY_RELIndex/start_descent;
[min_FZ_REL, min_FZ_RELIndex]=min(localFM_Relbow(1:start_descent,3));
min_FZ_RELphase=min_FZ_RELIndex/start_descent;
[min_MX_REL, min_MX_RELIndex]=min(localFM_Relbow(1:start_descent,4));
min_MX_RELphase=min_MX_RELIndex/start_descent;
[min_MY_REL, min_MY_RELIndex]=min(localFM_Relbow(1:start_descent,5));
min_MY_RELphase=min_MY_RELIndex/start_descent;
[min_MZ_REL, min_MZ_RELIndex]=min(localFM_Relbow(1:start_descent,6));
min_MZ_RELphase=min_MZ_RELIndex/start_descent;

```

```

REL_peakJComFM_lift=[peak_FX_REL peak_FY_REL peak_FZ_REL peak_MX_REL
peak_MY_REL peak_MZ_REL;...

```

```

    peak_FX_RELphase peak_FY_RELphase peak_FZ_RELphase peak_MX_RELphase
    peak_MY_RELphase peak_MZ_RELphase];
    REL_minJComFM_lift=[min_FX_REL min_FY_REL min_FZ_REL min_MX_REL
    min_MY_REL min_MZ_REL];...
    min_FX_RELphase min_FY_RELphase min_FZ_RELphase min_MX_RELphase
    min_MY_RELphase min_MZ_RELphase];
    save REL_MaxJointComFM_Lift.txt REL_peakJComFM_lift -ascii;
    save REL_MinJointComFM_Lift.txt REL_minJComFM_lift -ascii;

    %%%%%%%%% Right elbow component force rate
    Sim_FXRate_REL=diff(localFM_Relbow(1:start_descent,1)).*100; % simultaneous
    force rate of loading (Newton/second)
    [Max_Sim_FXRate_REL, Max_Sim_FXRate_RELIndex]=max(Sim_FXRate_REL(:,:));
    % maximal simultaneous force rate of loading
    Max_Sim_FXRate_RELPhase=Max_Sim_FXRate_RELIndex/(start_descent-1); %
    %phase at the max. simultaneous force rate

    Sim_FYRate_REL=diff(localFM_Relbow(1:start_descent,2)).*100; % simultaneous
    force rate of loading (Newton/second)
    [Max_Sim_FYRate_REL, Max_Sim_FYRate_RELIndex]=max(Sim_FYRate_REL(:,:));
    % maximal simultaneous force rate of loading
    Max_Sim_FYRate_RELPhase=Max_Sim_FYRate_RELIndex/(start_descent-1); %
    %phase at the max. simultaneous force rate

    Sim_FZRate_REL=diff(localFM_Relbow(1:start_descent,3)).*100; % simultaneous
    force rate of loading (Newton/second)
    [Max_Sim_FZRate_REL, Max_Sim_FZRate_RELIndex]=max(Sim_FZRate_REL(:,:));
    % maximal simultaneous force rate of loading
    Max_Sim_FZRate_RELPhase=Max_Sim_FZRate_RELIndex/(start_descent-1); %
    %phase at the max. simultaneous force rate

    Sim_MXRate_REL=diff(localFM_Relbow(1:start_descent,4)).*100; % simultaneous
    force rate of loading (Newton/second)
    [Max_Sim_MXRate_REL,
    Max_Sim_MXRate_RELIndex]=max(Sim_MXRate_REL(:,:)); % maximal simultaneous force
    rate of loading
    Max_Sim_MXRate_RELPhase=Max_Sim_MXRate_RELIndex/(start_descent-1); %
    %phase at the max. simultaneous force rate

    Sim_MYRate_REL=diff(localFM_Relbow(1:start_descent,5)).*100; % simultaneous
    force rate of loading (Newton/second)
    [Max_Sim_MYRate_REL,
    Max_Sim_MYRate_RELIndex]=max(Sim_MYRate_REL(:,:)); % maximal simultaneous force
    rate of loading
    Max_Sim_MYRate_RELPhase=Max_Sim_MYRate_RELIndex/(start_descent-1); %
    %phase at the max. simultaneous force rate

```

```

    Sim_MZRate_REL=diff(localFM_Relbow(1:start_descent,6)).*100; % simultaneous
force rate of loading (Newton/second)
    [Max_Sim_MZRate_REL,
Max_Sim_MZRate_RELIndex]=max(Sim_MZRate_REL(:,:)); % maximal simultaneous force
rate of loading
    Max_Sim_MZRate_RELPhase=Max_Sim_MZRate_RELIndex/(start_descent-1); %
%phase at the max. simultaneous force rate

    REL_JComFMrate_lift=[Max_Sim_FXRate_REL Max_Sim_FXRate_RELPhase
Max_Sim_FYRate_REL Max_Sim_FYRate_RELPhase Max_Sim_FZRate_REL
Max_Sim_FZRate_RELPhase;...
    Max_Sim_MXRate_REL Max_Sim_MXRate_RELPhase Max_Sim_MYRate_REL
Max_Sim_MYRate_RELPhase Max_Sim_MZRate_REL Max_Sim_MZRate_RELPhase];
    save REL_JointComFMrate_Lift.txt REL_JComFMrate_lift -ascii;

%%% Left elbow component forces
[peak_FX_LEL, peak_FX_LELIndex]=max(localFM_Lelbow(1:start_descent,1));
peak_FX_LELphase=peak_FX_LELIndex/start_descent;
[peak_FY_LEL, peak_FY_LELIndex]=max(localFM_Lelbow(1:start_descent,2));
peak_FY_LELphase=peak_FY_LELIndex/start_descent;
[peak_FZ_LEL, peak_FZ_LELIndex]=max(localFM_Lelbow(1:start_descent,3));
peak_FZ_LELphase=peak_FZ_LELIndex/start_descent;
[peak_MX_LEL, peak_MX_LELIndex]=max(localFM_Lelbow(1:start_descent,4));
peak_MX_LELphase=peak_MX_LELIndex/start_descent;
[peak_MY_LEL, peak_MY_LELIndex]=max(localFM_Lelbow(1:start_descent,5));
peak_MY_LELphase=peak_MY_LELIndex/start_descent;
[peak_MZ_LEL, peak_MZ_LELIndex]=max(localFM_Lelbow(1:start_descent,6));
peak_MZ_LELphase=peak_MZ_LELIndex/start_descent;

[min_FX_LEL, min_FX_LELIndex]=min(localFM_Lelbow(1:start_descent,1));
min_FX_LELphase=min_FX_LELIndex/start_descent;
[min_FY_LEL, min_FY_LELIndex]=min(localFM_Lelbow(1:start_descent,2));
min_FY_LELphase=min_FY_LELIndex/start_descent;
[min_FZ_LEL, min_FZ_LELIndex]=min(localFM_Lelbow(1:start_descent,3));
min_FZ_LELphase=min_FZ_LELIndex/start_descent;
[min_MX_LEL, min_MX_LELIndex]=min(localFM_Lelbow(1:start_descent,4));
min_MX_LELphase=min_MX_LELIndex/start_descent;
[min_MY_LEL, min_MY_LELIndex]=min(localFM_Lelbow(1:start_descent,5));
min_MY_LELphase=min_MY_LELIndex/start_descent;
[min_MZ_LEL, min_MZ_LELIndex]=min(localFM_Lelbow(1:start_descent,6));
min_MZ_LELphase=min_MZ_LELIndex/start_descent;

LEL_peakJComFM_lift=[peak_FX_LEL peak_FY_LEL peak_FZ_LEL peak_MX_LEL
peak_MY_LEL peak_MZ_LEL;...

```

```

    peak_FX_LELphase peak_FY_LELphase peak_FZ_LELphase peak_MX_LELphase
    peak_MY_LELphase peak_MZ_LELphase];
    LEL_minJComFM_lift=[min_FX_LEL min_FY_LEL min_FZ_LEL min_MX_LEL
    min_MY_LEL min_MZ_LEL];...
    min_FX_LELphase min_FY_LELphase min_FZ_LELphase min_MX_LELphase
    min_MY_LELphase min_MZ_LELphase];
    save LEL_MaxJointComFM_Lift.txt LEL_peakJComFM_lift -ascii;
    save LEL_MinJointComFM_Lift.txt LEL_minJComFM_lift -ascii;

    %%%%%%%%% Left elbow component force rate
    Sim_FXRate_LEL=diff(localFM_Lelbow(1:start_descent,1)).*100; % simultaneous
    force rate of loading (Newton/second)
    [Max_Sim_FXRate_LEL, Max_Sim_FXRate_LELIndex]=max(Sim_FXRate_LEL(:,:));
    % maximal simultaneous force rate of loading
    Max_Sim_FXRate_LELPhase=Max_Sim_FXRate_LELIndex/(start_descent-1); %
    %phase at the max. simultaneous force rate

    Sim_FYRate_LEL=diff(localFM_Lelbow(1:start_descent,2)).*100; % simultaneous
    force rate of loading (Newton/second)
    [Max_Sim_FYRate_LEL, Max_Sim_FYRate_LELIndex]=max(Sim_FYRate_LEL(:,:));
    % maximal simultaneous force rate of loading
    Max_Sim_FYRate_LELPhase=Max_Sim_FYRate_LELIndex/(start_descent-1); %
    %phase at the max. simultaneous force rate

    Sim_FZRate_LEL=diff(localFM_Lelbow(1:start_descent,3)).*100; % simultaneous force
    rate of loading (Newton/second)
    [Max_Sim_FZRate_LEL, Max_Sim_FZRate_LELIndex]=max(Sim_FZRate_LEL(:,:));
    % maximal simultaneous force rate of loading
    Max_Sim_FZRate_LELPhase=Max_Sim_FZRate_LELIndex/(start_descent-1); %
    %phase at the max. simultaneous force rate

    Sim_MXRate_LEL=diff(localFM_Lelbow(1:start_descent,4)).*100; % simultaneous
    force rate of loading (Newton/second)
    [Max_Sim_MXRate_LEL,
    Max_Sim_MXRate_LELIndex]=max(Sim_MXRate_LEL(:,:)); % maximal simultaneous force
    rate of loading
    Max_Sim_MXRate_LELPhase=Max_Sim_MXRate_LELIndex/(start_descent-1); %
    %phase at the max. simultaneous force rate

    Sim_MYRate_LEL=diff(localFM_Lelbow(1:start_descent,5)).*100; % simultaneous
    force rate of loading (Newton/second)
    [Max_Sim_MYRate_LEL,
    Max_Sim_MYRate_LELIndex]=max(Sim_MYRate_LEL(:,:)); % maximal simultaneous force
    rate of loading
    Max_Sim_MYRate_LELPhase=Max_Sim_MYRate_LELIndex/(start_descent-1); %
    %phase at the max. simultaneous force rate

```

```

    Sim_MZRate_LEL=diff(localFM_Lelbow(1:start_descent,6)).*100; % simultaneous
force rate of loading (Newton/second)
    [Max_Sim_MZRate_LEL,
Max_Sim_MZRate_LELIndex]=max(Sim_MZRate_LEL(:,:)); % maximal simultaneous force
rate of loading
    Max_Sim_MZRate_LELPhase=Max_Sim_MZRate_LELIndex/(start_descent-1); %
%phase at the max. simultaneous force rate

```

```

    LEL_JComFMrate_lift=[Max_Sim_FXRate_LEL Max_Sim_FXRate_LELPhase
Max_Sim_FYRate_LEL Max_Sim_FYRate_LELPhase Max_Sim_FZRate_LEL
Max_Sim_FZRate_LELPhase;...
    Max_Sim_MXRate_LEL Max_Sim_MXRate_LELPhase Max_Sim_MYRate_LEL
Max_Sim_MYRate_LELPhase Max_Sim_MZRate_LEL Max_Sim_MZRate_LELPhase];
    save LEL_JointComFMrate_Lift.txt LEL_JComFMrate_lift -ascii;

```

```

%% %% Right Wrist component forces
[peak_FX_RWR, peak_FX_RWRIndex]=max(localFM_Rwrist(1:start_descent,1));
peak_FX_RWRphase=peak_FX_RWRIndex/start_descent;
[peak_FY_RWR, peak_FY_RWRIndex]=max(localFM_Rwrist(1:start_descent,2));
peak_FY_RWRphase=peak_FY_RWRIndex/start_descent;
[peak_FZ_RWR, peak_FZ_RWRIndex]=max(localFM_Rwrist(1:start_descent,3));
peak_FZ_RWRphase=peak_FZ_RWRIndex/start_descent;
[peak_MX_RWR, peak_MX_RWRIndex]=max(localFM_Rwrist(1:start_descent,4));
peak_MX_RWRphase=peak_MX_RWRIndex/start_descent;
[peak_MY_RWR, peak_MY_RWRIndex]=max(localFM_Rwrist(1:start_descent,5));
peak_MY_RWRphase=peak_MY_RWRIndex/start_descent;
[peak_MZ_RWR, peak_MZ_RWRIndex]=max(localFM_Rwrist(1:start_descent,6));
peak_MZ_RWRphase=peak_MZ_RWRIndex/start_descent;

```

```

[min_FX_RWR, min_FX_RWRIndex]=min(localFM_Rwrist(1:start_descent,1));
min_FX_RWRphase=min_FX_RWRIndex/start_descent;
[min_FY_RWR, min_FY_RWRIndex]=min(localFM_Rwrist(1:start_descent,2));
min_FY_RWRphase=min_FY_RWRIndex/start_descent;
[min_FZ_RWR, min_FZ_RWRIndex]=min(localFM_Rwrist(1:start_descent,3));
min_FZ_RWRphase=min_FZ_RWRIndex/start_descent;
[min_MX_RWR, min_MX_RWRIndex]=min(localFM_Rwrist(1:start_descent,4));
min_MX_RWRphase=min_MX_RWRIndex/start_descent;
[min_MY_RWR, min_MY_RWRIndex]=min(localFM_Rwrist(1:start_descent,5));
min_MY_RWRphase=min_MY_RWRIndex/start_descent;
[min_MZ_RWR, min_MZ_RWRIndex]=min(localFM_Rwrist(1:start_descent,6));
min_MZ_RWRphase=min_MZ_RWRIndex/start_descent;

```

```

RWR_peakJComFM_lift=[peak_FX_RWR peak_FY_RWR peak_FZ_RWR
peak_MX_RWR peak_MY_RWR peak_MZ_RWR;...

```

```

    peak_FX_RWRphase peak_FY_RWRphase peak_FZ_RWRphase
peak_MX_RWRphase peak_MY_RWRphase peak_MZ_RWRphase];
    RWR_minJComFM_lift=[min_FX_RWR min_FY_RWR min_FZ_RWR
min_MX_RWR min_MY_RWR min_MZ_RWR;...
    min_FX_RWRphase min_FY_RWRphase min_FZ_RWRphase min_MX_RWRphase
min_MY_RWRphase min_MZ_RWRphase];
    save RWR_MaxJointComFM_Lift.txt RWR_peakJComFM_lift -ascii;
    save RWR_MinJointComFM_Lift.txt RWR_minJComFM_lift -ascii;

    %%%%%%%%% Right wrist component force rate
    Sim_FXRate_RWR=diff(localFM_Rwrist(1:start_descent,1)).*100; % simultaneous
force rate of loading (Newton/second)
    [Max_Sim_FXRate_RWR,
Max_Sim_FXRate_RWRIndex]=max(Sim_FXRate_RWR(:,:)); % maximal simultaneous force
rate of loading
    Max_Sim_FXRate_RWRPhase=Max_Sim_FXRate_RWRIndex/(start_descent-1); %
%phase at the max. simultaneous force rate

    Sim_FYRate_RWR=diff(localFM_Rwrist(1:start_descent,2)).*100; % simultaneous
force rate of loading (Newton/second)
    [Max_Sim_FYRate_RWR,
Max_Sim_FYRate_RWRIndex]=max(Sim_FYRate_RWR(:,:)); % maximal simultaneous force
rate of loading
    Max_Sim_FYRate_RWRPhase=Max_Sim_FYRate_RWRIndex/(start_descent-1); %
%phase at the max. simultaneous force rate

    Sim_FZRate_RWR=diff(localFM_Rwrist(1:start_descent,3)).*100; % simultaneous force
rate of loading (Newton/second)
    [Max_Sim_FZRate_RWR,
Max_Sim_FZRate_RWRIndex]=max(Sim_FZRate_RWR(:,:)); % maximal simultaneous force
rate of loading
    Max_Sim_FZRate_RWRPhase=Max_Sim_FZRate_RWRIndex/(start_descent-1); %
%phase at the max. simultaneous force rate

    Sim_MXRate_RWR=diff(localFM_Rwrist(1:start_descent,4)).*100; % simultaneous
force rate of loading (Newton/second)
    [Max_Sim_MXRate_RWR,
Max_Sim_MXRate_RWRIndex]=max(Sim_MXRate_RWR(:,:)); % maximal simultaneous force
rate of loading
    Max_Sim_MXRate_RWRPhase=Max_Sim_MXRate_RWRIndex/(start_descent-1); %
%phase at the max. simultaneous force rate

    Sim_MYRate_RWR=diff(localFM_Rwrist(1:start_descent,5)).*100; % simultaneous
force rate of loading (Newton/second)

```

```
[Max_Sim_MYRate_RWR,
Max_Sim_MYRate_RWRIndex]=max(Sim_MYRate_RWR(:,:)); % maximal simultaneous force
rate of loading
```

```
Max_Sim_MYRate_RWRPhase=Max_Sim_MYRate_RWRIndex/(start_descent-1); %
%phase at the max. simultaneous force rate
```

```
Sim_MZRate_RWR=diff(localFM_Rwrist(1:start_descent,6)).*100; % simultaneous
force rate of loading (Newton/second)
```

```
[Max_Sim_MZRate_RWR,
Max_Sim_MZRate_RWRIndex]=max(Sim_MZRate_RWR(:,:)); % maximal simultaneous force
rate of loading
```

```
Max_Sim_MZRate_RWRPhase=Max_Sim_MZRate_RWRIndex/(start_descent-1); %
%phase at the max. simultaneous force rate
```

```
RWR_JComFMrate_lift=[Max_Sim_FXRate_RWR Max_Sim_FXRate_RWRPhase
Max_Sim_FYRate_RWR Max_Sim_FYRate_RWRPhase Max_Sim_FZRate_RWR
Max_Sim_FZRate_RWRPhase;...
```

```
Max_Sim_MXRate_RWR Max_Sim_MXRate_RWRPhase Max_Sim_MYRate_RWR
Max_Sim_MYRate_RWRPhase Max_Sim_MZRate_RWR Max_Sim_MZRate_RWRPhase];
save RWR_JointComFMrate_Lift.txt RWR_JComFMrate_lift -ascii;
```

```
%%% Left Wrist component forces
```

```
[peak_FX_LWR, peak_FX_LWRIndex]=max(localFM_Lwrist(1:start_descent,1));
```

```
peak_FX_LWRphase=peak_FX_LWRIndex/start_descent;
```

```
[peak_FY_LWR, peak_FY_LWRIndex]=max(localFM_Lwrist(1:start_descent,2));
```

```
peak_FY_LWRphase=peak_FY_LWRIndex/start_descent;
```

```
[peak_FZ_LWR, peak_FZ_LWRIndex]=max(localFM_Lwrist(1:start_descent,3));
```

```
peak_FZ_LWRphase=peak_FZ_LWRIndex/start_descent;
```

```
[peak_MX_LWR, peak_MX_LWRIndex]=max(localFM_Lwrist(1:start_descent,4));
```

```
peak_MX_LWRphase=peak_MX_LWRIndex/start_descent;
```

```
[peak_MY_LWR, peak_MY_LWRIndex]=max(localFM_Lwrist(1:start_descent,5));
```

```
peak_MY_LWRphase=peak_MY_LWRIndex/start_descent;
```

```
[peak_MZ_LWR, peak_MZ_LWRIndex]=max(localFM_Lwrist(1:start_descent,6));
```

```
peak_MZ_LWRphase=peak_MZ_LWRIndex/start_descent;
```

```
[min_FX_LWR, min_FX_LWRIndex]=min(localFM_Lwrist(1:start_descent,1));
```

```
min_FX_LWRphase=min_FX_LWRIndex/start_descent;
```

```
[min_FY_LWR, min_FY_LWRIndex]=min(localFM_Lwrist(1:start_descent,2));
```

```
min_FY_LWRphase=min_FY_LWRIndex/start_descent;
```

```
[min_FZ_LWR, min_FZ_LWRIndex]=min(localFM_Lwrist(1:start_descent,3));
```

```
min_FZ_LWRphase=min_FZ_LWRIndex/start_descent;
```

```
[min_MX_LWR, min_MX_LWRIndex]=min(localFM_Lwrist(1:start_descent,4));
```

```
min_MX_LWRphase=min_MX_LWRIndex/start_descent;
```

```
[min_MY_LWR, min_MY_LWRIndex]=min(localFM_Lwrist(1:start_descent,5));
```

```
min_MY_LWRphase=min_MY_LWRIndex/start_descent;
```

```
[min_MZ_LWR, min_MZ_LWRIndex]=min(localFM_Lwrist(1:start_descent,6));
```

```

min_MZ_LWRphase=min_MZ_LWRIndex/start_descent;

LWR_peakJComFM_lift=[peak_FX_LWR peak_FY_LWR peak_FZ_LWR
peak_MX_LWR peak_MY_LWR peak_MZ_LWR;...
peak_FX_LWRphase peak_FY_LWRphase peak_FZ_LWRphase
peak_MX_LWRphase peak_MY_LWRphase peak_MZ_LWRphase];
LWR_minJComFM_lift=[min_FX_LWR min_FY_LWR min_FZ_LWR min_MX_LWR
min_MY_LWR min_MZ_LWR;...
min_FX_LWRphase min_FY_LWRphase min_FZ_LWRphase min_MX_LWRphase
min_MY_LWRphase min_MZ_LWRphase];
save LWR_MaxJointComFM_Lift.txt LWR_peakJComFM_lift -ascii;
save LWR_MinJointComFM_Lift.txt LWR_minJComFM_lift -ascii;

%%%%%%%%% Left wrist component force rate
Sim_FXRate_LWR=diff(localFM_Lwrist(1:start_descent,1)).*100; % simultaneous force
rate of loading (Newton/second)
[Max_Sim_FXRate_LWR,
Max_Sim_FXRate_LWRIndex]=max(Sim_FXRate_LWR(:,:)); % maximal simultaneous force
rate of loading
Max_Sim_FXRate_LWRPhase=Max_Sim_FXRate_LWRIndex/(start_descent-1); %
%phase at the max. simultaneous force rate

Sim_FYRate_LWR=diff(localFM_Lwrist(1:start_descent,2)).*100; % simultaneous force
rate of loading (Newton/second)
[Max_Sim_FYRate_LWR,
Max_Sim_FYRate_LWRIndex]=max(Sim_FYRate_LWR(:,:)); % maximal simultaneous force
rate of loading
Max_Sim_FYRate_LWRPhase=Max_Sim_FYRate_LWRIndex/(start_descent-1); %
%phase at the max. simultaneous force rate

Sim_FZRate_LWR=diff(localFM_Lwrist(1:start_descent,3)).*100; % simultaneous force
rate of loading (Newton/second)
[Max_Sim_FZRate_LWR,
Max_Sim_FZRate_LWRIndex]=max(Sim_FZRate_LWR(:,:)); % maximal simultaneous force
rate of loading
Max_Sim_FZRate_LWRPhase=Max_Sim_FZRate_LWRIndex/(start_descent-1); %
%phase at the max. simultaneous force rate

Sim_MXRate_LWR=diff(localFM_Lwrist(1:start_descent,4)).*100; % simultaneous
force rate of loading (Newton/second)
[Max_Sim_MXRate_LWR,
Max_Sim_MXRate_LWRIndex]=max(Sim_MXRate_LWR(:,:)); % maximal simultaneous force
rate of loading
Max_Sim_MXRate_LWRPhase=Max_Sim_MXRate_LWRIndex/(start_descent-1); %
%phase at the max. simultaneous force rate

```



```

else
  Fyratio_atMAX_RSHPOE=Fy_atMAX_RSHPOE/min_FY_RSH;
end
Fz_atMAX_RSHPOE=localFM_Rshoulder(RSHpeak_lift(1,1),3);
if Fz_atMAX_RSHPOE > 0;
  Fzratio_atMAX_RSHPOE=Fz_atMAX_RSHPOE/peak_FZ_RSH;
else
  Fzratio_atMAX_RSHPOE=Fz_atMAX_RSHPOE/min_FZ_RSH;
end
Mx_atMAX_RSHPOE=localFM_Rshoulder(RSHpeak_lift(1,1),4);
if Mx_atMAX_RSHPOE > 0;
  Mxratio_atMAX_RSHPOE=Mx_atMAX_RSHPOE/peak_MX_RSH;
else
  Mxratio_atMAX_RSHPOE=Mx_atMAX_RSHPOE/min_MX_RSH;
end
My_atMAX_RSHPOE=localFM_Rshoulder(RSHpeak_lift(1,1),5);
if My_atMAX_RSHPOE > 0;
  Myratio_atMAX_RSHPOE=My_atMAX_RSHPOE/peak_MY_RSH;
else
  Myratio_atMAX_RSHPOE=My_atMAX_RSHPOE/min_MY_RSH;
end
Mz_atMAX_RSHPOE=localFM_Rshoulder(RSHpeak_lift(1,1),6);
if Mz_atMAX_RSHPOE > 0;
  Mzratio_atMAX_RSHPOE=Mz_atMAX_RSHPOE/peak_MZ_RSH;
else
  Mzratio_atMAX_RSHPOE=Mz_atMAX_RSHPOE/min_MZ_RSH;
end
RF_atMAX_RSHPOE=resultantF_Rshoulder(RSHpeak_lift(1,1),1);
RFratio_atMAX_RSHPOE=RF_atMAX_RSHPOE/peak_RF_RSH;
RM_atMAX_RSHPOE=resultantM_Rshoulder(RSHpeak_lift(1,1),1);
RMratio_atMAX_RSHPOE=RM_atMAX_RSHPOE/peak_RM_RSH;

Fx_atMIN_RSHPOE=localFM_Rshoulder(RSHpeak_lift(1,2),1);
if Fx_atMIN_RSHPOE > 0;
  Fxratio_atMIN_RSHPOE=Fx_atMIN_RSHPOE/peak_FX_RSH;
else
  Fxratio_atMIN_RSHPOE=Fx_atMIN_RSHPOE/min_FX_RSH;
end
Fy_atMIN_RSHPOE=localFM_Rshoulder(RSHpeak_lift(1,2),2);
if Fy_atMIN_RSHPOE > 0;
  Fyratio_atMIN_RSHPOE=Fy_atMIN_RSHPOE/peak_FY_RSH;
else
  Fyratio_atMIN_RSHPOE=Fy_atMIN_RSHPOE/min_FY_RSH;
end
Fz_atMIN_RSHPOE=localFM_Rshoulder(RSHpeak_lift(1,2),3);
if Fz_atMIN_RSHPOE > 0;

```

```

Fzratio_atMIN_RSHPOE=Fz_atMIN_RSHPOE/peak_FZ_RSH;
else
  Fzratio_atMIN_RSHPOE=Fz_atMIN_RSHPOE/min_FZ_RSH;
end
Mx_atMIN_RSHPOE=localFM_Rshoulder(RSHpeak_lift(1,2),4);
if Mx_atMIN_RSHPOE > 0;
  Mxratio_atMIN_RSHPOE=Mx_atMIN_RSHPOE/peak_MX_RSH;
else
  Mxratio_atMIN_RSHPOE=Mx_atMIN_RSHPOE/min_MX_RSH;
end
My_atMIN_RSHPOE=localFM_Rshoulder(RSHpeak_lift(1,2),5);
if My_atMIN_RSHPOE > 0;
  Myratio_atMIN_RSHPOE=My_atMIN_RSHPOE/peak_MY_RSH;
else
  Myratio_atMIN_RSHPOE=My_atMIN_RSHPOE/min_MY_RSH;
end
Mz_atMIN_RSHPOE=localFM_Rshoulder(RSHpeak_lift(1,2),6);
if Mz_atMIN_RSHPOE > 0;
  Mzratio_atMIN_RSHPOE=Mz_atMIN_RSHPOE/peak_MZ_RSH;
else
  Mzratio_atMIN_RSHPOE=Mz_atMIN_RSHPOE/min_MZ_RSH;
end
RF_atMIN_RSHPOE=resultantF_Rshoulder(RSHpeak_lift(1,2),1);
RFratio_atMIN_RSHPOE=RF_atMIN_RSHPOE/peak_RF_RSH;
RM_atMIN_RSHPOE=resultantM_Rshoulder(RSHpeak_lift(1,2),1);
RMratio_atMIN_RSHPOE=RM_atMIN_RSHPOE/peak_RM_RSH;

Fx_atMAX_RSHAXIR=localFM_Rshoulder(RSHpeak_lift(1,3),1);
if Fx_atMAX_RSHAXIR > 0;
  Fxratio_atMAX_RSHAXIR=Fx_atMAX_RSHAXIR/peak_FX_RSH;
else
  Fxratio_atMAX_RSHAXIR=Fx_atMAX_RSHAXIR/min_FX_RSH;
end
Fy_atMAX_RSHAXIR=localFM_Rshoulder(RSHpeak_lift(1,3),2);
if Fy_atMAX_RSHAXIR > 0;
  Fyratio_atMAX_RSHAXIR=Fy_atMAX_RSHAXIR/peak_FY_RSH;
else
  Fyratio_atMAX_RSHAXIR=Fy_atMAX_RSHAXIR/min_FY_RSH;
end
Fz_atMAX_RSHAXIR=localFM_Rshoulder(RSHpeak_lift(1,3),3);
if Fz_atMAX_RSHAXIR > 0;
  Fzratio_atMAX_RSHAXIR=Fz_atMAX_RSHAXIR/peak_FZ_RSH;
else
  Fzratio_atMAX_RSHAXIR=Fz_atMAX_RSHAXIR/min_FZ_RSH;
end
Mx_atMAX_RSHAXIR=localFM_Rshoulder(RSHpeak_lift(1,3),4);

```

```

if Mx_atMAX_RSHAXIR > 0;
  Mxratio_atMAX_RSHAXIR=Mx_atMAX_RSHAXIR/peak_MX_RSH;
else
  Mxratio_atMAX_RSHAXIR=Mx_atMAX_RSHAXIR/min_MX_RSH;
end
My_atMAX_RSHAXIR=localFM_Rshoulder(RSHpeak_lift(1,3),5);
if My_atMAX_RSHAXIR > 0;
  Myratio_atMAX_RSHAXIR=My_atMAX_RSHAXIR/peak_MY_RSH;
else
  Myratio_atMAX_RSHAXIR=My_atMAX_RSHAXIR/min_MY_RSH;
end
Mz_atMAX_RSHAXIR=localFM_Rshoulder(RSHpeak_lift(1,3),6);
if Mz_atMAX_RSHAXIR > 0;
  Mzratio_atMAX_RSHAXIR=Mz_atMAX_RSHAXIR/peak_MZ_RSH;
else
  Mzratio_atMAX_RSHAXIR=Mz_atMAX_RSHAXIR/min_MZ_RSH;
end
RF_atMAX_RSHAXIR=resultantF_Rshoulder(RSHpeak_lift(1,3),1);
RFratio_atMAX_RSHAXIR=RF_atMAX_RSHAXIR/peak_RF_RSH;
RM_atMAX_RSHAXIR=resultantM_Rshoulder(RSHpeak_lift(1,3),1);
RMratio_atMAX_RSHAXIR=RM_atMAX_RSHAXIR/peak_RM_RSH;

Fx_atMIN_RSHAXIR=localFM_Rshoulder(RSHpeak_lift(1,4),1);
if Fx_atMIN_RSHAXIR > 0;
  Fxratio_atMIN_RSHAXIR=Fx_atMIN_RSHAXIR/peak_FX_RSH;
else
  Fxratio_atMIN_RSHAXIR=Fx_atMIN_RSHAXIR/min_FX_RSH;
end
Fy_atMIN_RSHAXIR=localFM_Rshoulder(RSHpeak_lift(1,4),2);
if Fy_atMIN_RSHAXIR > 0;
  Fyratio_atMIN_RSHAXIR=Fy_atMIN_RSHAXIR/peak_FY_RSH;
else
  Fyratio_atMIN_RSHAXIR=Fy_atMIN_RSHAXIR/min_FY_RSH;
end
Fz_atMIN_RSHAXIR=localFM_Rshoulder(RSHpeak_lift(1,4),3);
if Fz_atMIN_RSHAXIR > 0;
  Fzratio_atMIN_RSHAXIR=Fz_atMIN_RSHAXIR/peak_FZ_RSH;
else
  Fzratio_atMIN_RSHAXIR=Fz_atMIN_RSHAXIR/min_FZ_RSH;
end
Mx_atMIN_RSHAXIR=localFM_Rshoulder(RSHpeak_lift(1,4),4);
if Mx_atMIN_RSHAXIR > 0;
  Mxratio_atMIN_RSHAXIR=Mx_atMIN_RSHAXIR/peak_MX_RSH;
else
  Mxratio_atMIN_RSHAXIR=Mx_atMIN_RSHAXIR/min_MX_RSH;
end

```

```

My_atMIN_RSHAXIR=localFM_Rshoulder(RSHpeak_lift(1,4),5);
if My_atMIN_RSHAXIR > 0;
  Myratio_atMIN_RSHAXIR=My_atMIN_RSHAXIR/peak_MY_RSH;
else
  Myratio_atMIN_RSHAXIR=My_atMIN_RSHAXIR/min_MY_RSH;
end
Mz_atMIN_RSHAXIR=localFM_Rshoulder(RSHpeak_lift(1,4),6);
if Mz_atMIN_RSHAXIR > 0;
  Mzratio_atMIN_RSHAXIR=Mz_atMIN_RSHAXIR/peak_MZ_RSH;
else
  Mzratio_atMIN_RSHAXIR=Mz_atMIN_RSHAXIR/min_MZ_RSH;
end
RF_atMIN_RSHAXIR=resultantF_Rshoulder(RSHpeak_lift(1,4),1);
RFratio_atMIN_RSHAXIR=RF_atMIN_RSHAXIR/peak_RF_RSH;
RM_atMIN_RSHAXIR=resultantM_Rshoulder(RSHpeak_lift(1,4),1);
RMratio_atMIN_RSHAXIR=RM_atMIN_RSHAXIR/peak_RM_RSH;

Fx_atMAX_RSHELE=localFM_Rshoulder(RSHpeak_lift(1,5),1);
if Fx_atMAX_RSHELE > 0;
  Fxratio_atMAX_RSHELE=Fx_atMAX_RSHELE/peak_FX_RSH;
else
  Fxratio_atMAX_RSHELE=Fx_atMAX_RSHELE/min_FX_RSH;
end
Fy_atMAX_RSHELE=localFM_Rshoulder(RSHpeak_lift(1,5),2);
if Fy_atMAX_RSHELE > 0;
  Fyratio_atMAX_RSHELE=Fy_atMAX_RSHELE/peak_FY_RSH;
else
  Fyratio_atMAX_RSHELE=Fy_atMAX_RSHELE/min_FY_RSH;
end
Fz_atMAX_RSHELE=localFM_Rshoulder(RSHpeak_lift(1,5),3);
if Fz_atMAX_RSHELE > 0;
  Fzratio_atMAX_RSHELE=Fz_atMAX_RSHELE/peak_FZ_RSH;
else
  Fzratio_atMAX_RSHELE=Fz_atMAX_RSHELE/min_FZ_RSH;
end
Mx_atMAX_RSHELE=localFM_Rshoulder(RSHpeak_lift(1,5),4);
if Mx_atMAX_RSHELE > 0;
  Mxratio_atMAX_RSHELE=Mx_atMAX_RSHELE/peak_MX_RSH;
else
  Mxratio_atMAX_RSHELE=Mx_atMAX_RSHELE/min_MX_RSH;
end
My_atMAX_RSHELE=localFM_Rshoulder(RSHpeak_lift(1,5),5);
if My_atMAX_RSHELE > 0;
  Myratio_atMAX_RSHELE=My_atMAX_RSHELE/peak_MY_RSH;
else
  Myratio_atMAX_RSHELE=My_atMAX_RSHELE/min_MY_RSH;

```

```

end
Mz_atMAX_RSHELE=localFM_Rshoulder(RSHpeak_lift(1,5),6);
if Mz_atMAX_RSHELE > 0;
  Mzratio_atMAX_RSHELE=Mz_atMAX_RSHELE/peak_MZ_RSH;
else
  Mzratio_atMAX_RSHELE=Mz_atMAX_RSHELE/min_MZ_RSH;
end
RF_atMAX_RSHELE=resultantF_Rshoulder(RSHpeak_lift(1,5),1);
Rfratio_atMAX_RSHELE=RF_atMAX_RSHELE/peak_RF_RSH;
RM_atMAX_RSHELE=resultantM_Rshoulder(RSHpeak_lift(1,5),1);
RMratio_atMAX_RSHELE=RM_atMAX_RSHELE/peak_RM_RSH;

Fx_atMIN_RSHELE=localFM_Rshoulder(RSHpeak_lift(1,6),1);
if Fx_atMIN_RSHELE > 0;
  Fxratio_atMIN_RSHELE=Fx_atMIN_RSHELE/peak_FX_RSH;
else
  Fxratio_atMIN_RSHELE=Fx_atMIN_RSHELE/min_FX_RSH;
end
Fy_atMIN_RSHELE=localFM_Rshoulder(RSHpeak_lift(1,6),2);
if Fy_atMIN_RSHELE > 0;
  Fyratio_atMIN_RSHELE=Fy_atMIN_RSHELE/peak_FY_RSH;
else
  Fyratio_atMIN_RSHELE=Fy_atMIN_RSHELE/min_FY_RSH;
end
Fz_atMIN_RSHELE=localFM_Rshoulder(RSHpeak_lift(1,6),3);
if Fz_atMIN_RSHELE > 0;
  Fzratio_atMIN_RSHELE=Fz_atMIN_RSHELE/peak_FZ_RSH;
else
  Fzratio_atMIN_RSHELE=Fz_atMIN_RSHELE/min_FZ_RSH;
end
Mx_atMIN_RSHELE=localFM_Rshoulder(RSHpeak_lift(1,6),4);
if Mx_atMIN_RSHELE > 0;
  Mxratio_atMIN_RSHELE=Mx_atMIN_RSHELE/peak_MX_RSH;
else
  Mxratio_atMIN_RSHELE=Mx_atMIN_RSHELE/min_MX_RSH;
end
My_atMIN_RSHELE=localFM_Rshoulder(RSHpeak_lift(1,6),5);
if My_atMIN_RSHELE > 0;
  Myratio_atMIN_RSHELE=My_atMIN_RSHELE/peak_MY_RSH;
else
  Myratio_atMIN_RSHELE=My_atMIN_RSHELE/min_MY_RSH;
end
Mz_atMIN_RSHELE=localFM_Rshoulder(RSHpeak_lift(1,6),6);
if Mz_atMIN_RSHELE > 0;
  Mzratio_atMIN_RSHELE=Mz_atMIN_RSHELE/peak_MZ_RSH;
else

```

```

Mzratio_atMIN_RSHELE=Mz_atMIN_RSHELE/min_MZ_RSH;
end
RF_atMIN_RSHELE=resultantF_Rshoulder(RSHpeak_lift(1,6),1);
RFratio_atMIN_RSHELE=RF_atMIN_RSHELE/peak_RF_RSH;
RM_atMIN_RSHELE=resultantM_Rshoulder(RSHpeak_lift(1,6),1);
RMratio_atMIN_RSHELE=RM_atMIN_RSHELE/peak_RM_RSH;

FM_atRSHpeakA=[Fx_atMAX_RSHPOE Fxratio_atMAX_RSHPOE
Fy_atMAX_RSHPOE Fyratio_atMAX_RSHPOE Fz_atMAX_RSHPOE
Fzratio_atMAX_RSHPOE RF_atMAX_RSHPOE RFratio_atMAX_RSHPOE...
Mx_atMAX_RSHPOE Mxratio_atMAX_RSHPOE My_atMAX_RSHPOE
Myratio_atMAX_RSHPOE Mz_atMAX_RSHPOE Mzratio_atMAX_RSHPOE
RM_atMAX_RSHPOE RMratio_atMAX_RSHPOE;...
Fx_atMIN_RSHPOE Fxratio_atMIN_RSHPOE Fy_atMIN_RSHPOE
Fyratio_atMIN_RSHPOE Fz_atMIN_RSHPOE Fzratio_atMIN_RSHPOE RF_atMIN_RSHPOE
RFratio_atMIN_RSHPOE...
Mx_atMIN_RSHPOE Mxratio_atMIN_RSHPOE My_atMIN_RSHPOE
Myratio_atMIN_RSHPOE Mz_atMIN_RSHPOE Mzratio_atMIN_RSHPOE
RM_atMIN_RSHPOE RMratio_atMIN_RSHPOE;...
Fx_atMAX_RSHAXIR Fxratio_atMAX_RSHAXIR Fy_atMAX_RSHAXIR
Fyratio_atMAX_RSHAXIR Fz_atMAX_RSHAXIR Fzratio_atMAX_RSHAXIR
RF_atMAX_RSHAXIR RFratio_atMAX_RSHAXIR...
Mx_atMAX_RSHAXIR Mxratio_atMAX_RSHAXIR My_atMAX_RSHAXIR
Myratio_atMAX_RSHAXIR Mz_atMAX_RSHAXIR Mzratio_atMAX_RSHAXIR
RM_atMAX_RSHAXIR RMratio_atMAX_RSHAXIR;...
Fx_atMIN_RSHAXIR Fxratio_atMIN_RSHAXIR Fy_atMIN_RSHAXIR
Fyratio_atMIN_RSHAXIR Fz_atMIN_RSHAXIR Fzratio_atMIN_RSHAXIR
RF_atMIN_RSHAXIR RFratio_atMIN_RSHAXIR...
Mx_atMIN_RSHAXIR Mxratio_atMIN_RSHAXIR My_atMIN_RSHAXIR
Myratio_atMIN_RSHAXIR Mz_atMIN_RSHAXIR Mzratio_atMIN_RSHAXIR
RM_atMIN_RSHAXIR RMratio_atMIN_RSHAXIR;...
Fx_atMAX_RSHELE Fxratio_atMAX_RSHELE Fy_atMAX_RSHELE
Fyratio_atMAX_RSHELE Fz_atMAX_RSHELE Fzratio_atMAX_RSHELE
RF_atMAX_RSHELE RFratio_atMAX_RSHELE...
Mx_atMAX_RSHELE Mxratio_atMAX_RSHELE My_atMAX_RSHELE
Myratio_atMAX_RSHELE Mz_atMAX_RSHELE Mzratio_atMAX_RSHELE
RM_atMAX_RSHELE RMratio_atMAX_RSHELE;...
Fx_atMIN_RSHELE Fxratio_atMIN_RSHELE Fy_atMIN_RSHELE
Fyratio_atMIN_RSHELE Fz_atMIN_RSHELE Fzratio_atMIN_RSHELE RF_atMIN_RSHELE
RFratio_atMIN_RSHELE...
Mx_atMIN_RSHELE Mxratio_atMIN_RSHELE My_atMIN_RSHELE
Myratio_atMIN_RSHELE Mz_atMIN_RSHELE Mzratio_atMIN_RSHELE
RM_atMIN_RSHELE RMratio_atMIN_RSHELE];
save FMandRatio_atRSHpeakAngle.txt FM_atRSHpeakA -ascii;

%%%%% force and force ratio at the max Right Elbow angle %%%%%%

```

```

Fx_atMAX_RELFLE=localFM_Relbow(RELpeak_lift(1,1),1);
if Fx_atMAX_RELFLE > 0;
  Fxratio_atMAX_RELFLE=Fx_atMAX_RELFLE/peak_FX_REL;
else
  Fxratio_atMAX_RELFLE=Fx_atMAX_RELFLE/min_FX_REL;
end
Fy_atMAX_RELFLE=localFM_Relbow(RELpeak_lift(1,1),2);
if Fy_atMAX_RELFLE > 0;
  Fyratio_atMAX_RELFLE=Fy_atMAX_RELFLE/peak_FY_REL;
else
  Fyratio_atMAX_RELFLE=Fy_atMAX_RELFLE/min_FY_REL;
end
Fz_atMAX_RELFLE=localFM_Relbow(RELpeak_lift(1,1),3);
if Fz_atMAX_RELFLE > 0;
  Fzratio_atMAX_RELFLE=Fz_atMAX_RELFLE/peak_FZ_REL;
else
  Fzratio_atMAX_RELFLE=Fz_atMAX_RELFLE/min_FZ_REL;
end
Mx_atMAX_RELFLE=localFM_Relbow(RELpeak_lift(1,1),4);
if Mx_atMAX_RELFLE > 0;
  Mxratio_atMAX_RELFLE=Mx_atMAX_RELFLE/peak_MX_REL;
else
  Mxratio_atMAX_RELFLE=Mx_atMAX_RELFLE/min_MX_REL;
end
My_atMAX_RELFLE=localFM_Relbow(RELpeak_lift(1,1),5);
if My_atMAX_RELFLE > 0;
  Myratio_atMAX_RELFLE=My_atMAX_RELFLE/peak_MY_REL;
else
  Myratio_atMAX_RELFLE=My_atMAX_RELFLE/min_MY_REL;
end
Mz_atMAX_RELFLE=localFM_Relbow(RELpeak_lift(1,1),6);
if Mz_atMAX_RELFLE > 0;
  Mzratio_atMAX_RELFLE=Mz_atMAX_RELFLE/peak_MZ_REL;
else
  Mzratio_atMAX_RELFLE=Mz_atMAX_RELFLE/min_MZ_REL;
end
RF_atMAX_RELFLE=resultantF_Relbow(RELpeak_lift(1,1),1);
RFratio_atMAX_RELFLE=RF_atMAX_RELFLE/peak_RF_REL;
RM_atMAX_RELFLE=resultantM_Relbow(RELpeak_lift(1,1),1);
RMratio_atMAX_RELFLE=RM_atMAX_RELFLE/peak_RM_REL;

Fx_atMIN_RELFLE=localFM_Relbow(RELpeak_lift(1,2),1);
if Fx_atMIN_RELFLE > 0;
  Fxratio_atMIN_RELFLE=Fx_atMIN_RELFLE/peak_FX_REL;
else
  Fxratio_atMIN_RELFLE=Fx_atMIN_RELFLE/min_FX_REL;

```

```

end
Fy_atMIN_RELFLFLE=localFM_Relbow(RELpeak_lift(1,2),2);
if Fy_atMIN_RELFLFLE > 0;
  Fyratio_atMIN_RELFLFLE=Fy_atMIN_RELFLFLE/peak_FY_REL;
else
  Fyratio_atMIN_RELFLFLE=Fy_atMIN_RELFLFLE/min_FY_REL;
end
Fz_atMIN_RELFLFLE=localFM_Relbow(RELpeak_lift(1,2),3);
if Fz_atMIN_RELFLFLE > 0;
  Fzratio_atMIN_RELFLFLE=Fz_atMIN_RELFLFLE/peak_FZ_REL;
else
  Fzratio_atMIN_RELFLFLE=Fz_atMIN_RELFLFLE/min_FZ_REL;
end
Mx_atMIN_RELFLFLE=localFM_Relbow(RELpeak_lift(1,2),4);
if Mx_atMIN_RELFLFLE > 0;
  Mxratio_atMIN_RELFLFLE=Mx_atMIN_RELFLFLE/peak_MX_REL;
else
  Mxratio_atMIN_RELFLFLE=Mx_atMIN_RELFLFLE/min_MX_REL;
end
My_atMIN_RELFLFLE=localFM_Relbow(RELpeak_lift(1,2),5);
if My_atMIN_RELFLFLE > 0;
  Myratio_atMIN_RELFLFLE=My_atMIN_RELFLFLE/peak_MY_REL;
else
  Myratio_atMIN_RELFLFLE=My_atMIN_RELFLFLE/min_MY_REL;
end
Mz_atMIN_RELFLFLE=localFM_Relbow(RELpeak_lift(1,2),6);
if Mz_atMIN_RELFLFLE > 0;
  Mzratio_atMIN_RELFLFLE=Mz_atMIN_RELFLFLE/peak_MZ_REL;
else
  Mzratio_atMIN_RELFLFLE=Mz_atMIN_RELFLFLE/min_MZ_REL;
end
RF_atMIN_RELFLFLE=resultantF_Relbow(RELpeak_lift(1,2),1);
RFratio_atMIN_RELFLFLE=RF_atMIN_RELFLFLE/peak_RF_REL;
RM_atMIN_RELFLFLE=resultantM_Relbow(RELpeak_lift(1,2),1);
RMratio_atMIN_RELFLFLE=RM_atMIN_RELFLFLE/peak_RM_REL;

FM_atRELpeakA=[Fx_atMAX_RELFLFLE Fxratio_atMAX_RELFLFLE
Fy_atMAX_RELFLFLE Fyratio_atMAX_RELFLFLE Fz_atMAX_RELFLFLE
Fzratio_atMAX_RELFLFLE RF_atMAX_RELFLFLE RFratio_atMAX_RELFLFLE...
Mx_atMAX_RELFLFLE Mxratio_atMAX_RELFLFLE My_atMAX_RELFLFLE
Myratio_atMAX_RELFLFLE Mz_atMAX_RELFLFLE Mzratio_atMAX_RELFLFLE
RM_atMAX_RELFLFLE RMratio_atMAX_RELFLFLE;...
Fx_atMIN_RELFLFLE Fxratio_atMIN_RELFLFLE Fy_atMIN_RELFLFLE
Fyratio_atMIN_RELFLFLE Fz_atMIN_RELFLFLE Fzratio_atMIN_RELFLFLE RF_atMIN_RELFLFLE
RFratio_atMIN_RELFLFLE...

```

```

Mx_atMIN_RELFL E Mxratio_atMIN_RELFL E My_atMIN_RELFL E
Myratio_atMIN_RELFL E Mz_atMIN_RELFL E Mzratio_atMIN_RELFL E
RM_atMIN_RELFL E RMratio_atMIN_RELFL E];
save FMandRatio_atRELpeakAngle.txt FM_atRELpeakA -ascii;

%%%%%% force and force ratio at the max Right Wrist angle %%%%%
Fx_atMAX_RWRFLE=localFM_Rwrist(RWRpeak_lift(1,1),1);
if Fx_atMAX_RWRFLE > 0;
    Fxratio_atMAX_RWRFLE=Fx_atMAX_RWRFLE/peak_FX_RWR;
else
    Fxratio_atMAX_RWRFLE=Fx_atMAX_RWRFLE/min_FX_RWR;
end
Fy_atMAX_RWRFLE=localFM_Rwrist(RWRpeak_lift(1,1),2);
if Fy_atMAX_RWRFLE > 0;
    Fyratio_atMAX_RWRFLE=Fy_atMAX_RWRFLE/peak_FY_RWR;
else
    Fyratio_atMAX_RWRFLE=Fy_atMAX_RWRFLE/min_FY_RWR;
end
Fz_atMAX_RWRFLE=localFM_Rwrist(RWRpeak_lift(1,1),3);
if Fz_atMAX_RWRFLE > 0;
    Fzratio_atMAX_RWRFLE=Fz_atMAX_RWRFLE/peak_FZ_RWR;
else
    Fzratio_atMAX_RWRFLE=Fz_atMAX_RWRFLE/min_FZ_RWR;
end
Mx_atMAX_RWRFLE=localFM_Rwrist(RWRpeak_lift(1,1),4);
if Mx_atMAX_RWRFLE > 0;
    Mxratio_atMAX_RWRFLE=Mx_atMAX_RWRFLE/peak_MX_RWR;
else
    Mxratio_atMAX_RWRFLE=Mx_atMAX_RWRFLE/min_MX_RWR;
end
My_atMAX_RWRFLE=localFM_Rwrist(RWRpeak_lift(1,1),5);
if My_atMAX_RWRFLE > 0;
    Myratio_atMAX_RWRFLE=My_atMAX_RWRFLE/peak_MY_RWR;
else
    Myratio_atMAX_RWRFLE=My_atMAX_RWRFLE/min_MY_RWR;
end
Mz_atMAX_RWRFLE=localFM_Rwrist(RWRpeak_lift(1,1),6);
if Mz_atMAX_RWRFLE > 0;
    Mzratio_atMAX_RWRFLE=Mz_atMAX_RWRFLE/peak_MZ_RWR;
else
    Mzratio_atMAX_RWRFLE=Mz_atMAX_RWRFLE/min_MZ_RWR;
end
RF_atMAX_RWRFLE=resultantF_Rwrist(RWRpeak_lift(1,1),1);
RFratio_atMAX_RWRFLE=RF_atMAX_RWRFLE/peak_RF_RWR;
RM_atMAX_RWRFLE=resultantM_Rwrist(RWRpeak_lift(1,1),1);
RMratio_atMAX_RWRFLE=RM_atMAX_RWRFLE/peak_RM_RWR;

```

```

Fx_atMIN_RWRFLE=localFM_Rwrist(RWRpeak_lift(1,2),1);
if Fx_atMIN_RWRFLE > 0;
  Fxratio_atMIN_RWRFLE=Fx_atMIN_RWRFLE/peak_FX_RWR;
else
  Fxratio_atMIN_RWRFLE=Fx_atMIN_RWRFLE/min_FX_RWR;
end
Fy_atMIN_RWRFLE=localFM_Rwrist(RWRpeak_lift(1,2),2);
if Fy_atMIN_RWRFLE > 0;
  Fyratio_atMIN_RWRFLE=Fy_atMIN_RWRFLE/peak_FY_RWR;
else
  Fyratio_atMIN_RWRFLE=Fy_atMIN_RWRFLE/min_FY_RWR;
end
Fz_atMIN_RWRFLE=localFM_Rwrist(RWRpeak_lift(1,2),3);
if Fz_atMIN_RWRFLE > 0;
  Fzratio_atMIN_RWRFLE=Fz_atMIN_RWRFLE/peak_FZ_RWR;
else
  Fzratio_atMIN_RWRFLE=Fz_atMIN_RWRFLE/min_FZ_RWR;
end
Mx_atMIN_RWRFLE=localFM_Rwrist(RWRpeak_lift(1,2),4);
if Mx_atMIN_RWRFLE > 0;
  Mxratio_atMIN_RWRFLE=Mx_atMIN_RWRFLE/peak_MX_RWR;
else
  Mxratio_atMIN_RWRFLE=Mx_atMIN_RWRFLE/min_MX_RWR;
end
My_atMIN_RWRFLE=localFM_Rwrist(RWRpeak_lift(1,2),5);
if My_atMIN_RWRFLE > 0;
  Myratio_atMIN_RWRFLE=My_atMIN_RWRFLE/peak_MY_RWR;
else
  Myratio_atMIN_RWRFLE=My_atMIN_RWRFLE/min_MY_RWR;
end
Mz_atMIN_RWRFLE=localFM_Rwrist(RWRpeak_lift(1,2),6);
if Mz_atMIN_RWRFLE > 0;
  Mzratio_atMIN_RWRFLE=Mz_atMIN_RWRFLE/peak_MZ_RWR;
else
  Mzratio_atMIN_RWRFLE=Mz_atMIN_RWRFLE/min_MZ_RWR;
end
RF_atMIN_RWRFLE=resultantF_Rwrist(RWRpeak_lift(1,2),1);
Rfratio_atMIN_RWRFLE=RF_atMIN_RWRFLE/peak_RF_RWR;
RM_atMIN_RWRFLE=resultantM_Rwrist(RWRpeak_lift(1,2),1);
RMratio_atMIN_RWRFLE=RM_atMIN_RWRFLE/peak_RM_RWR;

FM_atRWRpeakA=[Fx_atMAX_RWRFLE Fxratio_atMAX_RWRFLE
Fy_atMAX_RWRFLE Fyratio_atMAX_RWRFLE Fz_atMAX_RWRFLE
Fzratio_atMAX_RWRFLE RF_atMAX_RWRFLE Rfratio_atMAX_RWRFLE...

```

```
Mx_atMAX_RWRFL Mxratio_atMAX_RWRFL My_atMAX_RWRFL  
Myratio_atMAX_RWRFL Mz_atMAX_RWRFL Mzratio_atMAX_RWRFL  
RM_atMAX_RWRFL RMratio_atMAX_RWRFL;...
```

```
Fx_atMIN_RWRFL Fxratio_atMIN_RWRFL Fy_atMIN_RWRFL  
Fyratio_atMIN_RWRFL Fz_atMIN_RWRFL Fzratio_atMIN_RWRFL  
RF_atMIN_RWRFL RFratio_atMIN_RWRFL...
```

```
Mx_atMIN_RWRFL Mxratio_atMIN_RWRFL My_atMIN_RWRFL  
Myratio_atMIN_RWRFL Mz_atMIN_RWRFL Mzratio_atMIN_RWRFL  
RM_atMIN_RWRFL RMratio_atMIN_RWRFL];
```

```
save FMandRatio_atRWRpeakAngle.txt FM_atRWRpeakA -ascii;
```

```
%%%%% the force and force ratio at the max Left Shoulder angle %%%%%%
```

```
Fx_atMAX_LSHPOE=localFM_Lshoulder(LSHpeak_lift(1,1),1);
```

```
if Fx_atMAX_LSHPOE > 0;
```

```
  Fxratio_atMAX_LSHPOE=Fx_atMAX_LSHPOE/peak_FX_LSH;
```

```
else
```

```
  Fxratio_atMAX_LSHPOE=Fx_atMAX_LSHPOE/min_FX_LSH;
```

```
end
```

```
Fy_atMAX_LSHPOE=localFM_Lshoulder(LSHpeak_lift(1,1),2);
```

```
if Fy_atMAX_LSHPOE > 0;
```

```
  Fyratio_atMAX_LSHPOE=Fy_atMAX_LSHPOE/peak_FY_LSH;
```

```
else
```

```
  Fyratio_atMAX_LSHPOE=Fy_atMAX_LSHPOE/min_FY_LSH;
```

```
end
```

```
Fz_atMAX_LSHPOE=localFM_Lshoulder(LSHpeak_lift(1,1),3);
```

```
if Fz_atMAX_LSHPOE > 0;
```

```
  Fzratio_atMAX_LSHPOE=Fz_atMAX_LSHPOE/peak_FZ_LSH;
```

```
else
```

```
  Fzratio_atMAX_LSHPOE=Fz_atMAX_LSHPOE/min_FZ_LSH;
```

```
end
```

```
Mx_atMAX_LSHPOE=localFM_Lshoulder(LSHpeak_lift(1,1),4);
```

```
if Mx_atMAX_LSHPOE > 0;
```

```
  Mxratio_atMAX_LSHPOE=Mx_atMAX_LSHPOE/peak_MX_LSH;
```

```
else
```

```
  Mxratio_atMAX_LSHPOE=Mx_atMAX_LSHPOE/min_MX_LSH;
```

```
end
```

```
My_atMAX_LSHPOE=localFM_Lshoulder(LSHpeak_lift(1,1),5);
```

```
if My_atMAX_LSHPOE > 0;
```

```
  Myratio_atMAX_LSHPOE=My_atMAX_LSHPOE/peak_MY_LSH;
```

```
else
```

```
  Myratio_atMAX_LSHPOE=My_atMAX_LSHPOE/min_MY_LSH;
```

```
end
```

```
Mz_atMAX_LSHPOE=localFM_Lshoulder(LSHpeak_lift(1,1),6);
```

```
if Mz_atMAX_LSHPOE > 0;
```

```
  Mzratio_atMAX_LSHPOE=Mz_atMAX_LSHPOE/peak_MZ_LSH;
```

```
else
```

```

Mzratio_atMAX_LSHPOE=Mz_atMAX_LSHPOE/min_MZ_LSH;
end
RF_atMAX_LSHPOE=resultantF_Lshoulder(LSHpeak_lift(1,1),1);
Rfratio_atMAX_LSHPOE=RF_atMAX_LSHPOE/peak_RF_LSH;
RM_atMAX_LSHPOE=resultantM_Lshoulder(LSHpeak_lift(1,1),1);
RMratio_atMAX_LSHPOE=RM_atMAX_LSHPOE/peak_RM_LSH;

Fx_atMIN_LSHPOE=localFM_Lshoulder(LSHpeak_lift(1,2),1);
if Fx_atMIN_LSHPOE > 0;
    Fxratio_atMIN_LSHPOE=Fx_atMIN_LSHPOE/peak_FX_LSH;
else
    Fxratio_atMIN_LSHPOE=Fx_atMIN_LSHPOE/min_FX_LSH;
end
Fy_atMIN_LSHPOE=localFM_Lshoulder(LSHpeak_lift(1,2),2);
if Fy_atMIN_LSHPOE > 0;
    Fyratio_atMIN_LSHPOE=Fy_atMIN_LSHPOE/peak_FY_LSH;
else
    Fyratio_atMIN_LSHPOE=Fy_atMIN_LSHPOE/min_FY_LSH;
end
Fz_atMIN_LSHPOE=localFM_Lshoulder(LSHpeak_lift(1,2),3);
if Fz_atMIN_LSHPOE > 0;
    Fzratio_atMIN_LSHPOE=Fz_atMIN_LSHPOE/peak_FZ_LSH;
else
    Fzratio_atMIN_LSHPOE=Fz_atMIN_LSHPOE/min_FZ_LSH;
end
Mx_atMIN_LSHPOE=localFM_Lshoulder(LSHpeak_lift(1,2),4);
if Mx_atMIN_LSHPOE > 0;
    Mxratio_atMIN_LSHPOE=Mx_atMIN_LSHPOE/peak_MX_LSH;
else
    Mxratio_atMIN_LSHPOE=Mx_atMIN_LSHPOE/min_MX_LSH;
end
My_atMIN_LSHPOE=localFM_Lshoulder(LSHpeak_lift(1,2),5);
if My_atMIN_LSHPOE > 0;
    Myratio_atMIN_LSHPOE=My_atMIN_LSHPOE/peak_MY_LSH;
else
    Myratio_atMIN_LSHPOE=My_atMIN_LSHPOE/min_MY_LSH;
end
Mz_atMIN_LSHPOE=localFM_Lshoulder(LSHpeak_lift(1,2),6);
if Mz_atMIN_LSHPOE > 0;
    Mzratio_atMIN_LSHPOE=Mz_atMIN_LSHPOE/peak_MZ_LSH;
else
    Mzratio_atMIN_LSHPOE=Mz_atMIN_LSHPOE/min_MZ_LSH;
end
RF_atMIN_LSHPOE=resultantF_Lshoulder(LSHpeak_lift(1,2),1);
Rfratio_atMIN_LSHPOE=RF_atMIN_LSHPOE/peak_RF_LSH;
RM_atMIN_LSHPOE=resultantM_Lshoulder(LSHpeak_lift(1,2),1);

```

```

RMratio_atMIN_LSHPOE=RM_atMIN_LSHPOE/peak_RM_LSH;

Fx_atMAX_LSHAXIR=localFM_Lshoulder(LSHpeak_lift(1,3),1);
if Fx_atMAX_LSHAXIR > 0;
  Fxratio_atMAX_LSHAXIR=Fx_atMAX_LSHAXIR/peak_FX_LSH;
else
  Fxratio_atMAX_LSHAXIR=Fx_atMAX_LSHAXIR/min_FX_LSH;
end
Fy_atMAX_LSHAXIR=localFM_Lshoulder(LSHpeak_lift(1,3),2);
if Fy_atMAX_LSHAXIR > 0;
  Fyratio_atMAX_LSHAXIR=Fy_atMAX_LSHAXIR/peak_FY_LSH;
else
  Fyratio_atMAX_LSHAXIR=Fy_atMAX_LSHAXIR/min_FY_LSH;
end
Fz_atMAX_LSHAXIR=localFM_Lshoulder(LSHpeak_lift(1,3),3);
if Fz_atMAX_LSHAXIR > 0;
  Fzratio_atMAX_LSHAXIR=Fz_atMAX_LSHAXIR/peak_FZ_LSH;
else
  Fzratio_atMAX_LSHAXIR=Fz_atMAX_LSHAXIR/min_FZ_LSH;
end
Mx_atMAX_LSHAXIR=localFM_Lshoulder(LSHpeak_lift(1,3),4);
if Mx_atMAX_LSHAXIR > 0;
  Mxratio_atMAX_LSHAXIR=Mx_atMAX_LSHAXIR/peak_MX_LSH;
else
  Mxratio_atMAX_LSHAXIR=Mx_atMAX_LSHAXIR/min_MX_LSH;
end
My_atMAX_LSHAXIR=localFM_Lshoulder(LSHpeak_lift(1,3),5);
if My_atMAX_LSHAXIR > 0;
  Myratio_atMAX_LSHAXIR=My_atMAX_LSHAXIR/peak_MY_LSH;
else
  Myratio_atMAX_LSHAXIR=My_atMAX_LSHAXIR/min_MY_LSH;
end
Mz_atMAX_LSHAXIR=localFM_Lshoulder(LSHpeak_lift(1,3),6);
if Mz_atMAX_LSHAXIR > 0;
  Mzratio_atMAX_LSHAXIR=Mz_atMAX_LSHAXIR/peak_MZ_LSH;
else
  Mzratio_atMAX_LSHAXIR=Mz_atMAX_LSHAXIR/min_MZ_LSH;
end
RF_atMAX_LSHAXIR=resultantF_Lshoulder(LSHpeak_lift(1,3),1);
RFratio_atMAX_LSHAXIR=RF_atMAX_LSHAXIR/peak_RF_LSH;
RM_atMAX_LSHAXIR=resultantM_Lshoulder(LSHpeak_lift(1,3),1);
RMratio_atMAX_LSHAXIR=RM_atMAX_LSHAXIR/peak_RM_LSH;

Fx_atMIN_LSHAXIR=localFM_Lshoulder(LSHpeak_lift(1,4),1);
if Fx_atMIN_LSHAXIR > 0;
  Fxratio_atMIN_LSHAXIR=Fx_atMIN_LSHAXIR/peak_FX_LSH;

```

```

else
  Fxratio_atMIN_LSHAXIR=Fx_atMIN_LSHAXIR/min_FX_LSH;
end
Fy_atMIN_LSHAXIR=localFM_Lshoulder(LSHpeak_lift(1,4),2);
if Fy_atMIN_LSHAXIR > 0;
  Fyratio_atMIN_LSHAXIR=Fy_atMIN_LSHAXIR/peak_FY_LSH;
else
  Fyratio_atMIN_LSHAXIR=Fy_atMIN_LSHAXIR/min_FY_LSH;
end
Fz_atMIN_LSHAXIR=localFM_Lshoulder(LSHpeak_lift(1,4),3);
if Fz_atMIN_LSHAXIR > 0;
  Fzratio_atMIN_LSHAXIR=Fz_atMIN_LSHAXIR/peak_FZ_LSH;
else
  Fzratio_atMIN_LSHAXIR=Fz_atMIN_LSHAXIR/min_FZ_LSH;
end
Mx_atMIN_LSHAXIR=localFM_Lshoulder(LSHpeak_lift(1,4),4);
if Mx_atMIN_LSHAXIR > 0;
  Mxratio_atMIN_LSHAXIR=Mx_atMIN_LSHAXIR/peak_MX_LSH;
else
  Mxratio_atMIN_LSHAXIR=Mx_atMIN_LSHAXIR/min_MX_LSH;
end
My_atMIN_LSHAXIR=localFM_Lshoulder(LSHpeak_lift(1,4),5);
if My_atMIN_LSHAXIR > 0;
  Myratio_atMIN_LSHAXIR=My_atMIN_LSHAXIR/peak_MY_LSH;
else
  Myratio_atMIN_LSHAXIR=My_atMIN_LSHAXIR/min_MY_LSH;
end
Mz_atMIN_LSHAXIR=localFM_Lshoulder(LSHpeak_lift(1,4),6);
if Mz_atMIN_LSHAXIR > 0;
  Mzratio_atMIN_LSHAXIR=Mz_atMIN_LSHAXIR/peak_MZ_LSH;
else
  Mzratio_atMIN_LSHAXIR=Mz_atMIN_LSHAXIR/min_MZ_LSH;
end
RF_atMIN_LSHAXIR=resultantF_Lshoulder(LSHpeak_lift(1,4),1);
RFratio_atMIN_LSHAXIR=RF_atMIN_LSHAXIR/peak_RF_LSH;
RM_atMIN_LSHAXIR=resultantM_Lshoulder(LSHpeak_lift(1,4),1);
RMratio_atMIN_LSHAXIR=RM_atMIN_LSHAXIR/peak_RM_LSH;

Fx_atMAX_LSHELE=localFM_Lshoulder(LSHpeak_lift(1,5),1);
if Fx_atMAX_LSHELE > 0;
  Fxratio_atMAX_LSHELE=Fx_atMAX_LSHELE/peak_FX_LSH;
else
  Fxratio_atMAX_LSHELE=Fx_atMAX_LSHELE/min_FX_LSH;
end
Fy_atMAX_LSHELE=localFM_Lshoulder(LSHpeak_lift(1,5),2);
if Fy_atMAX_LSHELE > 0;

```

```

Fyratio_atMAX_LSHELE=Fy_atMAX_LSHELE/peak_FY_LSH;
else
  Fyratio_atMAX_LSHELE=Fy_atMAX_LSHELE/min_FY_LSH;
end
Fz_atMAX_LSHELE=localFM_Lshoulder(LSHpeak_lift(1,5),3);
if Fz_atMAX_LSHELE > 0;
  Fzratio_atMAX_LSHELE=Fz_atMAX_LSHELE/peak_FZ_LSH;
else
  Fzratio_atMAX_LSHELE=Fz_atMAX_LSHELE/min_FZ_LSH;
end
Mx_atMAX_LSHELE=localFM_Lshoulder(LSHpeak_lift(1,5),4);
if Mx_atMAX_LSHELE > 0;
  Mxratio_atMAX_LSHELE=Mx_atMAX_LSHELE/peak_MX_LSH;
else
  Mxratio_atMAX_LSHELE=Mx_atMAX_LSHELE/min_MX_LSH;
end
My_atMAX_LSHELE=localFM_Lshoulder(LSHpeak_lift(1,5),5);
if My_atMAX_LSHELE > 0;
  Myratio_atMAX_LSHELE=My_atMAX_LSHELE/peak_MY_LSH;
else
  Myratio_atMAX_LSHELE=My_atMAX_LSHELE/min_MY_LSH;
end
Mz_atMAX_LSHELE=localFM_Lshoulder(LSHpeak_lift(1,5),6);
if Mz_atMAX_LSHELE > 0;
  Mzratio_atMAX_LSHELE=Mz_atMAX_LSHELE/peak_MZ_LSH;
else
  Mzratio_atMAX_LSHELE=Mz_atMAX_LSHELE/min_MZ_LSH;
end
RF_atMAX_LSHELE=resultantF_Lshoulder(LSHpeak_lift(1,5),1);
RFratio_atMAX_LSHELE=RF_atMAX_LSHELE/peak_RF_LSH;
RM_atMAX_LSHELE=resultantM_Lshoulder(LSHpeak_lift(1,5),1);
RMratio_atMAX_LSHELE=RM_atMAX_LSHELE/peak_RM_LSH;

Fx_atMIN_LSHELE=localFM_Lshoulder(LSHpeak_lift(1,6),1);
if Fx_atMIN_LSHELE > 0;
  Fxratio_atMIN_LSHELE=Fx_atMIN_LSHELE/peak_FX_LSH;
else
  Fxratio_atMIN_LSHELE=Fx_atMIN_LSHELE/min_FX_LSH;
end
Fy_atMIN_LSHELE=localFM_Lshoulder(LSHpeak_lift(1,6),2);
if Fy_atMIN_LSHELE > 0;
  Fyratio_atMIN_LSHELE=Fy_atMIN_LSHELE/peak_FY_LSH;
else
  Fyratio_atMIN_LSHELE=Fy_atMIN_LSHELE/min_FY_LSH;
end
Fz_atMIN_LSHELE=localFM_Lshoulder(LSHpeak_lift(1,6),3);

```

```

if Fz_atMIN_LSHELE > 0;
  Fzratio_atMIN_LSHELE=Fz_atMIN_LSHELE/peak_FZ_LSH;
else
  Fzratio_atMIN_LSHELE=Fz_atMIN_LSHELE/min_FZ_LSH;
end
Mx_atMIN_LSHELE=localFM_Lshoulder(LSHpeak_lift(1,6),4);
if Mx_atMIN_LSHELE > 0;
  Mxratio_atMIN_LSHELE=Mx_atMIN_LSHELE/peak_MX_LSH;
else
  Mxratio_atMIN_LSHELE=Mx_atMIN_LSHELE/min_MX_LSH;
end
My_atMIN_LSHELE=localFM_Lshoulder(LSHpeak_lift(1,6),5);
if My_atMIN_LSHELE > 0;
  Myratio_atMIN_LSHELE=My_atMIN_LSHELE/peak_MY_LSH;
else
  Myratio_atMIN_LSHELE=My_atMIN_LSHELE/min_MY_LSH;
end
Mz_atMIN_LSHELE=localFM_Lshoulder(LSHpeak_lift(1,6),6);
if Mz_atMIN_LSHELE > 0;
  Mzratio_atMIN_LSHELE=Mz_atMIN_LSHELE/peak_MZ_LSH;
else
  Mzratio_atMIN_LSHELE=Mz_atMIN_LSHELE/min_MZ_LSH;
end
RF_atMIN_LSHELE=resultantF_Lshoulder(LSHpeak_lift(1,6),1);
Rfratio_atMIN_LSHELE=RF_atMIN_LSHELE/peak_RF_LSH;
RM_atMIN_LSHELE=resultantM_Lshoulder(LSHpeak_lift(1,6),1);
RMratio_atMIN_LSHELE=RM_atMIN_LSHELE/peak_RM_LSH;

FM_atLSHpeakA=[Fx_atMAX_LSHPOE Fxratio_atMAX_LSHPOE
Fy_atMAX_LSHPOE Fyratio_atMAX_LSHPOE Fz_atMAX_LSHPOE
Fzratio_atMAX_LSHPOE RF_atMAX_LSHPOE Rfratio_atMAX_LSHPOE...
Mx_atMAX_LSHPOE Mxratio_atMAX_LSHPOE My_atMAX_LSHPOE
Myratio_atMAX_LSHPOE Mz_atMAX_LSHPOE Mzratio_atMAX_LSHPOE
RM_atMAX_LSHPOE RMratio_atMAX_LSHPOE;...
Fx_atMIN_LSHPOE Fxratio_atMIN_LSHPOE Fy_atMIN_LSHPOE
Fyratio_atMIN_LSHPOE Fz_atMIN_LSHPOE Fzratio_atMIN_LSHPOE RF_atMIN_LSHPOE
Rfratio_atMIN_LSHPOE...
Mx_atMIN_LSHPOE Mxratio_atMIN_LSHPOE My_atMIN_LSHPOE
Myratio_atMIN_LSHPOE Mz_atMIN_LSHPOE Mzratio_atMIN_LSHPOE
RM_atMIN_LSHPOE RMratio_atMIN_LSHPOE;...
Fx_atMAX_LSHAXIR Fxratio_atMAX_LSHAXIR Fy_atMAX_LSHAXIR
Fyratio_atMAX_LSHAXIR Fz_atMAX_LSHAXIR Fzratio_atMAX_LSHAXIR
RF_atMAX_LSHAXIR Rfratio_atMAX_LSHAXIR...
Mx_atMAX_LSHAXIR Mxratio_atMAX_LSHAXIR My_atMAX_LSHAXIR
Myratio_atMAX_LSHAXIR Mz_atMAX_LSHAXIR Mzratio_atMAX_LSHAXIR
RM_atMAX_LSHAXIR RMratio_atMAX_LSHAXIR;...

```

```

    Fx_atMIN_LSHAXIR Fxratio_atMIN_LSHAXIR Fy_atMIN_LSHAXIR
Fyratio_atMIN_LSHAXIR Fz_atMIN_LSHAXIR Fzratio_atMIN_LSHAXIR
RF_atMIN_LSHAXIR RFratio_atMIN_LSHAXIR...
    Mx_atMIN_LSHAXIR Mxratio_atMIN_LSHAXIR My_atMIN_LSHAXIR
Myratio_atMIN_LSHAXIR Mz_atMIN_LSHAXIR Mzratio_atMIN_LSHAXIR
RM_atMIN_LSHAXIR RMratio_atMIN_LSHAXIR;...
    Fx_atMAX_LSHELE Fxratio_atMAX_LSHELE Fy_atMAX_LSHELE
Fyratio_atMAX_LSHELE Fz_atMAX_LSHELE Fzratio_atMAX_LSHELE
RF_atMAX_LSHELE RFratio_atMAX_LSHELE...
    Mx_atMAX_LSHELE Mxratio_atMAX_LSHELE My_atMAX_LSHELE
Myratio_atMAX_LSHELE Mz_atMAX_LSHELE Mzratio_atMAX_LSHELE
RM_atMAX_LSHELE RMratio_atMAX_LSHELE;...
    Fx_atMIN_LSHELE Fxratio_atMIN_LSHELE Fy_atMIN_LSHELE
Fyratio_atMIN_LSHELE Fz_atMIN_LSHELE Fzratio_atMIN_LSHELE RF_atMIN_LSHELE
RFratio_atMIN_LSHELE...
    Mx_atMIN_LSHELE Mxratio_atMIN_LSHELE My_atMIN_LSHELE
Myratio_atMIN_LSHELE Mz_atMIN_LSHELE Mzratio_atMIN_LSHELE
RM_atMIN_LSHELE RMratio_atMIN_LSHELE];
    save FMandRatio_atLSHpeakAngle.txt FM_atLSHpeakA -ascii;

```

```

%%%%%% force and force ratio at the max Left Elbow angle %%%%%%%

```

```

Fx_atMAX_LELFLE=localFM_Lelbow(LELpeak_lift(1,1),1);
if Fx_atMAX_LELFLE > 0;
    Fxratio_atMAX_LELFLE=Fx_atMAX_LELFLE/peak_FX_LEL;
else
    Fxratio_atMAX_LELFLE=Fx_atMAX_LELFLE/min_FX_LEL;
end
Fy_atMAX_LELFLE=localFM_Lelbow(LELpeak_lift(1,1),2);
if Fy_atMAX_LELFLE > 0;
    Fyratio_atMAX_LELFLE=Fy_atMAX_LELFLE/peak_FY_LEL;
else
    Fyratio_atMAX_LELFLE=Fy_atMAX_LELFLE/min_FY_LEL;
end
Fz_atMAX_LELFLE=localFM_Lelbow(LELpeak_lift(1,1),3);
if Fz_atMAX_LELFLE > 0;
    Fzratio_atMAX_LELFLE=Fz_atMAX_LELFLE/peak_FZ_LEL;
else
    Fzratio_atMAX_LELFLE=Fz_atMAX_LELFLE/min_FZ_LEL;
end
Mx_atMAX_LELFLE=localFM_Lelbow(LELpeak_lift(1,1),4);
if Mx_atMAX_LELFLE > 0;
    Mxratio_atMAX_LELFLE=Mx_atMAX_LELFLE/peak_MX_LEL;
else
    Mxratio_atMAX_LELFLE=Mx_atMAX_LELFLE/min_MX_LEL;
end
My_atMAX_LELFLE=localFM_Lelbow(LELpeak_lift(1,1),5);

```

```

if My_atMAX_LELFLE > 0;
  Myratio_atMAX_LELFLE=My_atMAX_LELFLE/peak_MY_LEL;
else
  Myratio_atMAX_LELFLE=My_atMAX_LELFLE/min_MY_LEL;
end
Mz_atMAX_LELFLE=localFM_Lelbow(LELpeak_lift(1,1),6);
if Mz_atMAX_LELFLE > 0;
  Mzratio_atMAX_LELFLE=Mz_atMAX_LELFLE/peak_MZ_LEL;
else
  Mzratio_atMAX_LELFLE=Mz_atMAX_LELFLE/min_MZ_LEL;
end
RF_atMAX_LELFLE=resultantF_Lelbow(LELpeak_lift(1,1),1);
RFratio_atMAX_LELFLE=RF_atMAX_LELFLE/peak_RF_LEL;
RM_atMAX_LELFLE=resultantM_Lelbow(LELpeak_lift(1,1),1);
RMratio_atMAX_LELFLE=RM_atMAX_LELFLE/peak_RM_LEL;

Fx_atMIN_LELFLE=localFM_Lelbow(LELpeak_lift(1,2),1);
if Fx_atMIN_LELFLE > 0;
  Fxratio_atMIN_LELFLE=Fx_atMIN_LELFLE/peak_FX_LEL;
else
  Fxratio_atMIN_LELFLE=Fx_atMIN_LELFLE/min_FX_LEL;
end
Fy_atMIN_LELFLE=localFM_Lelbow(LELpeak_lift(1,2),2);
if Fy_atMIN_LELFLE > 0;
  Fyratio_atMIN_LELFLE=Fy_atMIN_LELFLE/peak_FY_LEL;
else
  Fyratio_atMIN_LELFLE=Fy_atMIN_LELFLE/min_FY_LEL;
end
Fz_atMIN_LELFLE=localFM_Lelbow(LELpeak_lift(1,2),3);
if Fz_atMIN_LELFLE > 0;
  Fzratio_atMIN_LELFLE=Fz_atMIN_LELFLE/peak_FZ_LEL;
else
  Fzratio_atMIN_LELFLE=Fz_atMIN_LELFLE/min_FZ_LEL;
end
Mx_atMIN_LELFLE=localFM_Lelbow(LELpeak_lift(1,2),4);
if Mx_atMIN_LELFLE > 0;
  Mxratio_atMIN_LELFLE=Mx_atMIN_LELFLE/peak_MX_LEL;
else
  Mxratio_atMIN_LELFLE=Mx_atMIN_LELFLE/min_MX_LEL;
end
My_atMIN_LELFLE=localFM_Lelbow(LELpeak_lift(1,2),5);
if My_atMIN_LELFLE > 0;
  Myratio_atMIN_LELFLE=My_atMIN_LELFLE/peak_MY_LEL;
else
  Myratio_atMIN_LELFLE=My_atMIN_LELFLE/min_MY_LEL;
end

```

```

Mz_atMIN_LELFLE=localFM_Lelbow(LELpeak_lift(1,2),6);
if Mz_atMIN_LELFLE > 0;
    Mzratio_atMIN_LELFLE=Mz_atMIN_LELFLE/peak_MZ_LEL;
else
    Mzratio_atMIN_LELFLE=Mz_atMIN_LELFLE/min_MZ_LEL;
end
RF_atMIN_LELFLE=resultantF_Lelbow(LELpeak_lift(1,2),1);
Rfratio_atMIN_LELFLE=RF_atMIN_LELFLE/peak_RF_LEL;
RM_atMIN_LELFLE=resultantM_Lelbow(LELpeak_lift(1,2),1);
RMratio_atMIN_LELFLE=RM_atMIN_LELFLE/peak_RM_LEL;

FM_atLELpeakA=[Fx_atMAX_LELFLE Fxratio_atMAX_LELFLE
Fy_atMAX_LELFLE Fyratio_atMAX_LELFLE Fz_atMAX_LELFLE
Fzratio_atMAX_LELFLE RF_atMAX_LELFLE Rfratio_atMAX_LELFLE...
Mx_atMAX_LELFLE Mxratio_atMAX_LELFLE My_atMAX_LELFLE
Myratio_atMAX_LELFLE Mz_atMAX_LELFLE Mzratio_atMAX_LELFLE
RM_atMAX_LELFLE RMratio_atMAX_LELFLE];...
Fx_atMIN_LELFLE Fxratio_atMIN_LELFLE Fy_atMIN_LELFLE
Fyratio_atMIN_LELFLE Fz_atMIN_LELFLE Fzratio_atMIN_LELFLE RF_atMIN_LELFLE
Rfratio_atMIN_LELFLE...
Mx_atMIN_LELFLE Mxratio_atMIN_LELFLE My_atMIN_LELFLE
Myratio_atMIN_LELFLE Mz_atMIN_LELFLE Mzratio_atMIN_LELFLE
RM_atMIN_LELFLE RMratio_atMIN_LELFLE];
save FMandRatio_atLELpeakAngle.txt FM_atLELpeakA -ascii;

%%%%%% force and force ratio at the max Left Wrist angle %%%%%%
Fx_atMAX_LWRFLE=localFM_Lwrist(LWRpeak_lift(1,1),1);
if Fx_atMAX_LWRFLE > 0;
    Fxratio_atMAX_LWRFLE=Fx_atMAX_LWRFLE/peak_FX_LWR;
else
    Fxratio_atMAX_LWRFLE=Fx_atMAX_LWRFLE/min_FX_LWR;
end
Fy_atMAX_LWRFLE=localFM_Lwrist(LWRpeak_lift(1,1),2);
if Fy_atMAX_LWRFLE > 0;
    Fyratio_atMAX_LWRFLE=Fy_atMAX_LWRFLE/peak_FY_LWR;
else
    Fyratio_atMAX_LWRFLE=Fy_atMAX_LWRFLE/min_FY_LWR;
end
Fz_atMAX_LWRFLE=localFM_Lwrist(LWRpeak_lift(1,1),3);
if Fz_atMAX_LWRFLE > 0;
    Fzratio_atMAX_LWRFLE=Fz_atMAX_LWRFLE/peak_FZ_LWR;
else
    Fzratio_atMAX_LWRFLE=Fz_atMAX_LWRFLE/min_FZ_LWR;
end
Mx_atMAX_LWRFLE=localFM_Lwrist(LWRpeak_lift(1,1),4);
if Mx_atMAX_LWRFLE > 0;

```

```

Mxratio_atMAX_LWRFLE=Mx_atMAX_LWRFLE/peak_MX_LWR;
else
Mxratio_atMAX_LWRFLE=Mx_atMAX_LWRFLE/min_MX_LWR;
end
My_atMAX_LWRFLE=localFM_Lwrist(LWRpeak_lift(1,1),5);
if My_atMAX_LWRFLE > 0;
Myratio_atMAX_LWRFLE=My_atMAX_LWRFLE/peak_MY_LWR;
else
Myratio_atMAX_LWRFLE=My_atMAX_LWRFLE/min_MY_LWR;
end
Mz_atMAX_LWRFLE=localFM_Lwrist(LWRpeak_lift(1,1),6);
if Mz_atMAX_LWRFLE > 0;
Mzratio_atMAX_LWRFLE=Mz_atMAX_LWRFLE/peak_MZ_LWR;
else
Mzratio_atMAX_LWRFLE=Mz_atMAX_LWRFLE/min_MZ_LWR;
end
RF_atMAX_LWRFLE=resultantF_Lwrist(LWRpeak_lift(1,1),1);
Rfratio_atMAX_LWRFLE=RF_atMAX_LWRFLE/peak_RF_LWR;
RM_atMAX_LWRFLE=resultantM_Lwrist(LWRpeak_lift(1,1),1);
RMratio_atMAX_LWRFLE=RM_atMAX_LWRFLE/peak_RM_LWR;

Fx_atMIN_LWRFLE=localFM_Lwrist(LWRpeak_lift(1,2),1);
if Fx_atMIN_LWRFLE > 0;
Fxratio_atMIN_LWRFLE=Fx_atMIN_LWRFLE/peak_FX_LWR;
else
Fxratio_atMIN_LWRFLE=Fx_atMIN_LWRFLE/min_FX_LWR;
end
Fy_atMIN_LWRFLE=localFM_Lwrist(LWRpeak_lift(1,2),2);
if Fy_atMIN_LWRFLE > 0;
Fyratio_atMIN_LWRFLE=Fy_atMIN_LWRFLE/peak_FY_LWR;
else
Fyratio_atMIN_LWRFLE=Fy_atMIN_LWRFLE/min_FY_LWR;
end
Fz_atMIN_LWRFLE=localFM_Lwrist(LWRpeak_lift(1,2),3);
if Fz_atMIN_LWRFLE > 0;
Fzratio_atMIN_LWRFLE=Fz_atMIN_LWRFLE/peak_FZ_LWR;
else
Fzratio_atMIN_LWRFLE=Fz_atMIN_LWRFLE/min_FZ_LWR;
end
Mx_atMIN_LWRFLE=localFM_Lwrist(LWRpeak_lift(1,2),4);
if Mx_atMIN_LWRFLE > 0;
Mxratio_atMIN_LWRFLE=Mx_atMIN_LWRFLE/peak_MX_LWR;
else
Mxratio_atMIN_LWRFLE=Mx_atMIN_LWRFLE/min_MX_LWR;
end
My_atMIN_LWRFLE=localFM_Lwrist(LWRpeak_lift(1,2),5);

```

```

if My_atMIN_LWRFLE > 0;
  Myratio_atMIN_LWRFLE=My_atMIN_LWRFLE/peak_MY_LWR;
else
  Myratio_atMIN_LWRFLE=My_atMIN_LWRFLE/min_MY_LWR;
end
Mz_atMIN_LWRFLE=localFM_Lwrist(LWRpeak_lift(1,2),6);
if Mz_atMIN_LWRFLE > 0;
  Mzratio_atMIN_LWRFLE=Mz_atMIN_LWRFLE/peak_MZ_LWR;
else
  Mzratio_atMIN_LWRFLE=Mz_atMIN_LWRFLE/min_MZ_LWR;
end
RF_atMIN_LWRFLE=resultantF_Lwrist(LWRpeak_lift(1,2),1);
RFratio_atMIN_LWRFLE=RF_atMIN_LWRFLE/peak_RF_LWR;
RM_atMIN_LWRFLE=resultantM_Lwrist(LWRpeak_lift(1,2),1);
RMratio_atMIN_LWRFLE=RM_atMIN_LWRFLE/peak_RM_LWR;

FM_atLWRpeakA=[Fx_atMAX_LWRFLE Fxratio_atMAX_LWRFLE
Fy_atMAX_LWRFLE Fyratio_atMAX_LWRFLE Fz_atMAX_LWRFLE
Fzratio_atMAX_LWRFLE RF_atMAX_LWRFLE RFratio_atMAX_LWRFLE...
Mx_atMAX_LWRFLE Mxratio_atMAX_LWRFLE My_atMAX_LWRFLE
Myratio_atMAX_LWRFLE Mz_atMAX_LWRFLE Mzratio_atMAX_LWRFLE
RM_atMAX_LWRFLE RMratio_atMAX_LWRFLE;...
Fx_atMIN_LWRFLE Fxratio_atMIN_LWRFLE Fy_atMIN_LWRFLE
Fyratio_atMIN_LWRFLE Fz_atMIN_LWRFLE Fzratio_atMIN_LWRFLE
RF_atMIN_LWRFLE RFratio_atMIN_LWRFLE...
Mx_atMIN_LWRFLE Mxratio_atMIN_LWRFLE My_atMIN_LWRFLE
Myratio_atMIN_LWRFLE Mz_atMIN_LWRFLE Mzratio_atMIN_LWRFLE
RM_atMIN_LWRFLE RMratio_atMIN_LWRFLE];
save FMandRatio_atLWRpeakAngle.txt FM_atLWRpeakA -ascii;

excelsheet1=[ave_LCFZ ave_RHandHF ave_RHandRF max_LCFZ max_RHandHF
max_RHandRF ...
trailing_VFIdex_liftPhase trailing_HFIdex_liftPhase trailing_RFIdex_liftPhase ...
peak_trailingVF_lift peak_trailingHF_lift peak_trailingRF_lift ave_LCFZ_lift ...
ave_RHandHF_lift ave_RHandRF_lift leading_VFIdex_liftPhase
leading_HFIdex_liftPhase ...
leading_RFIdex_liftPhase peak_leadingVF_lift peak_leadingHF_lift
peak_leadingRF_lift ...
ave_BNFZ_lift ave_LHandHF_lift ave_LHandRF_lift peak_landingVF landingHF
landingRF lift_phase];
excelsheet2=[ave_RF_RSH ave_RF_REL ave_RF_RWR peak_RF_RSH peak_RF_REL
peak_RF_RWR ...
peak_RF_RSHIndex_LiftPhase peak_RF_RELIndex_LiftPhase
peak_RF_RWRIndex_LiftPhase ...
Ave_RFRate_RSH Max_Sim_RFRate_RSH Max_Sim_RFRate_RSHPhase ...
Ave_RFRate_REL Max_Sim_RFRate_REL Max_Sim_RFRate_RELPhase ...

```

Ave_RFRate_RWR Max_Sim_RFRate_RWR Max_Sim_RFRate_RWRPhase ...
 ave_RM_RSH ave_RM_REL ave_RM_RWR peak_RM_RSH peak_RM_REL
 peak_RM_RWR ...
 peak_RM_RSHIndex_LiftPhase peak_RM_RELIndex_LiftPhase
 peak_RM_RWRIndex_LiftPhase ...
 Ave_RMRate_RSH Max_Sim_RMRate_RSH Max_Sim_RMRate_RSHPhase ...
 Ave_RMRate_REL Max_Sim_RMRate_REL Max_Sim_RMRate_RELPhase ...
 Ave_RMRate_RWR Max_Sim_RMRate_RWR Max_Sim_RMRate_RWRPhase];
 excelsheet3=[ave_RF_LSH ave_RF_LEL ave_RF_LWR peak_RF_LSH peak_RF_LEL
 peak_RF_LWR ...
 peak_RF_LSHIndex_LiftPhase peak_RF_LELIndex_LiftPhase
 peak_RF_LWRIndex_LiftPhase ...
 Ave_RFRate_LSH Max_Sim_RFRate_LSH Max_Sim_RFRate_LSHPhase ...
 Ave_RFRate_LEL Max_Sim_RFRate_LEL Max_Sim_RFRate_LELPhase ...
 Ave_RFRate_LWR Max_Sim_RFRate_LWR Max_Sim_RFRate_LWRPhase ...
 ave_RM_LSH ave_RM_LEL ave_RM_LWR peak_RM_LSH peak_RM_LEL
 peak_RM_LWR ...
 peak_RM_LSHIndex_LiftPhase peak_RM_LELIndex_LiftPhase
 peak_RM_LWRIndex_LiftPhase ...
 Ave_RMRate_LSH Max_Sim_RMRate_LSH Max_Sim_RMRate_LSHPhase ...
 Ave_RMRate_LEL Max_Sim_RMRate_LEL Max_Sim_RMRate_LELPhase ...
 Ave_RMRate_LWR Max_Sim_RMRate_LWR Max_Sim_RMRate_LWRPhase];
 excelsheet4=[peak_FX_RSH peak_FY_RSH peak_FZ_RSH peak_MX_RSH
 peak_MY_RSH peak_MZ_RSH ...
 peak_FX_RSHphase peak_FY_RSHphase peak_FZ_RSHphase peak_MX_RSHphase
 peak_MY_RSHphase peak_MZ_RSHphase ...
 min_FX_RSH min_FY_RSH min_FZ_RSH min_MX_RSH min_MY_RSH
 min_MZ_RSH ...
 min_FX_RSHphase min_FY_RSHphase min_FZ_RSHphase min_MX_RSHphase
 min_MY_RSHphase min_MZ_RSHphase ...
 Max_Sim_FXRate_RSH Max_Sim_FXRate_RSHPhase Max_Sim_FYRate_RSH
 Max_Sim_FYRate_RSHPhase Max_Sim_FZRate_RSH Max_Sim_FZRate_RSHPhase ...
 Max_Sim_MXRate_RSH Max_Sim_MXRate_RSHPhase Max_Sim_MYRate_RSH
 Max_Sim_MYRate_RSHPhase Max_Sim_MZRate_RSH Max_Sim_MZRate_RSHPhase];
 excelsheet5=[peak_FX_LSH peak_FY_LSH peak_FZ_LSH peak_MX_LSH
 peak_MY_LSH peak_MZ_LSH ...
 peak_FX_LSHphase peak_FY_LSHphase peak_FZ_LSHphase peak_MX_LSHphase
 peak_MY_LSHphase peak_MZ_LSHphase ...
 min_FX_LSH min_FY_LSH min_FZ_LSH min_MX_LSH min_MY_LSH
 min_MZ_LSH ...
 min_FX_LSHphase min_FY_LSHphase min_FZ_LSHphase min_MX_LSHphase
 min_MY_LSHphase min_MZ_LSHphase ...
 Max_Sim_FXRate_LSH Max_Sim_FXRate_LSHPhase Max_Sim_FYRate_LSH
 Max_Sim_FYRate_LSHPhase Max_Sim_FZRate_LSH Max_Sim_FZRate_LSHPhase ...
 Max_Sim_MXRate_LSH Max_Sim_MXRate_LSHPhase Max_Sim_MYRate_LSH
 Max_Sim_MYRate_LSHPhase Max_Sim_MZRate_LSH Max_Sim_MZRate_LSHPhase];

excelsheet6=[peak_FX_REL peak_FY_REL peak_FZ_REL peak_MX_REL
 peak_MY_REL peak_MZ_REL ...
 peak_FX_RELphase peak_FY_RELphase peak_FZ_RELphase peak_MX_RELphase
 peak_MY_RELphase peak_MZ_RELphase ...
 min_FX_REL min_FY_REL min_FZ_REL min_MX_REL min_MY_REL
 min_MZ_REL ...
 min_FX_RELphase min_FY_RELphase min_FZ_RELphase min_MX_RELphase
 min_MY_RELphase min_MZ_RELphase ...
 Max_Sim_FXRate_REL Max_Sim_FXRate_RELPhase Max_Sim_FYRate_REL
 Max_Sim_FYRate_RELPhase Max_Sim_FZRate_REL Max_Sim_FZRate_RELPhase ...
 Max_Sim_MXRate_REL Max_Sim_MXRate_RELPhase Max_Sim_MYRate_REL
 Max_Sim_MYRate_RELPhase Max_Sim_MZRate_REL Max_Sim_MZRate_RELPhase];
 excelsheet7=[peak_FX_LEL peak_FY_LEL peak_FZ_LEL peak_MX_LEL
 peak_MY_LEL peak_MZ_LEL ...
 peak_FX_LELphase peak_FY_LELphase peak_FZ_LELphase peak_MX_LELphase
 peak_MY_LELphase peak_MZ_LELphase ...
 min_FX_LEL min_FY_LEL min_FZ_LEL min_MX_LEL min_MY_LEL
 min_MZ_LEL ...
 min_FX_LELphase min_FY_LELphase min_FZ_LELphase min_MX_LELphase
 min_MY_LELphase min_MZ_LELphase ...
 Max_Sim_FXRate_LEL Max_Sim_FXRate_LELPhase Max_Sim_FYRate_LEL
 Max_Sim_FYRate_LELPhase Max_Sim_FZRate_LEL Max_Sim_FZRate_LELPhase ...
 Max_Sim_MXRate_LEL Max_Sim_MXRate_LELPhase Max_Sim_MYRate_LEL
 Max_Sim_MYRate_LELPhase Max_Sim_MZRate_LEL Max_Sim_MZRate_LELPhase];
 excelsheet8=[peak_FX_RWR peak_FY_RWR peak_FZ_RWR peak_MX_RWR
 peak_MY_RWR peak_MZ_RWR ...
 peak_FX_RWRphase peak_FY_RWRphase peak_FZ_RWRphase
 peak_MX_RWRphase peak_MY_RWRphase peak_MZ_RWRphase ...
 min_FX_RWR min_FY_RWR min_FZ_RWR min_MX_RWR min_MY_RWR
 min_MZ_RWR ...
 min_FX_RWRphase min_FY_RWRphase min_FZ_RWRphase min_MX_RWRphase
 min_MY_RWRphase min_MZ_RWRphase ...
 Max_Sim_FXRate_RWR Max_Sim_FXRate_RWRPhase Max_Sim_FYRate_RWR
 Max_Sim_FYRate_RWRPhase Max_Sim_FZRate_RWR Max_Sim_FZRate_RWRPhase ...
 Max_Sim_MXRate_RWR Max_Sim_MXRate_RWRPhase Max_Sim_MYRate_RWR
 Max_Sim_MYRate_RWRPhase Max_Sim_MZRate_RWR Max_Sim_MZRate_RWRPhase];
 excelsheet9=[peak_FX_LWR peak_FY_LWR peak_FZ_LWR peak_MX_LWR
 peak_MY_LWR peak_MZ_LWR ...
 peak_FX_LWRphase peak_FY_LWRphase peak_FZ_LWRphase
 peak_MX_LWRphase peak_MY_LWRphase peak_MZ_LWRphase ...
 min_FX_LWR min_FY_LWR min_FZ_LWR min_MX_LWR min_MY_LWR
 min_MZ_LWR ...
 min_FX_LWRphase min_FY_LWRphase min_FZ_LWRphase min_MX_LWRphase
 min_MY_LWRphase min_MZ_LWRphase ...
 Max_Sim_FXRate_LWR Max_Sim_FXRate_LWRPhase Max_Sim_FYRate_LWR
 Max_Sim_FYRate_LWRPhase Max_Sim_FZRate_LWR Max_Sim_FZRate_LWRPhase ...

Max_Sim_MXRate_LWR Max_Sim_MXRate_LWRPhase Max_Sim_MYRate_LWR
Max_Sim_MYRate_LWRPhase Max_Sim_MZRate_LWR Max_Sim_MZRate_LWRPhase];
excelsheet10=FM_atRSHpeakA;
excelsheet11=FM_atRELpeakA;
excelsheet12=FM_atRWRpeakA;
excelsheet13=FM_atLSHpeakA;
excelsheet14=FM_atLELpeakA;
excelsheet15=FM_atLWRpeakA;

BIBLIOGRAPHY

- 2013 Annual Disability Statistics Compendium*. (2013). The Research and Training Center on Disability Statistics and Demographics.
- Access Board, Figure 30b and 30c: Toilet Stalls, Alternate Stalls. Americans with Disabilities Act (ADA) - Accessibility Guidelines for Buildings and Facilities, U.S. Architectural and Transportation Barriers Compliance Board (Access Board).
- Allison, G. T., Singer, K. P., & Marshall, R. N. (1996). Transfer movement strategies of individuals with spinal cord injuries. *Disabil Rehabil*, 18(1), 35-41.
- Alm, M., Saraste, H., & Norrbrink, C. (2008). Shoulder pain in persons with thoracic spinal cord injury: prevalence and characteristics. *J Rehabil Med*, 40(4), 277-283.
- Americans with Disabilities Act (ADA) - Accessibility Guidelines for Buildings and Facilities. *U.S. Architectural and Transportation Barriers Compliance Board (Access Board)*(Fig. 28 and 29), 47.
- Americans with Disabilities Act (ADA) - Accessibility Guidelines for Buildings and Facilities. *U.S. Architectural and Transportation Barriers Compliance Board (Access Board)*(Fig. A6), A11.
- Bayley, J. C., Cochran, T. P., & Sledge, C. B. (1987). The weight-bearing shoulder. The impingement syndrome in paraplegics. *J Bone Joint Surg Am*, 69(5), 676-678.
- Boninger, M. L., Impink, B. G., Cooper, R. A., & Koontz, A. M. (2004). Relation between median and ulnar nerve function and wrist kinematics during wheelchair propulsion. *Arch Phys Med Rehabil*, 85(7), 1141-1145.
- Boninger, M. L., Koontz, A. M., Sisto, S. A., Dyson-Hudson, T. A., Chang, M., Price, R., et al. (2005). Pushrim biomechanics and injury prevention in spinal cord injury: recommendations based on CULP-SCI investigations. *J Rehabil Res Dev*, 42(3 Suppl 1), 9-19.
- Boninger, M. L., Robertson, R. N., Wolff, M., & Cooper, R. A. (1996). Upper limb nerve entrapments in elite wheelchair racers. *Am J Phys Med Rehabil*, 75(3), 170-176.

- Boninger, M. L., Waters, R. L., Chase, T., Dijkers, M. P. J. M., Gellman, H., Girona, R. J., et al. (2005). Preservation of upper limb function following spinal cord injury: a clinical practice guideline for health-care professionals. *J Spinal Cord Med*, 28(5), 434-470.
- Box, G. E. P., & Cox, D. R. (1964). An analysis of transformations. *Journal of the Royal Statistical Society, Series B*, 26(2), 211-252.
- Breusch, T. S., & Pagan, A. R. (1979). Simple test for heteroscedasticity and random coefficient variation. *Econometrica (The Econometric Society)*, 47(5), 1287 - 1294.
- Burnham, R. S., May, L., Nelson, E., Steadward, R., & Reid, D. C. (1993). Shoulder pain in wheelchair athletes. The role of muscle imbalance. *Am J Sports Med*, 21(2), 238-242.
- Burnham, R. S., & Steadward, R. D. (1994). Upper extremity peripheral nerve entrapments among wheelchair athletes: prevalence, location, and risk factors. *Arch Phys Med Rehabil*, 75(5), 519-524.
- Campbell, C. C., & Koris, M. J. (1996). Etiologies of shoulder pain in cervical spinal cord injury. *Clin Orthop Relat Res*(322), 140-145.
- Cobb, T. K., An, K. N., & Cooney, W. P. (1995). Externally applied forces to the palm increase carpal tunnel pressure. *J Hand Surg Am*, 20(2), 181-185.
- Cohen, J. (1992). A power primer. *Psychol Bull*, 112(1), 155-159.
- Cooper, R. A., Boninger, M. L., Shimada, S. D., & Lawrence, B. M. (1999). Glenohumeral joint kinematics and kinetics for three coordinate system representations during wheelchair propulsion. *Am J Phys Med Rehabil*, 78(5), 435-446.
- Curtis, K. A., Drysdale, G. A., Lanza, R. D., Kolber, M., Vitolo, R. S., & West, R. (1999). Shoulder pain in wheelchair users with tetraplegia and paraplegia. *Arch Phys Med Rehabil*, 80(4), 453-457.
- Curtis, K. A., Roach, K. E., Applegate, E. B., Amar, T., Benbow, C. S., Genecco, T. D., et al. (1995). Development of the Wheelchair User's Shoulder Pain Index (WUSPI). *Paraplegia*, 33(5), 290-293.
- Dalyan, M., Cardenas, D. D., & Gerard, B. (1999). Upper extremity pain after spinal cord injury. *Spinal Cord*, 37(3), 191-195.
- Desroches, G., Gagnon, D., Nadeau, S., & Popovic, M. R. (2013). Effects of sensorimotor trunk impairments on trunk and upper limb joint kinematics and kinetics during sitting pivot transfers in individuals with a spinal cord injury. *Clin Biomech (Bristol, Avon)*, 28(1), 1-9.
- Durbin, J., & Watson, G. S. (1950). Testing for serial correlation in least squares regression: I. *Biometrika*, 37(3/4), 409-428.

- Escobedo, E. M., Hunter, J. C., Hollister, M. C., Patten, R. M., & Goldstein, B. (1997). MR imaging of rotator cuff tears in individuals with paraplegia. *AJR Am J Roentgenol*, *168*(4), 919-923.
- Finley, M. A., McQuade, K. J., & Rodgers, M. M. (2005). Scapular kinematics during transfers in manual wheelchair users with and without shoulder impingement. *Clin Biomech (Bristol, Avon)*, *20*(1), 32-40.
- Finley, M. A., & Rodgers, M. M. (2004). Prevalence and identification of shoulder pathology in athletic and nonathletic wheelchair users with shoulder pain: A pilot study. *J Rehabil Res Dev*, *41*(3B), 395-402.
- Fleisig, G. S., Andrews, J. R., Dillman, C. J., & Escamilla, R. F. (1995). Kinetics of baseball pitching with implications about injury mechanisms. *Am J Sports Med*, *23*(2), 233-239.
- Fliess-Douer, O., Vanlandewijck, Y. C., & Van Der Woude, L. H. V. (2012). Most Essential Wheeled Mobility Skills for Daily Life: An International Survey Among Paralympic Wheelchair Athletes With Spinal Cord Injury. *Archives of physical medicine and rehabilitation*, *93*(4), 629-635.
- Forslund, E. B., Granstrom, A., Levi, R., Westgren, N., & Hirschfeld, H. (2007). Transfer from table to wheelchair in men and women with spinal cord injury: coordination of body movement and arm forces. *Spinal Cord*, *45*(1), 41-48.
- Fuchtmeier, B., May, R., Hente, R., Maghsudi, M., Volk, M., Hammer, J., et al. (2007). Proximal humerus fractures: a comparative biomechanical analysis of intra and extramedullary implants. *Arch Orthop Trauma Surg*, *127*(6), 441-447.
- Gagnon, D., Koontz, A., Mulroy, S., Nawoczenski, D. A., Butler-Forslund, E., Granstrom, A., et al. (2009). Biomechanics of Sitting Pivot Transfers Among Individuals with a Spinal Cord Injury: A Review of the Current Knowledge *Topics in Spinal Cord Injury Rehabilitation*, *15*, 33-58.
- Gagnon, D., Koontz, A. M., Brindle, E., Boninger, M. L., & Cooper, R. A. (2009). Does upper-limb muscular demand differ between preferred and nonpreferred sitting pivot transfer directions in individuals with a spinal cord injury? *J Rehabil Res Dev*, *46*(9), 1099-1108.
- Gagnon, D., Nadeau, S., Desjardins, P., & Noreau, L. (2008). Biomechanical assessment of sitting pivot transfer tasks using a newly developed instrumented transfer system among long-term wheelchair users. *J Biomech*, *41*(5), 1104-1110.
- Gagnon, D., Nadeau, S., Gravel, D., Noreau, L., Lariviere, C., & Gagnon, D. (2003). Biomechanical analysis of a posterior transfer maneuver on a level surface in individuals with high and low-level spinal cord injuries. *Clin Biomech (Bristol, Avon)*, *18*(4), 319-331.

- Gagnon, D., Nadeau, S., Noreau, L., Dehail, P., & Gravel, D. (2008). Quantification of reaction forces during sitting pivot transfers performed by individuals with spinal cord injury. *J Rehabil Med*, 40(6), 468-476.
- Gagnon, D., Nadeau, S., Noreau, L., Dehail, P., & Pottie, F. (2008). Comparison of peak shoulder and elbow mechanical loads during weight-relief lifts and sitting pivot transfers among manual wheelchair users with spinal cord injury. *J Rehabil Res Dev*, 45(6), 863-873.
- Gagnon, D., Nadeau, S., Noreau, L., Eng, J. J., & Gravel, D. (2008). Trunk and upper extremity kinematics during sitting pivot transfers performed by individuals with spinal cord injury. *Clin Biomech (Bristol, Avon)*, 23(3), 279-290.
- Gagnon, D., Nadeau, S., Noreau, L., Eng, J. J., & Gravel, D. (2009). Electromyographic patterns of upper extremity muscles during sitting pivot transfers performed by individuals with spinal cord injury. *J Electromyogr Kinesiol*, 19(3), 509-520.
- Gellman, H., Sie, I., & Waters, R. L. (1988). Late complications of the weight-bearing upper extremity in the paraplegic patient. *Clin Orthop Relat Res*(233), 132-135.
- Giphart, J. E., Brunkhorst, J. P., Horn, N. H., Shelburne, K. B., Torry, M. R., & Millett, P. J. (2013). Effect of plane of arm elevation on glenohumeral kinematics: a normative biplane fluoroscopy study. *J Bone Joint Surg Am*, 95(3), 238-245.
- Goldstein, B., Young, J., & Escobedo, E. M. (1997). Rotator cuff repairs in individuals with paraplegia. *Am J Phys Med Rehabil*, 76(4), 316-322.
- Goodman, C. M., Steadman, A. K., Meade, R. A., Bodenheimer, C., Thornby, J., & Netscher, D. T. (2001). Comparison of carpal canal pressure in paraplegic and nonparaplegic subjects: clinical implications. *Plast Reconstr Surg*, 107(6), 1464-1471; discussion 1472.
- Hanavan, E. P., Jr. (1964). A MATHEMATICAL MODEL OF THE HUMAN BODY. *Amrl tr*, 1-149.
- Hawkins, R. J., & Angelo, R. L. (1990). Glenohumeral osteoarthritis. A late complication of the Putti-Platt repair. *J Bone Joint Surg Am*, 72(8), 1193-1197.
- Hosseini, S. M., Oyster, M. L., Kirby, R. L., Harrington, A. L., & Boninger, M. L. (2012). Manual wheelchair skills capacity predicts quality of life and community integration in persons with spinal cord injury. *Arch Phys Med Rehabil*, 93(12), 2237-2243.
- Hurd, W. J., & Kaufman, K. R. (2012). Glenohumeral rotational motion and strength and baseball pitching biomechanics. *J Athl Train*, 47(3), 247-256.
- John, L. T., Cherian, B., & Babu, A. (2010). Postural control and fear of falling in persons with low-level paraplegia. *J Rehabil Res Dev*, 47(5), 497-502.
- Kaiser, H. (1974). An index of factorial simplicity. *Psychometrika*, 39(1), 31-36.

- Kaiser, H. F. (1960). The application of electronic computers to factor analysis. *Educational and Psychological Measurement*, 20, 141-151.
- Kankipati, P. (2012). *Investigation of transfer technique biomechanics among persons with tetraplegia and paraplegia*. University of Pittsburgh, Pittsburgh.
- Kankipati, P., Boninger, M. L., Gagnon, D., Cooper, R. A., & Koontz, A. M. (2014). Upper limb joint kinetics of three sitting pivot wheelchair transfer techniques in individuals with spinal cord injury. *J Spinal Cord Med*.
- Kankipati, P., Koontz, A. M., Vega, A., & Lin, Y. S. (2011). Phase Identification of Sitting Pivot Wheelchair Transfers, *American Society of Biomechanics*. Long Beach, CA.
- Keeley, D. W., Oliver, G. D., & Dougherty, C. P. (2012). A biomechanical model correlating shoulder kinetics to pain in young baseball pitchers. *J Hum Kinet*, 34, 15-20.
- Keir, P. J., Wells, R. P., Ranney, D. A., & Lavery, W. (1997). The effects of tendon load and posture on carpal tunnel pressure. *J Hand Surg Am*, 22(4), 628-634.
- Koontz, A. M., Kankipati, P., Lin, Y. S., Cooper, R. A., & Boninger, M. L. (2011). Upper limb kinetic analysis of three sitting pivot wheelchair transfer techniques. *Clin Biomech (Bristol, Avon)*.
- Koontz, A. M., Lin, Y. S., Kankipati, P., Boninger, M. L., & Cooper, R. A. (2011). Development of custom measurement system for biomechanical evaluation of independent wheelchair transfers. *J Rehabil Res Dev*, 48(8), 1015-1028.
- Lee, T. Q., & McMahon, P. J. (2002). Shoulder biomechanics and muscle plasticity: implications in spinal cord injury. *Clin Orthop Relat Res*(403 Suppl), S26-36.
- Marciello, M. A., Herbison, G. J., Cohen, M. E., & Schmidt, R. (1995). Elbow extension using anterior deltoids and upper pectorals in spinal cord-injured subjects. *Arch Phys Med Rehabil*, 76(5), 426-432.
- McCasland, L. D., Budiman-Mak, E., Weaver, F. M., Adams, E., & Miskevics, S. (2006). Shoulder pain in the traumatically injured spinal cord patient: evaluation of risk factors and function. *J Clin Rheumatol*, 12(4), 179-186.
- McClure, L. A., Boninger, M. L., Ozawa, H., & Koontz, A. (2011). Reliability and validity analysis of the transfer assessment instrument. *Arch Phys Med Rehabil*, 92(3), 499-508.
- McCullagh, P., Weiss, M. R., & Ross, D. (1989). Modeling considerations in motor skill acquisition and performance: an integrated approach. *Exerc Sport Sci Rev*, 17, 475-513.
- Meislin, R. J., Sperling, J. W., & Stitik, T. P. (2005). Persistent shoulder pain: epidemiology, pathophysiology, and diagnosis. *Am J Orthop (Belle Mead NJ)*, 34(12 Suppl), 5-9.

- Mercer, J. L., Boninger, M., Koontz, A., Ren, D., Dyson-Hudson, T., & Cooper, R. (2006). Shoulder joint kinetics and pathology in manual wheelchair users. *Clin Biomech (Bristol, Avon)*, *21*(8), 781-789.
- Minkel, J. L. (2000). Seating and mobility considerations for people with spinal cord injury. *Phys Ther*, *80*(7), 701-709.
- Minkel, J. L., Hastings, J., McClure, L. A., & Bjerkefors, A. (2010). Teaching transfers - safe and effective transfer techniques for persons with spinal cord injury, *4th International Interdisciplinary Conference on Posture and Wheeled Mobility*. Glasgow, UK.
- Mortenson, W. B., Miller, W. C., Backman, C. L., & Oliffe, J. L. (2012). Association between mobility, participation, and wheelchair-related factors in long-term care residents who use wheelchairs as their primary means of mobility. *J Am Geriatr Soc*, *60*(7), 1310-1315.
- Myers, R. H. (2000). *Classical and Modern Regression with Applications* (2nd ed.): Duxbury Press.
- Newton, A. M., Kirby, R. L., Macphee, A. H., Dupuis, D. J., & Macleod, D. A. (2002). Evaluation of manual wheelchair skills: is objective testing necessary or would subjective estimates suffice? *Arch Phys Med Rehabil*, *83*(9), 1295-1299.
- Nichols, P. J., Norman, P. A., & Ennis, J. R. (1979). Wheelchair user's shoulder? Shoulder pain in patients with spinal cord lesions. *Scand J Rehabil Med*, *11*(1), 29-32.
- Pentland, W. E., & Twomey, L. T. (1994). Upper limb function in persons with long term paraplegia and implications for independence: Part I. *Paraplegia*, *32*(4), 211-218.
- Perry, J., Gronley, J. K., Newsam, C. J., Reyes, M. L., & Mulroy, S. J. (1996). Electromyographic analysis of the shoulder muscles during depression transfers in subjects with low-level paraplegia. *Arch Phys Med Rehabil*, *77*(4), 350-355.
- Pynn, K., Tsai, C. Y., & Koontz, A. (2014). The relationship between lead hand positioning and proper wheelchair transfer techniques, *RESNA 2014 Annual Conference*. Indianapolis, IN.
- Pyo, J., Pasquina, P. F., DeMarco, M., Wallach, R., Teodorski, E., & Cooper, R. A. (2010). Upper limb nerve entrapment syndromes in veterans with lower limb amputations. *PM R*, *2*(1), 14-22.
- Qi, L., Wakeling, J., Grange, S., & Ferguson-Pell, M. (2013). Coordination patterns of shoulder muscles during level-ground and incline wheelchair propulsion. *J Rehabil Res Dev*, *50*(5), 651-662.
- Reinold, M. M., Macrina, L. C., Wilk, K. E., Fleisig, G. S., Dun, S., Barrentine, S. W., et al. (2007). Electromyographic analysis of the supraspinatus and deltoid muscles during 3 common rehabilitation exercises. *J Athl Train*, *42*(4), 464-469.

- Rice, I., Gagnon, D., Gallagher, J., & Boninger, M. (2010). Hand rim wheelchair propulsion training using biomechanical real-time visual feedback based on motor learning theory principles. *J Spinal Cord Med*, 33(1), 33-42.
- Rice, I. M., Jayaraman, C., Hsiao-Weckler, E. T., & Sosnoff, J. J. (2013). Relationship Between Shoulder Pain and Kinetic and Temporal-Spatial Variability in Wheelchair Users. *Arch Phys Med Rehabil*.
- Rice, L. A., Smith, I., Kelleher, A. R., Greenwald, K., Hoelmer, C., & Boninger, M. L. (2013). Impact of the Clinical Practice Guideline for Preservation of Upper Limb Function on Transfer Skills of Persons with Acute Spinal Cord Injury. *Arch Phys Med Rehabil*, 94(7), 1230-1246.
- Sie, I. H., Waters, R. L., Adkins, R. H., & Gellman, H. (1992). Upper extremity pain in the postrehabilitation spinal cord injured patient. *Arch Phys Med Rehabil*, 73(1), 44-48.
- Spinal Cord Injury Facts and Figures at a Glance. (2010). *National Spinal Cord Injury Statistical Center, Birmingham, Alabama*.
- Steinmetz, E. (2006). Americans With Disabilities: 2002. *U.S. Census Bureau Current Population Report*(May 2006), 70-107.
- Stevens, J. P. (2002). *Applied multivariate statistics for the social sciences* (4th ed.): Psychology Press.
- Subbarao, J. V., Klopstein, J., & Turpin, R. (1995). Prevalence and impact of wrist and shoulder pain in patients with spinal cord injury. *J Spinal Cord Med*, 18(1), 9-13.
- Toro, M. L., Koontz, A. M., & Cooper, R. A. (2013). The impact of transfer setup on the performance of independent wheelchair transfers. *Hum Factors*, 55(3), 567-580.
- Tsai, C.-Y., Hogaboom, N. S., Boninger, M. L., & Koontz, A. M. (2014). The Relationship between Independent Transfer Skills and Upper Limb Kinetics in Wheelchair Users. *BioMed Research International*, 2014, 12.
- Tsai, C. Y., Hogaboom, N. S., Boninger, M. L., & Koontz, A. M. (2014). The relationship between independent transfer skills and upper limb kinetics in wheelchair users. *BioMed Research International*, in press.
- Tsai, C. Y., Rice, L. A., Hoelmer, C., Boninger, M. L., & Koontz, A. M. (2013). Basic Psychometric Properties of the Transfer Assessment Instrument (Version 3.0). *Arch Phys Med Rehabil*, 94(12), 2456-2464.
- Van Drongelen, S., Van der Woude, L. H., Janssen, T. W., Angenot, E. L., Chadwick, E. K., & Veeger, D. H. (2005). Mechanical load on the upper extremity during wheelchair activities. *Arch Phys Med Rehabil*, 86(6), 1214-1220.

- Wang, Y. T., Kim, C. K., Ford, H. T., 3rd, & Ford, H. T., Jr. (1994). Reaction force and EMG analyses of wheelchair transfers. *Percept Mot Skills*, 79(2), 763-766.
- Wu, G., van der Helm, F. C., Veeger, H. E., Makhsous, M., Van Roy, P., Anglin, C., et al. (2005). ISB recommendation on definitions of joint coordinate systems of various joints for the reporting of human joint motion--Part II: shoulder, elbow, wrist and hand. *J Biomech*, 38(5), 981-992.
- Yanai, T., Fuss, F. K., & Fukunaga, T. (2006). In vivo measurements of subacromial impingement: substantial compression develops in abduction with large internal rotation. *Clin Biomech (Bristol, Avon)*, 21(7), 692-700.
- Youm, T., ElAttrache, N. S., Tibone, J. E., McGarry, M. H., & Lee, T. Q. (2009). The effect of the long head of the biceps on glenohumeral kinematics. *J Shoulder Elbow Surg*, 18(1), 122-129.